Politecnico di Torino

ScuDo
Scuola di Dottorato ~ Doctoral School
WHAT YOU ARE, TAKES YOU FAR

Doctoral Dissertation
Doctoral Program in Mechanical Engineering (38^{th}cycle)

MBSE and design of hydrogen storage and distribution system for UAVs

By

Filippo Mazzoni

******

Supervisor(s):
Prof. E.Brusa, Supervisor
Prof. C.Gastaldi, Co-Supervisor
Dr. Eng. G.Accardo, Company Supervisor

Doctoral Examination Committee:
Prof. A.B. , Referee, University of...
Prof. I.J, University of...

Politecnico di Torino
2026

Declaration

I hereby declare that, the contents and organization of this dissertation constitute my own original work and does not compromise in any way the rights of third parties, including those relating to the security of personal data.

Filippo Mazzoni
2026

* This dissertation is presented in partial fulfillment of the requirements for **Ph.D. degree** in the Graduate School of Politecnico di Torino (ScuDo).

To my father,
who recently left me,
and to my daughter,
who will soon come.

"Happiness can be found, even in the darkest of times,
if one only remembers to turn on the light".
J K. Rowling

Acknowledgements

These three years have been an unparalleled journey of personal and professional growth.

I want to express my deepest gratitude to Professors Brusa, Delprete, and Gastaldi of the Industrial Systems Engineering and Design research group, who, as academic supervisors, have continuously guided me throughout my PhD.
I would also like to thank Dr. Eng. Grazia Accardo, Principal Investigator of the Advanced Power and Energy Systems research unit of the Leonardo Innovation Hub & Intellectual Property, for her precious support, which allowed me to define and refine the direction of my research.

I thank my colleagues from the Leonardo Innovation Hub & Intellectual Property for the fruitful and inspiring collaboration, and my friends for their constant support and presence.

A special thanks goes to my family, both by birth and by bond: my uncles, grandparents, and cousins, for whom I feel fortunate.

I am profoundly thankful to my father, whose recent memory I carry with immense pride, to my mother, a fundamental pillar in my life, to my sister, whose presence has given me strength in the most difficult moments, to Diletta, the partner for my life, and to Teresa, the daughter I am ready to love boundlessly.

Abstract

The current work is the result of a doctoral activity conducted at the Leonardo Innovation Hub & Intellectual Property, specifically at the Advanced Power & Energy Systems R&D unit, during which Model-Based Systems Engineering (MBSE) has been applied to the design of a hydrogen storage and distribution system (H_2SDSys) for airborne applications. The purpose of the analysis was derived from Leonardo's need to investigate hydrogen-powered aircraft, while the MBSE is a must for the aerospace sector and for the company.

Thus, a conceptual design path for applying the MBSE has been described and initially applied to unmanned aerial vehicles (UAVs) through requirements and functional analyses. Then, a hydrogen tank parametric sizing model has been described and applied to two use cases to assess the feasibility of retrofitting two UAVs. Then, the MBSE design path has been newly applied at a deeper level of detail to design the H_2SDSys. Specifically, a set of requirements has been written for this system, the functional analysis has been applied, and a functional architecture has been created. Finally, the dynamic analysis has been conducted on the complete hydrogen storage and distribution system.

The contributions of the work conducted are both methodological, referring to the application of the MBSE, and technical, concerning the design of the H_2SDSys. Indeed, the implementation of the MBSE to an industrial product, such as the UAV, allowed the identification of both the obstacles and the advantages of such methodology, while in the design of the hydrogen storage and distribution system, the MBSE approach allowed for drawing both qualitative and quantitative conclusions for a straight finalisation of the H_2SDSys architecture. Conversely, the static analysis revealed that, for the same amount of energy stored onboard, the retrofitting of the two UAVs analysed could not be performed due to volume constraints. However, the high gravimetric and volumetric indexes of the liquid hydrogen tank obtained through the parametric design model, which, depending on the insulating material used, range

between 40% and 60% and between 60% and 70%, respectively, encouraged further investigation. Thus, the dynamic analysis has been conducted, leading to the final configuration of the H_2SDSys. The system demonstrated satisfactory performance, covering the entire flight mission without the need to evacuate hydrogen due to boil-off, consuming a relatively low amount of electric power during operation, efficiently conditioning hydrogen, and maintaining dormancy for more than 7 hours. Viewed holistically, the main contributions of this thesis include the application of the MBSE and the analyses conducted for the H_2SDSys design. Furthermore, as the thesis unfolds, the practical correlations between these two aspects gradually become appreciable.

Contents

List of Figures

List of Tables

Chapter 1

Introduction

1.1 Technical domain

The doctoral activity conducted covers two main domains: enabling technologies for hydrogen storage in aviation and Model-Based Systems Engineering (MBSE) for aircraft design.

The design of the hydrogen storage and distribution system represents a specific issue within the energy transition process that is gradually spreading across all industrial sectors, pushing the development of enabling technologies that enhance sustainable development. Among the several challenges characterising different domains, the high performance and the stringent requirements typical of the aviation sector pose significant obstacles to the design of the new generation of aircraft. The need for replacing fossil fuels with sustainable solutions for storing energy onboard leads to hydrogen as one of the most promising candidates, due to its high specific energy ($120\,\mathrm{MJ\,kg^{-1}}$) and the potential for nearly zero carbon emissions when produced from renewable sources [1, 2, 3, 4].
However, the inherently low density of hydrogen at environmental temperature, corresponding to $0.081\,\mathrm{kg\,m^{-3}}$, $25.86\,\mathrm{kg\,m^{-3}}$, and $47.44\,\mathrm{kg\,m^{-3}}$ at bar, 350 bar, and 700 bar, respectively, stands in contrast with the limited volumes available onboard. For this reason, hydrogen must be stored under cryogenic conditions, at approximately 20 K, which requires lightweight yet mechanically robust tanks, suitable materials with proper structural and chemical properties, and effective insulation systems capable of minimising boil-off losses while ensuring safety [5]. Moreover, the

design process of the hydrogen storage and distribution system (H_2SDSys) includes the identification of the most suitable solution, which, in turn, depends on various aspects such as the operational context, the duration of the filling and emptying phases, and the required storage capacity. Thus, the identification of an aircraft class to be used as a case study to conduct the analysis becomes mandatory. Considering the safety issues related to the presence of a human onboard, i.e. the pilot, and the advantages in terms of volumetric and gravimetric efficiencies of storing large amounts of hydrogen, long-endurance unmanned aerial vehicles (UAVs) have been selected as a potential application for hybrid-electric power-trains due to the missions they have to accomplish, which include continuous remotely piloted or autonomous flights lasting several hours, and thus requiring large amounts of fuel. Moreover, given the multiple purposes UAVs can serve, such as environmental monitoring, search and rescue operations in emergency scenarios, and the rapid delivery of medical supplies, the market is expected to grow in the coming years.

Nevertheless, the design of UAVs is characterised by a high degree of complexity, which is even increased by the introduction of innovative technologies such as the H_2SDSys. To manage risk and realise a successful system, the application of a proper methodology became mandatory. Systems Engineering (SE) and, in particular, MBSE are used to address this issue. SE is a well-established discipline, especially in specific industrial sectors such as aerospace and aviation. It includes a dedicated language, namely the Systems Modelling Language (SysML), as well as suitable processes and tools, which together constitute the three pillars of SE. The MBSE is indeed a methodology for applying SE through digital models (Model-Based), developed in SysML with dedicated tools [6].
However, the shift towards Model-Based Systems Engineering is yet to be assessed. From a theoretical perspective, several publications in the literature cover topics such as the Systems Modelling Language, examples and guidance for implementation, frameworks for applying Systems Engineering in specific domains, and assessed standards defining principles, concepts, and processes. Nevertheless, the practical shift towards MBSE represents a significant paradigm change, which encounters obstacles of a different nature, such as stakeholder resistance to change and the limited capabilities of the modelling tools.

Overall, the design of new systems involves risks associated with uncertainties, which can be associated, for example, with their behaviour in operational scenarios and their actual realisation. In this context, MBSE can be a suitable methodology

for managing risk, thereby increasing the probability of success. Throughout this work, the practical implications encountered while applying this methodology for the design of the H_2SDSys will be highlighted.

1.2 Research needs and industrial context

The author carried out his doctoral activity at intersection between industry and academia, being both a member of the Industrial Systems Engineering and Design (ISED) research group of the Department of Mechanical and Aerospace Engineering (DIMEAS) at Politecnico di Torino, and a member of the Advanced Power and Energy Systems (APES) R&D unit of the Leonardo Innovation Hub & Intellectual Property, at Leonardo S.p.A.. This dual affiliation allowed the candidate to benefit from both perspectives and to align the research direction with the methodological and scientific needs of academia, while developing a product and a robust framework that can be implemented on the platforms currently used by the company.

As a starting point, the needs identified by Leonardo can be summarised as follows:

- A state-of-the-art analysis of the current and previously applied technology to store and distribute hydrogen on board.
- The application of MBSE to show the advantages and limitations of MBSE through its practical application.
- The preliminary design of the H_2SDSys, including its functions and its architecture, a parametric analysis, and a simulation of its dynamic behaviour.
- The development of digital tools for creating numerical models of the aircraft systems, being compatible with the tools selected by the company.
- Coordinate modelling activities through parameter alignment across team members, enabling the integration of several models.
- Conduct the design taking into account that experimental activities are foreseen in the short to medium term.

1.3 Scope

The scope of this research activity is to apply the MBSE to the design of hydrogen storage and distribution systems for UAV applications. The research combines systems engineering practices, with particular emphasis on MBSE, and domain-specific knowledge of hydrogen technologies. The current work aims to apply MBSE to perform the preliminary design of a hydrogen storage and distribution system, supporting the development of sustainable aviation technologies.

In practice, the objectives of the current study can be grouped into methodological and technical aspects, both contributing to satisfying the needs of the customer. The application of Model-Based Systems Engineering aims to identify the advantages of this approach, to identify the issues that should be addressed, and those for which MBSE can be suitable, the advantages of applying MBSE from the perspective of the company, and the results obtained through its application.

In contrast, the need for sustainable technologies requires investigating technical aspects related to the hydrogen storage and distribution system. Determining the technical feasibility of the solution, its main characteristics and properties, its behaviour during operation, and the possibility of integrating the system onboard have to be investigated.

Overall, the objectives of the current analysis can be articulated into two levels: a methodological one, consisting of the application of the MBSE to a real system to assess its potential, and a practical one, including the design of the H_2SDSys for aviation. Thus, in the following, the MBSE will be applied to design the H_2SDSys, aiming at satisfying both the purpose of this work.

1.4 Thesis outline

An outline of the following chapters of the thesis has been provided to help the reader navigate through the study.

Chapter 2 proposes a comprehensive introduction to SE and MBSE to provide the elements necessary to understand the following analysis, introducing systems concepts, the modelling language, the methodology, and the tool. In addition, part of

the chapter has been elaborated to show the future of SE, which is now represented by the paradigm shift introduced by the new version of the modelling language, and to provide quantitative advantages retrieved from previous applications of SE and MBSE in industrial contexts.

Chapter 3 describes the unmanned aerial vehicles, their classification, and their applications. Subsequently, it focuses on two UAV classes, high-altitude long-endurance and medium-altitude long-endurance UAVs, which have been identified as suitable candidates to be used as test cases for the application of the hydrogen storage and distribution system. Then, considerations are delineated, analysing the sets of data retrieved from the literature. The MQ-1 Predator UAV by General Atomics and the RQ-4 Global Hawk UAV by Northrop Grumman are the selected and described for the subsequent analysis.

Chapter 4 provides a comprehensive historical description of the use of hydrogen in aviation. Then the focus is shifted towards a comparison between hydrogen and other storage technologies to understand the reason why hydrogen can represent the most promising solution to decarbonise aviation. The methods of storing hydrogen are described, focusing on the so-called physical-based methods, encompassing those technologies where hydrogen is stored as a fuel inside a containment volume. These include compressed, cryogenically compressed, and liquid hydrogen storage tanks. A description of the several design aspects is provided, drawing attention to compressed and liquid hydrogen storage, which are characterised by higher technological maturity.

Chapter 5 represents the core of the analysis, in which the tool, i.e., the MBSE, is applied to design the product, i.e., the hydrogen-powered UAV, focusing on the H_2SDSys.
A brief introduction about the advantages of applying SE to the design of UAVs is proposed. Then, the theoretical path for applying MBSE, namely the MBSE conceptual design path, is described. Then, the customer's needs are analysed, followed by the requirements and functional analyses applied to a specific use case of the UAV with the aim of creating a thread linking the customer's needs, i.e., the very first design phase, to the analysis of the hydrogen storage and distribution system.

Before proceeding with this analysis, the tank parametric sizing model is presented and applied to the two use cases previously mentioned to assess the potential for retrofitting, which resulted in unfeasibility, thus addressing the subsequent design steps towards a completely new aircraft configuration. Due to limited time available, MBSE has been applied only to the Predator UAV use case. The requirements and functional analyses have been carried out. The functional architecture has been created and translated into a logical one. Finally, dynamic simulations have been conducted, and the outputs have been analysed.

Chapter 6 draws the conclusion of the current work, highlighting both methodological and purely technical aspects, emphasising all the results and contributions provided by this work, also considering its marked practical connotations.

Chapter 2

The design methodology of Systems Engineering

2.1 Introduction to Systems Engineering

ISO/IEC/IEEE 15288 standard and the *Systems Engineering Handbook* ([7]) define Systems Engineering (SE) as:

a ***transdisciplinary*** *and* ***integrative*** *approach to enable the* ***successful realization, use, and retirement*** *of* ***engineered systems****, using* ***systems principles and concepts****, and* ***scientific, technological, and management methods****.*

Despite its conciseness, the definition provided is comprehensive, encompassing several elements worth exploring to gain a clearer view. The transdisciplinarity of SE makes it suitable to be applied both in technical and managerial domains, such as software, mechanical, or electrical engineering, as well as to fields related to quality assurance and project planning [8, 7, 6]. Covering such a wide spectrum of disciplines, SE encourages a holistic approach that integrates the various entities and aspects involved. By doing so, communication is improved, and traceability is ensured. SE can be very helpful in managing risk and reducing the probability of failure, which in turn leads to achieving its primary objective: realising successful systems. A life-cycle approach to system design is promoted, including analyses spanning from the very initial conceptual idea and needs through system realisation,

use, and retirement. Indeed, the definition reported above refers to an *engineered system* [7].

An engineered system is a system designed or adapted to interact with an anticipated operational environment to achieve one or more intended purposes while complying with applicable constraints.

The latter definition adds a few important elements to the definition of a system alone, highlighting interactions with the surrounding environment, emphasising that the system's design should take into account additional aspects such as the environment and the expected operational scenarios, the need to define clear purposes, and the presence of constraints. All the characteristics of SE are typically expressed through several concepts and principles, which are formally defined in standards such as the ISO/IEC/IEEE 15288, and applied through scientific, technological, and management methods, including practical suggestions, guidelines, and rules of thumb, known as SE heuristic, which offers easy access to SE knowledge, as well as structured approaches and frameworks [8, 7, 6, 9]. Moreover, to better clarify the meaning of the terms stakeholder, customer, and user, throughout the current thesis, a dedicated description has been added in Appendix A.

2.2 Model-Based Systems Engineering

So far, an introduction describing what SE is, along with its main characteristics, has been provided. Reminding that SE is an approach, a question should now arise: how can SE be applied?
There is neither a unique nor a correct answer to his question. However, in the current analysis, SE will be applied through the use of models of different natures, thus leveraging the Model-Based Systems Engineering (MBSE) approach, defined as:

The formalized application of modeling to support system requirements, design, analysis, verification, and validation activities beginning in the [concept stage] and continuing throughout development and later life cycle [stages].

A comprehensive theoretical description of MBSE can be found in the literature and will not be conducted here. However, an introduction to MBSE and to the elements

and characteristics that will be applied later throughout the analysis is proposed. To understand what MBSE is about, a comparison with document-based design is often proposed. Indeed, one of the main changes with respect to traditional approaches is the substitution of documents with models. Shifting to a model-based design involves transferring all the data and information, such as requirements, results from testing activities, and stand-alone numerical models, which were written in documents and papers, into models. In doing so, traceability must be assured throughout the whole life cycle. In addition, all selected stakeholders must have access to any necessary information, which must be unique. Thus, the concept of a *single source of truth* (SSoT) is introduced. In practice, the single source of truth can be a database, a shared repository, or the model itself, provided that all system artefacts are stored, maintained, and accessed in a consistent and traceable manner. MBSE will be applied using a top-down approach, starting from the macro-system and then decomposing it into subsystems and components [8, 7, 9].

In practice, to apply MBSE, it is essential to note that MBSE is built upon SE, serving as an application of SE through models. The tools, methodology, and language for applying SE through MBSE are referred to as *the three pillars*, and will be explored in the following sections. Considering the relevance and the large amount of data that has to be managed to properly apply MBSE, the *data management* can be added as a fourth pillar [6].

2.2.1 Methodology

From a conceptual perspective, defining the methodology involves answering two questions: what the design steps are, i.e., the *process*, and how they should be followed, i.e., the *method* [6]. In this sense, various methodologies exist, including the IBM Telelogic Harmony-SE, the INCOSE Object-Oriented Systems Engineering Method (OOSEM), the Rational Unified Process® (RUP®), the Vitech Model-Based System Engineering, the JPL State Analysis (SA), the Dassault MagicGrid, and several others [10]. As previously mentioned, the choice of a particular methodology can be based on several factors, or it may even be constrained by the company or the industrial application. In the current analysis, the V life cycle model has been selected, and a top-down approach will be followed. The Systems Modelling Language (SysML) will be utilised and described in the next section, while a black-box/white-box approach will be applied at each granularity level. This "SysML-

Based V-Model" MBSE methodology has been selected mainly due to industrial constraints, compliance with SE standards like the ISO/IEC/IEEE 15288 and with regulatory frameworks, ease of integration with and transition from traditional engineering processes in the aerospace field, and broad support from tools [6].

The V-model, as reported in Figure 2.1, describes the system life cycle, starting from the customer's need (top-left corner) and ending with system disposal (top-right corner). The actions to be performed are written in blue, and their sequence can be identified following the left branch of the V from top to bottom, and then moving upward along the right-hand branch (red arrows in Fig. 2.1). Indeed, requirements analysis, conceptual design, preliminary design, design synthesis, and testing and integration are the actions commonly followed during the design of a product. Moreover, proceeding along the same direction, the system granularity increases from system to subsystem and component levels. This particular V-model is designed to emphasise that interactions between stakeholders should be promoted throughout the entire life-cycle design, at any level of detail, as indicated by the horizontal arrows linking the left and right branches of the V. The last elements worth explaining are the yellow circular arrows that recur at any life-cycle stage, pointing out the recursive nature of the various phases. For instance, the requirements analysis is reported only once at the beginning of the diagram. However, requirements are continuously elicited for any system sub-system and components [7, 6, 9].
As can be inferred from the provided description of the V-model, selecting a specific methodology does not strongly constrain the design that will be performed. However, it can still be useful to have a baseline to follow.

2.2.2 Language

In the past, SE engineering was applied heavily, relying on documents, and information was mainly written in natural language in reports or documents, or accompanied by diagrams drawn without following specific rules, thus generating ambiguity, inconsistency, missing or scattered information, and a lack of traceability. These issues could easily get unmanageable, especially in large international companies where face-to-face dialogues are unfeasible and even the languages spoken become a barrier. The System Modelling Language brought a relevant paradigm change, introducing a series of diagrams, derived from the Unified Modelling Language (UML), that allow for the exchange of data through a shared language, facilitate

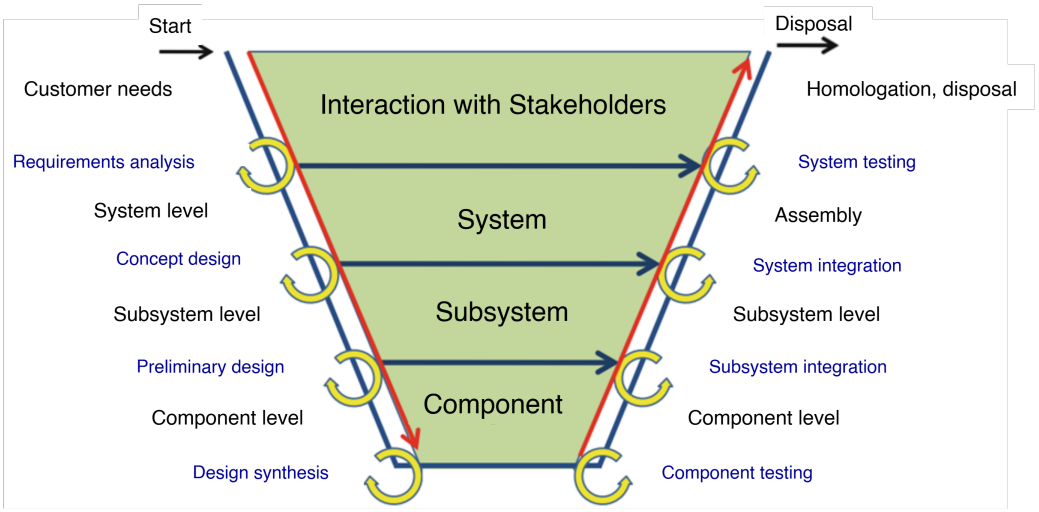

Fig. 2.1 System Engineering life-cycle V-model [6].

traceability, express information in a graphical form, and can be easily understood even by non-experts. Moreover, being explicitly tailored for SE, they are particularly suitable for describing the behaviour and structure of the system throughout the life cycle stages. They can be chained through allocation, are complementary, and can be reused or modified to deal with variants [11, 6, 9, 12].

Formally, SysML is expressed through nine diagrams classified into three groups (Fig. 2.2). As their names suggest, the *behaviour diagrams* describe the behaviour of the system, the *requirement diagram* collects all the requirements, and the *structure diagrams* describe the structures and architectures of the system. A description of each diagram is provided below. However, a better understanding of their usage will also be depicted when they are applied to the system under analysis in the following chapters.

Requirement diagram

Starting from the analysis of customers' needs, which must be translated into technical requirements, to the disposal phase, requirements have always been of paramount relevance, playing a key role in both engineering design and the formalisation of collaborations through legal contracts. In the requirements diagram (RD), all the requirements are collected and organised according to the established hierarchy. A

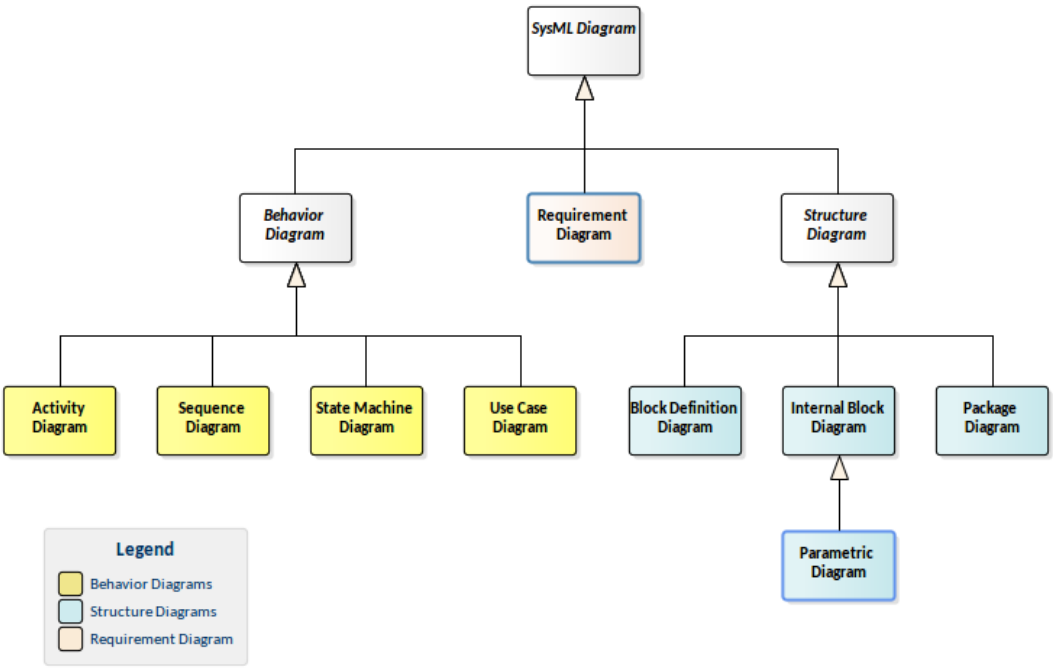

Fig. 2.2 Systems Modeling Language (SysML) diagrams taxonomy [13].

proper use of the RD ensures traceability covering the entire system life cycle, as well as the link to other views or elements. This is achieved by leveraging a set of predefined relationships: satisfy, verify, refine, derive, and trace.

Two examples of requirements diagrams have been reported in Figure 2.3 and Figure 2.4. Figure 2.3 shows a typical RD where the *requirement elements*, which are the frames containing the requirements, include the requirement in textual form, the requirement ID, and, eventually, the information describing the where the requirement was derived from (*derived*), how it is verified (*verify*), which are the elements providing further information to better describe it or deepening it (*refine*), how is is satisfied (*satisfy*), and, even if it is not shown, the element where to trace back the requirement (*trace*). These relationships can be contained in a unique box, as it is for the "All weather operation" requirement, or linked to external elements, as it is for the "Sensor Decision" requirement that is satisfied by the block "Camera". Also, the shapes of the connections between elements have a meaning. The line with a circle containing a cross that is linking the higher-level "Operating Environment" requirement to the two requirements below is a containment relation, meaning that the "All Weather Operation" and the "24/7 Operation" are contained inside the "Operating Environment" that, apart from being a requirements, it serves as a sot of

requirements container. This is done to organise requirements and define a hierarchy. The same information can be depicted from the requirements' IDs. Indeed, the high-level requirement ID is "S1", while those at a lower level are "S1.1" and "S1.2". However, the requirements diagram can also have a different structure (Fig. 2.4), es-

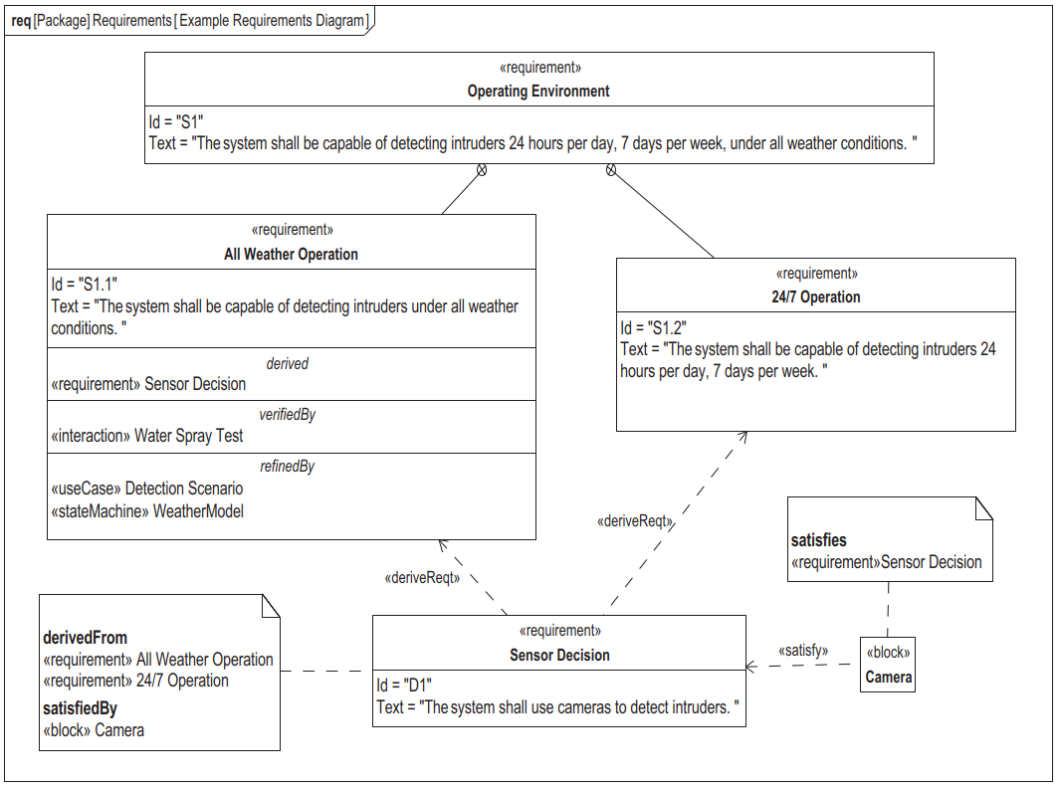

Fig. 2.3 Example of a general requirements diagram [12].

pecially when the model becomes large, making the use of a unique RD impractical, or when the design needs to focus on specific aspects without losing sight of the big picture. In this case, a more precise description of the "Start the process" use case is provided through a series of *refine* relationships which support the design during this specific use case, where it can be assumed that some users are involved and a particular procedure should be respected. Applying an analogous approach to all use cases, the system's description will be detailed for every scenario and application, ensuring a more manageable system design [6, 12].

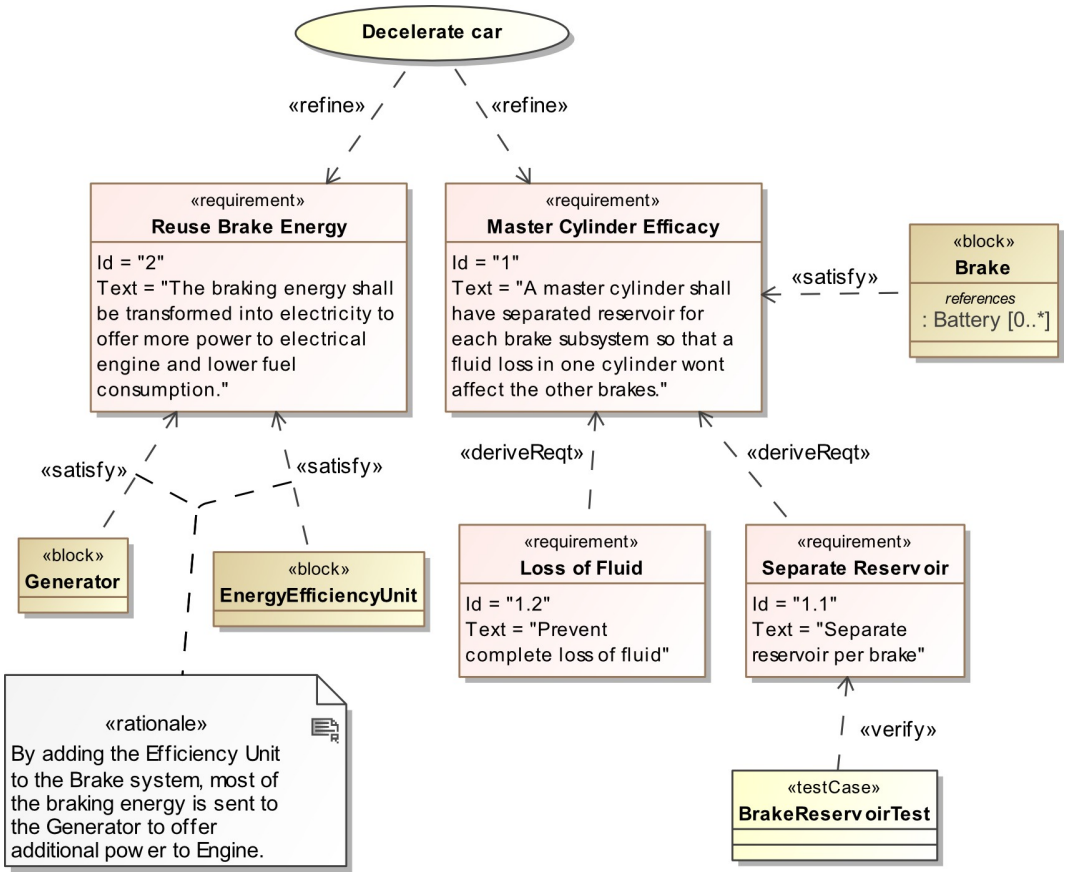

Fig. 2.4 Example of a requirements diagram [14].

Activity diagram

The activity diagram (AD) (Fig. 2.5) describes a sequence of actions emphasising the sequence and the triggering conditions. The activity starts from the filled dot (top centre in Fig 2.5). The first action ("lift of the rotor shaft") is performed given that the shaft is not unlocked ("[Shaft!=UNLOCKED]" condition). Then a *fork* is used to branch the activity into three *series* of *parallel* paths that must be conducted concurrently. The outputs of each action are compared to a reference value through a *decision node*, performing a *check*. Once all three tasks are performed and the decision nodes have been passed, the shaft starts rotating, the double concentric circle symbol is reached, and the activity is completed [6, 12].

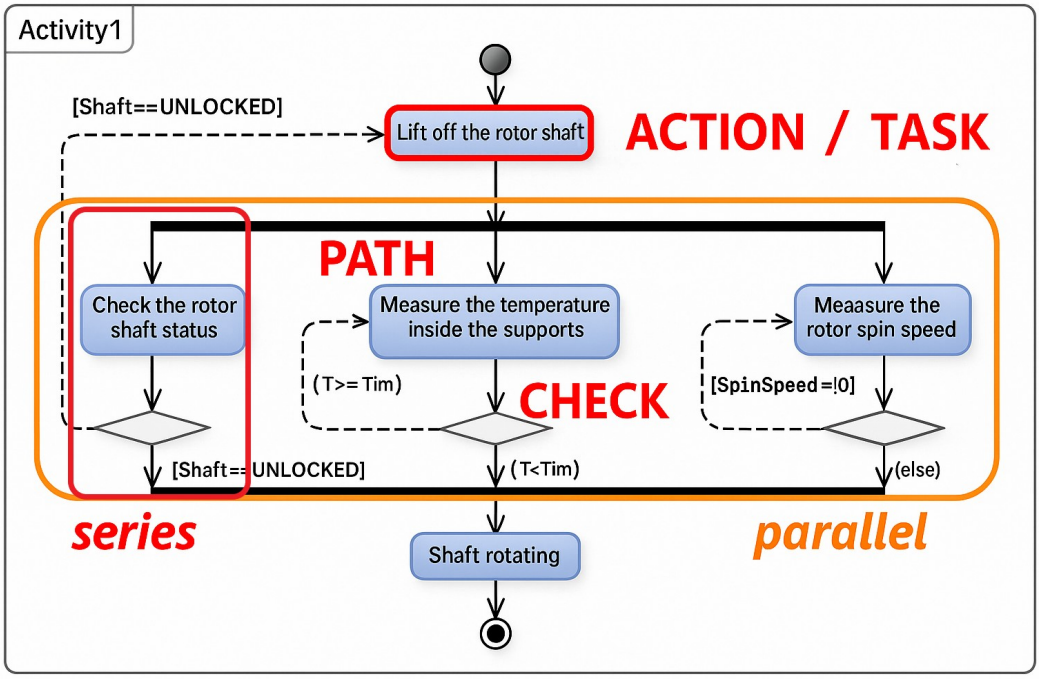

Fig. 2.5 SysML activity diagram [6].

Sequence diagram

In the sequence diagram (SD), the exchange of actions and messages between actors is described as a function of time. The diagram in Figure 2.6 describes the events applied in achieving the use case "Require suspension and rotation" (top-left in

the image), the stakeholders involved, which are each assigned to a vertical line, the ordered list of actions describing the use case (first column) that are performed according to the red "time" line. Even a frontier is present, highlighting the system's boundary. The horizontal arrows linking the vertical dashed lines of each stakeholder are also referred to as swim lanes because they should be followed moving back and forth according to the direction indicated by the arrowhead. So, the SD in Figure 2.6 should be read starting from the first action "Check the rotor" that is sent by the actor "Monitoring and emergency system" to the system, which sends back "Rotor info". The sequence then continues until the last event. Typically, swim lanes are represented by solid lines when they refer to an action, while dashed lines are used to describe an exchange of information, such as a message or feedback [6, 12].

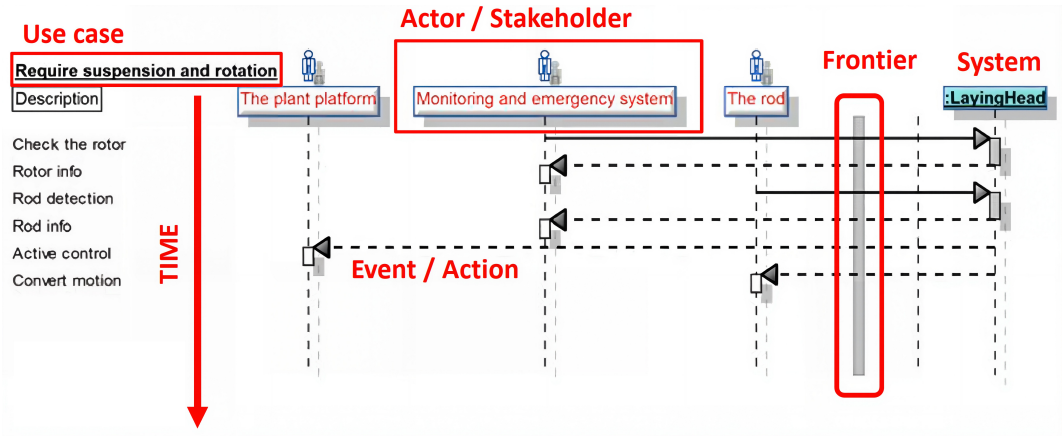

Fig. 2.6 SysML sequence diagram [6].

State machine diagram

The state machine diagram (SMD) is widely used in systems dynamic simulation. As highlighted in red in Figure 2.7, it describes the dynamics of a system transitioning from one state to another along a path, due to the occurrence of events. Analogously to activity diagrams, the starting and end points are represented as solid and half-empty dots. In the example provided, the initial state is "Rotor at standstill", once the rotor "levitate" event occurs, the system transitions to the "Rotor lift off" state. Actually, this includes two sub-states. Once that tuning operation is performed ("/Tuning") and the rotor is calibrated ("Rotor calibrated"), accelerating the rotor transitions the system to the next state ("Supercritical condition"), and so on. In

contrast to the diagrams previously described, the SMD highlights the events and states that the system must go through [6, 12].

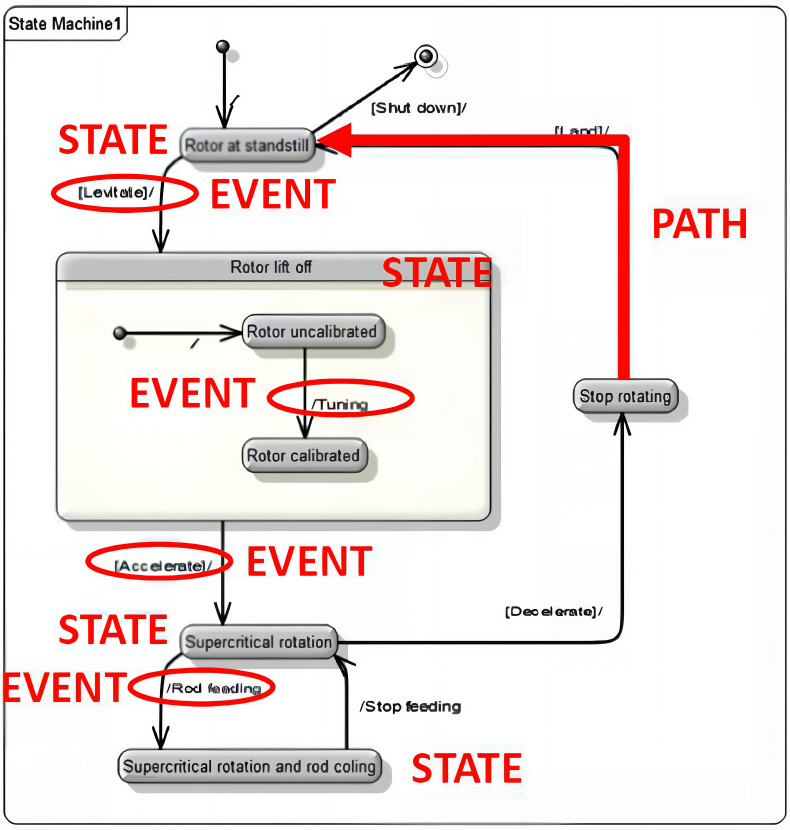

Fig. 2.7 SysML state machine diagram [6].

Use case diagram

A *use-case* is a description of the way someone could use a particular product or system in an effective way [15]. Starting from the definition of the term 'use-case', a use-case diagram (UCD) can be defined as a graphical representation of the interaction between stakeholders and the system, specifically concerning the system's usages, i.e., the use cases. In practice, observing the UCD, the actors involved during a specific system usage can be easily identified. In addition, the use cases can also be refined or decomposed, assigning links of specific types between them [6, 12].

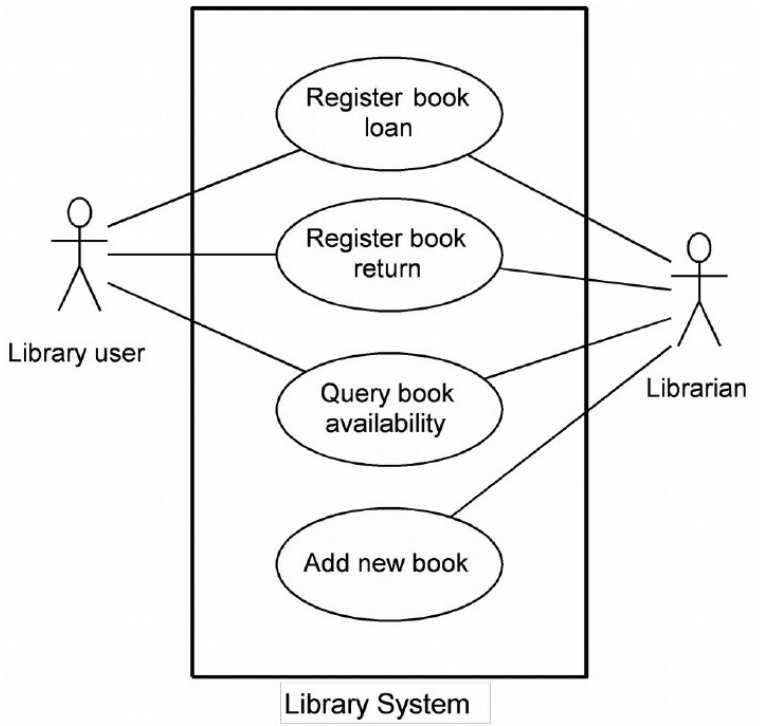

Fig. 2.8 SysML use case diagram [16].

Block definition diagram

The block definition diagram (BDD) (Fig. 2.9) is made of blocks, defining the system components and relations. It is typically used to show a decomposition of the system and describe its hierarchy. Moreover, it is also useful as a basis for other diagrams when the system's granularity increases. For instance, if the aircraft is the SoI, the engine will be a subsystem, and this relation will be set through a BDD. However, the engine will require an extended analysis, including many requirements and diagrams that can be traced back to the "engine" block, which, in this sense, becomes a sort of container for the engine lifecycle design artefacts [6, 12].

Internal block diagram

In contrast to the BDD, the internal block diagram (IBD) provides a white-box view of the system, detailing its internal elements, ports, and connectors. Following the previous example, to transition from the aircraft's black-box view to the engine, an IBD of the aircraft is required, which describes all the aircraft's internal subsystems

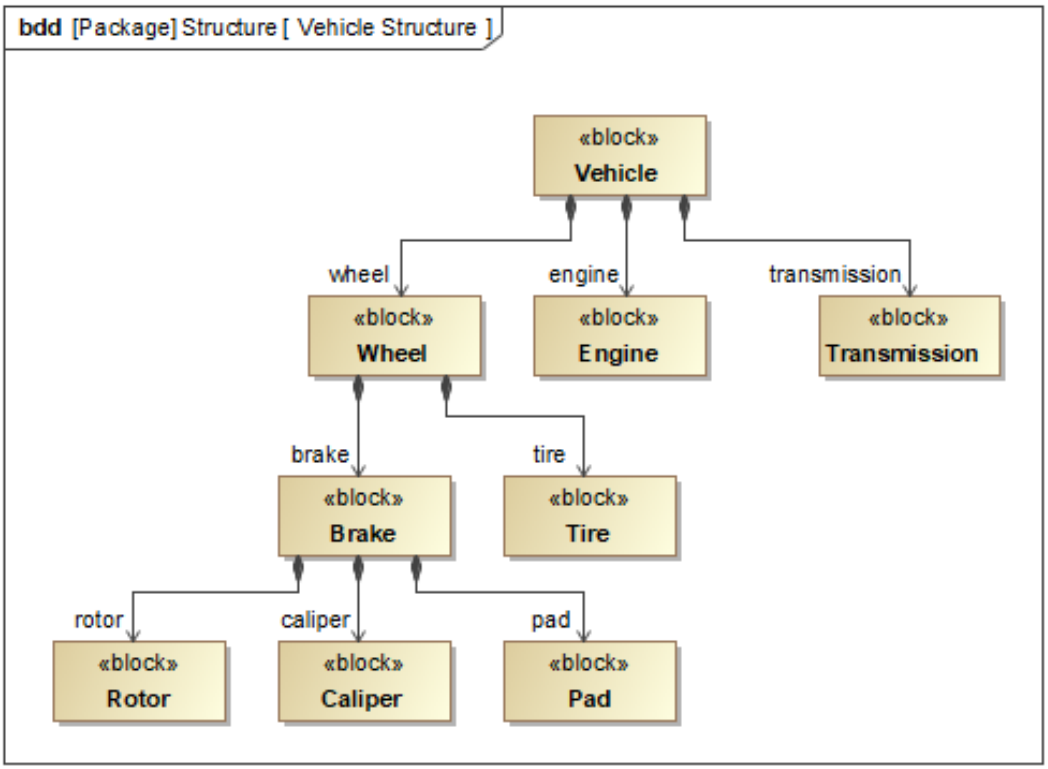

Fig. 2.9 SysML block definition diagram ([17]).

and components, including the engine block. Another example can be depicted from Figure 2.10, where the function "LayingHeadFunction" is explored, and three nested functions are identified. In addition, the IBD also specifies the flows between blocks, the connectors, the ports, specifying the direction in which they are meant to be traversed, as well as the actors involved [6, 12].

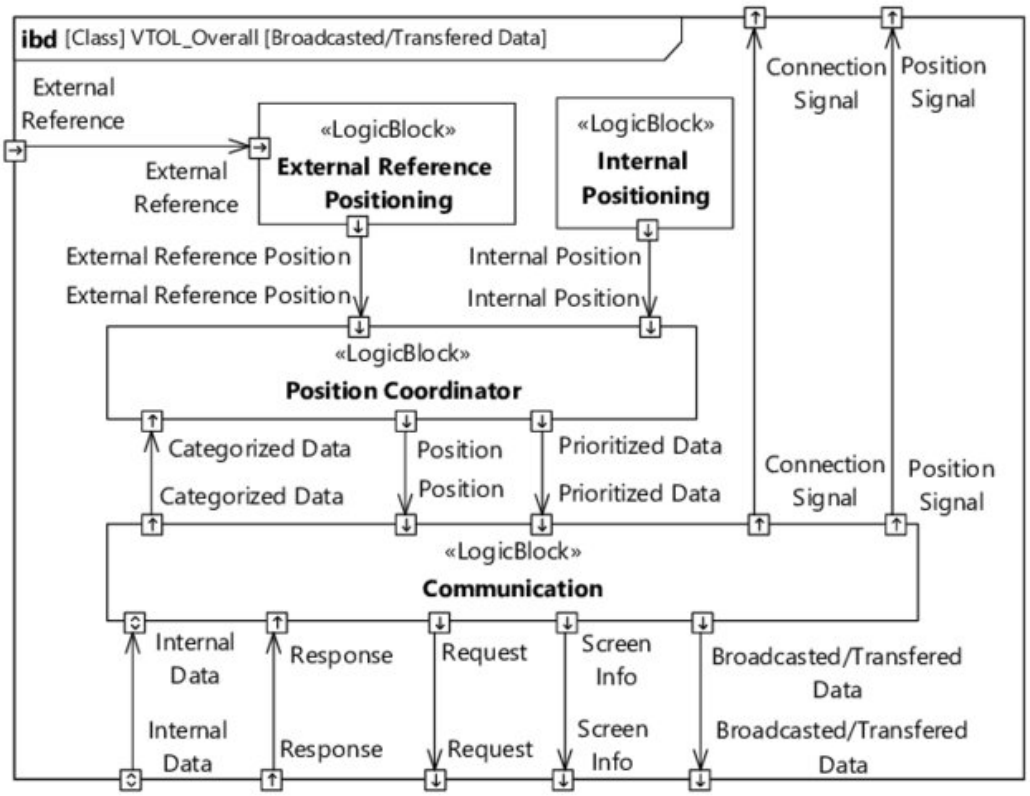

Fig. 2.10 SysML internal block diagram [18].

Parametric diagram

As can be seen from Figure 2.11, the parametric diagram (PMD) is a sort of IBD. It is the only diagram that includes formulas. Indeed, it should be used for preliminary calculations. However, there are more efficient software tools to perform calculations at different levels of detail, thus making PMDs impractical and poorly adopted [6, 12].

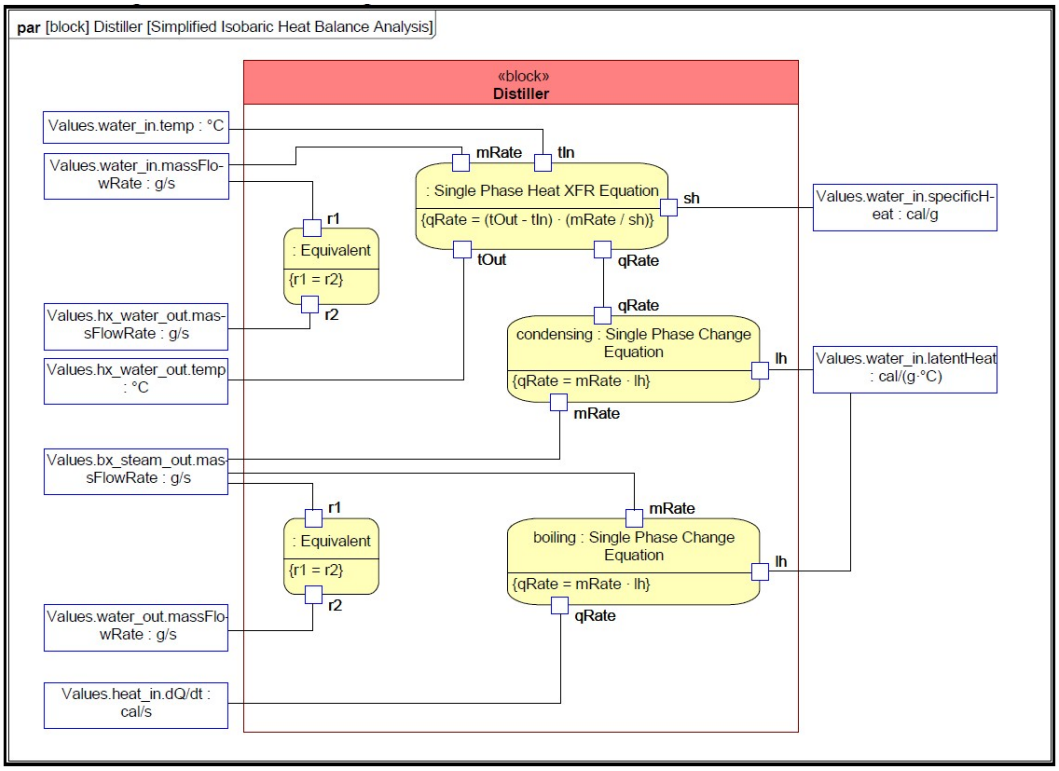

Fig. 2.11 SysML parametric diagram [19].

Package diagram

The package diagram is used to organise all the elements of the analysis into packages to structure large models and facilitate the reuse of artefacts. At first sight, looking at Figure 2.12, it might simply look like a sort of structured digital archive to be used in SE. However, it is fundamental to design a proper package structure because it resembles a top-level definition of the methodology to be implemented, apart from helping the engineers in separating the different layers and domains, and it can even mirror the internal organisation of the company, facilitating the integration among the design activities of different teams [6, 12].

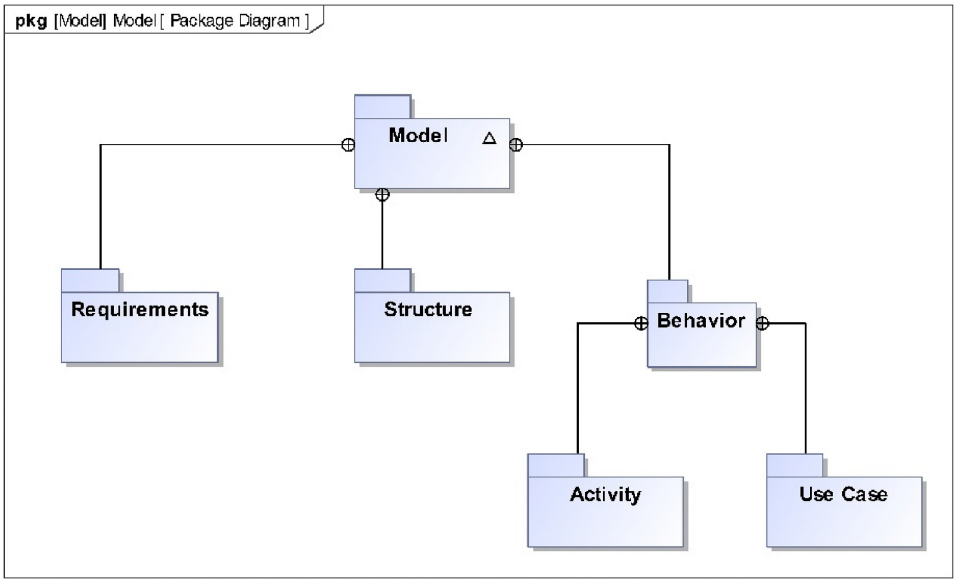

Fig. 2.12 SysML package diagram [20].

2.2.3 Tools

The tools commonly used can be classified into two main categories: theoretical tools and software tools. The former includes methodologies, guidelines, diagrams, and, in general, practical tools that help put the SE body of knowledge into practice [6]. The latter includes several software tools useful in different design phases. IBM Doors and Polarion are commonly used for requirements management, while IBM Rhapsody and Dassault No Magic (formerly Cameo System Modeler) are examples of software used for system modelling and architecture. Software used for simulation

or CAD, such as ANSYS Fluent or SOLIDWORKS, is typically not included among those used to apply MBSE. There are many more software programs available in the market besides the few mentioned here. However, as it will be shown in the following sections, the introduction of a new version of the System Modeling Language (SysML v2) is heavily affecting the software tools that have been used until now [6, 12].

2.3 New frontiers of SE: SysML v2

The next generation of the Systems Modeling Language, namely SysML v2, has been officially published in September 2025 as the result of years of development and collaboration between INCOSE and the Object Management Group (OMG) [21, 22]. Suitable standards and guidebooks are still under development, while the software tools implementing this new language have been released in beta versions. The version of the System Modelling Language used until now, SysML v1, was based on graphical elements derived from the UML that allow the drawing of the diagrams described above (Sec. 2.2.2). However, the diagrams generated, which are essentially images, can hardly be integrated with other software. A relevant paradigm shift is introduced with SysML v2, which is built as a coding language on top of what can be seen as the root language, the Kernel Modelling Language (KerML). However, this does not imply that the systems engineers who used to build SysML v1 diagrams will now need to code, because the new language can be used at different levels. This can be better depicted from Figure 2.13. The KerML is the foundation level os SysML v2, typically only software developers operate at that level to create new digital solutions. Systems engineers should be capable of operating at both the SysML and software tool levels, even if their previous experience can be directly applied to draw SysML diagrams using updated software tools, thus making the SysML v2 coding skills not strictly required. The advantages offered by SysML v2 will remain available, while many others are introduced. One of the leading innovations introduced is the SysML v2 application programming interface (API). In practice, the API is a tool enabling communication and data exchange among different software. Thus, the SysML v2 API should drastically enhance the interoperability of the language, allowing links between all the software used throughout the life cycle design. This enables a more agile and rigorous approach through the use of integrated software, resulting in a

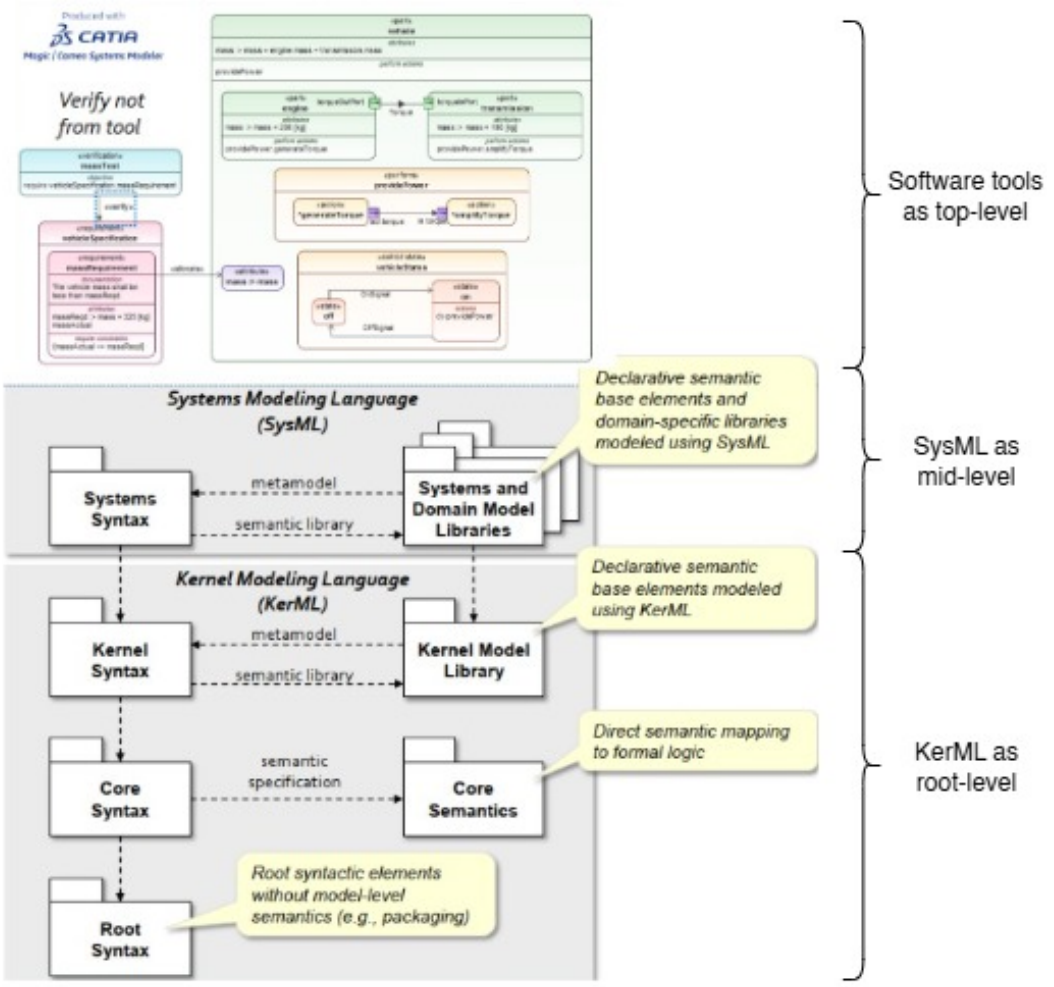

Fig. 2.13 SysML v2 levels and architecture (elaborated from [21, 23])

sort of digital design environment. Moreover, SysML v2 should enable more robust and flexible visualisations supporting the design and integration throughout all the life cycle phases [21, 22].

2.3.1 SysML v1 to v2 transition

The novelties introduced by SysML v2 are accompanied by significant changes that extend beyond the language itself. It is essential to remember that MBSE is built on three main pillars that must be taken into account. Moreover, in the so-called SysML v1 to v2 transition, a fourth important actor should be considered: people.

To better understand the magnitude of the transition, it can be helpful to divide it into two parts. The first focuses on technical aspects, while the second shows the approach to the transition at the managerial level.

From a technical point of view, the diagrams described in the previous section (Sec. 2.2.2) are conceptually unchanged. Variations in properties and attributes can be found in the literature. In the current study, changes in terminology have been reported to harmonise the following analysis and avoid confusion in the terms used (Fig. 2.14). Overall, the changes introduced should not considerably influence the

SysML v2	SysML v1
part / part def	part property / block
attribute / attribute def	value property / value type
port / port def	proxy port / interface block
action / action def	action / activity
state / state def	state / state machine
constraint / constraint def	constraint property / constraint block
requirement / requirement def	requirement
connection / connection def	connector / association block
view / view def	view

Fig. 2.14 SysML v1 and v2 terminology comparison [21]

way SysML diagrams have always been drawn. In fact, some aspects have been simplified, such as the types of ports (flow port, proxy port), which have been reduced to a single element, "port".

From a broad perspective, a transition strategy needs to be planned, which can be implemented through a practical project that engages multiple departments. This allows pursuing several activities. Concerning the language, the investigation of SysML v2 can be conducted, real case studies can be examined, and the potential and obstacles for the integration of SysML v2 into a specific company can be identified. Meanwhile, a market exploration of the existing tools can be done, and the possibility of collaborations and partnerships with tool vendors can be explored. In addition, mapping the tools available on the market helps the company in determining which software is worth developing and which ones are worth purchasing. Working on a project involving several departments results in advantages also from the point of view of the methodology. Indeed, within the same company, different approaches to applying MBSE often exist, which can also be in conflict. Thus, one of the first steps will be to assess the SE maturity within the organisation and map the methodologies adopted. A tool commonly used for this purpose is the Model-Based Enterprise Capabilities Matrix, but traditional surveys or other means of collecting feedback can also be very relevant, especially considering that shared consensus is crucial when relevant changes in the organisation have to be made. From a methodological perspective, the SysML v1 to v2 transition can be a very precious opportunity to align various approaches and foster cohesive collaboration across the organisation. Lastly, the company should carefully consider who must be involved. Once again, to gain different perspectives and obtain shared consensus, heterogeneous engineers and departments should collaborate on a common project. Additionally, the costs associated with training personnel should be considered, along with the number and roles of the individuals being trained [21, 22].

2.4 Why should industry apply MBSE?

As highlighted in Sec. 2.3.1, properly implementing SE and MBSE in an enterprise is not trivial. However, looking back at the origin of SE, one can be interested that this discipline was born and formalised from industrial contexts and, indeed, especially in sectors like aerospace and defence, specific processes and methodologies commonly adopted are already applying a SE approach. Several advantages have already been explored above. Nonetheless, quantifying such benefits from the economic point of view can be challenging. One of the most popular evidence of the economic advan-

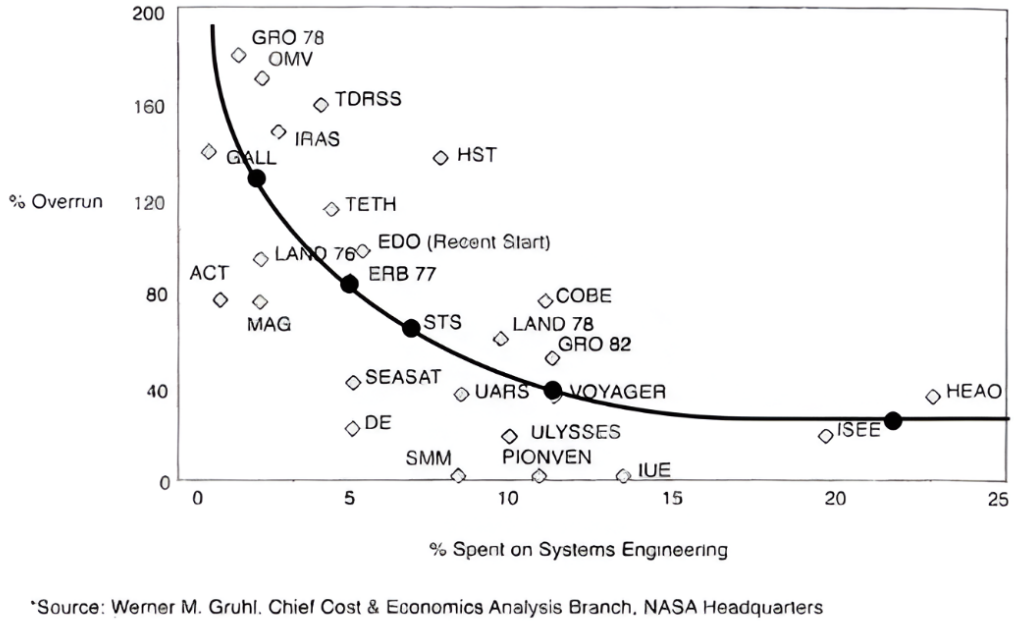

Fig. 2.15 Reduction in NASA projects' cost overruns compared to investments on SE [24].

tage of SE is published in the System Engineering Body of Knowledge (SEBoK) (Fig. 2.15 [24]. The curve reported in Figure 2.15 decreases until a value around 15% when it becomes horizontal. Actually, investing 7% to 12% of the project in SE and program management activities can avoid cost overruns accounting for 100% of the project budget. This can be approximately estimated in a return of ten times the investment [25]. Other studies set the optimal initial investment range in SE between 10% and 15% of the project budget [26].

Further industrial evidence of the benefits of implementing SE, the related tools, and even transitioning from SE to MBSE has also been published in the literature. The graph in Figure 2.16 describes the shift that Lockheed Martin performed transitioning from a document-based to an MBSE approach in the context of the Submarine Warfare Federated Tactical Systems (SWFTS) Systems Engineering & Integration (SE&I) program. The data collected refers to the years 2006-2013, even if major implementations in automation and baseline change request database (BCR), which could be seen as a sort of unique source of truth, have been made around 2007, the implementation of the requirements management tool (DOORS) dates back around 2009, while the transition to MBSE occurred in 2011. The yellow

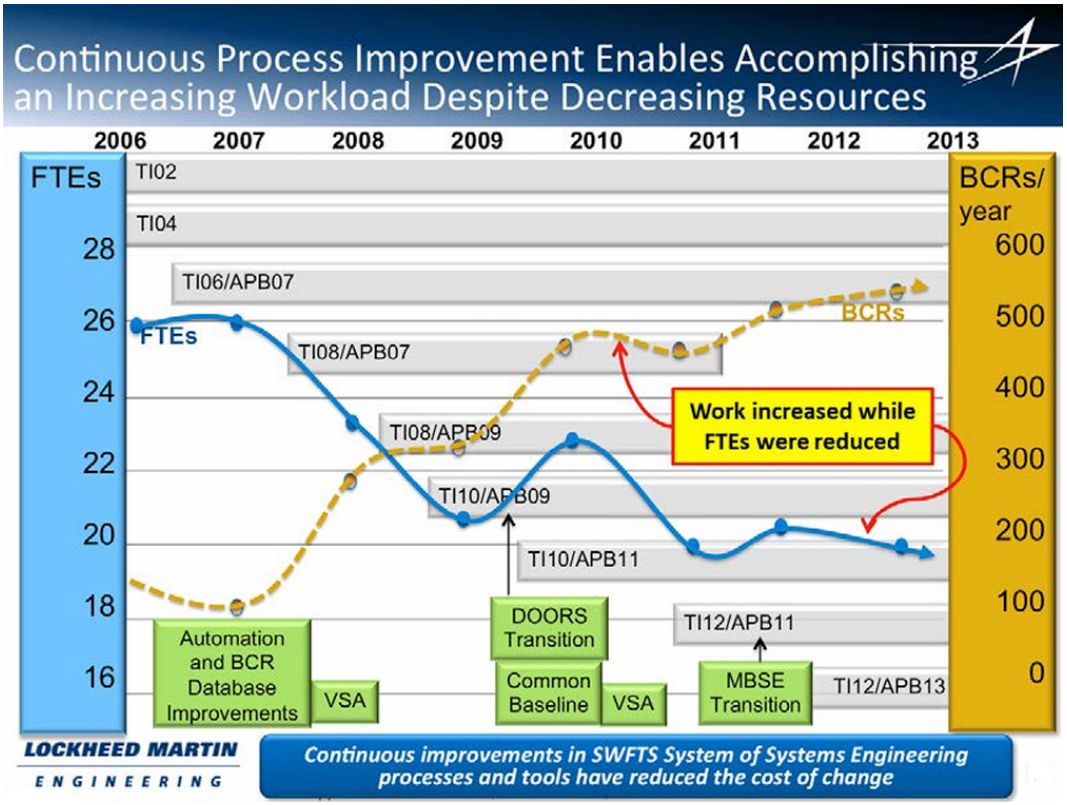

Fig. 2.16 Enter Caption [28]

dashed curve represents the project BCRs, which, as usual in long, complex projects, increase over time. The blue solid line, on the other hand, refers to the number of SE full-time equivalents (FTEs). In practical terms, the BCRs correspond to the workload, while FTEs are a unit of measurement used to describe the workload assigned to an individual employee. For instance, an FTE equal to one corresponds to work carried out by one person, typically on a forty-hour-per-week basis. From an operational standpoint, the curves indicate that a greater workload has been performed with fewer resources. Another is the trend that the FTEs curve assumes right after the DOOR and MBSE transitions. The increases in FTEs are due to a period of assessment, during which the changes are gradually implemented and the transition occurs. Such periods lasted for about one year for DOORS implementations and less than one year for MBSE transition [27, 28]. Apart from the difficulties in precisely quantifying the return on investment (ROI) in SE and MBSE, relevant economic advantages have been highlighted in the current section and can also be retrieved from the literature [29, 30, 31, 32, 33].

Chapter 3

Unmanned Aerial Vehicles: UAVs

3.1 Introduction

UAVs are pilotless aircraft, meaning there are no humans on board; however, it is worth providing additional information to establish a proper definition. The term "Unmanned" can be misleading since UAVs can be remotely operated up to a certain distance (i.e., range) without needing them to stay in view. Conversely, if any failure occurs, the UAV shall be able to return to the base autonomously or take corrective actions. Depending on its degree of automatic intelligence, the system demonstrates multiple operational capabilities, including real-time transmission of acquired data, monitoring of flight parameters such as position, velocity, and altitude, and environmental recognition of surrounding elements [34]. Actually, the capacity of a UAV to perform its task autonomously can be properly defined as the "degree of automation", and the more it is automated, the more the onboard computers take authority over the pilot [35]. In this context, it should be clarified that the term "autonomy" will be used hereafter to indicate the capability of the UAV to act without the need for human interaction, and not as the remaining operational duration, which in the case of UAV is the maximum flight time duration and is defined as "endurance" [36].

Among the numerous formal definitions presented in the literature, two have been identified by the authors as comprehensive and complete. The first one defines an Unmanned Vehicle as:

A powered vehicle that does not carry a human operator, can be operated autonomously or remotely, can be expendable or recoverable, and can carry a lethal or nonlethal payload. Ballistic or semi-ballistic vehicles, cruise missiles, artillery projectiles, torpedoes, mines, satellites, and unattended sensors (with no form of propulsion) are not considered unmanned vehicles. Unmanned vehicles are the primary component of unmanned systems.

U.S. Department of Defense. Office of the Secretary of Defense (2007)

Instead, the UAS has been described by EASA with reference to the elements composing its architecture:

An Unmanned Aircraft System (UAS) comprises individual system elements consisting of an "unmanned aircraft", the "control station" and any other system elements necessary to enable flight, i.e. "command and control link" and "launch and recovery elements". There may be multiple control stations, command & control links and launch and recovery elements within a UAS.

European Aviation Safety Agency (2009)

The description provided by the U.S. Department of Defence (U.S. DoD) is particularly interesting because it also delineates what is not a UAV, while the second clarifies the relationship between the UAS and the UAV [36]. UAVs are utilised in a wide range of both military and civilian applications. In the past, suitable applications were identified in the so-called dull, dirty, or dangerous (DDD) roles. Over time, the applications have expanded to include covert, diplomatic, research, and other roles [34]. According to the U.S. DoD, UAVs are promising candidates for missions such as aerial refuelling, electronic warfare, and battle management, which are typically conducted by crewed aircraft [37]. Research and development activities, together with civilian industrial applications, are also of great interest. Companies in the energy, telecommunications, and construction sectors can employ UAVs for monitoring the structural health of gas pipelines, telecommunications lines, bridges, and buildings under construction. In the context of research, for example, the University of Kansas measured the ice thickness at the North Pole using a UAV [38].

The large variety of applications requires different types of UAVs, which can be subdivided according to various criteria. One of the most common classification methods for UAVs is that proposed by NATO, which is primarily based on size, altitude, and endurance capabilities, as reported in Table 3.1.

Table 3.1 UAV classification according to NATO [39].

Class	Category	Nominal operating altitude	Normal mission radius
Class I (<150 kg)	Small >20 kg	Up to 5,000 ft AGL	50 km (LOS)
	Mini 2–20 kg	Up to 3,000 ft AGL	25 km (LOS)
	Micro <2 kg	Up to 200 ft AGL	5 km (LOS)
Class II (150–600 kg)	Tactical	Up to 10,000 ft AGL	200 km (LOS)
Class III (>600 kg)	HALE	Up to 65,000 ft AGL	Unlimited (BLOS)
	MALE	Up to 45,000 ft AGL	Unlimited (BLOS)

Looking at Table 3.1, the main characteristics can be immediately depicted. The three classes of UAVs primarily divide into three categories based on their gross take-off weight (GTOW). Typically, Class I includes the majority of UAVs used in civil applications, including those that can be purchased even in shops or on e-commerce websites. Class II and Class III enclose larger UAVs mainly used in research, industrial, or military applications. The nominal operating altitude ranges from approximately 70 m (200 ft) up to 20 km (65 000 ft). In the 'Nominal mission radius' column, a number is specified only for those UAVs that should remain in the Line Of Sight (LOS) to be controlled. In this case, the communication between the control system and the aircraft is typically based on direct radio communication. On the contrary, Class III UAVs have an unlimited radius because their communication system relies on satellite technology.

Despite its widespread use in the literature, the classification proposed by NATO in the table was introduced over 15 years ago and has certain limitations. Indeed, in the literature, numerous classifications can be found based on roles, applicable standards, military applications, wing types and configurations, degree of autonomy, and ownership. However, a comprehensive discussion goes beyond the scope of this study; therefore, the two categories, MALE and HALE, have already been selected in accordance with the needs expressed by Leonardo S.p.A., and will be explored in the following sections [36].

3.1.1 HALE UAVs

High altitude long endurance (HALE) UAVs typically operate at an altitude above 15 km (approximately 50 000 ft) and their endurance can exceed 24 hours. HALE UAVs are designed to fly in the stratosphere, where the environmental conditions are more stable. Their design is optimised for such conditions, allowing long endurance capabilities; indeed, they can even perform trans-global ISR missions. Flying at such an altitude allows for the performance of surveillance operations over a very wide area. They are among the largest UAVs and can carry a significant payload for applications spanning from military to telecommunications and environmental monitoring [40, 34].

The availability of technical data related to HALE UAVs in the literature is quite limited, sparse, and often incomplete. In Table 3.2, six HALE UAV models are reported together with their producers, nationalities, and roles. In Table 3.4 and Table 3.6, the dimensions and performance are collected. From Table 3.2 it can be noted that, even though their roles are expressed in slightly different ways, they all perform surveillance and combat operations. Despite their similar roles, their characteristics differ significantly, and this could be due to unverified data. The RQ-4 Global Hawk is considerably larger, especially compared to the Sharp Sword, which is primarily designed for combat roles and stealth capabilities, as is the CH-7.

Table 3.2 HALE UAV models (elaborated from [39, 41]).

Producer	Nationality	Model/Name	Role
Baykar	Turkey	Bayraktar Akıncı	Long-endurance strike
CASC	China	CH-6	High-altitude strike
CASC	China	CH-7	UCAV Stealth
Northrop Grumman	USA	RQ-4 Global Hawk	High-altitude ISR
Hongdu Aviation Industry Group	China	Sharp Sword	UCAV Stealth
Chengdu Aircraft Industry Group	China	Cloud Shadow	HALE ISR

Table 3.4 HALE UAV dimensions (elaborated from [39, 41, 42].

Model/Name	Length (m)	Wingspan (m)	Height (m)
Bayraktar Akıncı	12.2	20	N/A
CH-6	15.8	20.5	N/A
CH-7	10	22	3.5
RQ-4 Global Hawk	14.5	39.9	4.7
Sharp Sword	12.2	14.4	2.7
Cloud Shadow	9.0	20	3.66

Table 3.6 HALE UAV performances (elaborated from [39, 41].

Model/Name	MTOW (kg)	Payload (kg)	Max speed (knots)	Cruise speed (knots)	Range (km)	Endurance (hours)
Bayraktar Akıncı	5500	1350	90		7500	24
CH-6	7800	1700	N/A	N/A	N/A	18
CH-7	4000	2000	600	480	1500	15
RQ-4 Global Hawk	14628	1360	340	310	22780	34
Sharp Sword	20215	2000	1111	N/A	926	48
Cloud Shadow	3000	400	335	N/A	290	6

Northrop Grumman RQ-4 Global Hawk

Among the HALE UAVs mentioned in the current sections, the Northrop Grumman RQ-4A Global Hawk is widely recognised and renowned in the literature (Fig. 3.1). It is primarily designed to provide continuous reconnaissance and surveillance over a wide area, regardless of the weather and light conditions. It took its first flight in 1998 and has since successfully conducted both military and scientific research operations. For instance, the Global Hawk conducted 11 maritime surveillance missions during its deployment in Australia, but also supported NASA in hurricane monitoring and atmospheric analyses [43, 44]. In 2001, it was the first UAV to cross the Pacific Ocean, and it registered the longest flight of 13 840 km performed by a full-scale, jet-powered UAV.

For the purpose of the current analysis, it can be useful to identify the UAV's fuel capacity so as to have a preliminary estimate of the energy available onboard and, through basic formulas, compute the equivalent energy amount in terms of hydrogen. Different versions of the Global Hawk RQ-4 have been manufactured. The main changes relied on the payload capacities and other improvements implemented to meet the needs of different missions. The three most famous variants are the RQ-4A, the first produced, its direct upgraded version, the RQ-4B, and the naval variant for maritime surveillance, the MQ-4C Triton. With respect to the RQ-4A, the improved RQ-4B has longer wings and a nose allowing it to carry a heavier payload. In contrast, the MQ-4C Triton has a reinforced structure for improved weather resistance and slightly modified wings for steeper ascending and descending maneuvers [45]. However, for the purpose of the current analysis, estimates of the fuel capacity and the average and maximum fuel consumption are needed. Therefore, the following analysis will focus solely on these aspects related to the main variants of the Global Hawk: RQ-4A and RQ-4B.

The Global Hawk RQ-4A has a fuel capacity of 17 300 punds (7847 kg), while the RQ-4B carries 6500 kg of fuel, correspond approximately to 45% of its GTOW [46]. It is powered by a single Rolls Royce F137-RR-100 turbofan engine capable of generating a maximum thrust around 34 kN and has a specific fuel consumption (SPF) of 0.39 lb/lbfhr (10 g/(kNs)) at take-off, and 0.65 lb/lbfhr (18 g/(kNs)) at cruise speed (Mach 0.8 at 35 000 ft [38, 47, 48, 49]). However, as a first attempt, an average fuel consumption could be computed by dividing the total amount of fuel by the flight duration, but this would neglect a few basic assumptions that are

worth considering. Hence, more detailed data are provided in the following section (Sec. 3.1.3), where a more comprehensive description will be presented.

Fig. 3.1 NASA - Northrop Grumman RQ-4A Global Hawk [50].

3.1.2 MALE UAVs

Analogously to what has been discussed about HALE UAVs in Sec. 3.1.1, here the main characteristics of Medium Altitude Long Endurance (MALE) UAVs are investigated. Typically, MALE UAVs operate at an altitude between 5000 m and 15 000 m, their ranges are more limited compared to HALE UAVs, and their endurance is around 24 h, even though MALE UAVs are operated from fixed on-ground bases [34]. A general idea of the difference in the use between HALE and MALE UAVs can be summarised according to their difference in classification. MALE UAVs are tactical, also defined as "boots-on-the-ground" assets, meaning they are used in real-time battlefield surveillance and intervention, target acquisition and direct support to ground forces. Conversely, HALE UAVs are strategic UAVs and their role can be summarised as "eyes-in-the-sky for high-level decision-makers". Indeed, they can monitor extended geographical regions, and they are typically integrated into broader defence networks and operated by national-level commands [51, 52, 36].

After an extended review of the literature, a considerable amount of MALE UAVs' technical data has been collected in Tables. 3.8, 3.9, 3.11, and 3.13. As can be seen from Table 3.8 and Table 3.9, many countries are directly manufacturing MALE UAVs, all of which are intended to cover roles related to ISR. The dimensions are smaller than HALE UAVs (Table 3.11), and overall, the performances are lower as well as their associated costs [38].

Considering the significant number of male UAVs taken into account, it has been possible to identify some outliers with characteristics that were too far from the average trend. The deviations in the properties typical of MALE UAVs have been attributed both to the fact that specific UAVs are classified as MALE even though they are designed prioritising specific capabilities, such as the P.1HH HAMMERHEAD by Piaggio Aerospace and the Avenger by GA-ASI which have a maximum speed much higher than the others, and to the un-verified nature of this data that, being classified, is often manipulated before publication, as it could be for the CH-4 and CH-5 manufactured by CASIC that have an endurance of 40 h and 60 h, respectively. Thus, a selected number of models have been reported in Figure 3.2. These UAVs have an MTOW between 500 kg and 1400 kg, an endurance between 20 h and 30 h, and a maximum speed ranging between 50 kn and 180 kn.

Table 3.8 MALE UAV models [41].

Producer	Nationality	Model Name
DRDO	India	Archer-NG
Aeronautics Defense Systems	Israel	Dominator
TAI	Turkey	Anka
Airbus Defence & Space	Spain	Atlante
Stella tecnologia	Brazil	Atobá Tactical UAS
GA-ASI	USA	Avenger
Denel Dynamics	South Africa	Bateleur
Baykar	Turkey	Bayraktar TB2
Aurora Flight Sciences	USA	Centaur
CASIC	China	CH-4
CASIC	China	CH-5
China Academy of Aerospace Aerodynamics	China	CH-6
Carbon Fiber Technologies	Greece	DELAER RX-3

(CFT)		
DRDO	India	DRDO Rustom H
IAI	Israel	Eitan
Airbus Defence & Space	EU	Eurodrone
Leonardo	Italy	Falco Xplorer
Northrop Grumman	USA	Firebird
General Atomics	USA	Grey Eagle
HAI	Greece	HCUAV
Elbit Systems	Israel	Hermes 450
Elbit Systems	Israel	Hermes 900
IAI	Israel	Heron
BAE Systems	UK	HERTI
HESA	Iran	IAIO Fotros
Kronstadt Group	Russia	Kronshtadt Orion
KAL	South Korea	KUS-FS
BAE Systems	UK	Mantis
INTA	Spain	Milano
Milkor	South Africa	Milkor 380
Qods Aviation	Iran	Mohajer-6
Industry Company		
GA-ASI	USA	MQ-1 Predator
GA-ASI	USA	MQ-9 Reaper
Piaggio Aerospace	Italy	P.1HH HAMMERHEAD
HAI	Greece	Pegasus II
IAI	Israel	Searcher III
Denel Dynamics	South Africa	Seeker 400
HESA	Iran	Shahed 129
EADS and TAI	Europe/Turkey	Talarion
ADE	India	TAPAS-BH-201
Adcom Systems	UAE	United 40
Yabhon	UAE	United 40
Lentatek	Turkey	Vestel Karayel
Thales	UK	Watchkeeper WK450
Chengdu Aircraft Industry Group	China	Wing Loong I
Chengdu Aircraft Industry Group	China	Wing Loong II

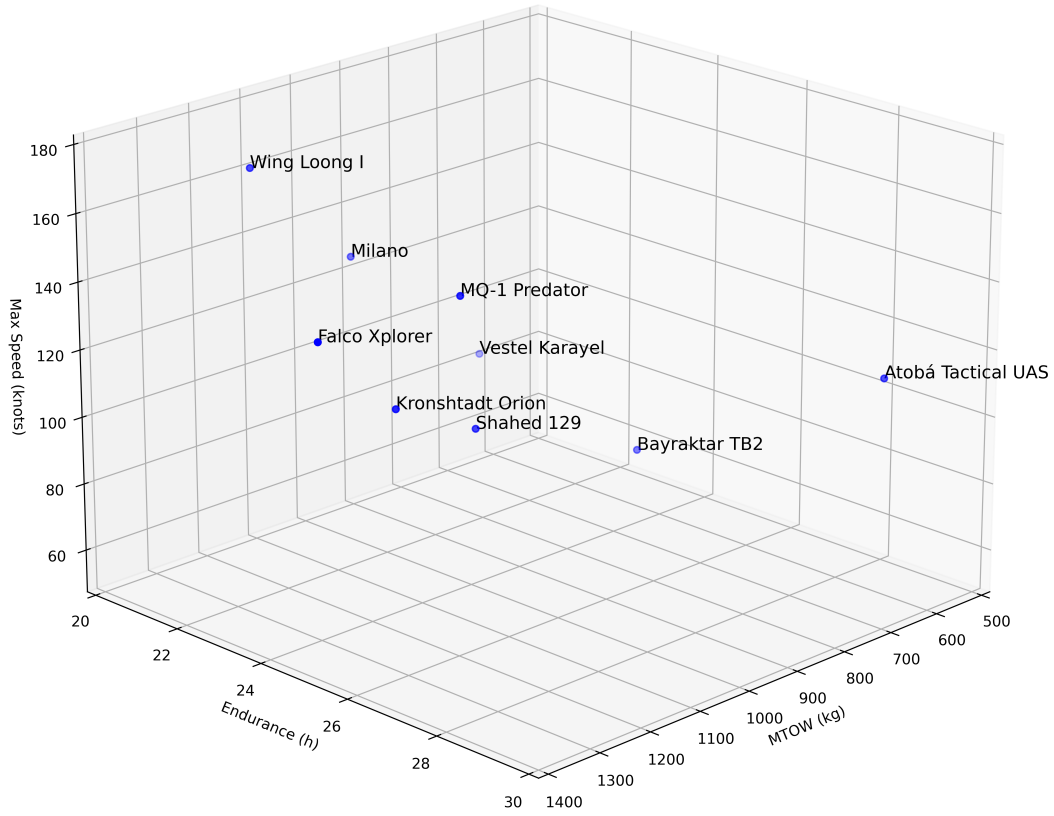

Fig. 3.2 Comparison between MALE UAVs limited to the following ranges: MTOW (500, 1400 kg), Endurance (20, 30 hours), Speed (50, 180 knots).

Table 3.9 MALE UAV roles [41].

Model/Name	Role
Atlante	Civil airspace operations
Avenger	ISR and strike
Bayraktar TB2	ISR and strike
Centaur	ISR and sensor-carrying aircraft
CH-4	ISR and strike
CH-5	ISR and strike
CH-6	ISR and strike
Eitan	ISR
Eurodrone	ISTAR missions
Falco Xplorer	ISR and targeting
Grey Eagle	ISR and precision strike
Hermes 450	ISR
Hermes 900	ISR and support
Heron	ISR
HERTI	ISR and reconnaissance
IAIO Fotros	ISR
Mantis	Surveillance and strike
MQ-1 Predator	ISR and strike
MQ-9 Reaper	ISR and strike
Searcher III	ISR and target acquisition
Seeker 400	ISR
Shahed 129	Reconnaissance / Light attack
United 40	Persistent surveillance
Watchkeeper WK450	ISR and target acquisition
Wing Loong I	ISR and strike
Wing Loong II	Multi-role ISR

Table 3.11 MALE UAV dimensions [41].

Model/Name	Length (m)	Wingspan (m)	Height (m)
Aeronautics Defense Dominator	8.00	13.42	
Atlante	5.47	8.00	1.99
Avenger	13.3	20.1	4.4
Bayraktar TB2	6.5	12.0	2.2
Centaur	8.5	13.4	2.5
CH-4	8.5	18.0	2.6
CH-5	10.0	21.0	3.1
CH-6	15.00	20.00	
DELAER RX-3	4.15	7.20	
Eitan	14.0	26.0	3.8
Eurodrone	16.0	30.0	6.0
Falco Xplorer	9.0	18.0	
Grey Eagle	8.0	17.0	2.1
HCUAV	4.0	6.4	
Hermes 450	6.1	10.5	1.8
Hermes 900	8.3	15.0	2.0
Heron	8.5	16.6	1.6
HERTI	3.5	8.5	
Kronshtadt Orion	8.0	16.0	
Mantis	11.0	20.0	
Milano	8.2	12.5	
Milkor 380	9.0	18.0	
Mohajer-6	7.50	10.00	
MQ-1 Predator	8.2	14.8	2.1
MQ-9 Reaper	11.0	20.1	3.6
P.1HH HAMMERHEAD	14.4	15.6	
Searcher III	5.8	8.5	1.5
Seeker 400	4.2	8.5	1.0
Shahed 129	8.0	16.0	
Talarion	10.0	28.0	3.5
TAPAS-BH-201	9.5	20.6	
United 40	11.1	17.5	4.4
Vestel Karayel	6.5	10.5	
Watchkeeper WK450	6.1	10.5	1.8
Wing Loong I	9.0	14.0	2.7
Wing Loong II	11.0	20.5	4.1

Table 3.13 MALE UAV performances [41].

Model/Name	MTOW (kg)	Payload (kg)	Max speed (knots)	Cruise speed (knots)	Range (km)	Endurance (hours)
Anka	1700		117		5000	30
Atlante	570	100	108	73	400	10
Atobá Tactical UAS	500	150	103	65		28
Avenger	8380	2948	460	350	926	18
Bateleur	1000		135		750	24
TB2	650	55	70		300	24
Centaur	1999	363	175	150	3700	24
CH-4	1330	350	180	150	2500	40
CH-5	3300	1200	220	180	2500	60
CH-6	7800	500	240	200	7000	20
DELAER RX-3	190	50	130	97		10
DRDO Rustom H	720		81		350	24
Eitan	5400	1000	220	180	1000	36
Eurodrone	11000	2300	270			40
Falco Xplorer	1300	350	135	115	1800	24
Grey Eagle	1450	360	150	120	2500	25
HCUAV	185	35	103	86		11
Hermes 450	450	180	95	80	300	20
Hermes 900	1180	350	120	90	1000	36
Heron	1250	250	130	110	1000	52
HERTI	170	50	70	60	150	24
IAIO Fotros	3500		216		2000	30
Kronshtadt Orion	1150	250	108	65		24
Mantis	9500	1500	278	240	1000	36
Milano	900	150	124			20
Milkor 380	1300	220	135	70		35
Mohajer-6	670	150	108	70	2000	12
MQ-1 Predator	1020	204	135	115	1110	24
MQ-9 Reaper	4760	1700	240	200	1852	27
P.1HH	6146	272	395	135		16
Searcher III	436	100	110	90	200	18
Seeker 400	550	100	150	120	300	16
Shahed 129	990	400	94	81	300	24
Talarion	10000	800	340		1700	20
TAPAS-BH-201	1800	350	121	94	1000	18
United 40	1000	100	108	108		25
Vestel Karayel	630		81			20
WK450	450	150	85	70	150	16
Wing Loong I	1100	200	160	130	4000	20
Wing Loong II	4200	480	140	100	6000	32

Fig. 3.3 General Atomics MQ-1 Predator MALE UAV [60].

Predator

Among the various UAVs, the MQ-1 Predator by General Atomics exhibit balanced performances (FIg. 3.2). Moreover, it is historically one of the most relevant MALE UAVs. Since its debut in 1995 during the conflicts in Bosnia, it has been widely used for both passive roles, such as surveillance and monitoring, and active roles thanks to its ability to detect and track moving targets, that, at that time, represented a relevant technological asset [53, 54]. It became the symbol of the American presence in the Middle East during operations in Iraq, Afghanistan, Syria, and Pakistan, and it represents a benchmark for all the MALE UAVs [38]. Due to its historical relevance to to the considerable amount of technical data that can be retrieved from the literature, the MQ-1 Predator will be considered as a baseline also in the current analysis.

To the purpose of the current analysis, only data related to the fuel capacity and the fuel consumption will be further investigated. The MQ-1 Predator has a fuel capacity of approximately 300 kg (665 lb) [55, 56]. To estimate the fuel consumption, information about the engine has been collected. The MQ-1 Predator is equipped with a four-stroke turbocharged engine manufactured by Rotax [57]. This engine is designed to maintain relevant performances even at high altitudes. It can deliver a maximum power of 84 kW (115 hp) at 5800 rpm for maximum 5 min, and 73 kW (100 hp) of continuos power [58]. The maximum fuel consumption for the Rotax 914 during take-off is around $33\,\mathrm{L\,h^{-1}}$, corresponding to $6.76\,\mathrm{g\,s^{-1}}$ [59]. Assuming a 10% fuel reserve, as it has been done for the Global Hawk in Sec. 3.1.1, the resulting amount of usable fuel is 270 kg. This will be the starting point to estimate the fuel consumptions throughout the mission profile phases, that will be performed in Sec. 3.1.3.

3.1.3 Class III UAVs mission

To perform the static and dynamic design of the H_2SDSys two main information are needed: the tank fuel capacity, and the value of the fuel mass flow rate throughout the mission profile, also referred to as fuel consumption profile. In the previous sections, the fuel capacities of the two aircraft selected as baselines were reported. Here, a typical flight mission profile will be delineated together with the fuel consumed in each time phase. It must be specified that both the static and dynamic sizing are performed at a preliminary level under the assumption that all the other power-train's components, like the engine and the transmission system's elements, hold the same properties and the same efficiencies of the "traditional" powertrains. This assumption will allow to convert the capacity and the mass flow rate referred to the traditional fuels into those referred to hydrogen only correlating the energy content of the fuels.

The starting point to estimate the fuel consumption throughout the whole mission profile is the data collected in the two sections dedicated to the RQ-4 Global Hawk (Sec. 3.1.1) and to the MQ-1 Predator (Sec. 3.1.2). In the case of the Global Hawk, the specific fuel consumption refers to the engine mounted on the RQ-4A model version and, accordingly, that model's fuel capacity will be considered. In the first step, a fuel reserve margin of 10% has been considered, thereby reducing the total fuel capacity to the available fuel. The data useful for the following calculations, which have been mentioned in the previous sections, have been grouped in Table 3.15.

Table 3.15 MQ-1 Predator and RQ-4A Global Hawk nominal fuel capacity and consumption.

		MQ-1 Predator	RQ-4A Global Hawk
Total fuel capacity	(kg)	300	7847
Total fuel available	(kg)	270	7062.3
Nominal Endurance	(h)	24	34

To move from this initial set of data to a more detailed fuel consumption profile, the fraction of time of each flight phase with respect to the total endurance has been elaborated through research in the literature. The UAV endurance, i.e. the total flying time per mission, has been divided into five phases: take-off & climb, cruise ingress, loiter, cruise egress, and descent & landing. However, due to the nature of cryogenic hydrogen storage, it is also necessary to consider the time that elapses between the end of the refuelling phase and the beginning of take-off. This interval has been

further subdivided into two phases: the post-refuelling and the ground idle & taxiing. During the post-refuelling the tank is filled at its maximum capacity and no hydrogen is extracted, while in the ground idle & taxiing a reduced amount of hydrogen is extracted. The ground idle & taxiing has been estimated to last for 25 minutes. Considering that both the UAVs belong to Class III they should undergo similar on-ground operations before flight, so the ground idle & taxiing has been assumed equal [61]. However, considering that the fuel consumption is minimum in idle, and that the ground idle & taxiing phase duration represents less than 2% compared to the total flight duration, this phase has been neglected from the calculations of the total fuel consumed to enable comparison of results with data available in the literature. Nonetheless, it will be taken into account when analysing the H_2SDSys dynamic behaviour. On the contrary, the duration of the post-refuelling phase will be investigated through a detailed dynamic analysis in the following chapters.

After extended research in the literature, typical values describing the fraction of the time covered by each phase of the flight mission with respect to the total endurance have been identified ("Duration (%)" column in Table 3.16). Then, assuming that during take-off and climb, the fuel consumption is maximum, the consumption during the other flight phases has been estimated iteratively until the fuel consumed equals the fuel available. As a reference, an example has been selected from the literature where the power fraction during climb is 100%, during cruise is 30%, and in descent and in ground-idle & taxing is 15% and 8%, respectively 3.16.

Table 3.16 Estimated Mission Phase Time Distribution for HALE and MALE UAVs (elaborated from [61, 62, 46, 63, 46]).

Mission Phase	Phase duration w.r.t. endurance
Take-off & Climb	5 - 10%
Cruise ingress	10 - 15%
Loiter	60 - 75%
Cruise egress	10 - 15%
Descent & Landing	5 - 10%

To estimate the fuel consumption profile, a "Ground idle and Taxiing" phase has been added. Even if the effect of considering this phase is negligible on the total fuel consumption, it will be relevant to analyse the dynamic behaviour of the H_2SDSys where a small amount of hydrogen flow rate will flow through the hydrogen

distribution system while safety checks are conducted. Typically, in the aviation domain, this phase lasts for a shorter time than that assumed here of 25 minutes (0.42 hours in Table 3.18. However, considering the novelty and complexity of the hydrogen storage system, and the lackness of specific indications from current standards, a longer time interval has been assumed where the fuel consumption is very low due to the hydrogen flow through the distribution system while the engine is still off, which can be useful to check the integrity of the distribution system and its components.
Considering the MQ-1 Predator, the fuel consumption profile has been estimated iteratively, and reasonable results have been obtained (Table 3.18). Different rates of consumption during loiter and cruise have been assumed to better reflect a realistic scenario and to impose more severe conditions on the H2SDSys [38].

Table 3.18 MQ-1 Predator Fuel consumption throughout the flight mission.

Flight phase	Duration (%)	Duration (h)	$\dot{m}_{fuel}$ w.r.t. $\dot{m}_{fuel,max}$	$\dot{m}_{fuel}$ (g/s)
Ground idle & Taxiing	1.7%	0.42	8%	0.54
Take-off & Climb	5%	1.2	100%	6.76
Cruise Ingress	15%	3.6	55%	3.72
Loiter	60%	14.4	40%	2.70
Cruise Egress	15%	3.6	55%	3.72
Descent & Landing	5%	1.2	15%	1.01

A double check was carried out later to verify the consistency of the Predator's fuel consumption. The specific fuel consumption ($276\,\mathrm{g\,kW^{-1}\,h}$) has been multiplied by the Rotax maximum and minimum power, 85 kW and 15 kW, resulting in a maximum fuel mass flow rate of $6.52\,\mathrm{g\,s^{-1}}$ and a minimum fuel mass flow rate $1.15\,\mathrm{g\,s^{-1}}$. These results have been considered aligned with those obtained iteratively (Table 3.18) and, even if the aircraft fuel consumption varies depending on the specific needs of each flight mission, the consumption profile described numerically in Table 3.18 has been considered adequately representative to be considered on the following analysis.
Analogous calculations have been conducted for the RQ-4A Global Hawk, but the resulting fuel consumption during cruise and loiter phases was around 11% of the maximum fuel consumption (Sec . 3.1.1). Unexpectedly, this result was extremely low; therefore, a different approach was used to estimate the average fuel consumption during cruise and loiter.

According to the fundamentals of flight mechanics, during cruise, the forces along the vertical direction (lift: L, and gravitational force: W) and along the horizontal direction (thrust: T, and drag: D) are in equilibrium. So, starting from the aerodynamic efficiency expressed through the lift-to-drag ratio (Eq. 3.1, the gravitational force and the lift have been computed (Eq. 3.2) at the beginning of the cruise ingress and at the end of the cruise egress phases, where the mass of fuel, has been assumed respectively equal to the 80% and 20% of the total fuel capacity. This mass of fuel has been summed to the operative empty weight (OEM) and the payload to obtain the aircraft's total mass. Then, through aerodynamic efficiency, the thrust and drag forces are also computed (Eq. 3.3. The mass flow rate of fuel during cruise ingress and cruise egress has been estimated (Eq. 3.4). Finally, the fuel mass flow rate during loiter has been computed as the average between the two values obtained at cruise ingress and egress [64, 49, 45].

$$E = \frac{L}{D} \tag{3.1}$$

$$W = L = (\text{OEM} + \text{Payload} + m_{\text{fuel}}) \cdot g \tag{3.2}$$

$$T = D = \frac{W}{E} \tag{3.3}$$

$$\dot{m}_{\text{fuel, cruise}} = \text{SFC} \cdot T \tag{3.4}$$

In agreement with results form the literature, the fuel consumption during the descent and landing phase has been estimated as one third of the fuel consumption during cruise [65]. Instead, concerning the fuel consumption during ground idle & taxiing, it was firs computed as the 8% of the maximum fuel rate [66]. However, the resulting value was higher that than that referred to the descent & landing phase, so it has been set equal to this last one.
As a final step, the mass of fuel burnt during one mission has been computed and it was exceeding the maximum fuel capacity. This inconsistency has been attributed to the fact that the computations have been conducted considering a full payload. In such conditions the aircraft endurance can be lower compared to the nominal one. So, a last tuning to make the fuel consumed equal to the fuel capacity resulted in a effective endurance of 29 hours, that will be the reference value for further analysis.

For reference, all the parameters related to the Global Hawk have been grouped in Table 3.19. Analogously to what has been previously done for the MQ-1 Predator, the data related to the Global Hawk's flight phases have been reported in Table 3.20.

Table 3.19 RQ-4 Global Hawk performance estimates.

Parameter	Value	Description
OEM	6,781 kg	Operating Empty Mass
Payload	1,360 kg	Mission payload
$m_{\text{fuel, capacity}}$	7,847 kg	Maximum fuel capacity
g	9.81 m/s^2	Gravitational acceleration
E	33	Lift-to-drag ratio in cruise
SFC_{cruise}	18 g/kN·s	Specific fuel consumption during cruise
$m_{\text{fuel, cruise ingress}}$	6,277.6 kg	Fuel remaining at start of cruise ingress
$m_{\text{fuel, cruise egress}}$	1,569.4 kg	Fuel remaining at end of cruise egress
W_{ingress}	141.45 kN	Total aircraft weight at cruise start
W_{egress}	95.26 kN	Total aircraft weight at cruise end
T_{ingress}	4.29 kN	Required thrust at cruise start
T_{egress}	2.89 kN	Required thrust at cruise end
$\dot{m}_{\text{fuel, ingress}}$	77.15 g/s	Fuel consumption rate during cruise ingress
$\dot{m}_{\text{fuel, egress}}$	51.96 g/s	Fuel consumption rate during cruise egress
$\dot{m}_{\text{fuel, avg}}$	64.56 g/s	Mean fuel consumption during loiter
$\dot{m}_{\text{fuel, descent}}$	21.52 g/s	Fuel consumption rate during descent
Endurance	29 hours	Estimated endurance at full payload

Table 3.20 Estimated Fuel Flow During RQ-4 Global Hawk Mission Phases. The *Duration (%)* is expressed with respect to the flight endurance of 29 hours.

Flight Phase	Duration (%)	Duration (h)	$\dot{m}_{fuel}$ (g/s)
Ground Idle & Taxiing	1.4%	0.42	21.52
Take-off & Climb	5%	1.45	314.00
Cruise Ingress	10%	2.90	77.15
Loiter	70%	20.30	64.56
Cruise Egress	10%	2.90	51.96
Descent & Landing	5%	1.45	21.52

All the data needed to provide a starting point for the static and dynamic sizing of the hydrogen storage and distribution system have been computed here and will be used in the following analysis.

Chapter 4

Hydrogen storage in aviation

4.1 History of hydrogen in aviation

The use of hydrogen in aviation dates back more than 100 years when hydrogen was used as lifting medium in airships. However, the year 1900 marked a turning point as the commercial use of airships began, leading to the use of hydrogen in commercial air transportation, which was interrupted during World War I, an then continued until the Hindenburg accident, where 35 of the 96 people on board died. The Hindenburg tragedy marked the end of airships and of the use of hydrogen in commercial aviation. It had such a strong resonance in public opinion that even today, discussions about the use of hydrogen in aviation still evoke memories of the event. It must be said that the Hindenburg completed 62 flights, including 10 ocean crossings, in just one year. Statistically speaking, this represents a huge result even in terms of operational safety. However, after the disaster, the public's perception of safety in the use of hydrogen in aviation was irreversibly damaged [67]. In 1940, in Germany, all the airships were dismantled to supply the Nazi war apparatus.

The use of hydrogen in aviation had been set apart until 1950, when the U.S. started several military projects to investigate the use of liquid hydrogen in aviation. The main objectives were to extend the range and to increase the service ceiling. Among the various projects, two are quite famous and have been selected here for further investigation: the Project Bee and the CL-400 Sultan aircraft project.
The Project Bee was conducted by the NACA, the precursor of NASA, to assess the feasibility of an LH_2 fuelled aircraft. The selected platform was a Martin B-57

Canberra configured with one engine running on jet fuel and the other capable of switching to hydrogen. So, the aircraft burned jet fuel until an altitude of 50 000 ft when one engine switched to hydrogen. The B-57 was equipped with two wing-tip tanks, one containing liquid hydrogen and the other containing helium, which was used to pressurise the LH_2 tank. (Fig. 4.1). The fuel lines crossed the wing to reach the fuel regulator and the air/hydrogen heat exchanger before entering the engine. The hydrogen fuel tank was made of stainless steel. It was 6.2 m long and

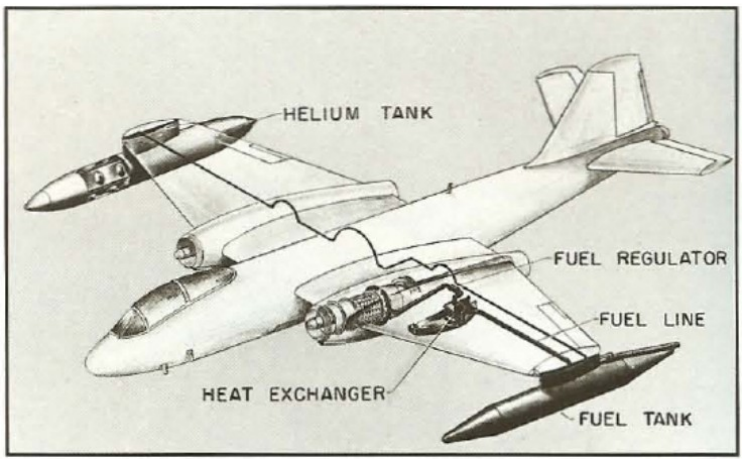

Fig. 4.1 Project Bee's modified Martin b-57 Canberra [68].

had a volume of 1.7 m^3. It was designed to bear a pressure of 3.4 bar. To maintain the hydrogen in cryogenic conditions and minimise boiloff, the tank was wrapped with 5 cm foam covered with an aluminium foil and enclosed inside a fiberglass shell. Helium that was stored at 200 bar in the other wing-tip tank. It was used both for purging the fuel lines from air before feeding them with hydrogen and to keep the fuel tank pressurised. The heat exchanger used ram air to vaporise hydrogen before injecting it into the engine. A vent pipe was also installed to discharge excess hydrogen safely. The Project Bee successfully demonstrated that cryogenic hydrogen could be safely stored and operated, and the technical feasibility of LH_2 powered aircraft. Indeed, the modified engine of the B-57 switched successfully from jet fuel to hydrogen 38 times while in-flight [69].

Another project worth mentioning, which took place in the same years, was led by Lockheed, which designed a CL-400 fully powered by liquid hydrogen. The goal of the project was to create a high-altitude spy aircraft capable of flying at Mach 2.5. The project included a massive fuselage containing three liquid hydrogen tanks, while the two engines were mounted on the wing tips to isolate them from

the cryogenic tanks (Fig. 4.2). In particular, there was one forward tank placed right behind the cockpit of 67 000 L, one in the rear part of the fuselage (aft. tank) of 54 000 L, and a smaller one located below and between the other two of 15 000 L. The working pressure of the two larger tanks was around 2.3 atm. The smaller central tank was also used as a mixing chamber and consequently kept at a pressure slightly lower.

Among the various tank configurations taken into account, one particularly promis-

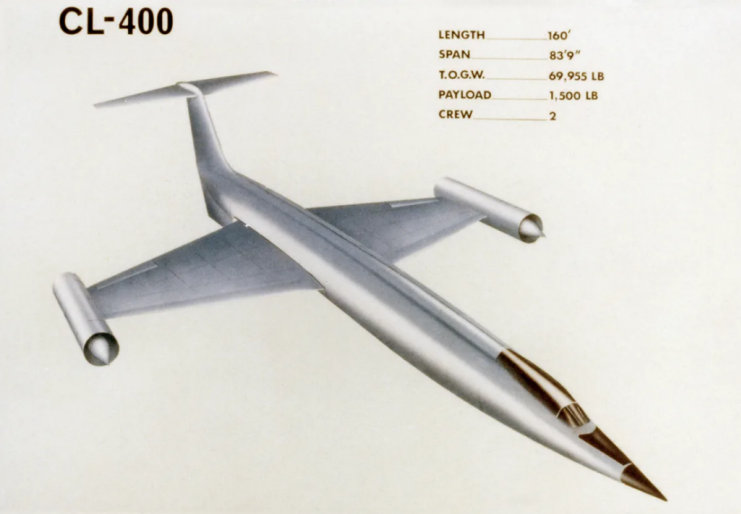

Fig. 4.2 Rendering of the fully hydrogen-powered Lockheed CL 400 [70].

ing was manufactured and tested. It consisted of a double-wall vacuum insulation made of aluminium. The 6.35 mm thickness between the two walls was filled with fibre-glass able to bear compressive loads from the outer shell. The inner shell was reinforced with circumferential beads, and it was only meant to sustain tensile stresses resulting from the internal pressures. Beads were also created on the outer shell to bear axial loads. These beads also allowed for adapting to thermal contraction and expansion. However, despite its initial theoretical relevance, this tank proved impractical mainly due to difficulties in keeping the vacuum between the two aluminium layers due to the welding at the bead tips, where the stresses were concentrated.

Thus, another tank was built and tested. The tank was a cylinder with ellipsoidal domes. It was made of a 1.27 mm 6061-T6 aluminium alloy layer wrapped with the insulation layer consisting of a 25.4 mm inner layer of styrofoam, and a 38.1 mm outer layer made of fiberglass [71]. Each of the insulating layers was enveloped with a mylar film of 0.127 mm to shield it from vapour and avoid gas permeation.

To prevent the condensation of gas at cryogenic temperatures (cryopumping), the void within the styrofoam layer was filled with helium and that within the fiberglass with nitrogen. Finally, an aluminium foil was wrapped around the tank to shield it from radiation. This tank holds notable performance. Indeed, the testing campaigns revealed that the boil-off amounted to 3% of the total fuel stored on board, but 2% was used to keep the tank pressurised, thus resulting in an effective boil-off of only 1% of the total hydrogen amount. Concerning the hydrogen distribution system, to transfer the hydrogen from the fuselage to the engine, the hydrogen pipes needed to cross the entire wings. However, at high speed, the wing could reach relatively high temperatures, while hydrogen had to be kept at low temperatures even inside the distribution lines. To solve this problem, vacuum jacketed pipes were applied. The CL-400 aircraft was never built mainly for two reasons. Firstly, it was considered limited in range capability, and the project did not reveal a significant margin for improvement. Secondly, the logistics associated with the use of liquid hydrogen would have introduced numerous challenges that were anything but trivial [71].

Both the Project Bee and the CL-400 were ahead of time. However, they are still considered milestones today, and their findings are often cited in current studies. Many of the lessons learned were reapplied to rocket design during the space programs.
Indeed, during the U.S. space program running from 1958 up to 2011, there has never been a failure of a hydrogen-fueled rocket. Similarly, during the U.S. nuclear rocket program, almost 10 000 ton of liquid hydrogen were handled without any serious injury.

Until this point, research into hydrogen for aeronautical applications had been conducted with the aim of exploiting its particular properties. The 1973 energy crisis marked the first time society faced the reality that fossil fuels are finite and inexhaustible.

In 1988, the Soviet Union flew the world's first hydrogen-powered passenger aircraft, modifying a Tupolev Tu-155 (Fig. 4.3). Apart from the historical relevance of this event, it also demonstrated that interest in the potential of hydrogen in aviation was not limited to the U.S. The Tupolev took its first flight in 1988. One of the engines was modified to run also on hydrogen or liquefied natural gas. The liquid hydrogen tank was placed in the rear part of the fuselage and had a volume of 17.5 m^3, corresponding approximately to a fuel capacity of 650 kg of hydrogen [73].

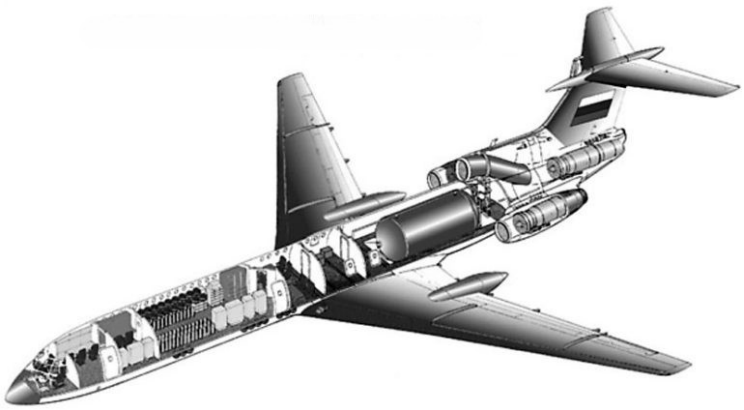

Fig. 4.3 Liquid hydrogen Tupolev TU-155 [72].

The large dimensions of the tank and its need to bear a certain inner pressure forced the engineers to design a large cylindrical vessel that, being so massive, could only be installed inside the fuselage. Despite the few data available in the literature, issues related to the volume occupied by hydrogen storage systems are still one of the significant drawbacks limiting their broader adoption [71].

Concerns about climate change grew in the following years. Indeed, in 1997, the Kyoto Protocol was signed. Starting from 2000, several projects took place. The CRYOPLANE project was conducted by the European Commission to study the feasibility of LH_2 as a commercial aviation fuel. It produced five aircraft concepts and concluded that a transition was possible by 2040-2050, provided that greater investments in research and development and support from institutions are made [74, 75].

NASA pursued a different objective with the X-43 Project: an aircraft powered by a scramjet engine that reached Mach 9.6. A peculiar feature of the X-43 was the shape of the frontal part of the aircraft, which was designed with a specific geometry capable of compressing the air before injecting it into the engine together with hydrogen, which was stored in gaseous form [76, 77].

The German Aerospace Center (DLR) has been at the forefront of sustainable aviation. Among the others, it conducted two relevant projects in the first decade of the 2000s. In one of them, the engineers from DLR replaced the auxiliary power unit of an Airbus A320 with a 20 kW fuel cell. The other project, the Antares DLR-H2, saw a collaboration between DLR and Lange Aviation GmbH that converted an Antares 20E aircraft to work on hydrogen by reinforcing the wing structures and installing two pods below the wings, one hosting the fuel cell while the other hosting

the hydrogen tank. The Antares was only using hydrogen, thus qualifying as the world's first manned aircraft entirely powered by fuel cells [78, 74].
Two attempts to exploit the hydrogen properties to increase the aircraft endurance were made by AeroVironment, the U.S. DoD and DARPA with the Global Observer UAV, and by Boeing with the Phantom Eye UAV. They were both high-altitude long-endurance (HALE) UAVs with an operational altitude in the 60 000-65 000 ft range. The Global Observer had an endurance of 5-7 days, while the Phantom Eye had an endurance of 4 days. Both aircraft stored liquid hydrogen on board. Although both programs were interrupted, the Global Observer ended after an aircraft crash, while the Phantom Eye was retired after nine flights and is now exhibited in a museum, they demonstrated the potential for multi-day endurance and stratospheric flights [79].

After the Paris agreement in 2015, the interest in hydrogen for aviation increased even among smaller companies and start-ups. Pipistrel flew a GH_2 aircraft in 2016 that later converted to LH_2, establishing the world's first liquid hydrogen electric-powered manned aircraft.
ZeroAvia is also an active player in the field. In 2023, it flew a Dornier 228 with one of the two engines replaced by a hydrogen-electric powertrain. Universal Hydrogen performed an analogous operation that substituted one engine of the Dash 8-300 with an electric motor powered by a fuel cell. Universal hydrogen addressed the issues related to cryogenic hydrogen handling, such as refuelling operations, using external liquid hydrogen tanks that were transported and placed inside the fuselage before take-off. With this solution, the company managed to save 15% of the hydrogen amount used to refuel the aircraft that would be lost otherwise due to boil-off losses during refuelling [80].
In 2024, France also had its first hydrogen-powered flight performed by Beyond Aero that substituted the traditional engine of a small aircraft with a 85 kW electric powertrain supplied by a gaseous hydrogen tank.

Apart from those mentioned, several other projects exploring innovative aircraft architectures aim to reduce the polluting emissions of the aviation sector. One of the most notable projects in Europe is HERA (Hybrid Electric Regional Aircraft), which is coordinated by Leonardo S.p.A. and involves all the leading companies and public institutions in the aerospace sector. HERA aims to develop a hybrid-electric regional aircraft for short-range routes under 500 km, seating 50–100 passengers, ready for service by 2030. It combines batteries or hydrogen fuel cells with Sustainable Aviation Fuel (SAF) or hydrogen combustion, targeting up to 90% emissions reduction.

To pursue this goal, innovative architectures related to high-power distribution, thermal management, and energy systems are investigated. Success relies on significant R&D investment and institutional support. HERA will support new certification, energy sources, and infrastructure, aligning with future mobility frameworks. A demonstration strategy in Clean Aviation Phase 2 will ensure readiness and early impact through high technological maturity [81].

As it is widely explored in the current section, the use of hydrogen as fuel in aviation is not new. However, in the last few decades, the interest in H_2 related technology has been increasing as it has never happened before. The main driver is the need to reduce global emissions, even though studies aiming at exploiting hydrogen properties are also present in the literature [77, 75, 74, 82].

The purpose of the work presented here is to investigate the hydrogen storage and distribution system that, as can be seen from the previous studies presented in this section, represents today, and represented in the past, one of the main obstacles to the broader development of hydrogen-powered aircraft. Hence, pursuing the primary author's objective, a deeper analysis focusing on all the key issues related to the hydrogen storage and distribution system will be conducted in the following.

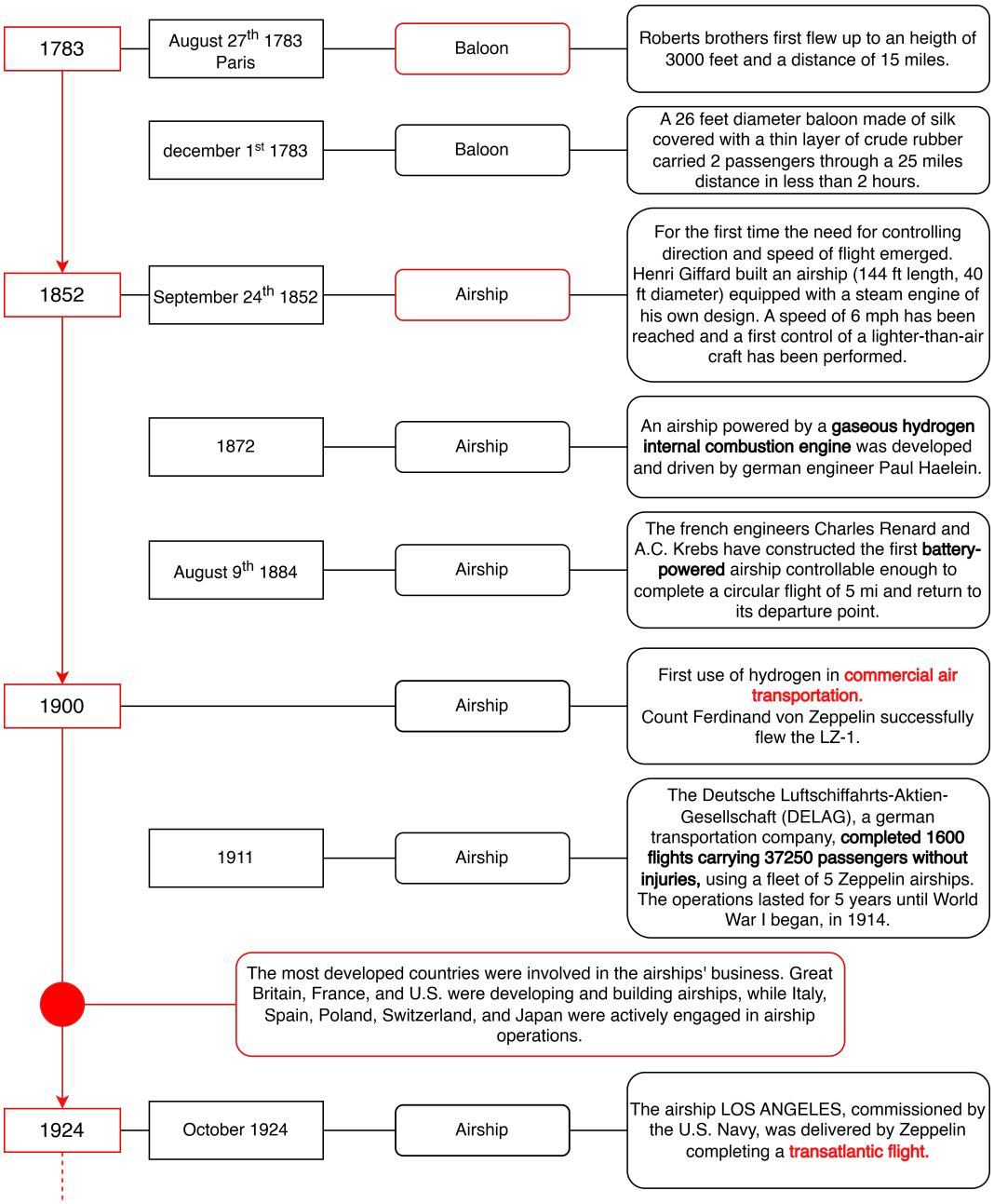

Fig. 4.4 Historical evolution of the use of hydrogen in aviation (1783-1924) [71, 83, 77, 75, 84, 85, 74, 82, 86].

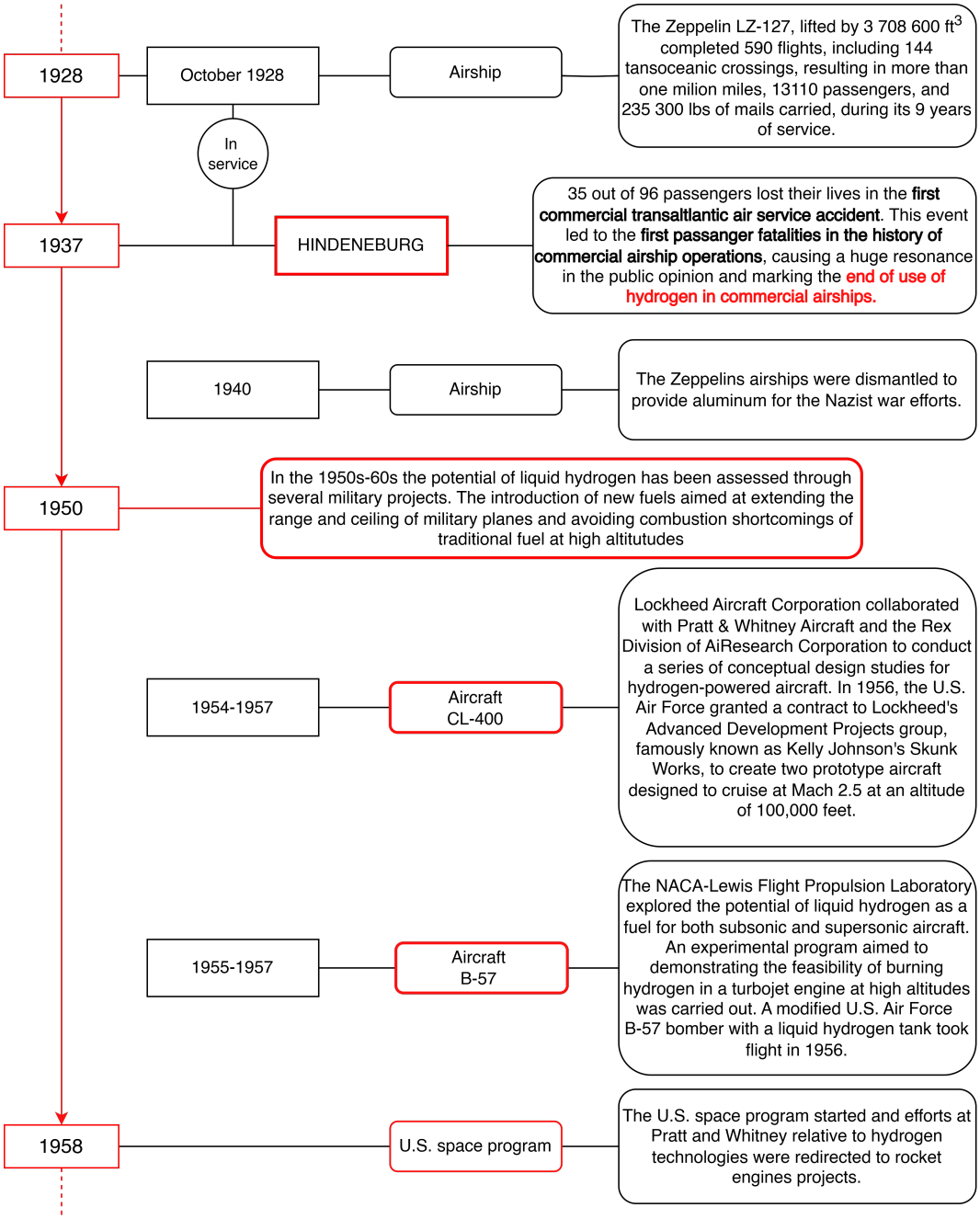

Fig. 4.5 Historical evolution of the use of hydrogen in aviation (1928-1958) [71, 83, 77, 75, 84, 85, 74, 82, 86].

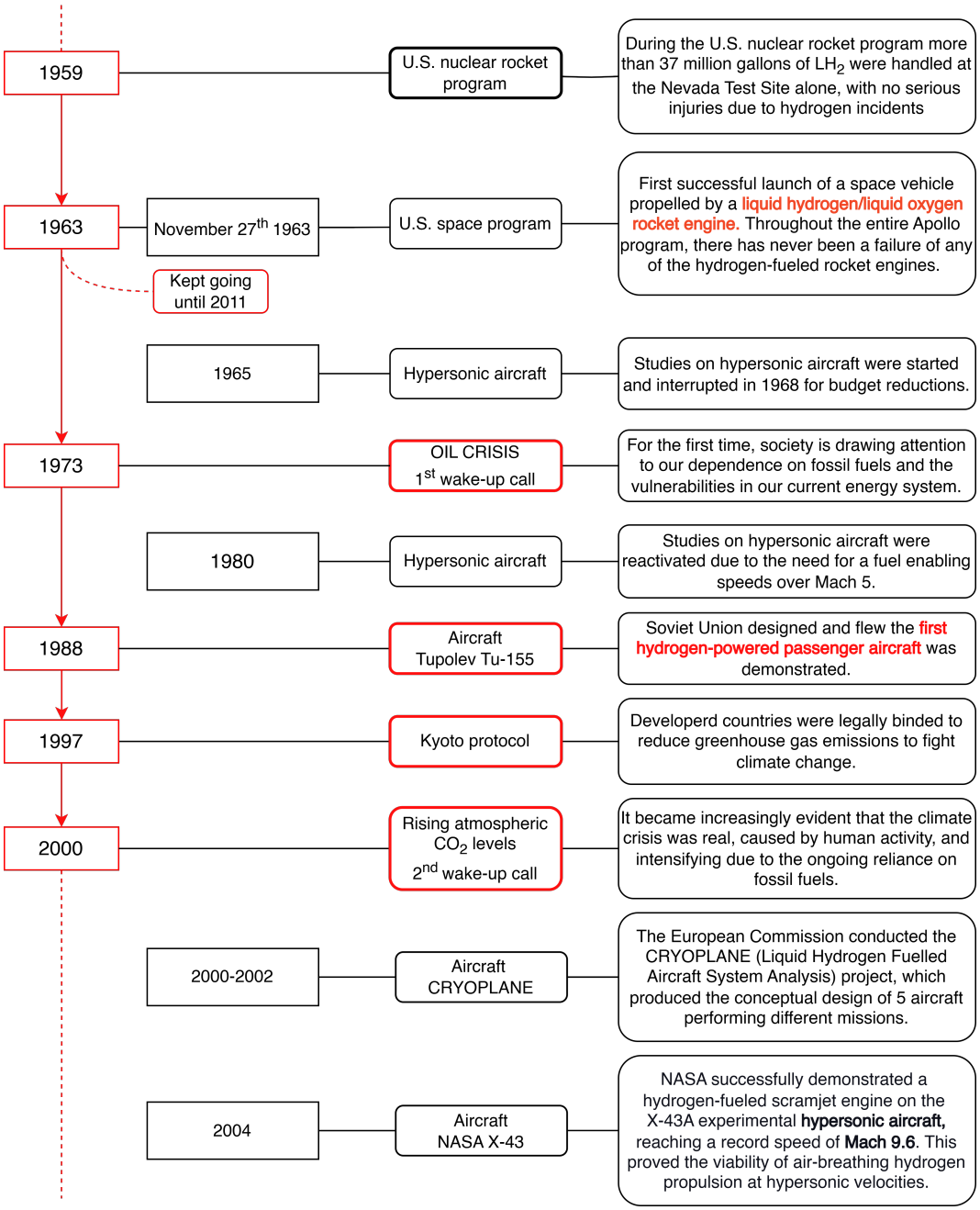

Fig. 4.6 Historical evolution of the use of hydrogen in aviation (1959-2004) [71, 83, 77, 75, 84, 85, 74, 82, 86].

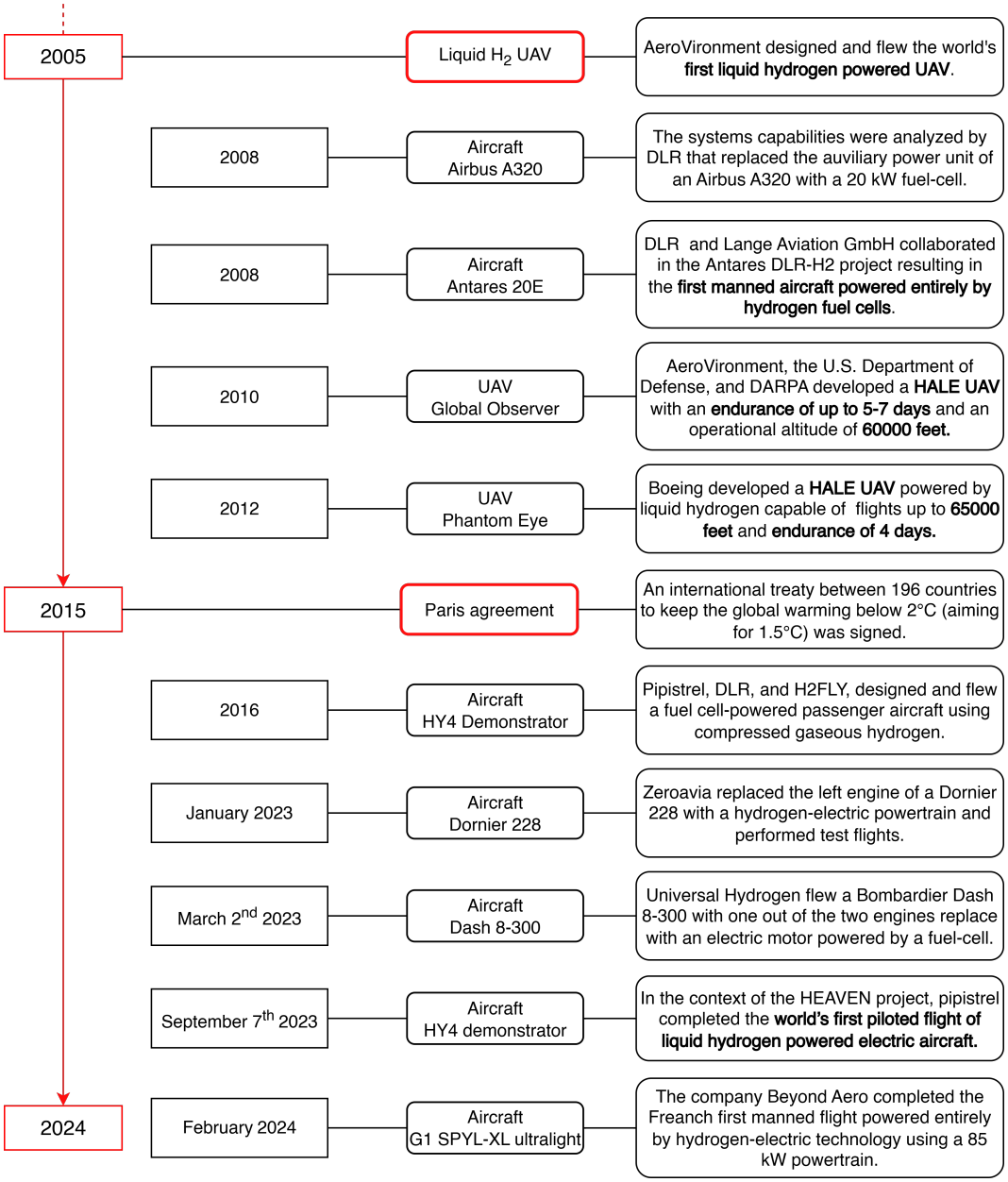

Fig. 4.7 Historical evolution of the use of hydrogen in aviation (2005-2024) [71, 83, 77, 75, 84, 85, 74, 82, 86].

4.2 Hydrogen fuel

Before analysing hydrogen storage technologies, it is helpful to provide a comprehensive description of hydrogen's thermo-physical properties and a comparison with other traditional fuels. However, before moving on, the reader might question the use of hydrogen in aviation itself, as the reason why hydrogen is being investigated instead of other energy storage solutions has not been explained so far. Although the author's objective is not to identify the best energy storage options for aviation, a concise yet clear and focused answer has been derived from the Fly Zero report by the Aerospace Technology Institute [87]. Starting from the Breguet range equation and assuming a lift-to-drag ratio equal to 12, a power-plant efficiency of 0.36 for fluid fuels, and of 0.76 for battery power-plants, the chart in Fig. 4.8 has been drawn. At first glance, it is immediately evident that hydrogen, particularly in its liquid form, is the only solution capable of providing greater performance than kerosene. However, this conclusion cannot be considered always accurate, and its validity should be verified on a case-by-case basis through more in-depth analysis.

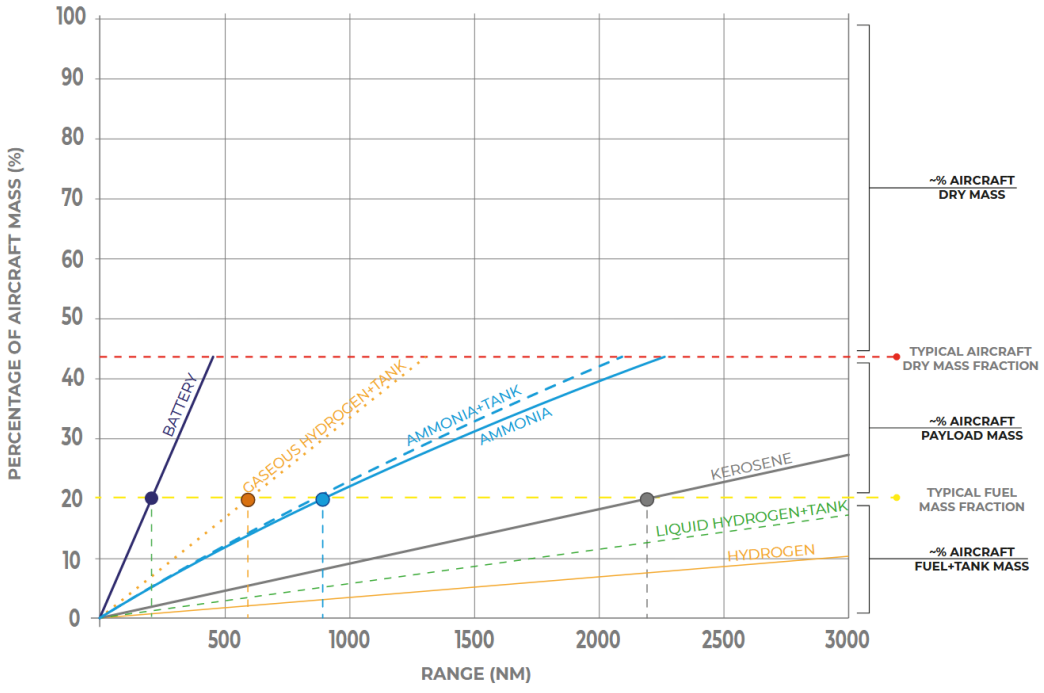

Fig. 4.8 Mass fractions of fuel, tanks, and payload as a function of aircraft range [87].

Hydrogen possesses relevant properties, even when compared to traditional fuels or batteries. For comparison, the main properties are reported in Table 4.1,

while a more comprehensive list of thermo-physical properties can be found in the literature [88].

Table 4.1 Typical values of fuel properties at standard conditions[1] (elaborated from [87, 89, 90])

Property	Hydrogen		Jet fuel	Gasoline	Diesel	Methane
	GH_2	LH_2[2]				
Gravimetric energy (MJ/kg)	120		43	44	45	∼52.5
Volumetric energy (MJ/m³)	10.8	8488	35000	33000	36000	36
Density (kg/m³)	0.0899	70.85	800	720	850	0.668
Boiling point (°C)	–252.9		150 to 300	100 to 170	180 to 360	–161.5
Freezing point (°C)	−259.2		−40	< -58	−60 to − 100	−182.5
Flammability range in air (%)	4 – 75	4 – 75	0.6 – 4.7	1.4 – 7.6	0.6 – 5.0	5 – 15

[1] Standard conditions refer to 15 °C and 1 atm pressure.
[2] LH_2 values are valid at cryogenic conditions: approximately 20.3 K and 1 atm.

Looking at Table 4.1, hydrogen stands out for having the highest specific gravimetric energy, which is almost four times that held by the other fuels. In contrast, the specific volumetric energy is dramatically lower even when hydrogen is stored in liquid form. The densities of jet fuel, gasoline, and diesel are significantly higher than the density of hydrogen. Additionally, they are available in liquid form over a wide range of temperatures, making them easy to store and transport. The wide flammability range of hydrogen makes it highly suitable for use in combustion

processes, but also dangerous if even small amounts are released into the air, thus making leakage avoidance a high-priority concern for designers [87, 89, 90].

Figure 4.9 provides an immediate visual perception of the hydrogen density with respect to other fuels. The high gravimetric density of hydrogen makes it one of the best candidates in sectors where lightweight is relevant. In contrast, due to its inherently low volumetric density, hydrogen cannot be stored under standard conditions. The necessity of employing either high-pressure containment systems or

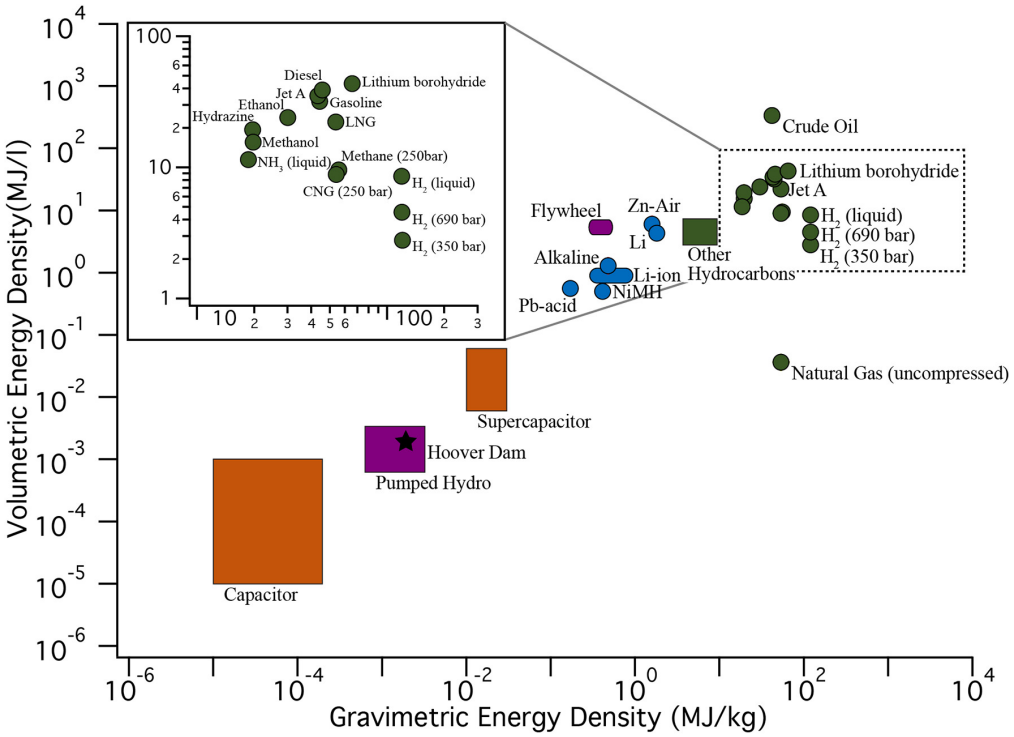

Fig. 4.9 Energy storage and fuels volumetric and gravimetric energy densities [91].

cryogenic temperatures significantly increases the complexity of its practical implementation. In the following section, a general overview of the different hydrogen storage methods will be provided.

4.3 Hydrogen storage methods

The low hydrogen density drove the need to investigate several solutions for storing hydrogen. Several technologies have been explored, and many others are under development. A classification based on the main approaches has been drawn (Fig. 4.10).

The various solutions can be broadly grouped into two categories: physical-based methods, which involve enclosing the fuel inside a confined space, typically a tank, and material-based methods, which exploit the ability of hydrogen molecules to bond with materials.

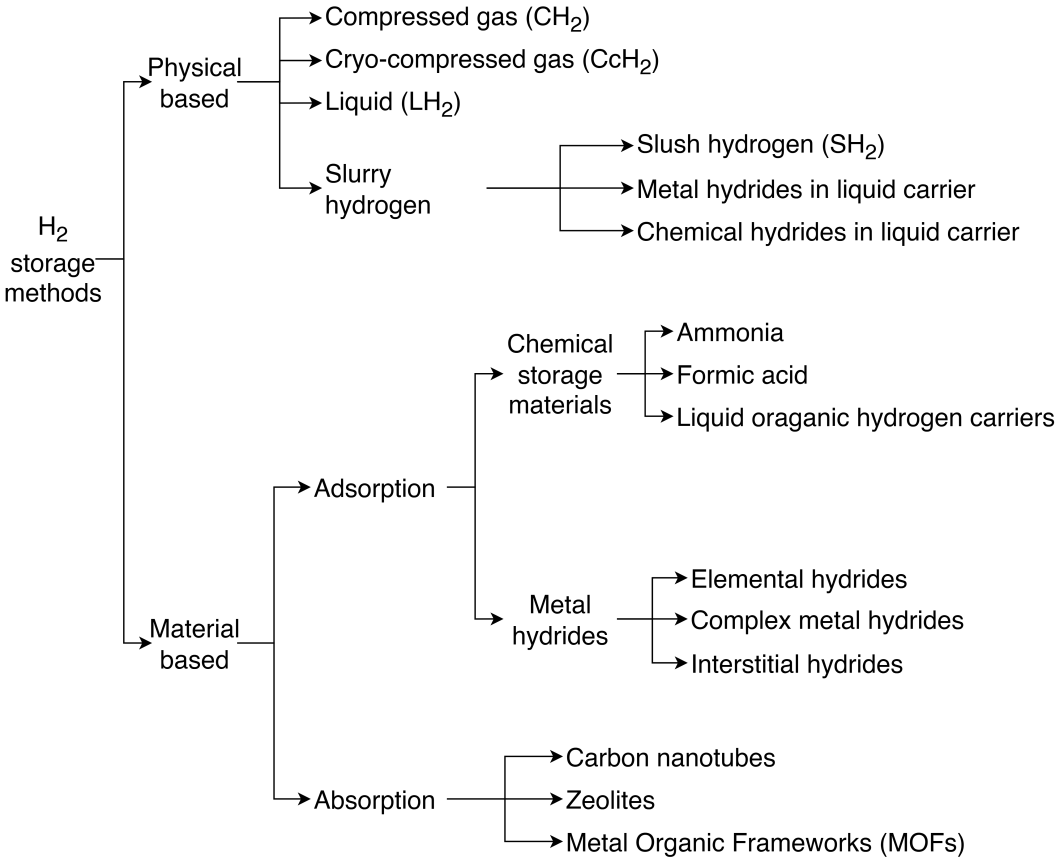

Fig. 4.10 Hydrogen storage technologies (elaborated from [92, 93, 94, 95, 85]).

In physical-based methods, hydrogen is stored inside a vessel designed to operate at specific temperatures and pressures. Compressed gas vessels typically operate at room temperature and have a working pressure of 350 bar or 700 bar. Liquid hydrogen is stored at low pressures, in the order of a few bars, and at a temperature close to the hydrogen boiling temperature (20.3 K). Hydrogen in cryo-compressed form can be placed halfway between CH_2 and LH_2. Typically temperature range from 30 K to 70 K, and pressures can span from 200 bar to 700 bar. A more detailed description of these three storage methods will be provided in the following sections.

In addition to the three states of matter, literature also mentions a sort of fourth state known as slurry hydrogen. Essentially, it is a solution of liquid hydrogen and solid elements. Such elements can be metal or chemical hydrides. In the simplest case, the solid fraction consists of solid hydrogen particles, and it is referred to as Slush Hydrogen (SH_2). Slush hydrogen can be produced in different ways. Still, all of them require further cooling of the liquid hydrogen to, or below, the triple point (13.81 K), thus demanding more energy if compared to hydrogen liquefaction. If the solid fraction is equal to or below 55% of the total mixture and the particle sizes are limited in dimension, slush hydrogen can flow through vacuum-insulated pipes and orifices, and it can also be handled by centrifugal pumps. Depending on the fraction of solid particles, the density of SH_2 can be higher than that of LH_2 (SH_2 with 50% solids has a density of $81.49\,\mathrm{kg\,m^{-3}}$, 5.5% higher than LH_2), and may have a higher heat capacity, which helps manage boil-off. This is because all the solid hydrogen inside the liquid must be melted before it evaporates. Despite offering certain advantages, SH_2 has not attracted much interest in either literature or industry, likely due to its higher production costs compared to those of liquid hydrogen [96].
In addition to slush hydrogen, slurry hydrogen can also be produced by adding metal or chemical hydrides to liquid hydrogen. Metal hydride slurries can be obtained by adding magnesium (MgH_2) or aluminium (AlH_3), while an example of chemical hydride is the ammonia borane (NH_3BH_3), even though many more can be found in the literature. Generally, hydride slurries offer advantages in terms of safety and ease of thermal management in transportation applications. In contrast, their wider adoption is limited by various issues, such as increased system complexity and reduced regeneration efficiency [85].

Materials-based methods encompass a broad variety of solutions. However, this current analysis presents a brief overview, focusing on the materials most frequently found in the literature, which have been classified into two categories: adsorption and absorption, based on their working principles. Adsorption, also known as physisorption, describes the process where hydrogen atoms or molecules are bonded to the surface of a material. In contrast, absorption, or chemisorption, involves the dissociation of hydrogen molecules into atoms that are integrated within the material's network. Adsorption-based methods, in turn, include chemical storage and metal hydrides. The most famous chemical storage material is probably ammonia. The ammonia molecule (NH_3) contains hydrogen that can be separated through a

process called ammonia cracking. It is liquid at higher temperatures than LH_2 and it contains a greater amount of hydrogen per unit volume. It is used in the chemical sector, while technologies exploiting this solution in aviation are at a low Technology Readiness Level (TRL) [97].
Hydrogen can also react with metal alloys or intermetallic compounds to form metal hydrides. Elemental hydrides are formed by hydrogen and a single element, like lithium hydride (LiH) or aluminium hydride (AlH_3). In interstitial hydrides, hydrogen atoms are bonded to the structure of metals like palladium (palladium hydride: PdH_x), and Titanium (Titanium Iron Hydride: $TiFeH_2$).In complex hydrides, the hydrogen atom is part of a complex anion. Examples include lithium borohydride ($LiBH_4$) and sodium alanate (-$NaAlH_4$). Overall, research has shown that elemental hydrides can be safe and utilise the residual heat of other processes to operate. Still, their performance is too low to be of interest for the mobility sector [93]. Interstitial hydrides offer advantages in terms of safety. They operate at low pressures and are quite compact. On the other hand, they have a low hydrogen-to-weight ratio, making them unsuitable for airborne applications. Finally, complex hydrides offer interesting potential in terms of weight and hydrogen storage capacity. However, the presence of a catalyst and a precise thermal control system is often necessary, which increases the weight, volume, and complexity of the storage solution [98, 99]. Materials-based method solutions relying on absorption are also a field of research. In Fig. 4.10, three among the most studied materials have been reported. They are all characterised by a high porosity, thanks to which hydrogen can weakly bond to their surface. Carbon nanotubes form C-H bonds with hydrogen; indeed, graphene is also a subject of ongoing research. The porosity of carbon nanotubes can be tuned. Consequently, the amount of hydrogen they can store depends on various parameters [100]. Zeolites store hydrogen at cryogenic temperature, around 70 K, and release it at higher temperatures. Despite offering economic and safety advantages, the operating temperatures of zeolites require a temperature management system that is anything but trivial [101]. Among the material-based methods, Metal-Organic Frameworks (MOFs) exhibit a notable hydrogen storage capacity. However, typical values are in the order of 9% in weight, which is too low for aeronautical applications, apart from being costly and barely integrable on board [102]. Additionally, material-based methods are also unsuitable due to their slow loading and/or unloading [103].

Overall, physical methods are technologically more mature than material-based methods [104, 105, 106].

Hence, in the analysis proposed here, to satisfy customer needs, the author chose to investigate those storage technologies that are more mature, to comply with the customer's need for short-term industrial applicability. In the following sections, the physical hydrogen storage methods will be explored, with a greater focus on compressed and liquid hydrogen storage, which are more developed at the industrial level.

4.4 Physical hydrogen storage methods

In physical storage methods, hydrogen is contained inside a tank. However, the storage conditions entirely change the design of each vessel. As highlighted in Figure 4.11, three main options are available. Compressed gaseous hydrogen (region 2 in Fig. 4.11) is stored at room temperature at pressures ranging from 250 bar to 700 bar. Cryo-compressed hydrogen (region 3 in Fig. 4.11), is stored at cryogenic temperature approximately between 30 K and 70 K. The operating pressures range for CcH_2 can actually be broader than that reported in Figure 4.11, spanning from 200 bar to 1000 bar. Finally, liquid hydrogen is stored at temperatures around the hydrogen boiling temperature (20 K and at pressures slightly above the external environmental pressure. The main aspects of these three methods will be discussed in more detail in the following sections. Among the three storage types, CH_2 and LH_2 are mainly adopted mature. Compressed hydrogen is the most mature technology. In the mobility sector, it is already a well-established technology in the automotive industry. It is an efficient technology, although it is more expensive compared to traditional vehicles' fuel tanks, and solutions for fast filling are yet to be fully developed. Liquid hydrogen holds a much higher storage density. However, the production and transport of liquid hydrogen is demanding both in terms of energy and time. In addition, keeping the hydrogen at a low temperature to limit boil-off losses significantly increases the system complexity [108]. In contrast, hydrogen stored as a cryogenic compressed gas can achieve densities even higher than those of the liquid. However, the combined effect of low temperatures and high pressures poses several challenges to the tank's integrity. Moreover, this technology still remains less explored in aircraft applications [109, 94].

In any case, the transition from traditional fuel to hydrogen involves a substantial change in the design approach to the storage system. To provide a preliminary

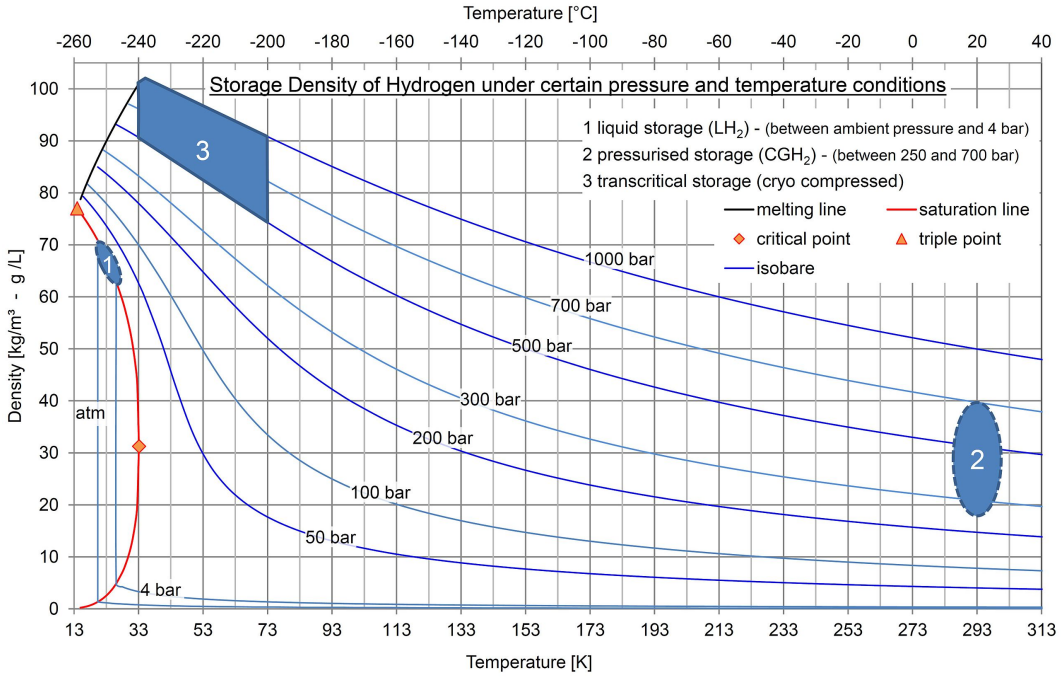

Fig. 4.11 Hydrogen density vs. temperature for various pressure levels [107].

quantitative measure on how impactful the hydrogen fuel storage system is compared to jet fuel, it can be useful to observe the chart published by the University of Cambridge and the Aviation Impact Accelerator at the World Economic Forum (Fig 4.12. Regardless of the fact that Figure 4.12 refers to 1 kWh of energy stored that does not make it applicable to any case, the substantial impact of storage system mass in hydrogen applications is immediately evident. In the case of jet fuel, the mass of the fuel storage is, in practice, almost negligible, and values of the gravimetric efficiency of the entire system approaching higher than 95% are reasonable. In contrast, translating the graphical information into percentage values for CH_2 tanks yields 6%, 10%, and 15%, for current, optimised, and future tanks, respectively. Analogously, for LH_2 tanks, the mass of hydrogen corresponds to 20%, 60%, and 75% of the total storage system weight for the configurations just mentioned.
It is clear that the margin for improvement in the case of liquid hydrogen is significantly greater than that of compressed hydrogen, which, even in the best-case scenario, may not prove efficient enough to justify substantial resource investment. Nevertheless, CH_2 remains a well-established technology currently suitable for implementation during experimental and testing phases.

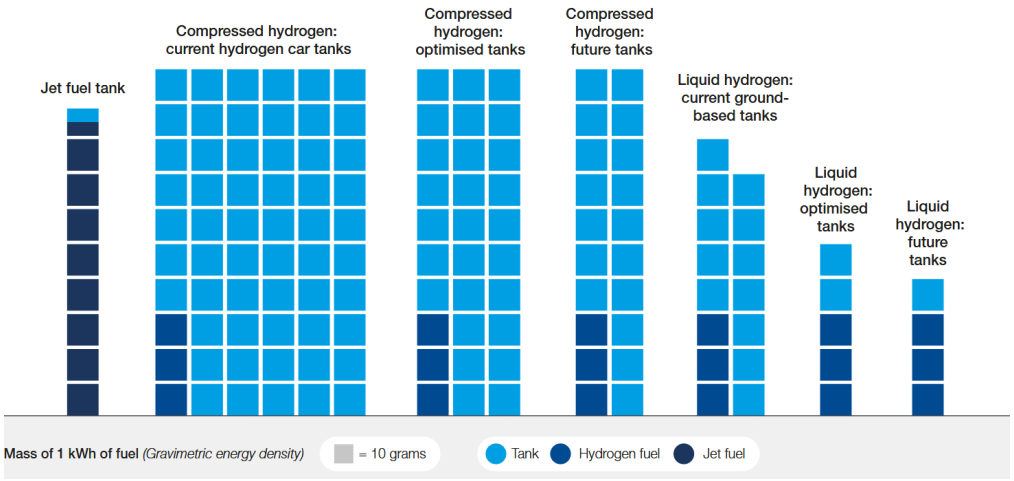

Fig. 4.12 Comparison of the mass required to store 1 kWh of energy using hydrogen and kerosene-based jet fuel across different tank configurations [110].

In the following sections, CH_2, CcH_2, and LH_2 will be further explored. However, in light of the evidence gathered through the literature review and to satisfy the customer's need, the author will mainly focus on compressed and liquid hydrogen storage systems.

4.4.1 Compressed hydrogen storage

Over the last two decades, the need to reduce the carbon footprint in aviation has increased interest in the use of hydrogen fuel in both industry and academia. As shown in Sec. 4.1, different prototypes have been manufactured to investigate the use of hydrogen-based propulsion systems. Additional examples include the ZeroE project developed by Airbus, and the RAPID 200-Fuel Cell, an aeroplane developed within the European Union's ENFICA-FC project coordinated by the Politecnico di Torino [111]. Most of the experiments conducted rely on CH_2 storage. Indeed, high-pressure vessels are the most widely adopted and mature technology in the mobility sector, as also demonstrated by the relevant amount of studies that can be found in the literature [112, 113, 114, 115, 116, 117].

High-pressure vessels are commonly classified into five types (Fig. 4.13). Type I vessels are entirely made of metal. Type II are also made of metal, but the central cylindrical part of the vessel is wrapped with composites. Types III, IV, and V are

all fully wrapped in composite materials, but Type III has an internal metallic liner, Type IV has a polymeric liner, while Type V has no liner and is therefore also called "liner-less". This latter tank type is gaining considerable research interest, although its commercial deployment remains limited [112].

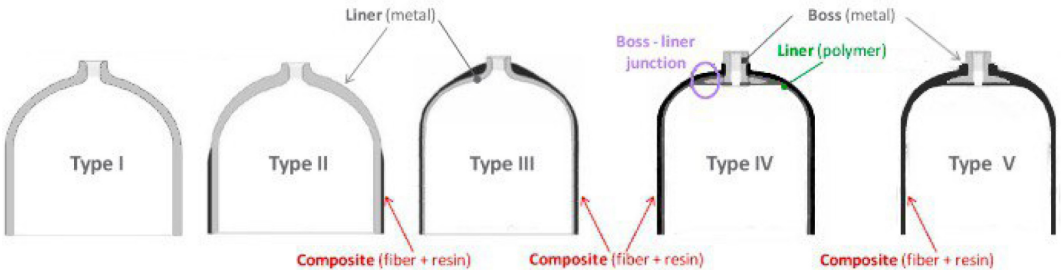

Fig. 4.13 Compressed hydrogen storage tank types [118]).

Typical values of the working pressure, and the gravimetric and volumetric densities of the different Types of CH_2 tank are reported in Table 4.2. Apart from Type V vessels, which are still under research, the other four types exhibit different characteristics that meet the requirements of various industrial applications. Type I and Type II tanks are heavy but inexpensive. They are typically adopted in stationary applications or for transportation of goods by trucks or trains. They are usually made of steel and have an operational lifespan of about 15 years. Type III and Type IV are more expensive, but being lightweight, they are suitable for mobile applications. The internal liner materials are selected to be compatible with hydrogen, and their service life can reach 20 years [108, 119].

Table 4.2 Working pressure and typical ranges of the gravimetric and volumetric density for compressed hydrogen tanks (elaborated from [108, 119, 120, 86]).

Type	Working pressure (MPa)	Gravimetric density (%)	Volumetric density (g/L)
Type I	17.5–20	1	14–17
Type II	26.3–30	1.5	14–17
Type III	35–70	2.4–5	35–40
Type IV	35-70	∼5	38–40
Type V[1]	up to 100	∼6.5	–

[1] Due to low technological maturity, gravimetric density value is and estimate elaborated from the literature.

Observing the values reported in Table 4.2, the tank properties, types, and operating pressure levels can be immediately correlated. For increasing working pressures, both the gravimetric and volumetric densities increase, describing an improvement in tank performance. Moreover, it can be intuitively deduced that the tank storage performance improves from Type I to Type IV due to the use of more advanced materials, and further to Type V, where the absence of a liner contributes to reducing the overall tank weight. This increase in gravimetric and volumetric densities with increasing pressure reflects the physical properties of hydrogen. Indeed, as shown in Fig.4.14, the density rises for increasing pressure levels, as it is common for gases.

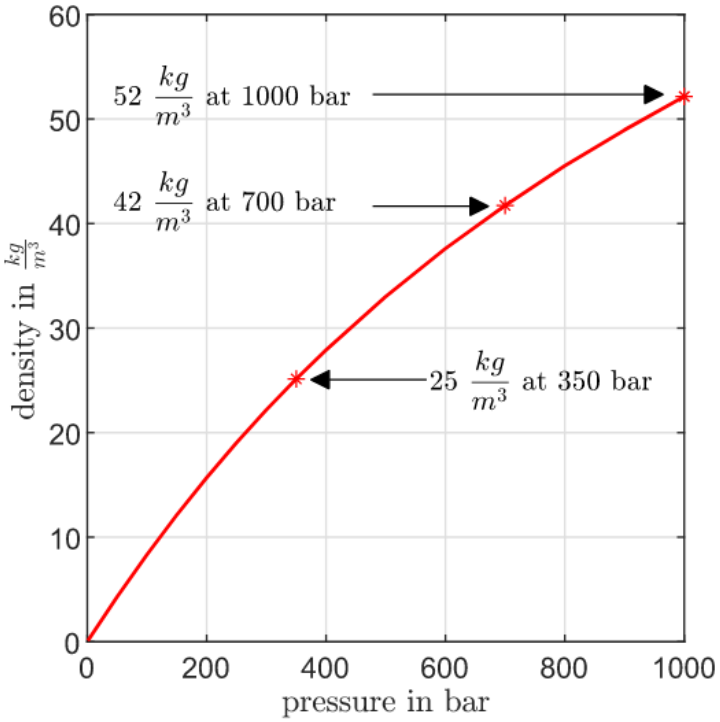

Fig. 4.14 Hydrogen storage density vs. pressure at 275.15 K [103].

However, it is equally straightforward to demonstrate the inadequacy of this conclusion. Roughly analysing the values reported in Fig.4.14, the density at 350 bar is 25 $\mathrm{kg\,m^{-3}}$, while the density at twice the pressure (700 bar) bar does not double but it is equal to 42 $\mathrm{kg\,m^{-3}}$. The trend is even smoother at higher pressures. Indeed, at 1000 bar the density is 52 $\mathrm{kg\,m^{-3}}$, approximately twice of that at 350 bar. It becomes

crucial to conduct further investigation, and it is also evident that there is a need for a model capable of predicting the tank characteristics at different pressure levels.

Thus, further extensive research in the literature has been conducted. The existing literature provides thorough analyses of hydrogen storage technologies, including high-pressure composite tanks and cryogenic systems. It also features in-depth modelling plus experimental validation for tank performance under operational conditions [121, 122]. In aviation purposes, digital twins and multi-physics simulations optimise tank configurations and improve structural integrity using cutting-edge design techniques [123, 124]. Many studies, however, mainly experiment on a small scale or perform digital simulations only. This limits the applicability of these findings to full-scale aircraft systems. Since practical difficulties regarding large-scale implementation are limited, the challenges of integrating hydrogen storage with aircraft design, which include issues related to weight and volume, are still not fully addressed [125, 122].

Focusing on the hydrogen vessel design for the mobility sector, where lightweight is relevant, Types III, IV, and V are those mainly investigated, which, basically, are made of three elements: the resin and the fiber, constituting the composite, and the liner, which is absent in Type V vessels.
The resins, also known as matrices, are categorised into two types: thermoset and thermoplastic. Thermoset resins are easier to process, and their manufacturing techniques, such as resin transfer moulding and filament winding, are well-established industrial knowledge. Epoxy resins are the most commonly adopted, even though interest in vinyl-ester resins is increasing, mainly due to their lower densities, higher burst pressures, and lower susceptibility to intra-laminar cracking. Conversely, the thermo-mechanical cycles created by repeated refuelling operations can create severe fatigue-induced damage.
On the other hand, thermoplastic matrices can be processed faster than thermosets, are easier to repair, and are more easily recyclable. However, the high viscosity of these resins makes the fiber impregnation process more difficult. Pre-impregnated components, such as towpregs, may be suitable for addressing this issue, enabling wider adoption. However, increasing interest in thermoplastic matrices is also due to their potential suitability for Type V tanks. Several analyses are moving in this direction, and some prototypes have also been manufactured [113, 112]. Additionally, studies that, starting from the requirements needed from the resin, identify new types of resins are also present in the literature [126].

Moving to fibres, carbon fibre dominates the scene due to its strength, fatigue resistance, and chemical stability, although it is expensive. The choice of the proper fibre mainly depends on the application. Typical alternatives include glass fibres, which are cheaper but less performing, and basalt fibre, which is also more affordable and more environmentally sustainable compared to carbon fibre, although it is heavier. Steel wire is better for stationary applications where a trade-off in favour of lower prices is desirable. Aramid fibres also exhibit notable mechanical properties but at a higher price. Recent studies also investigate the use of natural fibres and the impact of different fibres made from the same material [112].
Despite the various options available, the vast majority of high-pressure hydrogen storage vessels are made of carbon fibres. A further choice must be made between the different types of carbon fibres. However, such a level of detail exceeds the scope of the preliminary design phase conducted in the current study; therefore, typical or average properties will be selected as needed [113].

The last of the main three elements composing the hydrogen vessel is the innermost layer, i.e., the liner. The choice of the proper liner is crucial as it must serve as a barrier between hydrogen and the outer composite layer. Formally, the tank liner shall prevent hydrogen penetration and resist or avoid hydrogen embrittlement (HE). Indeed, hydrogen atoms are tiny and, especially for prolonged exposures at high pressures and room temperature, they can permeate both metals and polymeric materials. The result is a decrease in ductility and in the stress needed to initiate a crack inside the material, which is commonly referred to as hydrogen embrittlement, but it is also referred to as hydrogen-induced cracking or hydrogen-assisted cracking [127].
Assessing the material sensitivity to hydrogen embrittlement is an essential step in choosing the proper liner. Type III vessels have a metallic liner. Generally, all metals are susceptible to hydrogen embrittlement. Steels, nickel, titanium, and cobalt alloys are all susceptible to HE, while stainless steels, copper, and aluminium alloys resist HE better. In particular, it has been found that aluminium alloys 1100, 6061-T6, and 7075-T73, and stainless steels A286, 310, and 316 exhibit negligible susceptibility to HE [119]. Polymeric materials composing the liner of Type IV tanks are also prone to permeability. In this case, polyether-based materials are typically used, including high-density polyethylene (HDPE), polyethylene (PE), polyamide (PA), and polyethylene terephthalate (PET). Generally, polymers with a dense inner structure are less susceptible to hydrogen permeation [113, 119].

The selection of the material strongly influences the following fabrication process. Traditionally, wet winding methods have been broadly adopted to fabricate composite vessels. However, more recent and innovative techniques, such as tape winding, automated fibre placement (AFP) for Type V vessels, and towpreg, are also under development [113, 112, 128].

Overall, meaningful progress has been made to improve HE resistance and improve gravimetric efficiency of Type IV and V vessels [121, 128]. Brand new materials are explored through computational chemistry and machine learning techniques [129]. At the same time, the application of promising materials, such as graphene, to tank fabrications is being investigated, showing potential for performance improvements [130, 131]. In contrast, the behaviour of novel materials in long-term applications is still to be fully explored, and the transition from laboratory to industry requires certification for aviation. For these reasons, obstacles to a wider industrial implementation still have to be overcome [123, 124, 128]. Indeed, the gravimetric efficiency of commercial tanks is now around 6%. However, flight test data reported improved efficiencies up to 13%. Such results highlight margin for improvements that could be achieved if research and development efforts are sustained [132].

At this point, it can be helpful to introduce a more detailed classification method supporting the choice of the proper tank configuration. The data reported in Table 4.3 is intentionally limited to those tanks that are most promising for on-board application, however an extended analysis can be retrieved from the literature [113].
The Type names are assigned according to the format: Type N - X Y Z, where:

- N is the tank Type (I, II, III, IV, or V).
- X is the reinforcement type, and it can alternatively be:
  - M: metal wire,
  - F: fibre,
  - H: hybrid, expressing a combination of M and F.
- Y is the matrix type, and it can alternatively be:
  - S: thermoset,
  - P: thermoplastic.

- Z express the type of winding process:
  - W: wet winding,
  - T: tape placement.

Table 4.3 CH_2 Type IV sub-types and Type V vessels cost and weight comparison [113]

Type	Resin[1]	Fiber[2]	Cost	Light Weight
Type IV—FSW[3]	TS	CF	very-low	high
Type IV—FST	TS	CF	low	very-high
Type IV—FPT	TP	CF	low	very-high
Type IV—FPW	TP	CF	low	very-high
Type IV—MSW	TS	SW	very-high	low
V	TS/TP	CF	low	very-high

[1] TS = Thermoset,TP = Thermoplastic. [2] CF = Carbon Fiber; SW = Steel Wire. [3] Most common configuration.

The features of the tanks that are mainly relevant to the current analysis are also reported in Table 4.3 and expressed on a five-level scale, ranging from very low to low, average, high, and very high. Apart from the Type V vessel that is at a lower TRL, it can be observed that the Type IV tanks fabricated with carbon fibres (CF) are all at a high or very-high level in terms of lightweight. The first one is also very low-cost, probably due to its broad adoption. It can be preliminarily concluded that, depending on the available resources and manufacturing constraints, due to very strict mass and volume constraints, the choice of a hydrogen vessel for aeronautical applications to be tested in the short term will likely fall within one of these options.

Several studies have deepened the economic aspects of hydrogen storage in aviation, including analyses of cost reduction through advanced manufacturing methods and economies of scale [133, 113]. Studies have also highlighted the impact of design optimisation on reducing system weight and cost [134]. However, from a macroscopic point of view, production volumes are low, and the infrastructure is costly and still to be built. Forecasts are often based on optimistic assumptions, including very high technological targets and relevant support from institutions and policymakers, which are not yet assured. In addition, hydrogen competitiveness is significantly lower than that of traditional fuels, discouraging short-term utilisation if not stimulated by institutional funds supporting the development of the new

technologies [135].
Given that the present study focuses on analysing the storage system with an emphasis on technical aspects, it can be concluded that composite materials are also cost-effective. Indeed, composite hydrogen vessels are lightweight, easy to fabricate, reducing manufacturing expenses, have a long operational life, and require minimal maintenance during service. All these characteristics contribute to reducing the overall life-cycle costs [114].

Additional aspects worth mentioning include the integration of the storage system onboard and safety considerations. Explorations on the integration of the storage system into the aircraft highlight the need for a holistic approach that considers both other systems, such as the fuel-cell and thermal management systems, as well as the installation analysis aimed at guaranteeing the aircraft's balance, and the refuelling system [136, 134]. Considering the substantial changes introduced by hydrogen fuel storage systems, a redesign of the entire aircraft may be necessary, along with further analysis to quantify the impact on aircraft performance and operations, thereby providing a system-level validation [125, 122]. Moreover, airports' infrastructure and regulatory standards are still at an early stage of development, even though they should evolve concurrently [137].

Concerning safety, studies analysing hydrogen's flammability, diffusivity, and embrittlement, and proposing measures addressing safe containment and leak prevention can be found in the literature [138, 137]. Additional measures related to structural health monitoring can also be useful to decrease the risk of failure [123, 139]. However, extended analyses and comprehensive standards providing guidelines are yet to be fully developed [132].

Environmental impact and refuelling are also topics under investigation. Even if they will be briefly introduced here, there are lines of research in the literature that primarily focus on these aspects. SAE J2601 is the standard commonly referred to for refuelling activities using compressed hydrogen. It provides guidance through qualitative and quantitative data such as the working pressures and the hydrogen filling rate [126]. An operational window for refuelling has also been elaborated from the SAE J2601 standard [140]. Indeed, the temperature and state of charge (SOC) of the hydrogen tank during refuelling depend on many factors, and it has been observed that pre-cooling the hydrogen to control its inlet temperature and regulating the filling rate are crucial if fast filling operations are to be achieved [108].

However, it is worth noting that the SAE J2601 standard primarily applies to the automotive sector. At the moment of writing, reference standards for refuelling operations at airports have not been published yet.

Most publications in the literature investigate different aspects of hydrogen, primarily with the aim of obtaining environmental benefits [141]. Indeed, a multitude of studies related to emission abatement, greenhouse gases, carbon footprint, contrail reduction, net-zero emissions goals, energy supply, comparisons with traditional fuels, and other environmental aspects can be found in the literature [3, 2, 142, 143, 144, 145, 146, 147, 148, 1, 114]. Environmental issues are now one of the most critical concerns to be addressed in aviation, as well as in other sectors. These aspects are becoming increasingly important, although the evaluation and analysis techniques are still under development. Therefore, at this stage, a preliminary study is carried out, focusing primarily on the other aspects mentioned above.

Future research trends in compressed hydrogen storage encompass various innovative solutions. As previously mentioned, Type V tanks are among the most promising solutions, despite still having some open issues. The absence of a liner further reduces the complexity of these vessels, thereby avoiding concerns about the thermo-mechanical compatibility between the materials that compose the inner and outer layers. However, the composites should be designed to avoid hydrogen permeation and embrittlement by using reliable, microcrack-resistant resins or barrier coatings. A proposed solution is to embed nanoparticles inside the resins, thereby reducing their permeability. Encouraging results have been obtained after laboratory tests, but the path to potential industrial commercialisation still needs to be explored [113, 112].

Less popular solutions include the use of glass capillaries, hollow glass microspheres, or carbon nanotubes. Glass capillaries are long and thin glass tubes, with diameters ranging from a few microns to a few millimetres. They can store hydrogen at pressures up to 1500 bar. Glass capillaries seem a promising solution due to their low susceptibility to hydrogen permeation and high geometric flexibility, allowing them to be used individually or bundled and to adapt effectively to the available space [103].

Another method for storing hydrogen is the use of hollow glass microspheres (HGMs). They are not a new technology, as they were first introduced in 1977, demonstrating at that time that HGMs could meet U.S. DoE targets. However, recent studies investigated their usage due to HGMs' capability of storing hydrogen

safely and at high pressures. In addition, investigations to assess the possibility of producing HGMs from recycled materials are also ongoing [149, 119].
Carbon nanotubes (CNTs) are cylindrical nanostructures made of carbon atoms. They have exceptional mechanical properties while being lightweight and resistant to hydrogen operation. The use of CNTs in tank manufacturing can notably reduce the weight and volume of the vessels while increasing their lifespan. Experiments incorporating CNTs within the composite structure resulted in a 30% increase in burst pressure and a 75% reduction in weight [114].
Another study explores the possibility of increasing the vessel by wrapping it with an insulating layer, enabling it to store both compressed and liquid hydrogen. Tests have also been conducted to assess the possibility of commercial high-pressure vessels working at cryogenic temperatures. No significant damages or performance losses have been detected. However, safety issues still need to be fully addressed, and a comprehensive characterisation of materials behaviour under cryogenic fatigue phenomena should be conducted [150].

In conclusion, despite several ongoing research trends in compressed hydrogen storage, composite pressure vessels remain the most widely adopted solution in all industrial sectors where lightweight solutions are necessary. Forecasts estimate the market value growing from 1.7 billion dollars in 2024, to 5.2 billion in 2030, following a compound annual growth rate CAGR of 19.7%. While fuel cell electric vehicles (FCVEs) are considered the main driver in the development of hydrogen storage vessels, space and aviation also play a significant role [151]. Reinforced by robust industrial knowledge and excellent mechanical properties, composite pressure vessels are in a strong position to remain the preferred solution for next-generation energy and mobility systems.

4.4.2 Liquid hydrogen storage

Liquid hydrogen has a higher density ($70\,\mathrm{kg\,m^{-3}}$) compared to compressed gaseous hydrogen ($24\,\mathrm{kg\,m^{-3}}$ at 350 bar and $40\,\mathrm{kg\,m^{-3}}$ at 700 bar), is stored at cryogenic temperatures ($-253\,^{\circ}\mathrm{C}$), and is the most promising candidate for aerospace applications. In contrast, the hydrogen liquefaction costs are high, accounting for approximately 30% of the LH_2 energy content. In addition, LH_2 storage suffers from evaporation losses, which are indeed a key driver during design [71]. These and other relevant aspects will be investigated throughout the current study.

After an extensive review of the literature, the author identified several topics worth mentioning and different research trends. Specifically, most of the publications cover two macro-areas. The first one includes aircraft-level analyses, such as retrofitting of existing aircraft, investigating the replacement of thermal powertrains with hybrid-electric solutions ([152, 153, 154, 155, 156, 157, 158]), designs tailored for specific aircraft types or completely unexplored solutions ([5, 71, 159, 160, 161]), as well as methodologies for design and optimisation including the whole aircraft and its subsystems ([132, 162, 163, 75]). Instead, the second category encompasses more detailed analysis focusing on the hydrogen tank ([164, 165]), or on specific aspects of its design, such as analyses of vessel insulating techniques, including well assessed and innovative solutions like the use of vapour-cooled shields ([166, 167, 168]), advanced cryogenic cooling insulation systems ([169]), advanced supports ([79]), and hollow glass microspheres ([170]).
Overall, the design approaches identified in the literature fall into one of two categories: one emphasising a holistic system approach, and the other focusing more on the detailed exploration of specific aspects. However, the several publications identified are all very valuable, even though their suitability may vary depending on the problem under investigation.

In this section, studies from both categories mentioned are retrieved, aiming to explore the main aspects related to the liquid hydrogen storage and distribution system. However, it was considered appropriate to start the analysis with a section focusing on the properties and behaviour of cryogenic hydrogen.

Hydrogen cryogenic properties and behaviour

Before analysing the several issues involved with liquid hydrogen storage systems, it is helpful to understand the cryogenic properties and behaviour of hydrogen, to avoid making unrealistic assumptions or setting unfeasible design parameters. Therefore, a brief description of hydrogen liquefaction and its properties will be presented in the following section.

Hydrogen is typically stored in liquid form at a temperature around 20.39 K, corresponding to its boiling point at room temperature (Fig. 4.15. There are various processes for liquefying hydrogen. The Linde cycle, also known as the Joule-Thomson cycle, is the most popular, but others, such as the Claude cycle, the Linde cycle with double expansion, and the Haydlandt cycle, are also used. In

the Linde cycle, hydrogen is liquefied through sequential stages of compression, cooling, and expansion. However, it must be cooled down below its inversion temperature of 200 K. Indeed, when hydrogen undergoes an expansion, it warms up if its temperature is above 200 K and it cools down if its temperature is below. Through liquefaction, hydrogen reaches a density of 70.79 $kg\,m^{-3}$, which is notably higher than gaseous hydrogen. However, being one-fourteenth as dense as water, it is one of the lightest liquids in nature. The ideal liquefaction work for hydrogen is relatively high (3.228 $kW\,h\,kg^{-1}$) if compared to other substances like nitrogen (0.207 $kW\,h\,kg^{-1}$), even if increasing the pressures involved in the cycle, the ideal liquefaction work can be decreased by 25-30% [171]. Undoubtedly, one of the main issues is that hydrogen liquefaction is an energy-intensive process, requiring from 25% to 40% of the energy contained in the hydrogen itself [114].
Looking at diagrams in Figure 4.15 and Figure 4.16, it can be easily depicted how hydrogen stays in liquid in a quite limited range of pressure and temperatures. Such "LH_2 window" must be carefully considered, especially during the dynamic system modelling. Preliminary estimates would set the vessel's maximum operating pressure around 6 bar and its operating temperature below 30 K, even though a more cautious approach may suggest setting it equal to or below the boiling temperature of 20.3 K also considering that hydrogen cannot condense for temperature below 33 K [172]. However, the technical feasibility of a storage system guaranteeing such storage conditions should be assessed, even though few tools are available to predict the behaviour of hydrogen cryogenic systems, and their suitability to aerospace applications should be verified [173].

A peculiar behaviour of hydrogen is the ortho-para transition. The hydrogen molecule is made of two atoms that can have equal direction of spinning (ortho-hydrogen: o-H_2) or opposite direction (para-hydrogen: p-H_2). As shown in Figure 4.17, the fraction of ortho and para hydrogen depends on the fluid temperature. At room temperature, hydrogen is composed of 25% p-H_2 and 75% o-H_2. Through liquefaction, the composition changes to 99.8% p-H_2 and 0.2% o-H_2 [164]. In practice, liquid hydrogen is composed entirely of para-hydrogen. The process is referred to as "ortho-to-para" transition and generates a heat of conversion of 527.14 $kJ\,kg^{-1}$. Reminding that the liquid hydrogen's latent heat of vaporisation is 446 $kJ\,kg^{-1}$, the ortho-to-para conversion may theoretically cause the evaporation of approximately 50% of the liquid hydrogen stored in approximately ten days. The exact time required for ortho-to-para conversion to take place can vary significantly and may

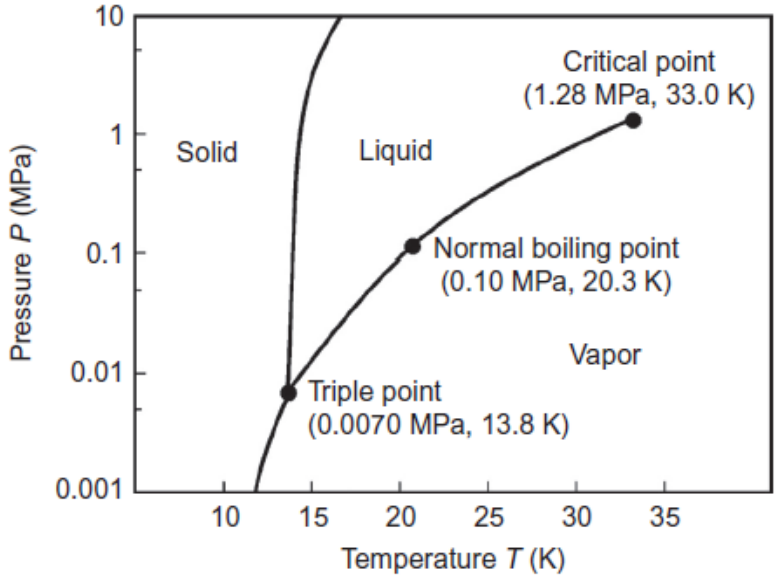

Fig. 4.15 Hydrogen phase diagram ([171]).

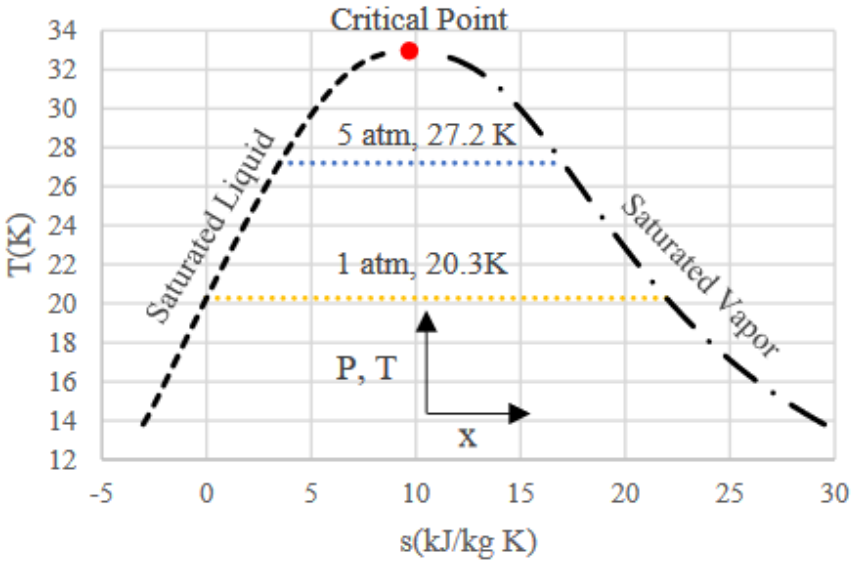

Fig. 4.16 Temperature-entropy diagram for hydrogen at saturated conditions ([84]).

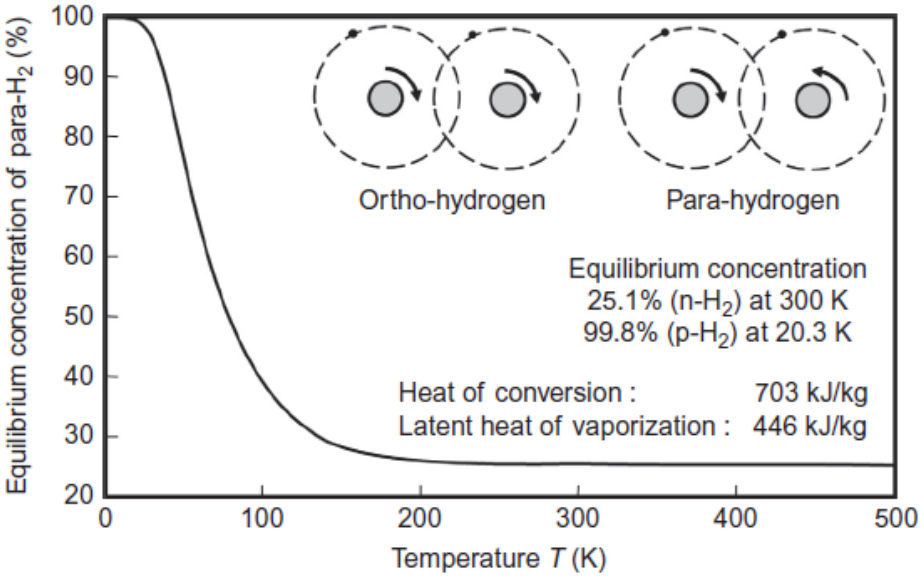

Fig. 4.17 Orto-para hydrogen fractions as function of temperature ([171]).

theoretically last for weeks or even months [172].
Nevertheless, this issue is avoided through the use of catalysts that accelerate the ortho-to-para hydrogen conversion, thus ensuring a para-hydrogen fraction within the liquid of nearly 100%. In the following chapters, it will be assumed that the liquid hydrogen has a negligible fraction of ortho-H_2, and the effects of the ortho-to-para conversion will not be taken into account. On the other hand, the impact of the para-to-ortho transition will not be considered once hydrogen is heated up. Two primary considerations justify this latter assumption. Firstly, the para-to-ortho conversion is an endothermic process that absorbs hydrogen and would not generate any evaporation. Secondly, as a preliminary consideration, hydrogen will be extracted from the tank, heated, and then fed into an engine or a fuel cell just a few seconds later. Such short time intervals make the conversion from para- to ortho-hydrogen impossible [174, 171]. However, if precise estimates of the transition time are needed, one could refer to various references in the literature [175, 176, 177, 178].

Considering the sizing activities that will be performed in the following, it can be helpful to briefly observe how few of the main hydrogen properties vary with temperature. Then, throughout the design, other properties will be computed or retrieved from the literature whenever needed [179]. Generally, considerable variations occur in the thermo-physical properties where rotational heat capacity is relevant [180]. Thus, in the following, hydrogen's ideal-gas enthalpy (Fig. 4.18),

isobaric heat capacity (Fig. 4.19), and thermal conductivity (Fig. 4.20) are reported. The properties follow different curves depending on the ortho-para composition. If not specified, normal hydrogen typically corresponds to the para-ortho composition at that specific temperature [176].

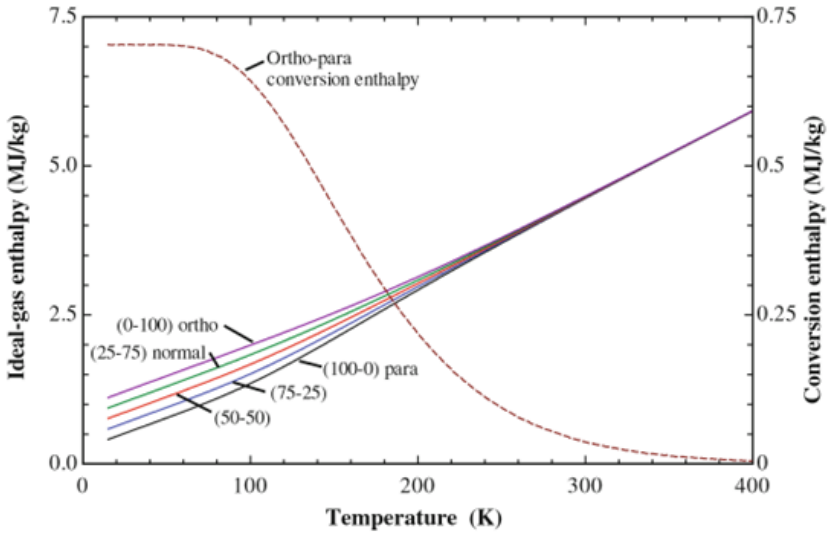

Fig. 4.18 Hydrogen enthlpy as function of temperature ([176]).

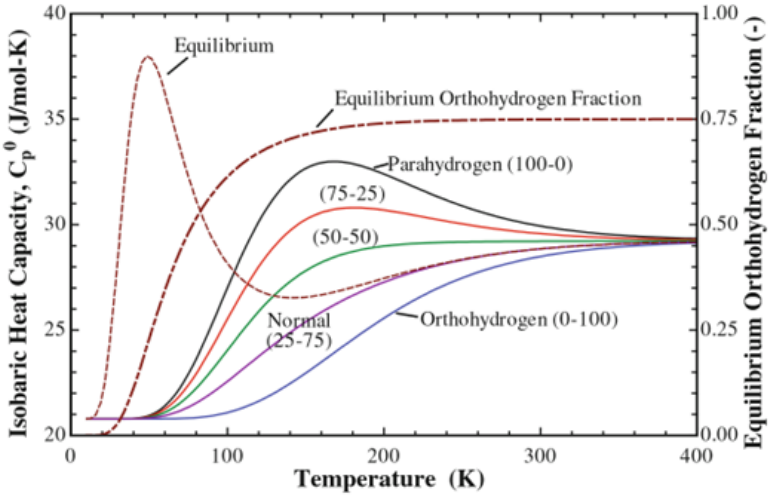

Fig. 4.19 Hydrogen heat capacity as function of temperature ([176]).

It can be immediately perceived that these properties vary significantly with temperature, even under the assumption of 100% para-H_2 fraction at any temperature. Moving from cryogenic temperatures up to 400 K, ideal-gas enthalpy increases ap-

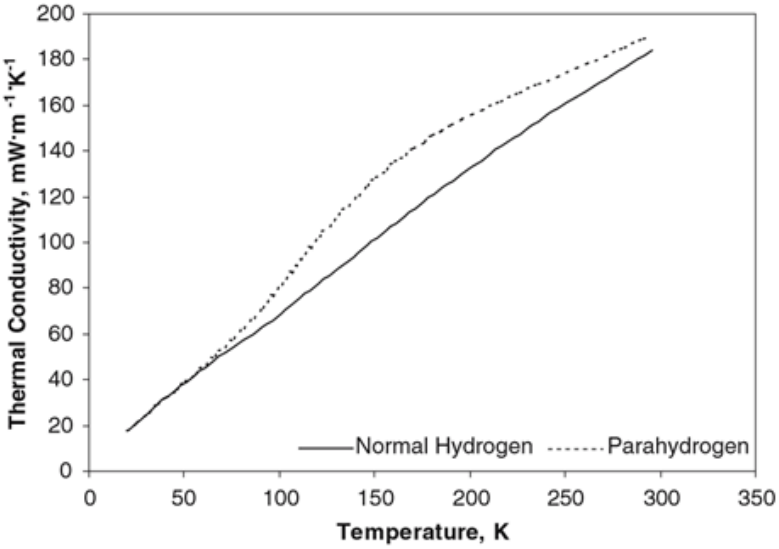

Fig. 4.20 Hydrogen thermal conductivity as function of temperature ([180]).

proximately by a factor of six. At the same time, the isobaric heat capacity spans from 21 J mol^{-1} K to 28 J mol^{-1} K, reaching its maximum of about 33 J mol^{-1} K around 160 K. The trend of thermal conductivity is more linear, but its increase is far more pronounced, ranging from 20 mW m^{-1} K at 20 K to approximately 180 mW m^{-1} K at 300 K.

From the design point of view, assumptions involving constant hydrogen properties over wide temperature ranges should be taken very carefully, as they could prove to be so strong that they would invalidate any meaningful analysis. In contrast, being aware of such variations in properties, confident design choices can take advantage of the natural behaviour of hydrogen and exploit it, for example, in the design of a conditioning system that performs specific functions within certain temperature ranges, where the intrinsic properties of hydrogen make it easier to achieve.

Liquid hydrogen tank configuration

In the current section, an overview of the main aspects concerning the design will be proposed. Typically, LH_2 vessels present a multilayered structure. Thus, the discussion will begin with the innermost layer, directly in contact with hydrogen, before proceeding to the external insulating layer. A discussion about integral vs. non-integral solutions will also be proposed, and, finally, a few words will be spent

on the tank supports, representing the connecting elements between the aircraft fuselage and the LH_2 tank.

Structural layer The innermost layer is the one in contact with hydrogen, and it should therefore be capable of operating at cryogenic temperatures and resisting hydrogen permeation, so as not to be affected by hydrogen embrittlement (HE). There are different types of embrittlement, including hydrogen environmental embrittlement, internal embrittlement, and reaction embrittlement. The main factors influencing embrittlement are the conditions at which hydrogen is stored, the stresses applied, and the type of material. In any case, embrittlement can seriously affect the properties of the material in contact with hydrogen [181].

Moreover, the innermost layer should also withstand the mechanical stresses caused by internal storage pressure and liquid sloshing. This is the reason why it will also be referred to as the mechanical layer or the structural layer.

Candidate materials must comply with a series of requirements. Apart from being lightweight, the selected material should be fully characterised both at ambient and cryogenic temperatures. So the static behaviour, fatigue behaviour, crack propagation mechanisms, ductile-to-brittle transition, and hydrogen interaction under prolonged exposures should be well-assessed [173, 182]. These aspects, in addition to the customer's need for a solution at a reasonably high Technology Readiness Level (TRL), that is approximately above TRL 6 or 7, significantly narrow the spectrum of available options to well-assessed materials. In contrast, the need for characterising novel materials, like composites, remains critical [77]. Studies in the literature identify aluminium alloys as the most suitable structural material. It has been previously adopted in various projects, such as the AIRBUS ZEROe and the Boeing Phantom Eye, and its fatigue behaviour under cryogenic conditions has been widely investigated. Specifically, alloy Al 2219 is pointed out in several analyses [77, 162, 75, 163]. However, other alloys are also used, such as the Al 2014, with a minimum thickness of 5 mm due to manufacturing constraints, the Al 5083, showing better characteristics after welding, and the Al 2195, which has been used in the Ariane space rocket project and exhibits better characteristics than the Al 2219 over all temperatures [183, 184, 164, 167, 185].

Thermal layer Moving to the outer layer, the thermal insulation can be found. Due to the need to maintain a cryogenic environment inside the tank, the thermal design is one of the most extensively investigated topics in the literature. There are studies in the literature that evaluated the hypothesis of placing the insulating layer in contact with hydrogen. However, insulating materials typically do not hold relevant structural properties, and they are not meant to be in contact with hydrogen. Additionally, the outermost layer should also prevent the penetration of air inside the tank layers, as it would condense and then freeze, reducing insulation performance and increasing system weight. Air penetration is typically avoided using vacuum jackets that should maintain a vacuum level of at least 0.001 33 bar, while the air already present inside the system is usually purged with helium or nitrogen. Placing the insulating layer internally results in having the mechanical layer externally, allowing it to operate at environmental temperatures. This eliminates the need to address its thermal contractions and expansions and simplifies the fixation of supports. However, avoiding the diffusion of hydrogen into the thermal layer is hardly feasible, and the consequent rise in thermal conductivity of the insulating material would not be acceptable [165]. Indeed, in most of the studies, the configuration with the external thermal layer is preferred [165, 71]

Before going into details, it is worth mentioning that, at the system level, two types of solutions can be applied, defined as passive and active insulation. Active insulation implies cooling the tank through a conditioning system. Consequently, a set of components must be designed and installed onboard. On the other hand, passive insulation relies on the use of materials or analogous solutions that do not require additional components. The primary difference between the two approaches lies in their energy consumption. Active insulation systems require a continuous supply of energy, whereas passive insulation systems do not. Most studies employ passive insulation. Very few analyses have mentioned that active insulation may be potentially investigated for very large aircraft performing long flights, where the amount of energy spent to power an active insulation system could be very low compared to the energy required by the aircraft. An additional advantage of the active cooling system is the ability to regulate the hydrogen temperature and its evaporation rate, thereby controlling the tank's internal pressure. However, there is no practical evidence of the benefits of active insulation systems due to their low TRL, i.e., below TRL 4 [173].
Overall, passive insulation is preferred because it does not add complexity to the

system, is more technologically mature, and requires no energy supply, making it more suitable for critical applications where lightweight structure is fundamental. This is why passive insulation will be used in the current analysis.

There are various solutions, some are more traditional, consisting simply of one or more layers of materials wrapped around the tank, while others employ more innovative solutions, such as vapour-cooled shields.

The main driver in the selection of the insulating material is lightweight, which translates into materials characterised by low thermal conductivity, low thermal diffusivity, and low density [186]. In practice, a lower thermal conductivity (k) reduces the steady-state heat flux into the tank, while a lower thermal diffusivity (a) extends the time needed to reach equilibrium with the external environment. In addition, their ratio (k/a) expresses the material's capacity to retain energy. Once the storage system is cooled down, it will require more thermal energy to return to equilibrium conditions, resulting in a tank with higher performance [165]. In addition, the capacity of dealing with large expansions and contractions is also relevant [183].

Typical insulating solutions include the use of foams, which are simple and lightweight, multi-layer insulation (MLI), vacuum insulation, which is more effective but usually heavier, or a combination of the two [173]. Foams, aerogels, and MLI are investigated by Winnefeld et. al, who identified Rohacell-foam as an ideal candidate satisfying all the requirements, even compared to MLI [165]. Instead, Verstraete preferred using high vacuum insulation coupled with MLI. However, a failure of the vacuum jacket would result in a fast decrease of the vessel's insulating capacity, so he decided also to explore foam-based solutions. Moreover, the use of foams may require only one tank wall, which is the inner structural layer, whereas a vacuum layer requires at least two walls, making the weight advantages questionable and necessitating quantitative analyses [183]. Indeed, other studies identify the vacuum insulation as thermally more efficient but heavier [173].

Apart from considering the characteristics separately, the compatibility between the mechanical and thermal layers should also be investigated. At the preliminary level, this is typically done by comparing the thermal expansion coefficients of the selected materials. However, to obtain an initial estimate of the system's weight and volume, this aspect is often neglected in favour of other aspects [165].

Integral vs. non-integral Considering the LH_2 tank installation into the aircraft, two configurations are possible: integral or non-integral tank. Integral tanks are designed to be part of the airframe and utilise the fuselage's structural elements as part of the tank structure. In a certain sense, the fuel tank and the aircraft structure are merged into a single structural entity. On the other hand, a non-integral tank can be seen as an element that is built separately and then installed inside the aircraft, fixed to the aircraft structure using supports. Integral tanks are more challenging to inspect, install, remove, and even model, test, and certify. In non-integral tanks, thermal expansion and mechanical stresses are easier to manage, even though the solutions for attaching the tank to the airframe, i.e., the supports, should be carefully designed [173]. These considerations are generally shared in the literature, even though there can be exceptions. For instance, studies suggest that repairing an integral tank is easier because it is sufficient to remove part of the external skin of the aircraft, whereas fixing a non-integral tank requires extracting it from the fuselage, making the operation significantly more complex [183]. In this specific case, each solution should be investigated individually. In general, integral tanks should be lighter, ensuring higher gravimetric efficiencies, while non-integral tanks should be easier to design but heavier. Nonetheless, a final remark should be made. Regardless of the choice between integral and non-integral configurations, liquid hydrogen must be stored in an enclosed volume, and a specific insulation thickness should be guaranteed. So, even if an integral tank is selected, hydrogen cannot be in contact with any structural element, because it would be subject to hydrogen permeation and cryogenic temperatures. In substance, integral LH_2 tanks still require an enclosed volume wrapped with a layer of insulation. Indeed, they cannot be approached like a kerosene tank, because the structural elements of the fuselage should be designed against hydrogen penetration, they should avoid leakages of gaseous or liquid hydrogen and be designed to operate in a temperature range spanning from a few Kelvin degrees to more than 300 K, significantly hindering the aircraft feasibility.

Tank supports After an extensive review of the literature, it has been noted that tank supports are typically less investigated. However, they are crucial elements as they should adequately support the vessel, avoiding any fracture or damage that would cause hydrogen leakages even in the case of hard landings. Moreover, supports should accommodate any contraction and expansion of the vessel while minimising the heat flow. Reminding that the LH_2 tank configuration to be analysed

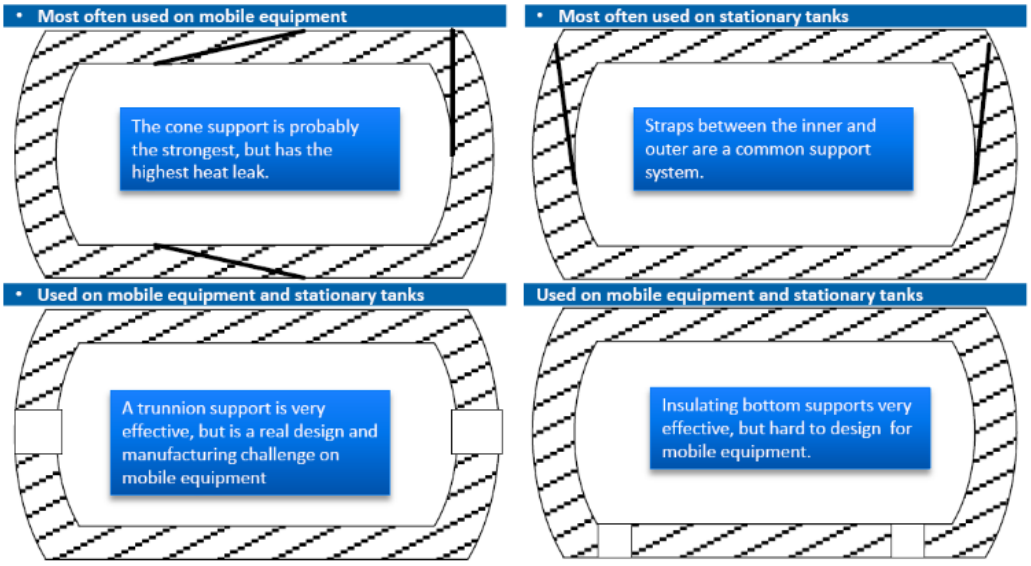

Fig. 4.21 Typical supports in double walled containers [182].

in the following has an internal structural layer wrapped in insulation, the supports should be attached to the thermal layer. This would mean that the insulating layer should withstand the weight of the vessel itself. However, due to the poor structural properties typical of insulating materials, this solution is often not feasible. Thus, the supports should be attached to the innermost structural layer. The supports and the mechanical layer are both made of metallic alloys mainly because, being structural elements meant to work at cryogenic temperatures, they are not characterised by a ductile-to-brittle transition, which would make them fragile and poorly suitable, especially in the case of impact or severe dynamic loads. In contrast, they should also be designed to minimise the heat inflow into the tank [187, 188]. Standard supports for minimising heat leakages are already present in the market, especially in sectors working with liquid natural gas (Figure 4.21).

An interesting approach is that of minimising the contact between surfaces, which somehow applies the same logic used in ball bearings to minimise friction between moving parts. Experiments have been conducted, showing that the heat leakages through supports were reduced by 85% using ceramic balls, and, even though the maximum stresses, which have been investigated using the Hertz theory, can be nine times larger, the structural requirements were still met [82, 79]. At a preliminary design level, the heat transfer through the tank wall has been increased by 30% to account for the pipes and supports [183]. Another design utilises G-10 CR supports

to connect the inner and outer shells of a 6 L LH_2 tank. G-10 CR are composite tubes made of fibreglass and epoxy resin specifically manufactured for cryogenic environments. It is interesting to note that these particular pipes serve not only as structural support but also to refill and extract hydrogen from the vessel [189].

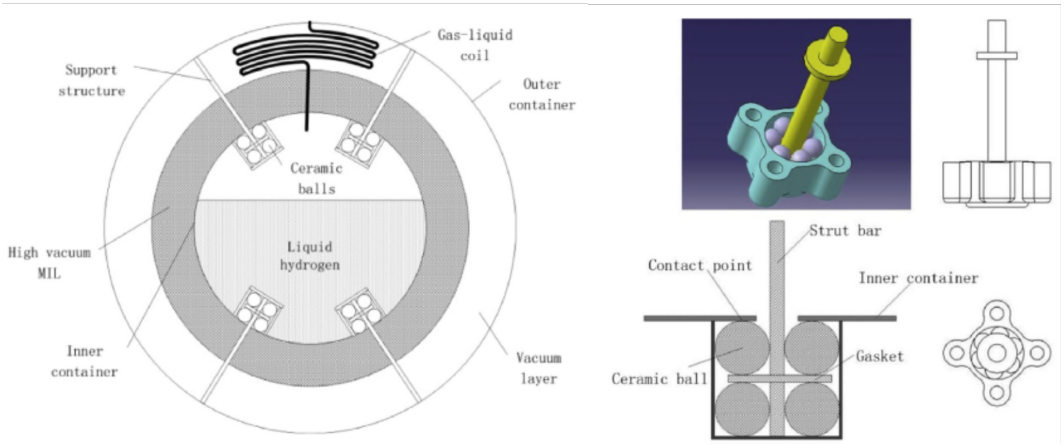

(a) Tank section (left) and views of the support (right).

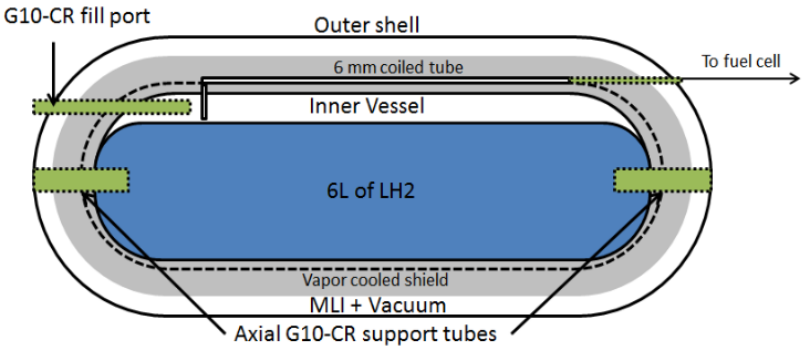

(b) Schematic of a double-walled tank configuration.

Fig. 4.22 Innovative tank supports: (a) minimum contact ceramic ball-based supports [79], and (b) configuration of a 6 L LH_2 tank with G-10 CR supports (b) [189].

Overall, it can be concluded that, regardless of the case-specific solution, supports are fundamental elements in the design of hydrogen vessels. During conceptual design, can be approximated by increasing the heat influx, but in the subsequent design phases, they should be carefully designed to meet both structural and thermal requirements.

4.4.3 Cryo-compressed hydrogen storage

For the sake of completeness, the last of the three main physical hydrogen storage methods will also be briefly introduced in the current section, even if it will not be explored through quantitative analysis.
Cryo-compressed hydrogen (CcH_2) tanks operate at low temperatures and relatively moderate pressure. CcH_2 density can higher than LH_2 density (Fig. 4.23). For example, CcH_2 stored at 240 bar has a density of 87 $kg\,m^{-3}$ while the LH_2 maximum density is approximately 71 $kg\,m^{-3}$. As it can be depicted from Figure 4.23, the advantages of CcH_2 are more pronounced up to 20 MPa. At higher pressures, the increasing weight of the tank may not justify the slight increase in density. Typically, operating temperatures span between 30 K and 80 K, while pressures range between 100 bar to 300 bar [171].

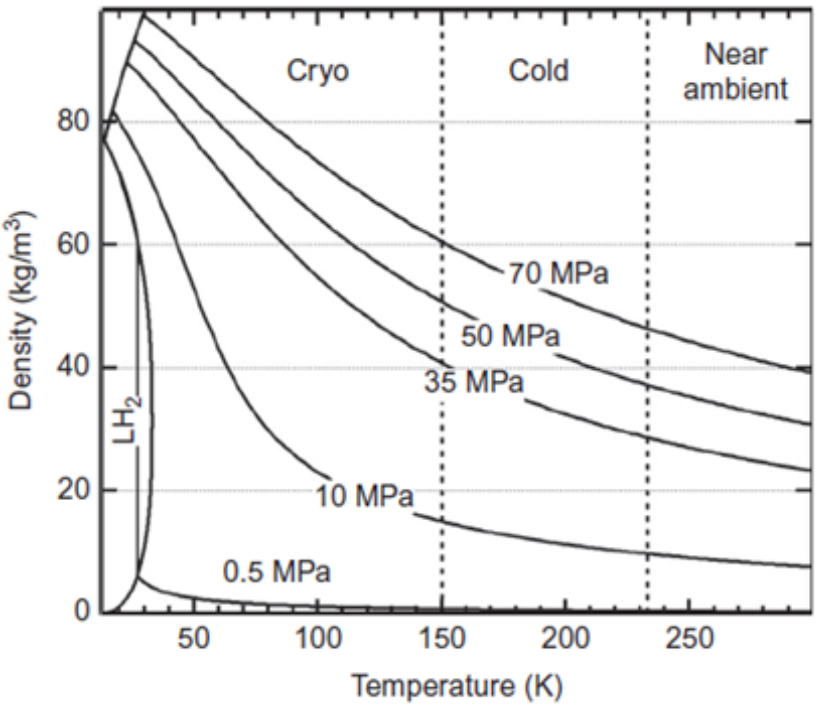

Fig. 4.23 CryoH2 density ([171]).

Practically speaking, CcH_2 vessels can be placed halfway between compressed and liquid hydrogen tanks. The large volumes required and the high pressures needed by the CH_2 tank are here reduced, while the issues related to boil-off losses are here overcome. Indeed, the vessel's capability to withstand high pressures allows

the internal pressure to increase without venting hydrogen, thereby extending the dormancy periods. Moreover, operating at lower pressures compared to CH_2 tanks, that usually operates at 350 bar or 700 bar, CcH_2 vessels requires composites and this turns into lower costs [114].
Another advantage of CcH_2 tanks derives from the fact that they are designed to both withstand relatively high pressures and to be thermally isolated. However, these systems may also be used to store CH_2 at room temperature, or LH_2 at environmental pressure, significantly enhancing the flexibility of CcH_2 tanks, which, in case of missing infrastructures, can be alternatively refuelled with gaseous or liquid hydrogen [171].
In addition, the production of CcH_2 requires approximately $10\,MJ\,kg^{-1}$, corresponding to 50% – 70% of the work needed for hydrogen liquefaction and to the work required to compress hydrogen to approximately 500 bar [190].

On the other hand, the presence of cyclic stresses generated by the combined effects of cryogenic temperatures and high pressures poses several challenges to the tank design. Apart from being capable of withstanding such stresses, CcH_2 tanks should accommodate more pronounced deformations. The building materials, which also encompass composites, should maintain their properties under any working conditions and for long-time periods, to ensure the tank safety and durability [171, 114]. There are studies investigating liner-less cryogenic vessels, as well as the application of graphene or carbon nanotubes based composites, but they are at a low maturity level [191, 192, 193].

Cryo-compressed hydrogen exhibits great potential worth further investigation. However, this technology is less mature compared to compressed and liquid storage. The scalability of CcH_2 is yet to be assessed, as well as the materials behaviour under cyclic cryogenic thermo-mechanical loads and hydrogen embrittlement phenomena. This is the main reason why CcH_2 will not be considered in the following analysis [109, 191, 194, 195].

Chapter 5

MBSE applied to hydrogen storage and distribution system for UAVs

In this chapter, the suitability of Systems Engineering for the design of UAVs is first explored (Sec. 5.1). Then, a conceptual path for the application of MBSE is delineated (Sec. 5.2). The core of the study starts with the examination of customer's needs (Sec. 5.3), followed by a simplified RFL analysis applied to the UAV, aimed at showing the design thread linking the very first step, i.e. the customer's needs, to the identification of the hydrogen storage and distribution system. The analysis applied to the UAV can be helpful both for understanding the methodology and for providing a more comprehensive analysis. Then, before continuing to apply MBSE to the H_2SDSys, a feasibility analysis to assess the possibility for retrofitting the Predator and the Global Hawk UAVs is proposed, together with the description of the Python parametric sizing model used to carry out the analysis (Sec. 5.5). The outcomes revealed that retrofitting activities would lead to UAVs exhibiting poorer performance with respect to their traditional configuration based on aviation fuel, thus addressing further analysis towards the design of entirely new aircraft concepts. Due to time constraints, the study proceeds with the application of the MBSE design path to the Predator UAV only (Sec. 5.6). The requirements have been elicited and managed, the functional analysis is deployed, the functional architecture is proposed, and the systems architecture is drawn. The outcomes of the dynamic analysis of the system are finally traced, providing interesting insights relevant for further design steps.

5.1 Systems Engineering for the design of UAVs

The UAVs are systems composed of several subsystems, and sub-systems part of a larger system, namely the Unmanned Aerial System (UAS). Formally, the UAS can be defined as "a group of coordinated multidisciplinary elements for an aerial mission by employing various payloads in flying vehicle(s)", while UAVs are "remotely piloted or self-piloted aircraft that can carry payloads" [38]. These systems nested inside other systems are defined in the literature as System-of-Systems (SoS). A SoS is defined as “a collection of systems, each capable of independent operation, that interoperate together to achieve additional desired capabilities.” [37]. Practically speaking, the UAS include multiple sub-systems, and one of them is the UAV. Regardless of the UAV type, all the UAS used for large UAVs such as MALE or HALE types share a series of main sub-systems [38, 34]:

- UAV
- ground control station
- payload
- launch and recovery system
- maintenance and support system

Actually, these systems can be seen as those to be designed or, at least, strictly needed to ensure that the UAS can operate.
A series of sub-systems can also be identified in the UAVs, which are typically composed of [38]:

- flight control subsystem,
- power transmission subsystem,
- fuel subsystem,
- airframe subsystem,
- propulsion system,
- landing system,

- payload.

Being UAVs complex systems characterised by high costs and high risk, they are an ideal candidate for the application of SE. Traditionally, this process involves starting with the definition of requirements, followed by functional analysis and allocation, design synthesis, and validation. The design should comprehend the whole life cycle of the system, properly applying SE principles, concepts, methodologies and tools. Moreover, the purposes must be clear from the beginning, and the product must be competitive in the market. The design should concurrently consider several factors, both concerned with the customer needs and life-cycle aspects, including manufacturing, testing, maintenance, logistics, costs, upgrades, decommissioning, satisfying requirements related to performance, stability, operational effectiveness, survivability, interoperability, autonomy, while complying with all the applicable standards [38, 196]. The risk of failure can be dramatically high when dealing with such complex systems, and the need to follow a well-structured procedure becomes imperative. This is why the application of MBSE, together with a rigorous methodology, a proper language, and suitable tools, is explored in the current study.

5.2 MBSE conceptual design path

The proposed MBSE design approach has been selected to satisfy the general customer's need for exploring the application of MBSE in an agile manner, to explore its potential, and to establish a preliminary, albeit general, framework for its application in the initial design phases capable of supporting the first interactions with stakeholders.
The concepts highlighted by the V diagrams (Fig. 5.1) have been primarily followed, along with practical guidelines proposed by the MagicGrid® framework (Fig. 5.2) [6, 197].

The design path followed can be better depicted in Fig. 5.3, somehow representing a combination of the two V diagrams in Fig. 5.1. The analysis starts from the customer's needs that cover both methodological aspects, related to the application of MBSE, and technological elements, concerned with the modelling of the hydrogen storage and distribution system. Then, in theory, the requirements, functional, logical, and physical analyses ("RFLP", V diagram on the left-hand side of Fig. 5.1) should

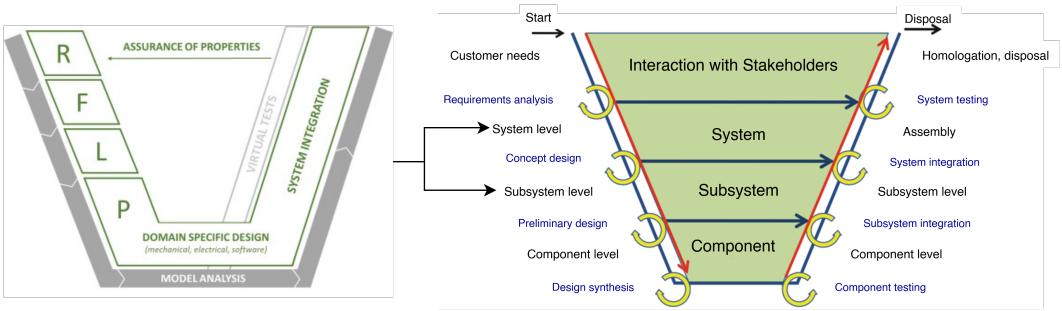

Fig. 5.1 Reference V-diagrams for MBSE product life cycle development [6, 198]

.

			Pillar				
			Requirements	Structure	Behavior	Parameters	Safety & Reliability
Domain	Problem	Black Box	Stakeholder Needs	System Context	Use Cases	Measures of Effectiveness (MoEs)	Conceptual and Functional Failure Mode & Effects Analysis (FMEA)
		White Box		Conceptual Subsystems	Functional Analysis	MoEs for Subsystems	Conceptual Subsystems FMEA
	Solution		System Requirements	System Structure	System Behavior	System Parameters	System Safety & Reliability (S&R)
			Subsystem Requirements	Subsystem Structure	Subsystem Behavior	Subsystem Parameters	Subsystem S&R
			Component Requirements	Component Structure	Component Behavior	Component Parameters	Component S&R
	Implementation		Implementation Requirements				

Fig. 5.2 Dassault MagiGrid® [197].

be applied at the system, subsystem, and component levels (blue label on the left side of Fig. 5.3). The desired level of detail, i.e., the granularity, depends on the objectives of each specific analysis. A black-box white-box approach is applied at each level of detail (grey and white areas within the analysis column in Fig. 5.3). The underlying logic of this approach can be easily understood from Fig. 5.4. Whenever a system, subsystem, or component is analysed, the black-box approach takes into account all aspects external to the system, such as scenarios, interfacing systems, actors, and stakeholders having any interaction with the object under analysis. In contrast, in the white-box approach, the box itself is somehow opened, and the internal elements composing the system are identified. The functions to be performed can then be allocated to the subsystems or to the components, which together compose the

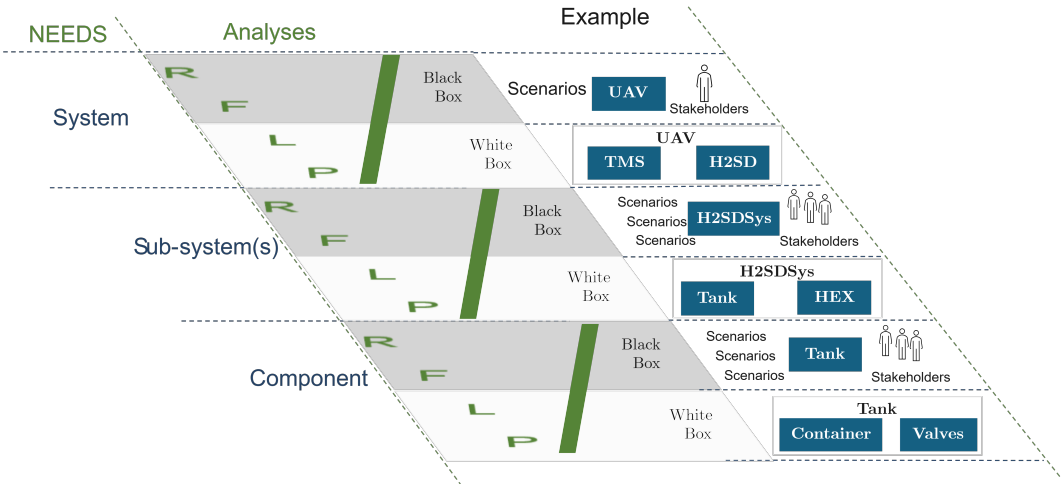

Fig. 5.3 MBSE design path.

system's architecture.

Summarising, the RFLP analyses are subdivided into black-box and white-box approaches, which are applied at each level of detail within the system. As the design progresses, new elements emerge, such as new requirements, functions, or actors, making the design path characterised by several iterations, which are indicated by yellow circular arrows in the V diagram on the right side of Fig. 5.1. An additional element of paramount relevance is the interactions between the left

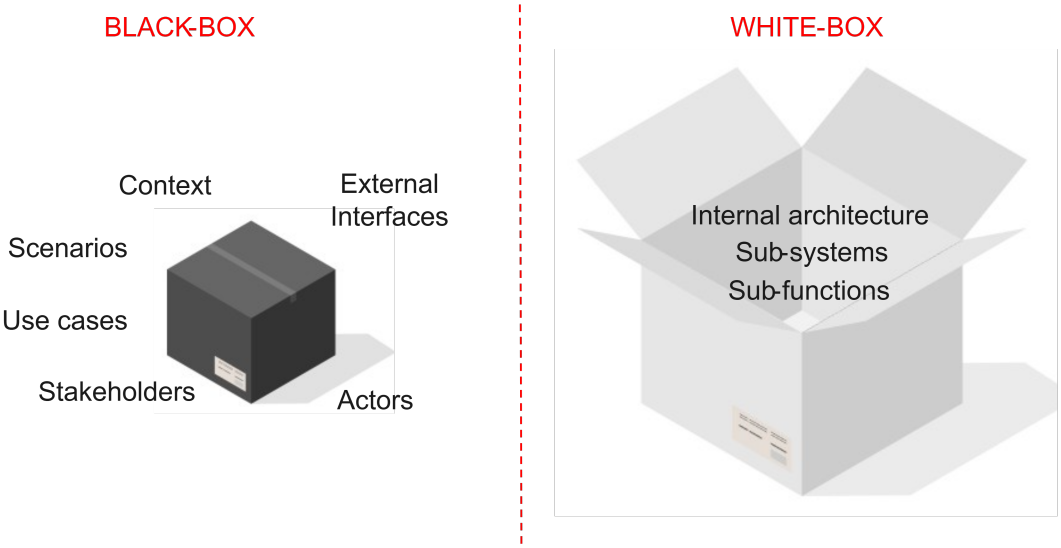

Fig. 5.4 Black-box white-box approach.

and right branches of the V diagram (horizontal arrows in the V diagram on the left

of Fig. 5.1). Indeed, among the various graphical representations of the life-cycle design that can be found in the literature, the V diagram emphasises the interactions between the left-branch, typically containing engineering design-related activities, and the right-branch, which includes production-related activities such as integration, prototyping, testing, manufacturing, homologation, and disposal. Such interaction is implemented in the current analysis through constant communication with other stakeholders, within the limits of the undertaken activities. A practical example can be depicted from Fig. 5.5, the author of the current analysis has been in charge of the H_2SDSys, and has been including into the analysis both requirements and constraints resulted by the activities conducted with a system supplier and with other systems engineers responsible for the other systems at the interface with the H_2SDSys, such as the thermal managements system (TMS).

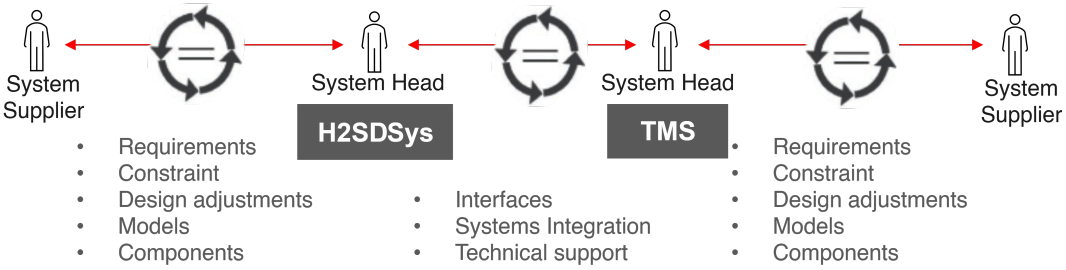

Fig. 5.5 Stakeholders iterative and concurrent interactions.

5.3 Customer's need

As just mentioned, the very first step of the analysis involves identifying the customer's needs and defining the objective of the study. Although the objectives will likely be revised and refined, it is essential at this initial stage to have at least a draft of the needs to provide a starting point. The first need can be depicted from the title of the doctoral activity itself:

System Engineering applied to the design of hydrogen storage and distribution systems for aviation.

The customer, i.e. Leonardo, is interested in a hydrogen storage and distribution system for airborne applications, and it expects the candidate to investigate the

technology and design the system applying Systems Engineering. Three main topics can already be identified: Systems Engineering, hydrogen storage, and aviation. However, this need is too general and further investigation is required. The customer has been interviewed to better understand his needs and priorities, and to guide him through a sort of negotiation process if his desires were unfeasible or inconvenient. A series of general questions were raised, such as:

- Which type of aerial platform do you want to investigate?
- Which relevance should be given to the environmental sustainability-related aspects?
- In which scenarios do you want your platform to work?
- Which types of mission should the platform perform?
- Which type of powertrains do you want to investigate?
- When do you want the platform to be ready?

The answers to such questions are definitely not independent of each other. Typically, in this context, the negotiation process just mentioned takes place through a discussion with a subject-matter expert who can guide the customer towards the best-fitting solution. For instance, the choice of a certain power-train constrains the polluting emissions produced during flight, while the choice of a specific platform can have a drastic influence on all subsequent activities.
Indeed, in the current analysis, the choice of an unmanned platform has been pushed by the author mainly due to the critical safety implications of storing hydrogen on board. Additionally, among the various unmanned platforms categories, the greatest potentials has been identified in large long-endurance UAVs, mainly due to the intrinsic properties of hydrogen having a high energy density, and to the fact that typically hydrogen storage system exhibit higher gravimetric efficiencies if a greater amount of hydrogen is stored, which is the case of long-endurance UAV that must store huge amounts of fuel with respect to their own weight. Despite the analysis focusing on hydrogen storage, some attention had to be given to UAVs strictly within the scope necessary for the design of the H_2SDSys. Essentially, the result of the discussion with the customer has been translated into a first need:

We want a UAV fully powered by hydrogen. The UAV should be multi-purpose, meaning that it should be capable of performing different tasks, such as observation and monitoring, transport, and defence. The UAV should be fully autonomous once programmed; for example, it should be capable of continuously communicating with the control station on the ground while also performing the mission autonomously and returning to the base if something unexpected occurs. It should be able to carry a payload and ensure sufficient endurance to remain competitive with existing and future technologies. It must be able to operate in any condition. The UAV we want is a MALE (Medium Altitude Long Endurance) type. We want the system to be compliant with the available standards. As this will be the first time we produce a full electric vehicle, we also want to use it to enhance our expertise over the next few years and validate the models we already have, as well as those we will develop.

Despite being rough and somehow incomplete, this need enables the identification of several key elements, providing relevant information on the customer's expectations. Indeed, satisfying such a need involves acquiring relevant knowledge about the technology of interest and, simultaneously, ensuring the possibility of manufacturing a prototype within the next few years, which in turn means selecting among the various solutions those that have an acceptable level of maturity. In the following analysis, a set of requirements, including aspects that emerged from the customer interview will be proposed.

5.4 RFLP analysis: UAV

As mentioned above, the modelling activity related to the UAV is limited to those elements strictly needed for the design of the hydrogen storage and distribution system. However, for the sake of completeness, a simplified thread linking the very first customer's need to the beginning of the design of the H_2SDSys is also shown to provide a practical example of the MBSE design path mentioned in Section 5.2.
Some system-level requirements, which, in the aviation sector, are typically referred to as top-level aircraft requirements, are reported in the requirements table (Fig. 5.6). It can be observed that a hierarchy exists among requirements. Indeed, certain requirements are created solely to serve as containers for others. For instance, in the first row, the "TLAR" serves as a container for all the top-level aircraft requirements, i.e., the TLAR themself. All the requirements are general and cover

various aspects, such as the environment of operation, the payload that the UAV shall carry, communication, reliability, and autonomy aspects. The problem is viewed from a black-box perspective, and indeed, this point of analysis can also be located on the MagicGrid® at the intersection of the "Problem"-"Black Box" domain row and the "Requirements" column (top-left yellow rectangle in Fig. 5.2, Sec. 5.2). Not all requirements are included for brevity, but a preliminary review of their consistency and a check on the congruence of their level of detail have been conducted to ensure similar granularity. Since certain requirements are not directly relevant to the scope of this work, they have been deliberately left incomplete, but have been reported to ensure that no aspect is unintentionally omitted if further design phases will eventually be conducted.

After deriving a first set of requirements starting from the customer's needs and from the review of the literature, a number of stakeholders and actors have been included in the context diagram (Fig. 5.7), which has been modelled through an internal block diagram, even though it can also be represented using a use case diagram. The basic rule followed in the current analysis to build the context diagram is to include any stakeholder who has any direct interaction with the system. In addition, it can be observed that there is a stereotyped symbol of a person inside the rectangles of the pilot, of the birds, and of the maintenance personnel. This symbol is used in the current analysis when the stakeholder is an actor. The dashed line surrounding the central block representing the SOI is just a graphical addition to highlight the system under analysis. The primary purpose of the context diagram is to group all stakeholders interacting with the SOI within a single diagram, but if the system grows significantly, more than one context diagram may be used to improve readability. Stakeholders can interact with the system through various usages, which are formalised as use cases.

One use case will be explored here (Fig. 5.8). The Interaction between the pilot and the UAV can occur in various forms under different scenarios. However, in practice, it is always true that the pilot should control the aircraft, which can involve steering it, issuing commands to perform specific operations, or controlling its speed and direction. This latter activity, included in the use case "control the aircraft", has been detailed through the activity diagram "change speed and direction" (Fig. 5.9) that, indeed, is directly linked to the use case control the aircraft.

Name	Text
22 TLAR	The aircraft shall satisfy the Top Level Aircraft Requirements
22.1 STOL	The UAV shall possess Short Take-Off and Landing (STOL) capabilities
22.2 Flight	The UAV shall fly
22.3 Mission	The aircraft shall satisfy the mission requirements
22.4 Environment	The UAV shall operate under any environmental condition
22.4.1 Day_Night	The UAV shall be capable of operating under day and night
22.4.2 Weather	The UAV shall operate under any weather condition
22.5 Payload	The UAV shall carry the Payload
22.6 Communication	The UAV shall communicate with dedicated stakeholders
22.6.1 Sensor_Integration	The UAV shall integrate all the necessary sensors
22.7 Survivability	The UAV shall hold enenched features to survive to any hostile scenario
22.7.1 Countermeasures	If events of any kind occur, the UAV shall apply countermeasures.
22.8 Standards	The UAV shall be compliant to all the relevant standards.
22.8.1 Airworthiness	The UAV shall satisfy Airworthiness requirements
22.9 Reliability	The UAV shall be reliable
22.9.1 Mainteinance	The UAV shall be desinged to comply with mainteinance requirements.
22.9.2 Redundancy	The designer shall ensure critical systems redundancy.
22.10 Energy_Storage	The energy shall be stored through specified sources
22.10.1 H2_Storage	The primary energy storage shall be based on hydrogen
22.11 Competitiveness	The UAV shall be competitive
22.11.1 Cost	The UAV shall be cost efficient and cost effective
22.12 Autonomy	The UAV shall be able to perform tasks fully automously.
22.13 Multi-purpose	The UAV shall be multi-purpose
22.14 Stealth	The aircraft shall exhibit stealth capabilities
22.15 Flight_Performances	Te aircraft shall exhibit the required flight performances

Fig. 5.6 Top-level aircraft requirements.

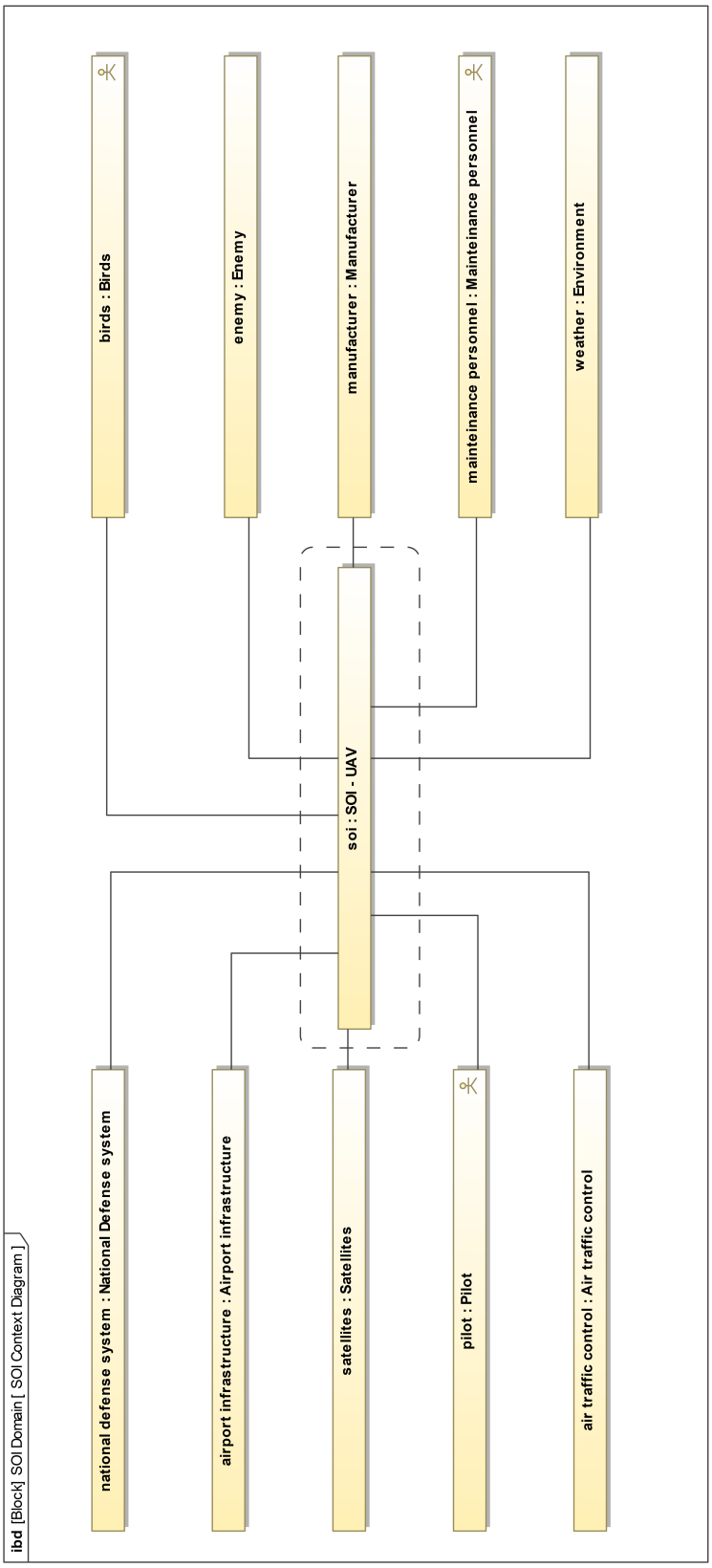

Fig. 5.7 UAV system context diagram.

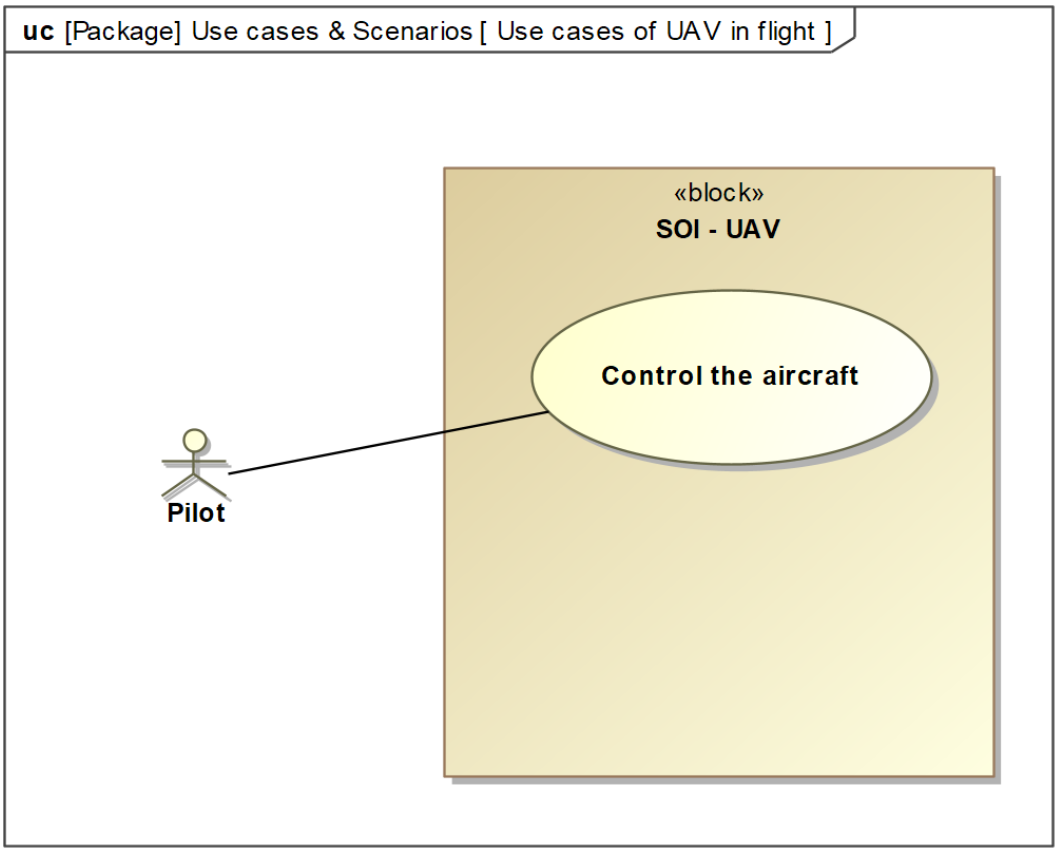

Fig. 5.8 UC diagram.

The AD in Fig. 5.9 contain itself actions and information detailing the "change speed and direction activity". The diagram starts from the black circle when the aircraft's speed is detected. The desired speed, received as an external input, is compared with the actual speed. On the left side of the image, the direction is corrected if needed, while on the right side, the speed is controlled by adjusting the power supply. Ultimately, the information on the aircraft's speed is newly detected and transmitted as "real flight data". Actually, it must be mentioned that this diagram was created for demonstrative purposes, once the UAV configuration was already selected. Upon careful observation of the AD, it can be noted that to compute the corrective manoeuvres, the control surfaces are adjusted, while to change the aircraft speed, the power is regulated. These two aspects alone narrow the range of possible solutions, assuming that the direction will be controlled through the control surface and the speed through the power supply. At this point, the UAV should be seen as a black box, and its subsystems should be unknown. However, it must be mentioned

that MBSE can also be applied to an existing system, for example, to create an upgraded version of the SOI. At this point in the analysis, these details are of lesser importance with respect to the objective previously mentioned, which is to show how the customer's needs and the H_2SDSys are linked through MBSE.

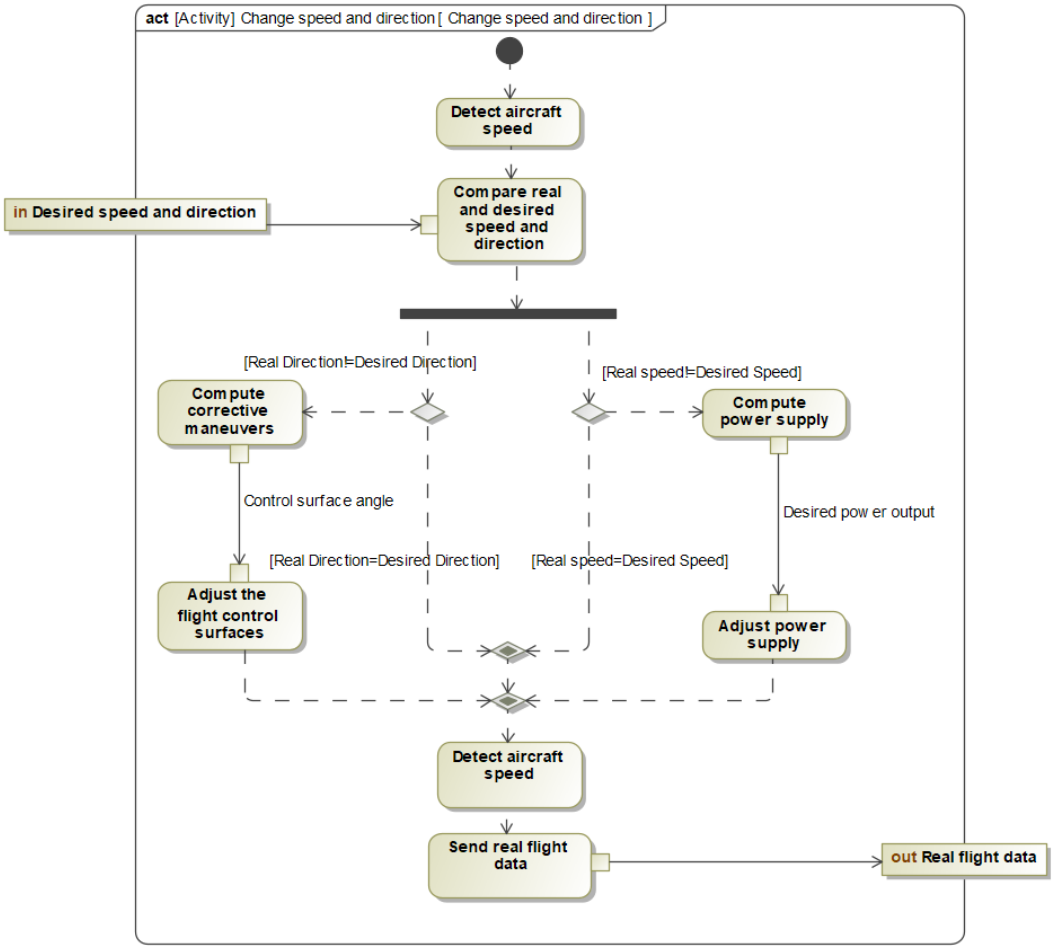

Fig. 5.9 AD diagram.

Once the various use cases are explored and several activities are identified, the activity decomposition map can be created (Fig. 5.10). At this point, the analysis is situated close to the border between black-box and white-box approaches. Functional blocks are identified, and a functional architecture can eventually be created.

Nonetheless, at this point, the functions have been directly connected to logical blocks that perform these functions. A simplified BDD has been reported, showing the three logical blocks composing the UAV. The "flight control system" manages

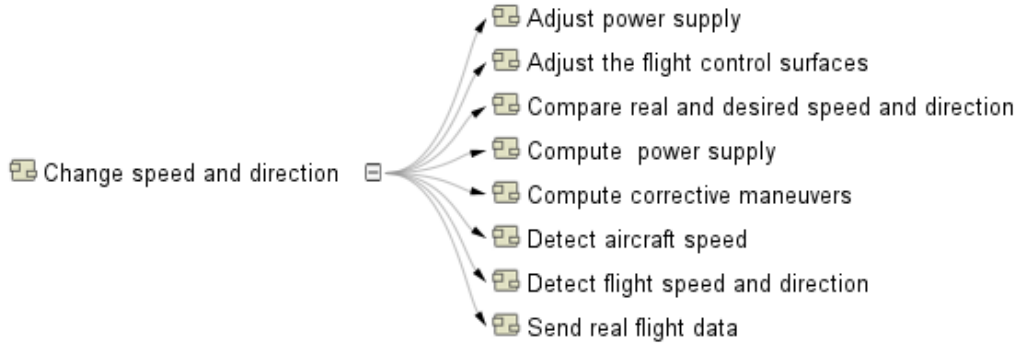

Fig. 5.10 Activity decomposition map.

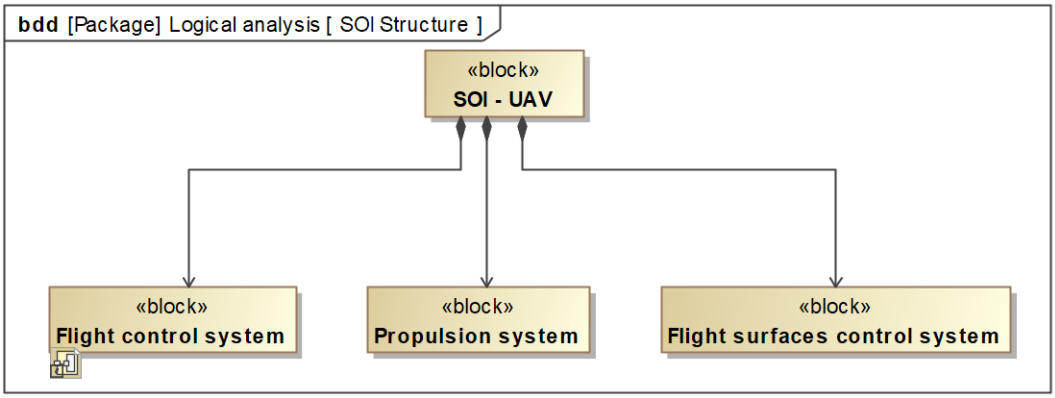

Fig. 5.11 Partial UAV logical structure.

and elaborates the information exchanged, the propulsion system is responsible for supplying power, and the flight surface control system must physically move the flight surfaces whenever needed. The propulsion system contains the hydrogen storage and distribution system, which will be analysed in the following section.

5.5 Preliminary feasibility analysis

Before developing a broader analysis using the MBSE approach previously described, it was considered useful to design a parametric sizing model to explore possible solutions and obtain preliminary quantitative results to assess the technical feasibility of the proposed solutions. Thus, a parametric sizing model has been developed in Python and will be introduced in the following (Sec. 5.5.1). Then, a brief investigation of materials properties at cryogenic temperatures is presented (Sec. 5.5.1).

Finally, the model is applied to the use case of the Predator and the Global Hawk UAVs to assess the feasibility of a retrofitting activity (Sec. 5.5.3).

5.5.1 Hydrogen tank parametric sizing model

The hydrogen tank parametric sizing model structure and capabilities have already been described in the literature [199]. However, it can be helpful to introduce it here, briefly emphasising its architectural and programming aspects, which have been less covered in the literature.

The sizing model has been created in Python according to object-oriented programming (OOP) guidelines. In brief, OOP is based on four fundamental principles [200]:

1. Abstraction: representing complex concepts through simplified models built upon classes which describe the objects under analysis, highlighting their main properties and characteristics.

2. Encapsulation: nesting properties and behaviours of the objects under analysis, allowing and controlling the access of only those needed to reduce complexity and improve clarity.

3. Inheritance: the principle according to which one class can inherit the properties and behaviour of another class, allowing the reuse and ordered hierarchical structuring of large models

4. Polymorphism: the capability of using a single operation, method, or interface in different ways depending on the object that implements it.

It can be difficult to grasp the importance of these four OOP principles immediately. However, their meaning and advantages will be illustrated in the following explanation of the hydrogen tank sizing model.
Looking at Fig. 5.12, it can be seen that the structure of the tank sizing model is made of three main design classes (in red), three tank design classes (in blue), three additional design classes (in orange), and two properties databases (in green). The three red classes can be seen as the three pillars of the model. The *HydrogenTankGeometry* class encloses all the geometrical parameters and formulas that allow for

the computation of various tank dimensions, including diameter, length, height, and surface area, for cylindrical tanks with hemispherical or ellipsoidal domes, even if a vessel geometry can also be created by accessing only two parameters (abstraction). Additionally, regardless of the dome type selected, this class allows for the generation of a three-dimensional mesh of the vessel that can even be refined (polymorphism). All these parameters and capabilities are also possessed by *HydrogenTankMechanics* (inheritance), as indicated by the arrow pointing from *HydrogenTankMechanics* to *HydrogenTankGeometry*. The other two main classes, *HydrogenTankMechanics* and *HydrogenTankThermal*, contain all the parameters needed to perform the structural and thermal analyses in the cases of compressed cryo-compressed and compressed hydrogen. The *HydrogenTankMechanics* inherits the features of the *MaterialsDF* and the *CryoMaterialsEquations*. The latter two classes are necessary to retrieve information from the two materials databases, which, for ease of use, were created in Excel. The *OptiClass* linked to *HydrogenTankThermal* has been created to perform a constrained optimisation whenever the number of equations of the system to be solved is lower than the number of unknowns. This occurs when the thickness of one or more thermal layers has to be computed. The minimum and maximum thickness values can be set for each layer, as well as the desired materials and the optimisation goal, which is set by default to find the solution leading to the highest gravimetric index. All these parameters and methods (as the functions contained in a class are formally referred to) are inherited by the three blue classes, which are the ones the user interacts with directly. These three classes are designed with one or a few methods which encapsulate all the others needed to perform the design, which have been inherited from upper-level classes (encapsulation). For instance, to perform the sizing of a liquid hydrogen tank, the user will only access the *HydrogenTankThermal*. Selecting a few parameters, such as the mass of hydrogen to be stored, the structural and insulating materials, the desired boil-off rate, and the tank diameter, and executing only one method ("compute_tank_sizing()"), the sizing will be performed. The model automatically retrieves the materials data and the equations needed from all the inherited classes and provides a full set of tank properties.

To provide an overview of the complexity of the three main classes used in the design (highlighted in red in Fig 5.12), and thereby illustrate how the proper application of the four principles of OOP can be beneficial, the list of properties and methods contained in classes *HydrogenTankGeometry*, *HydrogenTankMechanics*, and *HydrogenTankThermal* is presented in Fig. 5.13.

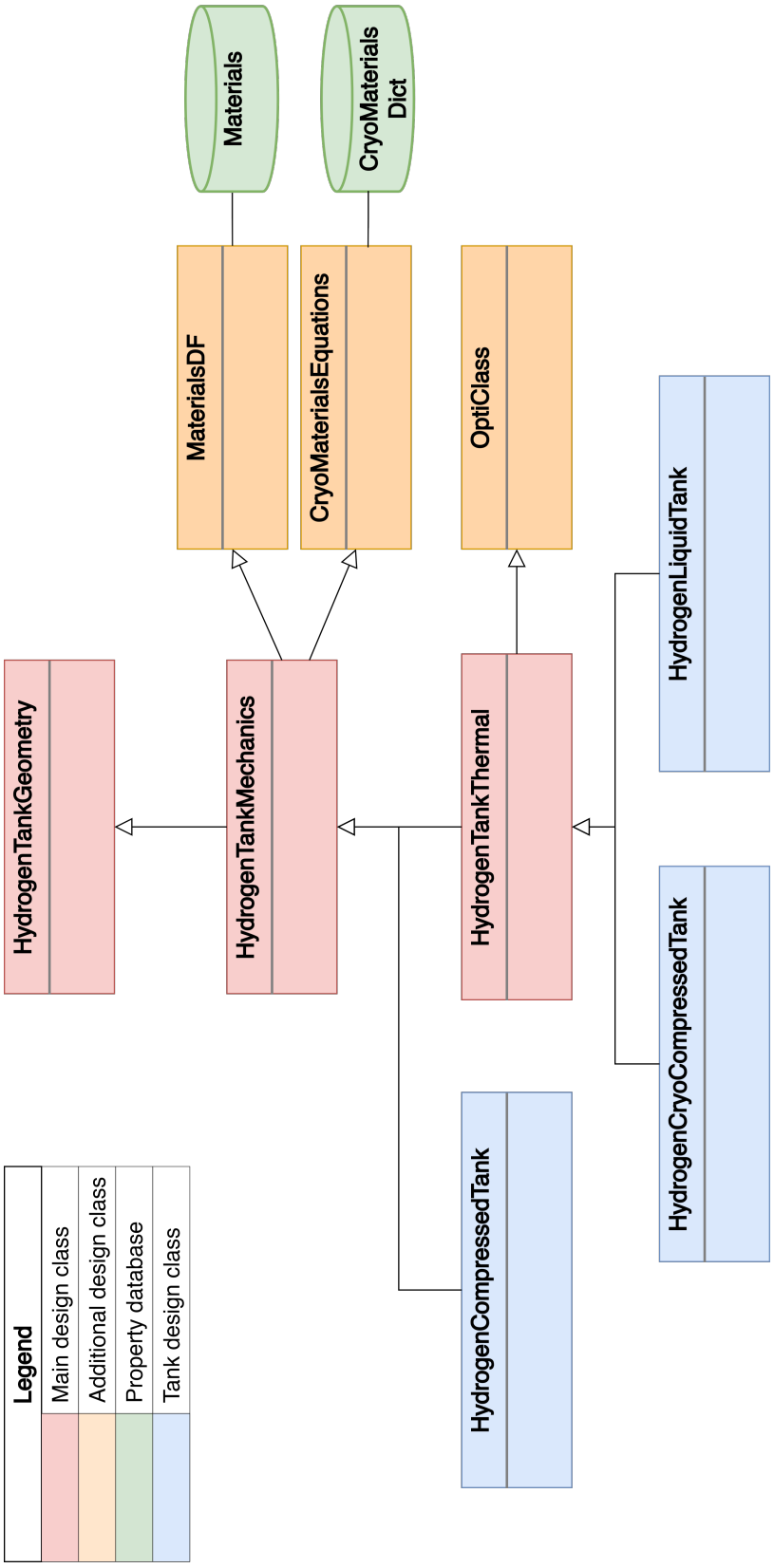

Fig. 5.12 Hydrogen tank parametric sizing model structure.

The *HydrogenTankGeometry* class contains 22 attributes and six methods, while the *HydrogenTankMechanics* class contains 49 attributes and 19 methods. The *HydrogenTankThermal* class contains 28 attributes and 34 methods. It is worth noting that the methods created can contain a single equation or a few equations. In principle, this aligns with the OOP logic, which suggests that it is preferable to have a higher number of simpler functions rather than a lower number of more complex functions.

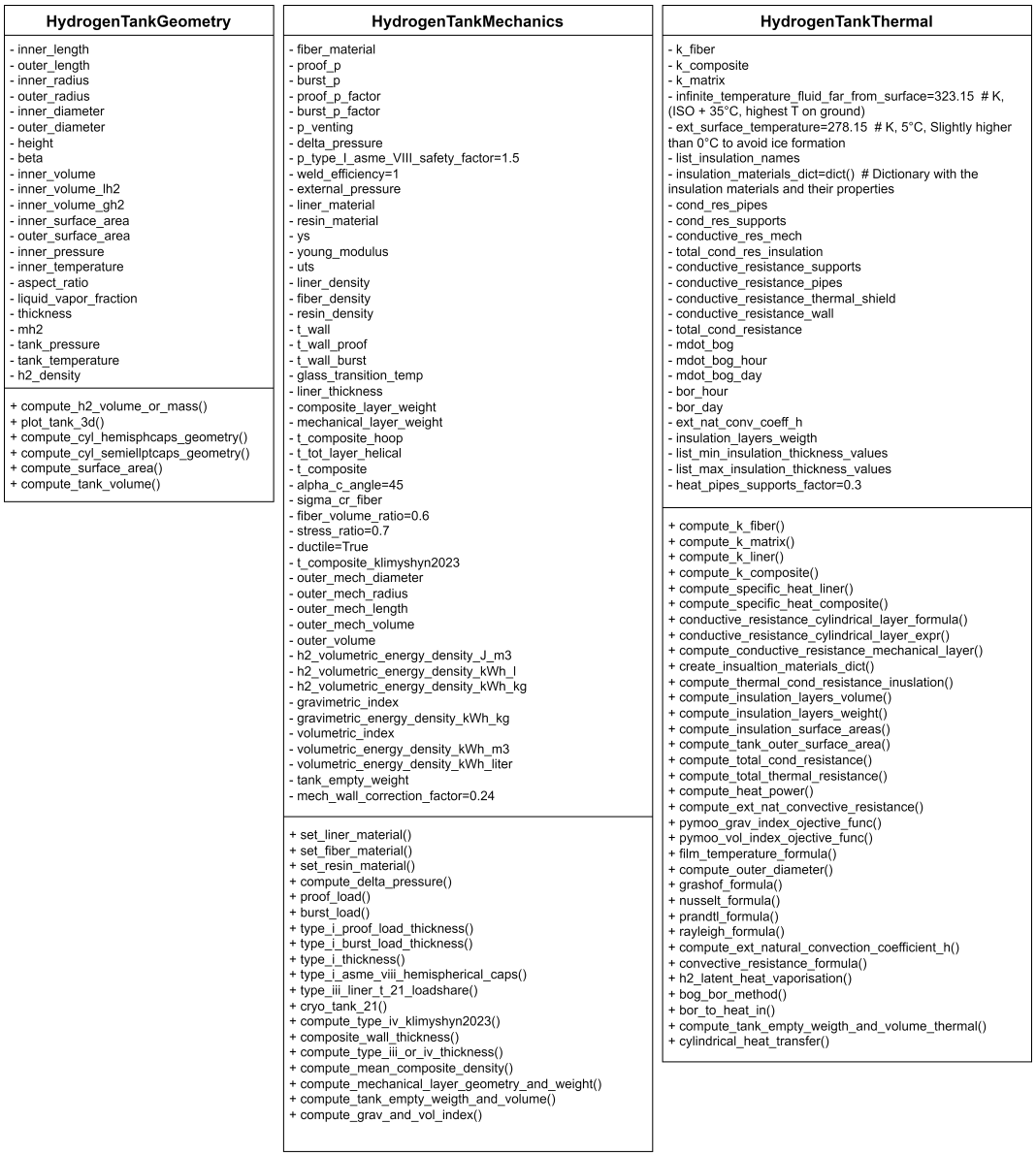

Fig. 5.13 Geometrical, mechanical, and thermal classes attributes and methods.

The architectural description of the model provided above highlights the more programming-oriented aspects and should be considered complementary to the more engineering-focused perspective available in the literature [199].

Materials analysis

As already highlighted in Ch. 4, the selection of materials is a critical step that directly affects mechanical integrity, thermal stability, hydrogen compatibility, and overall system efficiency. However, in addition to the considerations that have already been made in Sec. 4.4 and in the articles published in the literature ([199, 201]), it was considered of particular interest to show and discuss the materials included in the dedicated database and, most importantly, to investigate how the properties of certain metals, that are typically employed in direct contact with hydrogen, are affected by cryogenic temperatures.

The metal alloys and polymers considered in the mechanical analysis are reported in Table 5.1 and Table 5.2. The behaviour of metallic alloys is typically well-known, and their usage at cryogenic temperatures can be preferred over polymers because, regardless of their behaviour, they do not undergo a ductile-to-brittle transition. Among the metal alloys, aluminium alloys are the most commonly adopted in aviation due to their good balance between strength and lightweight. In addition, many materials become embrittled when exposed to hydrogen and aluminium alloys exhibit minimal susceptibility to H_2 embrittlement. Among those shown in Tables 5.1 and 5.2, Al 6061 is typically used for pressure vessels in the nuclear industry, Al 5086 has been recommended by NASA and it was chosen in the Cryoplane project. At the same time, Al 2219 has also been suggested by Air Liquide and used in projects to store liquid hydrogen. Al 5083-O has also been identified as a good candidate for storing hydrogen at cryogenic temperatures due to its excellent properties, its good weldability, its slightly lower density compared to the other aluminium alloys, and its low sensitivity to hydrogen-induced corrosion, and it will be used in the following analysis [183, 202]. In addition, a 5 mm thickness layer of polymeric material HDPE UHMW will be applied as an external humidity barrier to avoid environmental air penetrating the insulation layer.

Analogously to what has been done for structural materials, also the insulating materials included in the *Materials* database are reported in Table 5.3. Thermally insulating the storage tank is crucial to guarantee an efficient storage system, to limit

Table 5.1 Structural materials mechanical properties.

Name	Density	UTS	YS	Elongation at break	Modulus of Elasticity	Poisson Ratio	Fatigue Strength	Shear Modulus	Shear Strength	Ref.
	(kg/m^3)	(MPa)	(MPa)	(%)	(GPa)	(-)	(MPa)	(GPa)	(MPa)	
Al 6061-O	2700	124	55.2	25	68.9	0.33	62.1	26.0	82.7	[203]
Al 6061-T6	2700	310	276	17	68.9	0.33	96.5	26.0	207	[203]
Al 5083-O	2660	290	145	25	71.0	0.33	150	26.4	172	[203]
Al 5086-O	2660	262	117	30	71.0	0.33	145	26.4	159	[203]
Al 2219-T87	2840	476	393	10	73.1	379	103	27.0	280	[203]
SS 304	8000	505	215	70	193	0.29				[203]
SS 316	8000	565	250	55	193					[203]
Ti6Al4V	4430	860	790	15	113.8	0.342	140	44.0	550	[203]
PTFE	2170	25.6	131	336	0.599	0.46				[203]
HDPE UHMW	953	36.0	19.6	247	0.715				33.0	[203]
ETFE	1730	41.5	17.0	444	1.48					[203]
PFA	2150	27.1		314	0.519					[203]
PCTFE	2040	36.9		164	1.48					[203]
PI	1360	97.9	103	25.5	6.08	0.37	21.4		90.5	[203]
Carbon fiber	1760	3530		1.5	230					[204]
Delrin	1380									[126]
Epoxy	1350	33.1	563	9.35	35.2	0.389		3.2	80.1	[203]

Table 5.2 Structural materials thermal properties.

Name	CTE linear (μm/mK)	Specific Heat (J/gK)	Thermal conductivity (W/mK)	Mimum Service Temperature (°C)	Brittleness Temperature (°C)	Tg (°C)	Ref.
Al 6061-O	23.6	0.896	180				[203]
Al 6061-T6	23.6	0.896	167				[203]
Al 5083-O	23.8	0.900	117				[203]
Al 5086-O	23.8	0.900	125				[203]
Al 2219-T87	22.3	0.864	121				[203]
SS 304	17.3	0.500	16.2				[203]
SS 316	16.0	0.500	16.3				[203]
Ti6Al4V	8.6	0.5263	6.7				[203]
PTFE	294	1.50	0.292	-270			[203]
HDPE UHMW	159	1.82	0.428	-269	-70	-120	[203]
ETFE	103	1.18	0.179		-76		[203]
PFA	143	1.02	0.230	-200			[203]
PCTFE	58.7	0.920	0.207	-273			[203]
PI	40.9	1.02	0.367			-20	[203]
Carbon fiber	-0.41		10.5				[204]
Delrin		1.47	0.330				[126]
Epoxy	64.7		0.440	-62		123	[203]

Acronyms: PTFE = Polytetrafluoroethylene; HDPE UHMW = High-Density Polyethylene Ultra-High Molecular Weight; ETFE = Ethylene Tetrafluoroethylene; PFA = Perfluoroalkoxy Alkane; PCTFE = Polychlorotrifluoroethylene; PI = Polyimide.

the boil-off rate to acceptable values and overall, to increase the operational capabilities of the whole aircraft. Insulating foams, such as polystyrene, polyurethane, and polymethacrylimide, are well-assessed solutions which can provide low thermal conductivity values and are widely used in several applications where the volume and weight requirements are not stringent. In contrast, more innovative solutions rely on the use of aerogels and multilayer insulation (MLI), which hold thermal conductivities in the order of $0.0006\,\mathrm{W\,m^{-1}\,K}$ when vacuum is also used. These materials, though fragile and costly, are indispensable in a tank used in an aerial vehicle where minimal thermal losses are required. Unlike the approach adopted for selecting the structural metal alloy, no thermal insulator has been preselected in this case. In the following analysis, the use of various thermal insulation materials will be compared, and their impact on system performance will be quantitatively assessed.

As previously mentioned, it may be worthwhile to mention an aspect that is typically less explored in the literature, both due to simplifying assumptions that often make a more detailed investigation unnecessary, or due to the limited experimental data available in the literature. However, analysing the variation in the properties of certain metal alloys allows us to assess whether assuming constant material properties during the design of the storage system is a reasonable assumption. The cryogenic properties of the materials available from the NIST databases have been reported in Table 5.4, and used to trace the following charts. Al 5083-O, Al 6061-T6, stainless steels 304 and 316 are the only alloys for which data related to all four properties is provided (in bold in Table 5.4). However, properties of other alloys will be represented if available. The limited data available, especially referring to the Young's Modulus, hinders the possibility of verifying if assuming constant material properties during the design of the storage system is a reasonable assumption. In practice, the Young's Moduli of Al 5083-O, Al 6061-T6, Stainless Steel 304, and Stainless Steel 316 are lower at environmental temperature, thus assuming it is constant and equal to the value at environmental temperature ensures that the structure can withstand the required load also at cryogenic temperatures. In contrast, the same assumption cannot be verified for other materials, limiting the reliability of the analysis. The temperature range considered for all the properties spans from approximately 20 K up to 300 K.

Looking at Fig. 5.14, the thermal conductivity of stainless steels, titanium, and Inconel can be assumed constant. In contrast, for aluminium alloys, variations in

Table 5.3 Insulating materials properties.

Type	Name	Density (kg/m^3)	Thermal conductivity (W/mK)	Operating pressure (Pa)	roh · k	Bib. Ref.
Polystyrene foam	PS	25.6	0.03		0.768	[75]
Polymethacrylimide foam (PMI)	PMI	51.1	0.021		1.0731	[75]
Polyurethane foam (PRU)	PRU	32	0.015		0.48	[75]
Expanded perlite	Perlite	16	0.052		0.832	[205]
Silica aerogel	Silica aerogel	122	0.025		3.05	[205]
Fiberglass	Fiberglass	50	4.00E-02		2	[182]
Glass Bubble	Glass Bubble	230	0.13		29.90327	[206]
EPS spray-on foam	EPS	26	0.02594		0.674346	[206]
Polyvinilchloride	Polyvinychloride	49.7	0.015		0.7455	[186]
Rohacell® 41S	Rohacell	51.1	0.0311	1.01E+05	1.58921	[77]
Polyurethane	PU	40	0.0245	101325	0.98	[205]
Aerogel/Glass Fibre	Aerogel_low_p	125	0.0033	100	0.4125	[77]
Aerogel/Glass Fibre	Aerogel_very_low_p	125	0.0006	1.00E-02	0.075	[77]
High Density Aerogel	HD_Aerogel	41.8	0.035	101325	1.463	[77]
High Density Aerogel	HD_Aerogel_low_p	41.8	0.0175	1.00E-02	0.7315	[77]
Perlite powder	Perlite_low_p	128	0.016	100	2.048	[77]
Perlite powder	Perlite_very_low_p	128	0.0015	1.00E-02	0.192	[77]
MLI Mylar/Dacron	MLI_MD	40	0.035	101325	1.4	[77]
MLI Mylar/Dacron	MLI_MD_low_p	40	7.00E-05	1.00E-04	0.0028	[77]

Table 5.4 Cryogenic properties of materials available from NIST.

	Thermal conductivity (W/(m-K))	Specific Heat (J/(kg-K))	Young's Modulus (GPa)	Linear expansion (-)
Al 1100	X			
Al 3003-F	X	X		X
Al 5083-O	**X**	**X**	**X**	**X**
Al 6061-T6	**X**	**X**	**X**	**X**
Al 6063-T5	X			
Fiberglass Epoxy G-10	X	X		X
Glass Fabric/polyester	X			X
Glass mat/epoxy				X
Inconel 718	X			X
Kevlar-49 Fiber	X			
Kevlar-49 Composite	X			
PET (Mylar)	X			
Polyimide (Kapton)	X	X		
Polystyrene	X	X		X
Polyurethane	X	X		X
Polyvinyl Chloride (PVC)	X	X		X
Stainless Steel 304	**X**	**X**	**X**	**X**
Stainless Steel 316	**X**	**X**	**X**	**X**
Teflon	X	X		X
Ti-6Al-4V	X			X

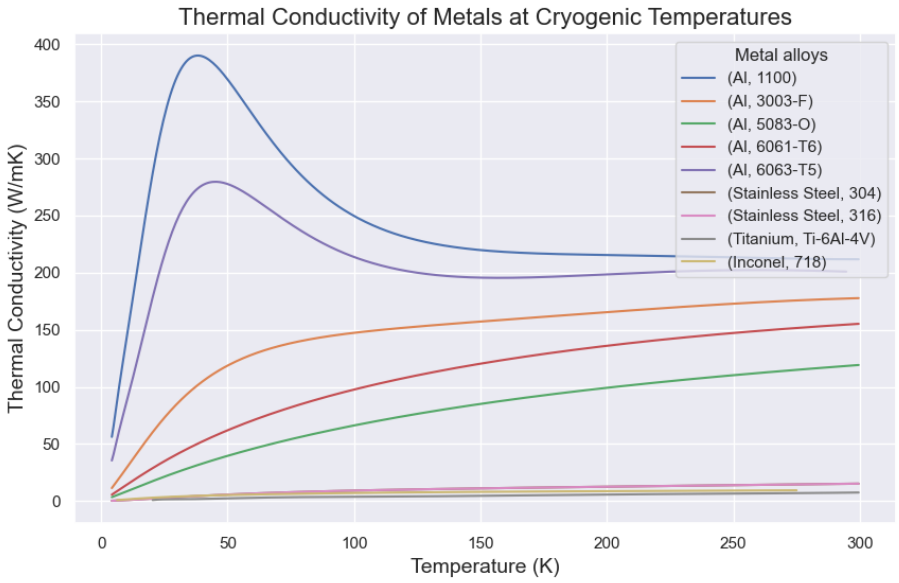

Fig. 5.14 Thermal conductivity of various metallic alloys at cryogenic temperatures [207].

the thermal conductivity up to almost two orders of magnitude can be observed. In general, the thermal conductivity increases with increasing temperature. However, the trends exhibited for Al 1100 and Al 6063-T5 increase steeply from around 50 $\mathrm{W\,m^{-1}\,K}$ up almost 400 $\mathrm{W\,m^{-1}\,K}$ and 275 $\mathrm{W\,m^{-1}\,K}$ at a temperature near 40 K, respectively. Then, the trends decrease until 150 K when the thermal conductivity of the two alloys stabilises around a constant value of approximately 200 $\mathrm{W\,m^{-1}\,K}$.

Considering the similarity between them, the linear expansion coefficients have been reported for each alloy family rather than for each individual alloy (Fig. 5.15). Aluminium is again the material showing the highest variation over the temperature range. However, all the materials in this case should be carefully considered since, even in the best case when titanium is selected, the value of the linear expansion coefficient ranges from zero to less than $-150\,\mathrm{K^{-1}}$.

Data on the Young modulus were only available for four alloys (Fig. 5.16). The Young modulus increases with decreasing temperature, even if for stainless steel 304, a sort of step can be observed at about 50 K. Overall, for stainless steel 304 and 316, the Young modulus is approximately between 190 GPa and 220 GPa. Analogously, the Young modulus of Al 5083-O and Al 6061-T6 increases in value, ranging from approximately 70 GPa to SI80. To improve readability, the Young's modulus of

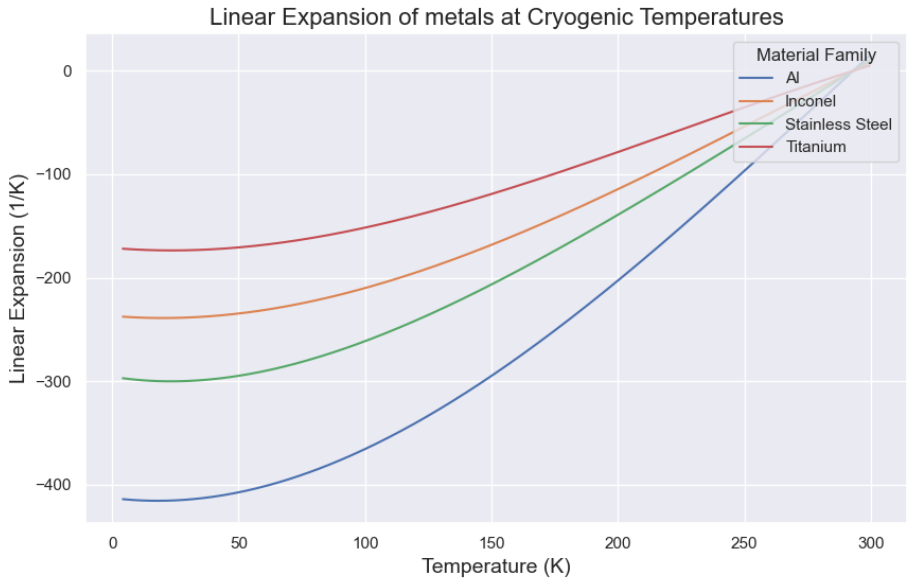

Fig. 5.15 Linear expansion coefficient of aluminium, stainless steel, Inconel, and titanium alloys at cryogenic temperatures [207].

the two aluminium alloys has been isolated and presented in Fig. 5.17. The trends shown are almost linear and approach constant values at temperatures below 50 K.

Overall, aside from the specific behaviour observed in the thermal conductivity of the aluminium alloys Al 1100 and Al 6063-T5, it can generally be stated that, as temperature increases, thermal conductivity tends to increase, the linear thermal expansion coefficient increases while approaching zero, and the Young's modulus decreases. This implies that assuming metal properties at room temperature generally sets the design on the safe side in terms of the thermal conductivity and the Young modulus, since, typically, the worst case scenario when performing a structural sizing is given when the materials exhibit the lowest structural properties, while for the thermal design it corresponds to the condition leading to the highest heat influx. So, in the case of static design, the lowest Young modulus and the highest thermal conductivity values should put the designer on the most cautious side. The linear expansion should be carefully considered in relation to the other materials composing the vessel to assess the overall compatibility among the selected materials, even though a thermal expansion coefficient closer to zero should lead to less pronounced deformations that may lead to a solution that is less complex to manage. However,

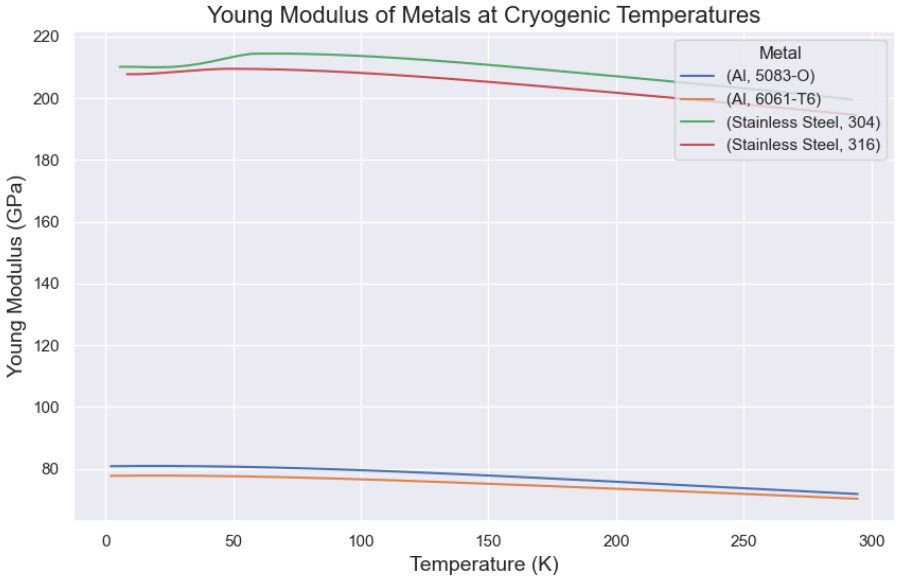

Fig. 5.16 Young's Modulus of aluminium and stainless steel metallic alloys at cryogenic temperatures [207].

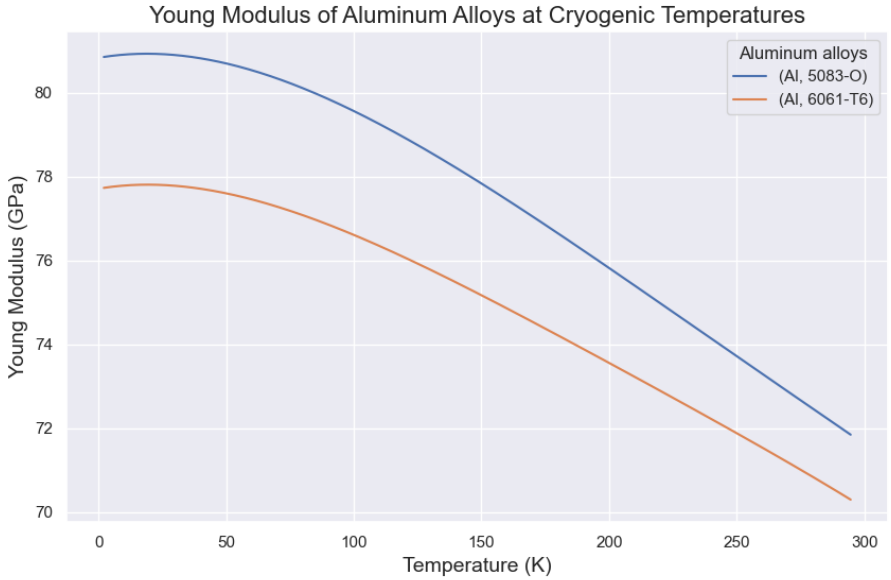

Fig. 5.17 Young's Modulus of Al 5083-O and Al 6061-T6 alloys at cryogenic temperatures [207].

without additional information, the conclusions that can be drawn in terms of thermal expansion remain highly general.

5.5.2 Hydrogen tank model validation

A validation of the model, performed relying on experimental data, was unfeasible due to the absence of a testing facility. However, in the analysis previously published, the outputs of the model for compressed and liquid hydrogen storage have been compared with data retrieved from an extensive research in the literature [199, 201]. To further improve the reliability of the sizing model, a set of data has been derived from publicly available sources, including websites, technical brochures, and product catalogues of manufacturers specialising in pressure vessels for compressed hydrogen storage, as part of the current analysis. These specifications have been reported in Table B.1 (appendix B), and plotted in Fig. 5.18 and Fig. 5.20. It is necessary to specify that only data related to Type III and Type IV CH_2 tanks have been collected. These types are lightweight and well-established industrial technologies, and are the only ones commonly used in the mobility sector. In contrast, Type I and Type II tanks are typically heavy and used for stationary storage, while data for Type V tanks refer to prototypes or less mature technologies rather than commercial products. An analogous attempt has been made to collect data about liquid hydrogen storage. However, due to the lower technological maturity and the limited number of manufacturers, it was not possible to collect data. Thus, a validation of the model against commercial data has been conducted for compressed hydrogen storage only.

Looking at Fig. 5.18, it can be observed that the Type III tanks working at 700 bar always exhibit a higher gravimetric index than those working at 350 bar. Type III vessels storing hydrogen at 700 bar have a gravimetric index between 6% and 8%, while those operating at 350 bar approximately between 3% and 5.5%. Actually, these trends are in contrast with the result typically found in the literature, where Type III tanks operating at 350 bar typically show higher gravimetric indexes than those working at 350 bar, which, in contrast, exhibit higher volumetric efficiencies [199].

In contrast, examining the gravimetric index trends of Type IV tanks reveals that vessels operating at 350 bar exhibit higher gravimetric indexes for storage capacities exceeding 3 kg (Fig 5.19). However, the scattered data makes this latter conclusion somewhat uncertain. In case of Type IV tanks, the gravimetric index approximately

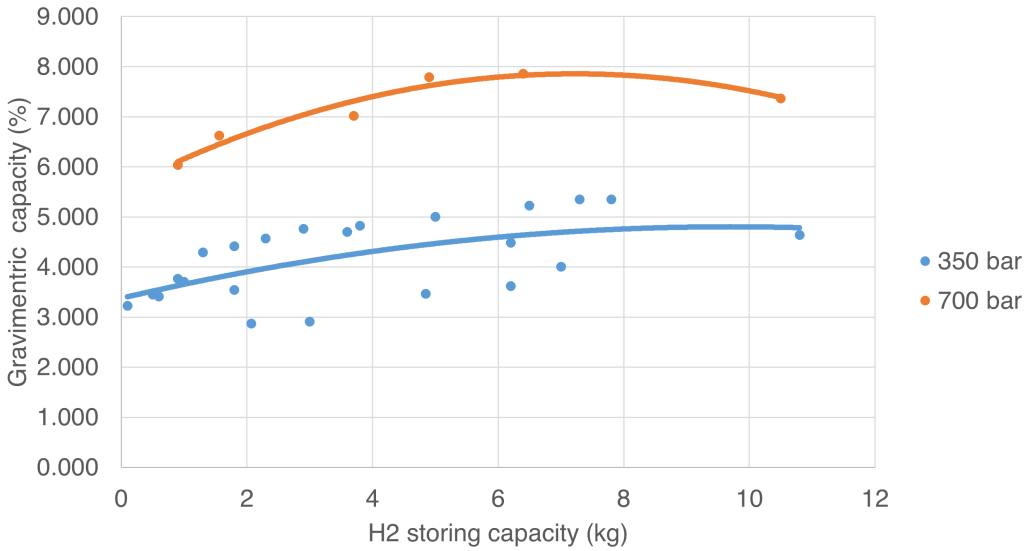

Fig. 5.18 Type III high-pressure tank data for validation.

ranges between 4% and 7% for 700 bar tanks, and between 3% and 8% for vessels operating at 350 bar.

Although the trends shown in Fig. 5.18 and Fig 5.19 may be considered approximate due to the scattering of the data points fitted by the curves, the ranges encompassing all values in the four cases discussed above can be regarded as more general but reliable.

The outputs of the tank sizing model have been reported in Fig. 5.20, where the Type III tanks are those where the liner is made of Al 6061 (blue and orange curves), while those where the liner is made of HDPE UHMH are of Type IV (green and red curves). Comparing the model outputs with the commercial data collected, it can be seen that for Type III tanks operating at 350 bar the commercial data range is slightly lower (commercial range: 3% - 5.5% vs. model range: 5.25% - 6.15%), while it is the opposite in the case of 700 bar (commercial range: 6% - 8% vs. model range: 4.75% - 5.25%). Conversely, the data corresponding to Type IV tanks exhibit a better alignment. For 350 bar service pressure, the gravimetric index for the commercial data ranges between 3% and 8%, and that of the model approximately between 6% and 6.5%. Finally, at a pressure of 700 bar, the ranges of commercial data and model-derived values are, respectively, 4% and 7%, and, approximately, 5.15% and 5.4%. The intervals derived through the model are obviously much narrower because the same materials were used to compute the vessel properties. However, a detailed

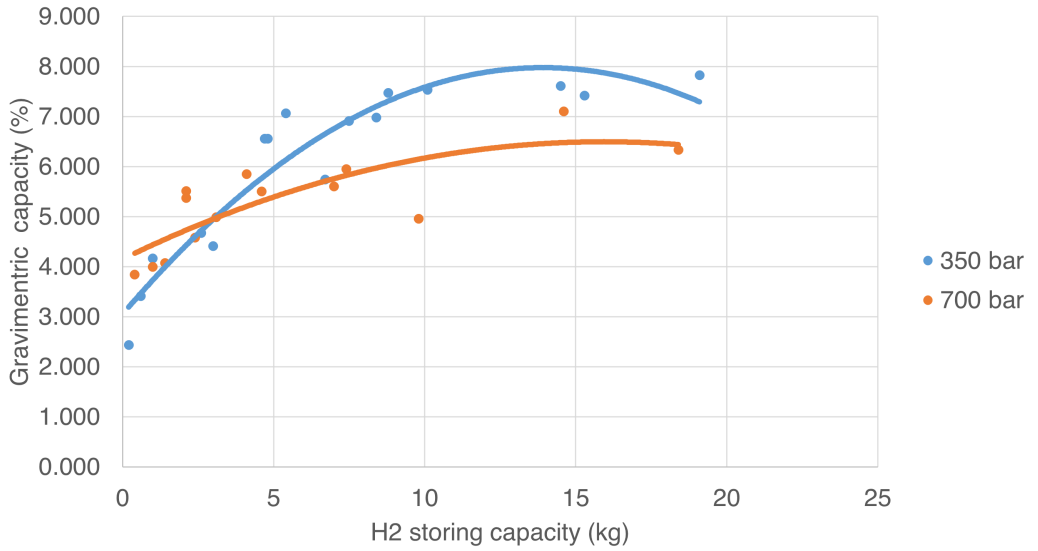

Fig. 5.19 Type IV high-pressure tank data for validation.

description of the materials used for commercial vessels was not available, and it is improbable that different companies use precisely the same materials.

Apart from the opposite trends found in the case of Type III tanks, where the vessels operating at 700 bar unexpectedly exhibit higher gravimetric indexes, the values of the gravimetric indexes can be considered aligned. Considering that a preliminary system analysis was conducted here, the discrepancies were considered negligible.

5.5.3 Case studies

In order to evaluate the potential for retrofitting a long-range UAV, an initial estimation of the onboard hydrogen storage requirement is essential, serving as a basis for the subsequent design of the storage system. It follows that, to approximately determine the amount of hydrogen to be stored on board the UAVs, it has been assumed that the energy content stored onboard using traditional aviation fuel should be equal to that of hydrogen. Even if the Predator and Global Hawk UAVs are respectively fuelled with aviation gasoline and kerosene, which can hold slightly different energy densities, at this preliminary stage their energy densities have been estimated at 43 $MJ\,kg^{-1}$, and they are referred to as aviation fuel (av.fuel) [208]. The specific energies per mass and the densities of CH_2 and LH_2 are:

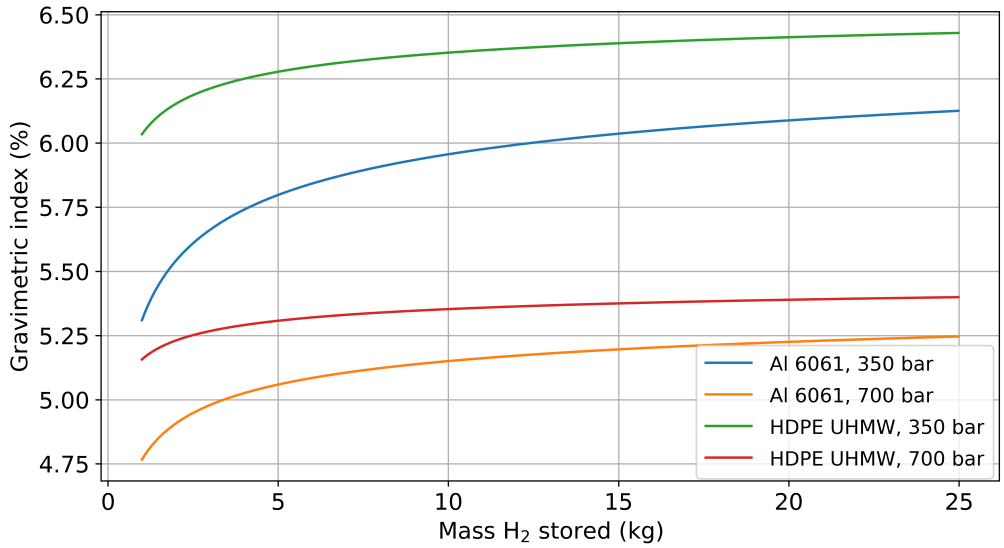

Fig. 5.20 Type III and IV high-pressure tank data generated through the sizing model.

- Energy content of aviation fuel: $e_{\text{av.fuel}} = 43\,\text{MJ}\,\text{kg}^{-1}$
- Energy content of hydrogen: $e_{H_2} = 120\,\text{MJ}\,\text{kg}^{-1}$
- Density of aviation fuel: $\rho_{\text{av.fuel}} = 810\,\text{kg}\,\text{m}^{-3}$
- Densities of hydrogen (by storage type):
  - CH_2 at 350 bar: $\rho_{H_2,350} = 23\,\text{kg}\,\text{m}^{-3}$
  - CH_2 at 700 bar: $\rho_{H_2,700} = 40\,\text{kg}\,\text{m}^{-3}$
  - LH_2: $\rho_{\text{LH}_2} = 70.85\,\text{kg}\,\text{m}^{-3}$

Under the assumption that the total amount of energy stored should be equal, regardless of the type of fuel used, the mass of hydrogen to be stored can be computed through Eq. 5.1.

$$m_{H_2} = \frac{m_{\text{av.fuel}} \cdot e_{\text{av.fuel}}}{e_{H_2}} \tag{5.1}$$

Then, the corresponding volumes occupied by the fuel amounts are computed by Eq. 5.2

$$V = \frac{m}{\rho} \tag{5.2}$$

The results for the two UAVs under analysis are reported in Table 5.5.
It is essential to note that the masses and volumes reported in the table above refer

Table 5.5 Equivalent hydrogen fuel capacity for Global Hawk and Predator UAVs

	Global Hawk	Predator
Total energy stored (MJ)	337421	12900
Aviation fuel mass (kg)	7847	300
H_2 Mass (kg)	2811.84	107.5
Aviation fuel Vol. (m^3)	9.69	0.37
H_2 Vol. 350 bar (m^3)	122.25	4.67
H_2 Vol. 700 bar (m^3)	70.3	2.69
LH_2 Vol. (m^3)	39.67	1.52

only to the fuel and do not account for the storage system. For aviation fuel, the mass and volume of the fuel alone can be assumed to be nearly equal to that of the system; however, a deeper analysis is required to quantify the weight of the hydrogen tank and distribution system.

Looking at Table 5.5, it can be quantitatively perceived how impactful the resulting volumes are. Even storing hydrogen in liquid form requires approximately four times the volume occupied by aviation fuel. Considering that these results can be directly traced back to the densities of LH_2 and jet fuel, and that they account for the fuels alone without considering the storage systems, it can be stated that storing the same energy amount as liquid hydrogen would always require at least four times the volume occupied by aviation fuel. In contrast, the hydrogen mass is much lower than that of aviation fuel. Considering that the mass of the hydrogen tank should be added to that of hydrogen, it can be interesting to identify a sort of break-even point for the gravimetric index. In practice, it is helpful to determine a value of the gravimetric index below which the total weight of the hydrogen and the storage system is higher than that of aviation fuel for the same amount of energy stored. Such a value can be used as a reference to evaluate the system's performance in terms of weight. To compute what it can be defined as the gravimetric index break-even point in terms of specific energy, it is sufficient to find the value for which the gravimetric efficiency of the hydrogen storage system becomes equal to that of the aviation fuel storage system, thus solving the following proportion (Eq. 5.3).

$$e_{H_2} \cdot \eta_{H_2} = e_{\text{av.fuel}} \cdot \eta_{\text{av.fuel}} \tag{5.3}$$

Assuming a gravimetric index of the aviation fuel storage system equal to 99%, the value of the break-even point can be computed (Eq. 5.4).

$$\eta_{H_2} = \frac{e_{\text{av.fuel}} \cdot \eta_{\text{av.fuel}}}{e_{H_2}} = \frac{43 \cdot 0.99}{120} = 0.35475 \tag{5.4}$$

So, if the gravimetric index of the hydrogen storage system is higher than 35.5%, its mass efficiency is superior to that of aviation fuel. On the other hand, if its value is lower, there are no advantages in terms of weight.

The same reasoning could be applied to find analogous values for CH_2 stored at 350 bar and 700 bar. However, due to the significantly higher volumes compared to those needed to store jet fuel, and to the low gravimetric indexes typical of high-pressure vessels, computing such values has been considered unjustified, and only liquid hydrogen storage and distribution systems will be analysed. In the following, the impact of the insulating materials is quantified, and the resulting dimensions of the hydrogen tank are compared with the space available that has been estimated for the Predator and the Global Hawk UAVs. The starting inputs for the analysis are the required tank capacity and the desired instantaneous boil-off rate, which has been set to 1.6% of the total amount of liquid hydrogen stored [199, 201].

Predator case study

The results for the various insulating materials are reported in Table 5.6 and graphically represented in Fig. 5.21. The complete names of the insulating materials can be depicted from Table 5.3 (Sec. 5.5.1). Overall, observing the bar charts, it can be immediately concluded that the gravimetric indexes are between 40% and 50% and the volumetric indexes are between 60% and 70% for most materials. Two exceptions arise for the polyurethane foam (PRU) and the glass bubble insulation, which exhibit notably lower performances. In the case of glass bubble, the reason can be traced back to the poor insulating properties of the material, which has a relatively high thermal conductivity combined with a high density.
In contrast, the PRU insulating capabilities are comparable to those of other foams, such as the polymethacrylimide (PMI) or polystyrene (PS). Thus, this outlier value can be attributed to a model numerical error in the optimisation loop. A comprehensive analysis of the optimisation algorithms goes beyond the scope of the current

study. However, for the sake of completeness, it is useful to address this anomaly in the value briefly. The optimisation algorithm has been set in collaboration with an optimisation expert, as part of the doctoral activity, aiming to implement a solution that ensures reliability while maintaining a relevant speed. To deal with this compromise, the model may find a local minimum of the solution instead of a global one. The design choice ultimately favoured a faster solution over an extremely time-consuming one that would require hours to perform a preliminary static analysis. Instead, the identification of potential outliers was left to the designer's judgment, as in this case, where such anomalies emerge when comparing the results of multiple simulations that can be executed in a very short time.

Table 5.6 Predator Tank Data

Insulation material	Tank empty weight (kg)	Tank volume (m^3)	Gravimetric index (%)	Volumetric index (%)
PS	2308.45	60.70	54.92	68.05
PMI	2310.71	60.62	54.89	68.14
PRU	2305.17	60.57	54.95	68.20
Perlite	2310.11	60.90	54.90	67.83
Silica aerogel	2328.46	60.65	54.70	68.10
Fiberglass	2320.36	60.80	54.79	67.94
Glass Bubble	2577.59	61.62	52.17	67.04
EPS	2307.42	60.66	54.93	68.09
Polyvinychloride	2307.52	60.57	54.93	68.20
Rohacell	2668.76	61.08	51.31	67.63
PU	2310.06	60.65	54.90	68.11
Aerogel_low_p	2303.95	60.46	54.96	68.32
Aerogel_very_low_p	2300.98	60.44	55.00	68.35
HD_Aerogel	2314.87	60.74	54.85	68.00
HD_Aerogel_low_p	2307.52	60.59	54.93	68.18
Perlite_low_p	2320.11	60.58	54.79	68.19
Perlite_very_low_p	2301.98	60.44	54.99	68.34
MLI_MD	2314.31	60.74	54.85	68.00
MLI_MD_low_p	2300.26	60.43	55.00	68.35

The solution showing the highest performance is that relying on multi-layer insulation Mylar/Dacron used in combination with vacuum at low pressures ("MLI_MD_low_p"). Thus, additional data have been reported for this tank in Table 5.7. The dimensions of the Predator have been reported in Fig. 5.22. Typically, the payload and, in general,

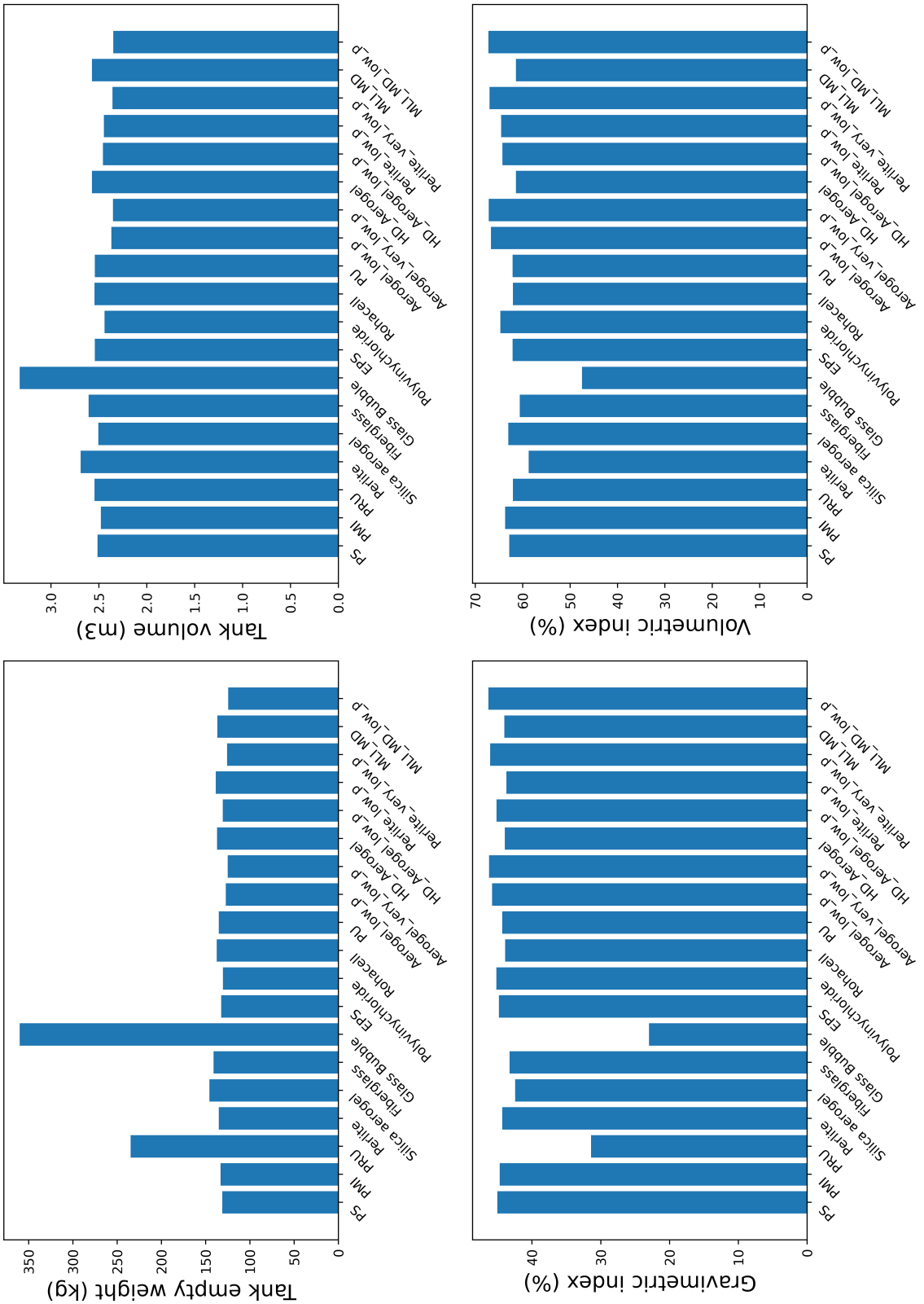

Fig. 5.21 Predator UAV hydrogen tank performances for various insulating materials.

Table 5.7 Predator liquid hydrogen tank data for MLI Mylar/Dacron insulation.

Data	Value
Liner material	Al 5083-O
Liner weight (kg)	69.52
Insulation layers materials	MLI_MD_low_p & HDPE UHMW
Insulation weight (kg)	54.99
Tank empty weight (kg)	124.52
Tank diameter (m)	1.21
Tank length (m)	1.84

all the electronic equipment for communication and data acquisition, such as antennas and radar, are installed in the front section of the fuselage, while the powertrain is located in the rear half, where the propeller is also positioned [209]. It follows that the cylindrical hydrogen tank should be installed inside an available space that, from Fig. 5.22, has a diameter of maximum 0.6 m, assuming that the tank wall is in contact with the aircraft skin. Estimating the length of the volume available for the installation is hardly feasible in this context, considering that the other components constituting the powertrain should also be sized. However, considering only the diameter of the tank, which measures 1.21 m, the maximum available dimension within the fuselage is largely exceeded. Moreover, by comparing the gravimetric and volumetric index values obtained for all the insulations adopted (Table 5.6) with the typical values from the literature, the outputs here shown appear quite optimistic, also due to the fact the only the shells of the vessels account for the overall system weight and no additional, but strictly necessary, components are considered.
In conclusion, the installation of a liquid hydrogen tank containing the same amount of energy stored via aviation fuel inside the fuselage of a Predator UAV was deemed unfeasible due to volume constraints. A smaller tank could be designed for testing purposes, but considering that the flight endurance is one of the most essential aircraft strengths, retrofitting a Predator UAV would lead to a less performing and, in turn, non-competitive solution.

Global Hawk case study

An analogous analysis to that conducted for the Predator UAV (Sec. 5.5.3) will be applied in the current section to the Global Hawk UAV. The tank properties for all the insulation materials considered are reported in Table 5.8 and represented graphically

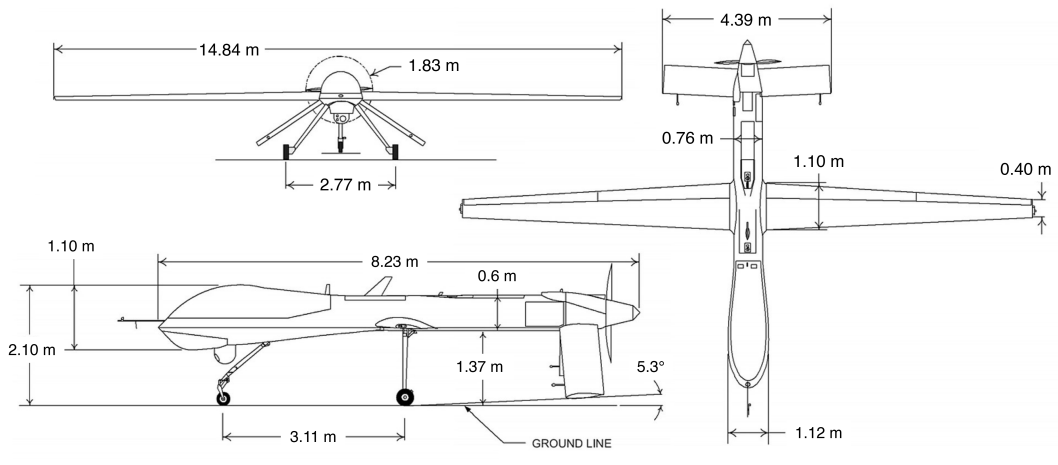

Fig. 5.22 Reference dimensions for the MQ1 Predator UAV [56, 210].

in Fig. 5.23. In this case, the gravimetric indexes range between 50% and 60%. The higher values compared to the Predator use case can be attributed to the greater tank capacities. Typically, storing a greater amount of liquid hydrogen leads to higher tank performances, because their higher volume-to-surface ratios translate into a reduced heat exchange surface in proportion to the hydrogen stored. Observing the bar charts in Fig. 5.23, no anomalies are identified. The lower performances in the case of glass bubble and rohacell insulation can be attributed to their lower thermal capabilities.

The solution exhibiting the highest gravimetric and volumetric indexes is again that implementing the multilayer Mylar/Dacron (MLI_MD_low_p). This can be attributed to the fact that the sizing model computes the insulation thickness based on a sort of maximum admissible heat flux. At this preliminary level, the weight and volume of additional elements, such as supports, pipes, and valves, are estimated through correction factors which increase the system weight by a preselected percentage value [199, 201]. It follows linearly that the insulating material with the best thermal and lightweight properties leads to the most efficient tank.

The data referred to the tank implementing the MLI_MD_low_p insulation is reported in Table 5.9. Similarly to what has been done in the previous section, the volume available to install the tank inside the fuselage has been estimated from the lateral cross-section of the Global Hawk retrieved from the literature (Fig. 5.24). Considering that also in this case the frontal region of the UAV is meant to host the payload, the length of the volume available (red dotted rectangle in Fig. 5.24) has been computed by summing the length of zone 3 (green arrow in the lower part

Table 5.8 Global Hawk Tank Data

Insulation material	Tank empty weight (kg)	Tank volume (m^3)	Gravimetric index (%)	Volumetric index (%)
PS	131.22	2.514	45.03	62.82
PMI	133.09	2.479	44.68	63.70
PRU	234.72	2.546	31.41	62.04
Perlite	135.08	2.690	44.31	58.71
Silica aerogel	145.74	2.505	42.45	63.03
Fiberglass	141.09	2.606	43.24	60.61
Glass Bubble	360.14	3.326	22.99	47.49
EPS	132.42	2.542	44.81	62.13
Polyvinychloride	130.45	2.441	45.18	64.69
Rohacell	137.43	2.546	43.89	62.04
PU	135.10	2.542	44.31	62.12
Aerogel_low_p	127.26	2.369	45.79	66.67
Aerogel_very_low_p	124.98	2.352	46.24	67.14
HD_Aerogel	137.10	2.572	43.95	61.41
HD_Aerogel_low_p	130.63	2.457	45.14	64.27
Perlite_low_p	138.46	2.447	43.71	64.53
Perlite_very_low_p	125.77	2.358	46.08	66.98
MLI_MD	136.71	2.572	44.02	61.41
MLI_MD_low_p	124.52	2.349	46.33	67.23

of Fig. 5.24) and zone 25 (red arrow in the lower part of Fig. 5.24), and measures 4.064 m. The height of the selected region has been computed by multiplying by two the height of zone 22 (blue arrow in the lower part of Fig. 5.24) and equals 0.712 m. Instead, the width is 1.46 m, and can be directly depicted from the schematic in the upper part of Fig. 5.24. The tank length and diameter vastly exceed the dimensions of the available volume inside the fuselage. Therefore, similar considerations to those outlined for the Predator also apply to the Global Hawk, which can hardly be competitive with one powered by jet fuel if it is retrofitted with a hydrogen-based powertrain.

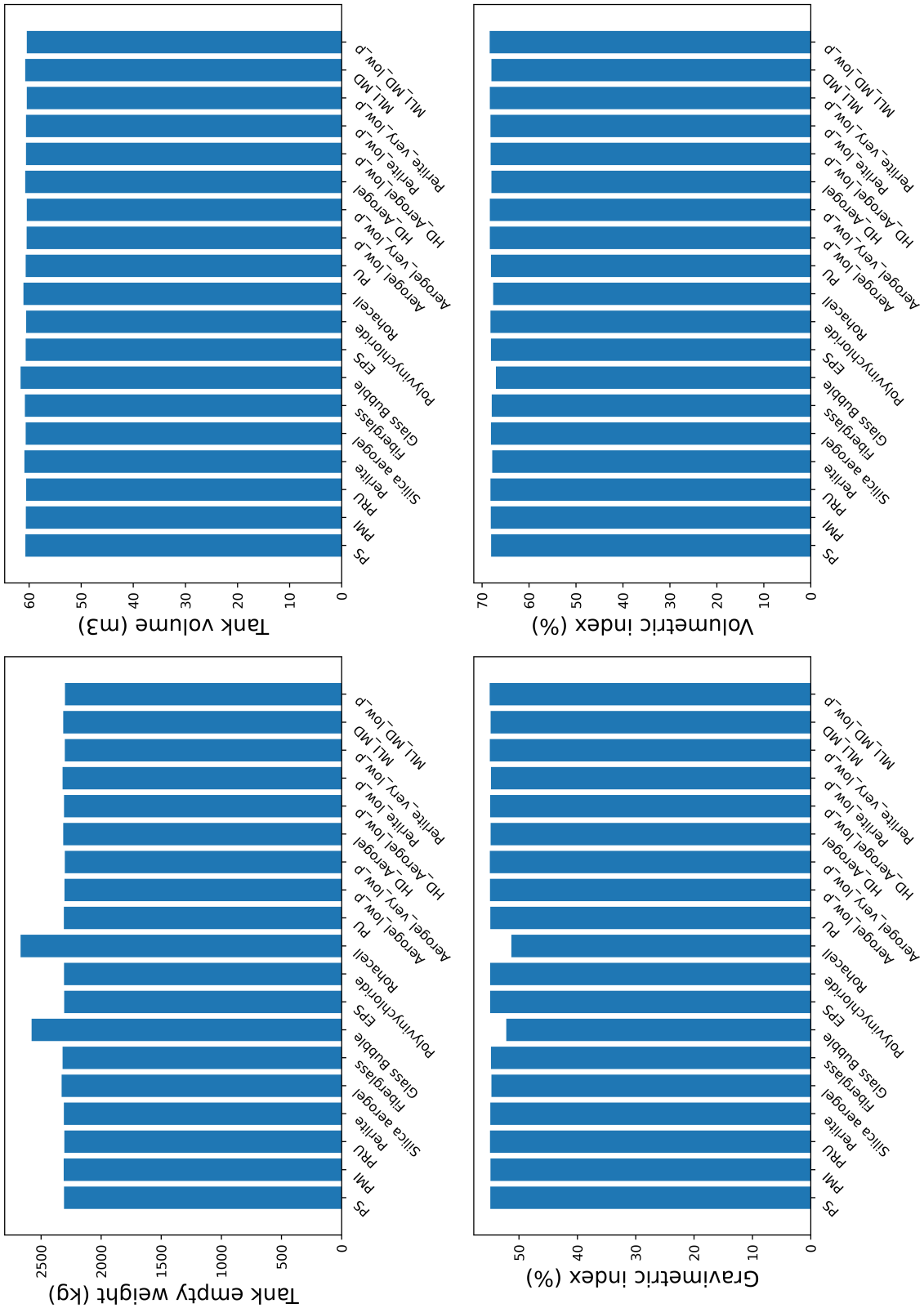

Fig. 5.23 Global Hawk UAV hydrogen tank performances for various insulating materials.

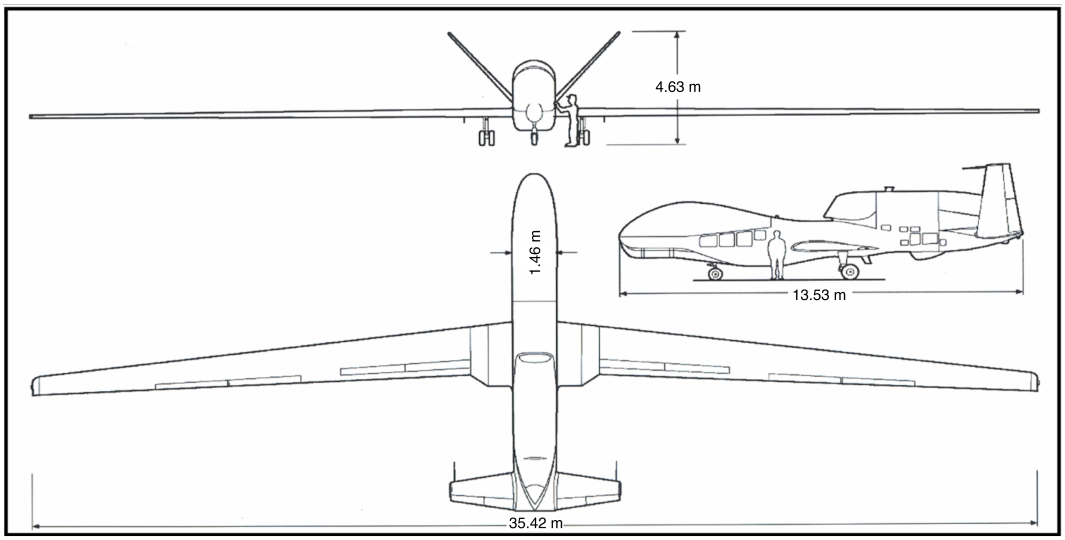

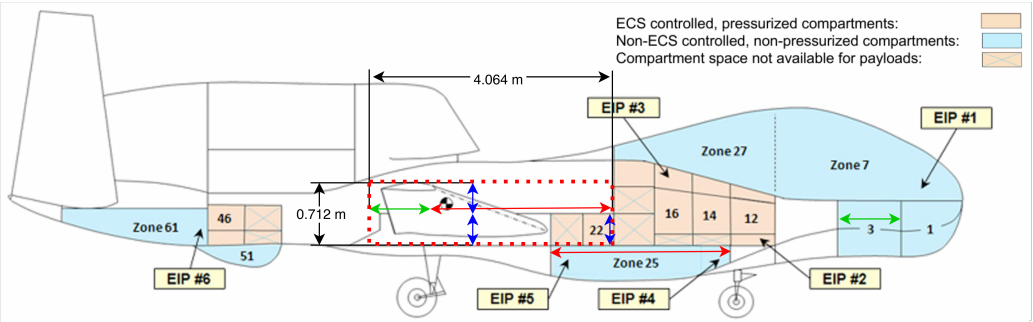

Payload Zone ID	Length (m)	Width (m)	Height (m)
1	0.66	0.991	0.838
3	1.016	0.584	0.686
7	2.667	1.422	0.914
11	0.483	0.533	0.33
12	0.483	0.533	0.33
13	0.483	0.508	0.432
14	0.483	0.508	0.432
16	0.381	0.508	0.508
22	0.483	0.635	0.356
25	3.048	1.422	0.457
27	1.829	1.27	0.66
46	0.508	0.508	0.356
51	1.143	0.356	0.305
61	1.778	1.118	0.508

Fig. 5.24 Reference dimensions for the RQ-4 Global Hawk UAV [44].

Table 5.9 Global Hawk liquid hydrogen tank data for MLI Mylar/Dacron insulation.

Liner material	Al 5083-O
Liner weight (kg)	1818.50
Insulation layers materials	MLI_MD_low_p & HDPE UHMW
Insulation weight (kg)	481.77
Tank empty weight (kg)	2300.26
Tank diameter (m)	3.58
Tank length (m)	5.42

5.6 MBSE for the H_2SDSys design

In this section, the MBSE conceptual design path previously shown will be tailored to be applied to the design of the hydrogen storage and distribution system. The study begins with the requirements analysis. Then, the operational analysis, aimed at defining the system's mission and context, is carried out as a distinct and separate step to highlight the relevance of use cases and scenarios. Then, the investigation of one representative use case is proposed ("UAV in Flight Mission"). The functional analysis is performed, and the transition from black-box to white-box approaches is performed, relying also on the activities decomposition map and on the functional architecture. Considering the preliminary level of the analysis and the need for exploring an unknown technology, the logical analysis has been somehow merged with the physical one. Finally, the dynamic analysis has been conducted by performing different simulations, and the primary outcomes have been reported and evaluated.

5.6.1 Requirements analysis

Once the H_2SDSys has been identified as a subsystem of the Propulsion system included in the UAV, the requirements analysis is reapplied to the system of interest, that is now the hydrogen storage and distribution system.
In line with the methodology previously applied (Sec. 5.4), the requirements analysis is again started from the customer's needs, from which a series of requirements applicable to the H_2SDSys are derived. Other stakeholders' needs were added to the customer's needs and collected in a table, clustered and ordered hierarchically. Then, several requirements have been derived as shown in Table 5.10, where the customer's and stakeholders' needs can be identified by the prefix 'SN' at the beginning of their name, while the requirements derived from them start with 'R'. General statements

were decomposed into specific and, whenever possible, measurable requirements. For instance, the statement *"We are designing a fuel-cell hydrogen-powered aircraft, we need a hydrogen storage and distribution system"* (SN_H2SDSys_H2_Aircraft) was refined into specific requirements on storage capacity, output pressure, output temperature, and installation constraints (e.g., R_H2SDSys_Storage_Capacity, R_H2SDSys_Output_Pressure, R_H2SDSys_Max_Weight). This process ensures that the needs collected in the previous steps of the analysis related to the UAV are also linked and quantified in the H_2SDSys analysis whenever possible.

Table 5.10 First draft of H_2SDSys requirements derived from customer's needs

Name	Text
70 SN_H2SDSys_H2_Aircraft	We are designing a fuel-cell hydrogen-powered aircraft; we need a hydrogen storage and distribution system.
70.1 R_H2SDSys_Storage_Capacity	The H2SDSys shall store a mass of hydrogen equal to XXX kg.
70.2 R_H2SDSys_Output_Pressure	The H2SDSys shall supply hydrogen to the fuel cell at $p_{out} = XX \pm X$ bar.
70.3 R_H2SDSys_Installation	The H2SDSys shall be installed on the aircraft.
70.4 R_H2SDSys_Output_Temperature	The H2SDSys shall supply hydrogen to the fuel cell at $T_{out} = XX^{\circ}C \pm X^{\circ}C$.
70.5 R_H2SDSys_H2_Out_Conditions	The H2SDSys shall supply hydrogen to the fuel cell in gaseous form.
70.6 R_H2SDSys_Refueling	The H2SDSys shall be refilled by an external supplier.
73 SN_H2SDSys_Live_Monitoring	We need to control and monitor the system both during flight and during stationary operations and parking.
73.1 R_H2SDSys_Live_Monitoring	The H2SDSys conditions shall be monitored.
74 SN_H2SDSys_Safety_Autonomy	If something unexpected occurs, we want the system to automatically activate countermeasures.
74.1 R_H2SDSys_Autonomy	In both normal and unexpected operating conditions, the H2SDSys shall operate autonomously.
75 SN_H2SDSys_Operative_Life	We don't yet know the aircraft type, but the system should last for the aircraft's lifetime and support its most demanding missions.

Name	Text
75.1 R_H2SDSys_Service_Life	The H2SDSys lifetime shall not limit the aircraft's lifetime.
75.2 R_H2SDSys_Operational_Capabilities	The H2SDSys lifetime shall not limit the aircraft's capabilities.
76 SN_H2SDSys_Installation_Constraints	The system will be installed on a UAV, so its dimensions must allow for that.
76.1 R_H2SDSys_Max_Volume	The H2SDSys volume shall be limited to XXX m³ (XX m length, XX m height).
76.2 R_H2SDSys_Max_Weight	The H2SDSys weight shall be limited to XXX kg.
78 SN_H2SDSys_External_Supplier	We plan to outsource the system's production to a third party.
78.1 R_H2SDSys_External_Supplier_Requests	If a component is produced by a supplier, its requirements shall hold legal validity and include detailed technical specifications.
79 SN_H2SDSys_Standard_Compliance	The system must comply with applicable standards to be eligible for a "permit to fly."
79.1 R_H2SDSys_Standards_Driven_Design	The H2SDSys design shall follow relevant standards.
79.2 R_H2SDSys_Standard_Authority_Interaction	The H2SDSys design shall be developed in cooperation with a certification body or authority.
80 SN_H2SDSys_Data_Acquisition	We want to extract data from the UAV for further analysis.
80.1 R_H2SDSys_Data_Acquisition_Equipment	The H2SDSys shall be equipped with tools for data monitoring and acquisition.
81 SN_H2SDSys_Electric_Powertrain	We aim to power the UAV with a fully electric hydrogen-based powertrain.

Name	Text
81.1 R_H2SDSys_Electric_Compatibility	The H2SDSys integration with hybrid-electric aircraft components shall be analysed and optimised.
82 SN_H2SDSys_Competitiveness	UAV performance must be at least comparable to those with conventional powertrains; ideally, it should be superior for market appeal.
82.1 R_H2SDSys_Performance_Competitiveness	The H2SDSys shall guarantee UAV performance levels comparable to conventional powertrains.
82.2 R_H2SDSys_Market_Competitiveness	The H2SDSys shall offer advantages that make the UAV competitive in the market.

Then, further research has been conducted, and additional requirements have been derived from relevant standards. The results of this whole process are synthesised in the first draft of requirements (Table 5.11), where, for brevity, a selection of these requirements was included to highlight the various design aspects that should be covered and to conduct the following analysis at a preliminary level. In Table 5.11, the "Source" of each requirement is explicit whenever the requirement is derived from a standard; in other cases, the requirement has been derived from the needs or from analysis of the literature. The "Source" column has been added as an additional feature. However, requirements are typically linked to documents or upper-level requirements and needs via a traceability matrix, which does not provide further insights into the current analysis and is therefore not included. Carefully reviewing the proposed requirements list (Table 5.11) it can be immediately depicted how several different aspects should be considered in the design. In this preliminary design phase, a deep knowledge of the system is yet to be gained, and the majority of requirements are not measurable. Indeed, priority has been given to collect all the aspects that should be considered in later stages, where, after several requirements elicitation, a more proper granularity could also be applied. For instance, the requirement *"The H_{2SDSys} shall safely store and distribute hydrogen"* (R_H2SDSys_Safety) is of broad applications an may include many requirements which are actually useful in making the system safe, such as *"Tapered thread fittings shall be replaced when joints are disassembled"* (R_H2SDSys_Joints_Replacement) and *"Materials shall resist hydrogen-accelerated fatigue phenomena"* (R_H2SDSys_Fatigue_Resistance). Practically speaking, if the tapered thread fittings are not replaced when the joints are disassembled or if the materials selected do not resist hydrogen-accelerated fatigue phenomena, the system may not work correctly, or a failure may occur. In both cases, the safety of the system would be compromised. This does not mean that such requirements should be grouped under one related to safety. As the analysis progresses, it may prove more useful to include the requirement concerning the replacement of tapered thread fittings (R_H2SDSys_Joints_Replacement) within those related to maintenance activities. Conversely, the requirement addressing hydrogen-accelerated fatigue phenomena (R_H2SDSys_Fatigue_Resistance) could be associated with specific standards for material selection and assigned to stakeholders responsible for supplying and certifying the materials used.

Table 5.11 First requirements draft for the H_2SDSys.

Name	**Requirement Description**	**Source**
R_H2SDSys_Safety	The H2SDSys shall safely store and distribute hydrogen	
R_H2SDSys_Effectiveness	The H2SDSys shall effectively store and distribute hydrogen	
R_H2SDSys_Efficiency	The H2_System shall efficiently store and distribute hydrogen	
R_H2SDSys_Industrial_Manufacturing	The H2_System shall be suitable for industrial production	
R_H2SDSys_Standard_Compliance	The H2_System shall be compliant with applicable standards	
R_H2SDSys_H2_Compatibility	The H2_System shall be compatible with hydrogen environment	
R_H2SDSys_Operating_Temperature	The design shall clearly define the temperature ranges required for each component.	
R_H2SDSys_Operating_Pressure	The design shall clearly define the pressure ranges required for each component.	
R_H2SDSys_SetUp	Design shall define the in-service set-up of all components	

Name	Requirement Description	Source
R_H2SDSys_Components_Standards	Specific standard reference for each component shall be specified	
R_H2SDSys_Embrittlement	The H2_Storage_System shall be able to resist hydrogen embrittlement phenomena	NASA safety standards for hydrogen and hydrogen systems
R_H2SDSys_Operating_Tempreature_01	Design shall consider operating temperatures	NASA safety standards for hydrogen and hydrogen systems
R_H2SDSys_Manufaturing_Standards	H2_System manufacturing shall comply with appropriate standards and codes	NASA safety standards for hydrogen and hydrogen systems
R_H2SDSys_Testing_Standards	H2_System testing shall comply with appropriate standards and codes	NASA safety standards for hydrogen and hydrogen systems
R_H2SDSys_Inspections_Standards	H2_System inspections shall comply with appropriate standards and codes	NASA safety standards for hydrogen and hydrogen systems
R_H2SDSys_Maintenance_Standards	H2_System maintenance shall comply with appropriate standards and codes	NASA safety standards for hydrogen and hydrogen systems
R_H2SDSys_Stress_Resistance	H2_System shall maintain functionality under mechanical stresses, deformations, corrosion, or degradation	ISO 12619
R_H2SDSys_Steel_Cracking	If stainless steel is used, design shall consider chloride stress corrosion cracking	ISO 12619
R_H2SDSys_Aluminum_Cracking	If aluminium is used, design shall consider load cracking	ISO 12619

Name	Requirement Description	Source
R_H2SDSys_Joints_Sealing	Jointing components shall provide gas-tight sealing performance	ISO 12619
R_H2SDSys_Joints_Replacement	Tapered thread fittings shall be replaced when joints are disassembled	ISO 12619
R_H2SDSys_Components_Temperatures	Components shall be suitable for service within specified temperature ranges	ISO 12619
R_H2SDSys_Fatigue_Resistance	Materials shall resist hydrogen-accelerated fatigue phenomena	ISO 12619
R_H2SDSys_Materials_Temperature	Design shall consider material properties at operating temperatures	NASA safety standards for hydrogen and hydrogen systems
R_H2SDSys_Materials_Mech_Temperature	Design shall consider mechanical properties of materials at operating temperatures	NASA safety standards for hydrogen and hydrogen systems
R_H2SDSys_Air_Condensation	H2_System shall avoid air condensation	NASA safety standards for hydrogen and hydrogen systems
R_H2SDSys_Boiloff_Losses_Minimizazion	Design shall minimise evaporation losses when storing hydrogen in liquid form	NASA safety standards for hydrogen and hydrogen systems
R_H2SDSys_Liquid_Sloshing	Design shall consider the influence of fluid sloshing	
R_H2SDSys_Wiring_Protection	Openings for wiring shall prevent chafing and abrasion of insulation	ISO 12619
R_H2SDSys_Sloshing_UAV_Balance	Design shall consider the influence of fluid sloshing on aircraft behaviour	

Name	Requirement Description	Source
R_H2SDSys__Sloshing_on_UAV	Design shall consider mechanical and thermal consequences of fluid sloshing	
R_H2SDSys_Natural_Performance	Design shall leverage natural component behaviour to maximise performance	
R_H2SDSys_Thermal_Deformation	Design shall consider thermal deformation due to temperature gradients	
R_H2SDSys_H2_ExtractionManagement	Design shall consider hydrogen extraction management in multiphase conditions	
R_H2SDSys_Backflow_Refilling	During refilling, H2_System shall avoid hydrogen backflow	
R_H2SDSys_Safety_Manouvres	Emergency manoeuvres shall reduce or avoid adverse safety consequences	
R_H2SDSys_Harmless_H2_Evacuation	In emergencies, H2_System shall evacuate or neutralize hydrogen within X seconds	
R_H2SDSys_Off_Design_Stresses	Design shall analyse emergency scenarios causing extraordinary stresses	
R_H2SDSys_Harmful_Deformations	Design shall assess maximum strains leading to crack initiation under emergencies	
R_H2SDSys_Crash	Preventing aircraft crash or H2_System damage shall be a primary design goal	
R_H2SDSys_External_Pressure_Stress	The tank shall withstand external pressures	ASME VIII

Name	Requirement Description	Source
R_H2SDSys_External_Pressure_Source	Design shall identify sources of external pressure in all operating conditions	ASME VIII
R_H2SDSys_Manufacturer_Instructions	Manufacturer shall provide clear instructions and diagrams for safe use	ISO 12619

Thus, at this point of the analysis, considering the relatively reduced number of requirements which make them easily manageable, few general requirements categories have been identified (Fig. 5.25). The "E" and "R" labelling each requirement in Fig. 5.25 stand for "Requirement" and "Extended Requirement". The software tool offers the possibility to extend the attributes of a typical requirement by creating an extended requirement. However, for the purpose of the work conducted here, they can both be interpreted simply as requirements. To address the customer desire of having the H_2SDSys modelled while complying with reasonable deadlines, only a subset of requirements were selected in accordance with upper-level systems engineers (Fig. 5.26), which to assess the technical feasibility of the whole project needed to have an estimate of the weight and volume of all the sub-systems to be installed on board. Thus, the first set of requirements applicable as starting inputs for the design includes the H_2SDSys volume and weight, as well as the storage capacity, the external environmental conditions, and the hydrogen fuel properties at supply.

Name
R_H2SDSys_1 R_H2SDSys_Safety
R_H2SDSys_2 R_H2SDSys_Effectiveness
R_H2SDSys_3 R_H2SDSys_Efficiency
R_H2SDSys_4 R_H2SDSys_Industrial_Manufacturing
R_H2SDSys_6 R_H2SDSys_H2_Compatibility
R_H2SDSys_5 R_H2SDSys_Standard_Compliance
R_H2SDSys_7 R_H2SDSys_Autonomy
R_H2SDSys_8 R_H2SDSys_Electric_Interaction
R_H2SDSys_9 R_H2SDSys_Maintenance
R_H2SDSys_10 R_H2SDSys_Design_Guidelines
R_H2SDSys_11 R_H2SDSys_Design_Reqs
R_H2SDSys_13 R_H2SDSys_Monitoring
R_H2SDSys_14 R_H2SDSys_Refueling

Fig. 5.25 High-level requirements of the H_2SDSys, indicating the topics used to classify the requirements ("E": extended requirement, "R": requirement; both can be interpreted as standard requirements).

Name	Text	Derived From
R_H2SDSys_11 R_H2SDSys_Design_Reqs		
R_H2SDSys_11.1 R_H2SDSys_Storage_Capacity	The H2SDSys shall store a m_h2 equal to XXX kg	SN-1
R_H2SDSys_11.7 R_H2SDSys_Max_Volume	The H2SDSys volume shall be limited to XXX m3 (XX m length, XX m heigth).	SN-5
R_H2SDSys_11.5 R_H2SDSys_H2_Out_Conditions	The H2SDSys shall be supply to the fuel cell hydrogen in gaseous form.	SN-1
R_H2SDSys_11.5.1 R_H2SDSys_Output_Temperature	The H2SDSys shall supply hydrogen to the Fuel-cell at T_out = XX °C +- X °C	SN-1
R_H2SDSys_11.5.2 R_H2SDSys_Output_Pressure	The H2SDSys shall supply hydrogen to the Fuel-cell at p_out = XX +-X bar	SN-1
R_H2SDSys_11.8 R_H2SDSys_Max_Weight	The H2SDSys weight shall be limited to XXX kg	SN-5
R_H2SDSys_11.9 R_H2SDSys_Air_Condensation	H2_System shall avoid air condensation	
R_H2SDSys_11.10 R_H2SDSys_Refueling		
R_H2SDSys_11.10.1 R_H2SDSys_Backflow_Refilling	During H2_System refilling, H2_System shall avoid hydrogen backflow	

Fig. 5.26 Set of design ("D") and functional ("F") requirements of the H_2SDSys derived from the customer's needs.

5.6.2 Operational analysis

The objective of the operational analysis is to determine the mission of the system, its context, and scenarios [6]. The operational analysis is not always included or, at least, explicit among the steps typically included in the MBSE. Indeed, looking back at the V diagrams (Fig 5.1), at the MagicGrid® (Fig 5.2), and at the MBSE design path (Fig 5.3), the reader will not find the operational analysis, which can be formalised differently or included between the requirements and functional analysis. However, in the current analysis, it was considered appropriate to separate the operational analysis from the others, both to facilitate the reusability of the approach and to emphasise the definition of contexts and scenarios. The black-box approach is applied in this phase to explore the problem domain. Indeed, this analysis covers the "system context" and Use Cases" phases in the MagicGrid® framework (Fig 5.2), while, in the MBSE path the operational analysis can be located at the sub-system level between the requirement ("R") and the functional ("F") analyses inside the black-box region in Fig. 5.3. The SysML diagram used is the internal block diagram, where the stakeholders and actors interacting with the system can be identified, and the use case diagram, which collects the usages of the system. The stakeholders and

actors interact with the SOI through functions, which will then be the object of the following design step (functional analysis).

Starting from the customer's needs, the H_2SDsys mission has been reduced to the minimum terms as:

"The H_2SDSys shall supply hydrogen to the fuel-cell."

The use cases have been identified at the system level and are referred to the UAV (Fig. 5.27). These use cases encompass various life cycle stages, including system manufacturing, integration, and maintenance, as well as specific system usages, such as the UAV during flight (Flight Mission) and maritime operations. Naturally, these usages also affect the design of the UAV subsystems, among which is the H_2SDSys. Consistent with the system mission just defined, the use case explored is "UAV in Flight Mission". This does not mean that the "hydrogen system shall supply hydrogen to the fuel" request excludes other use cases from investigation or attributes them less relevance. The choice has been made considering that it is during the flight that the system physically supplies hydrogen to the fuel cell. To enable quantitative analysis and deal with future potential suppliers, a priority was devoted to this use case.

Fig. 5.27 Use cases for the UAV.

The H_2SDSys context has been modelled through the IBD in Fig. 5.28. Looking at the top-left corner of the image, a reference to the use case under analysis is reported. The context diagram is composed of seven parts, including the SOI itself. The interfacing systems are the structure of the aircraft to which the SOI is anchored (Airframe), with which a mutual exchange of mechanical stresses occurs. The

external environment (Environment), exchanging air with the SOI, which should indeed be sealed, while the H_2SDSys sends hydrogen, for example, during venting operations. The Flight control system has been conceptually modelled as a sort of "UAV Brain" which manages all the data exchanges and commands. The Fuel-Cell System (FCS) sends the desired conditions for hydrogen production, which in turn is supplied by the H_2SDSys. The Thermal Management System (TMS) and the Electrical Power System (EPS) have also been included to exchange thermal and electric power with the SOI.

Then, the interaction between the FCS and the H_2SDSys, which actually reflects the mission of the system, is described through the UCD in Fig 5.29. The use case "Supply Hydrogen" had been detailed into two separate usages, "Supply Hydrogen at desired pressure" and "Supply Hydrogen at desired temperature", through the «include» relationship. The boundary of the system can also be identified as the perimeter of the rectangular block "UAV in Flight Mission," which describes the use case.

As previously mentioned, the system interacts with stakeholders and actors through functions. In practical terms, the H_2SDSys will "Supply Hydrogen" to the FCS through a sequence of functions which will be described in the following section.

5.6.3 Functional analysis

The functional analysis has been performed according to the steps already applied to the UAV (Sec. 5.4), which have been elaborated from both the approaches proposed by the MagicGrid® framework and by Brusa et al. [197, 6].
In practice, a series of functions has been drawn through activity diagrams. In this first phase, the actors should still be unknown, and the ADs should look like previously created for the UAV (Fig 5.9). Then, once the stakeholders and actors have been identified, they are allocated to the swimlanes (black columns with titles of sub-systems in Fig. 5.30, Fig. 5.31, and Fig. 5.32). The ADs reported in the current section may somehow resemble sequence diagrams, which have been described in Ch. 2. However, it is worth noting that activity diagrams describe a series of actions, and the addition of swimlanes serves to assign the responsibility of actions to subsystems and actors or, formally, to allocate functions to subsystems.

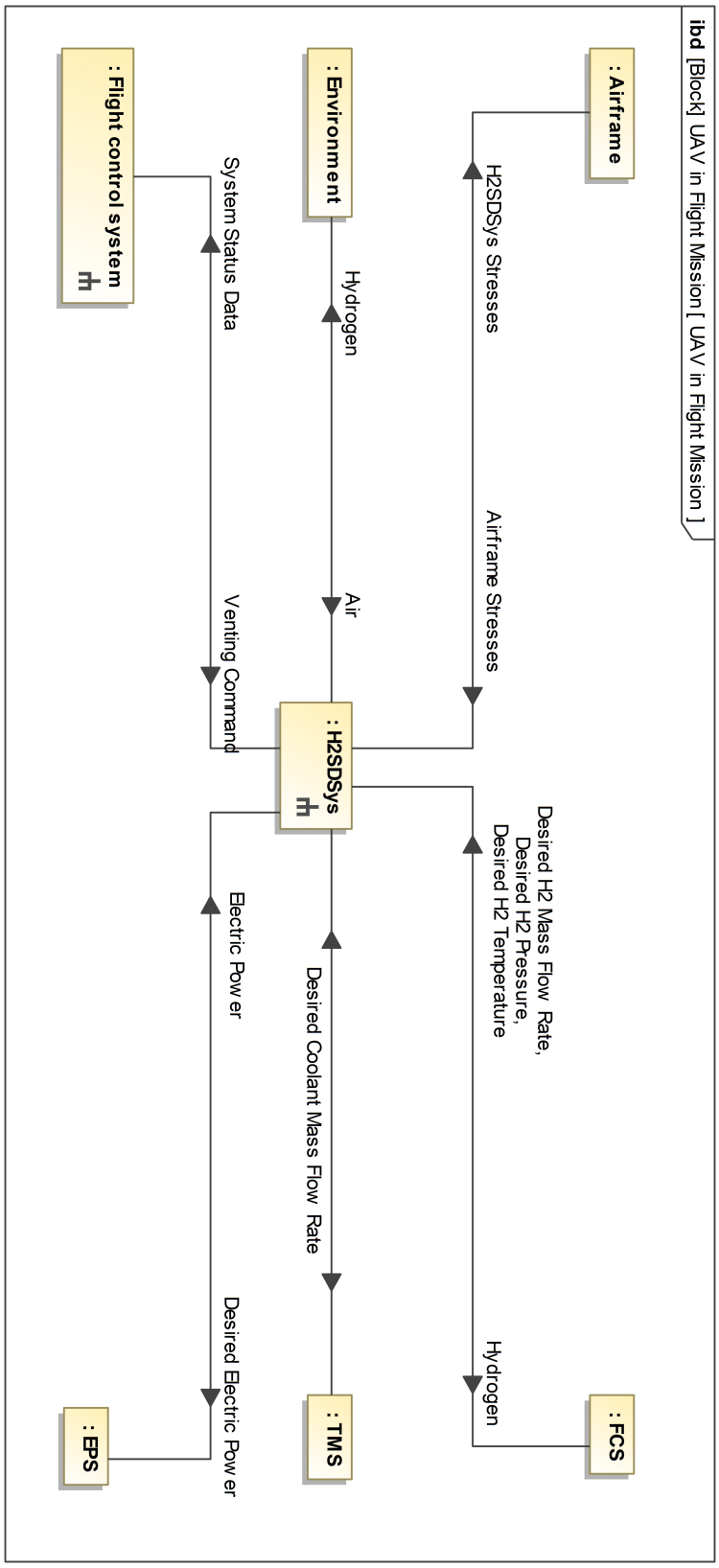

Fig. 5.28 Context diagram for the H_2SDSys.

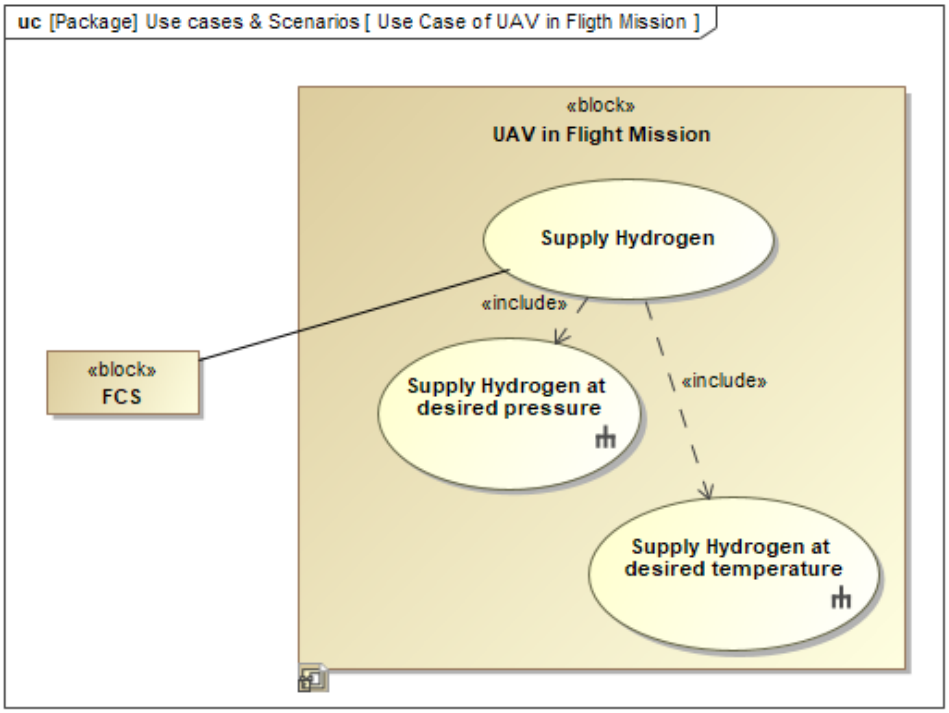

Fig. 5.29 Use case diagram of "UAV in Flight Mission".

In contrast, the sequence diagram describes the temporal sequence of messages exchanged between systems and actors, highlighting the dynamic interactions. In the activity diagrams reported here, it was considered useful to add the items exchanged, which have been placed along the connection lines between the functions, somehow recalling the structure of sequence diagrams. Nonetheless, the main objective is not to describe the temporal sequence of messages, but to identify and allocate the functions useful to perform an activity.

Initially, the "Supply Hydrogen" was a unique use case. The following activity diagram resulted in too much complexity, so in the second design iteration, the use case was decomposed into the two use cases previously shown, one related to pressure and the other to temperature (Fig. 5.29). Then, a higher-level AD for the "supply Hydrogen" has been created (Fig 5.30). This contains the two functions, "Supply Hydrogen at desired pressure" and "Supply Hydrogen at desired temperature", which are directly linked to their respective activity diagrams, as indicated by the small fork symbols in the bottom-right corner of their block in Fig 5.30.

The pressure at which hydrogen has to be supplied to the FCS has been determined by the systems engineer responsible for the system to be approximately 3 bar.

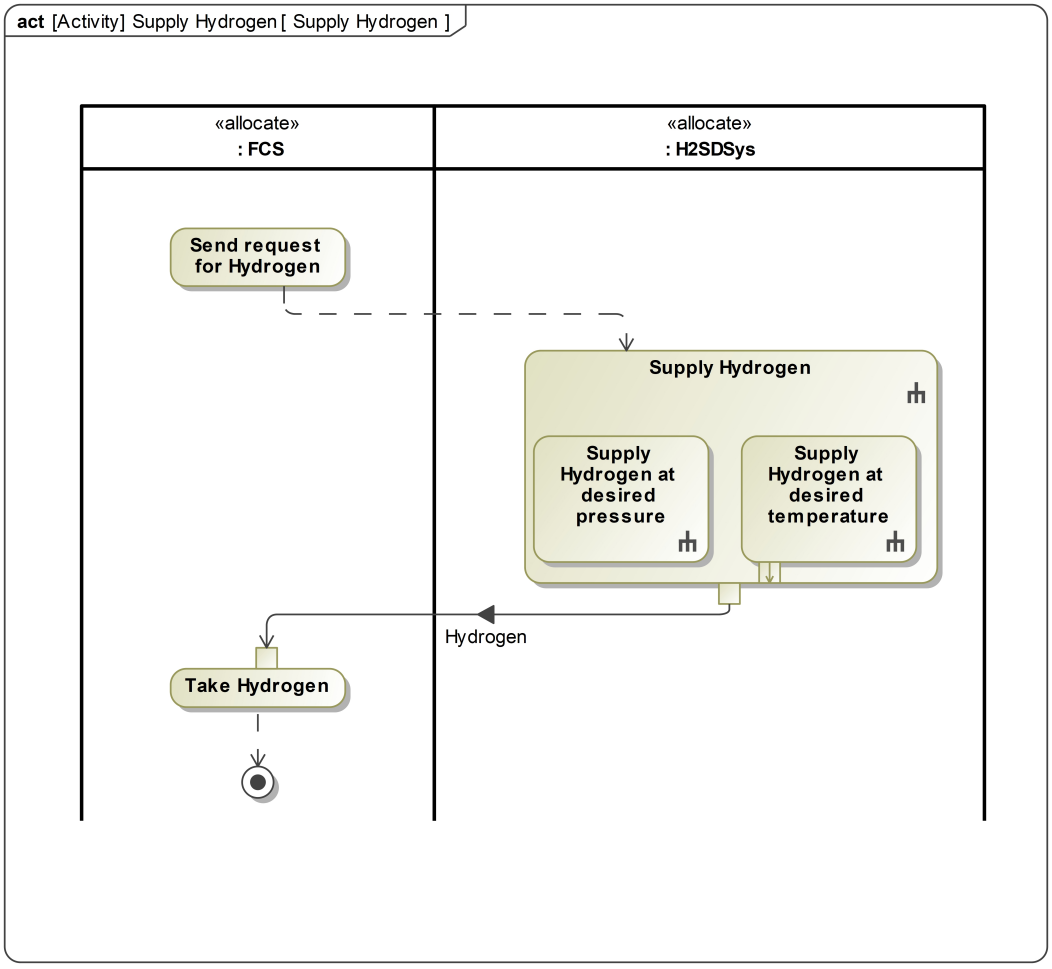

Fig. 5.30 Activity diagram of the "Supply Hydrogen" use case.

This means that, assuming that along the hydrogen distribution line the pressure will remain constant or, more realistically, decrease, a minimum pressure level to the fuel cell can only be guaranteed if the storage pressure is higher than 3 bar, or if a component increasing the hydrogen pressure is inserted along the distribution line. However, this latter solution requires the addition of a component to the system and increases the risk for hydrogen backflow. So, to keep the system complexity as low as possible, it has been decided not to add components to those that were strictly needed. Moreover, to deal with the requirements imposing that the storage pressure should be higher than the external environmental pressure to avoid air penetrating the system in case of cracks or failures, the storage pressure should be in any case kept at least higher than a 1 bar, corresponding to the environmental pressure at sea level, while, apart from the occurrence of particular phenomena in the H_2SDSys surrounding environment, at higher altitudes the external pressure is lower.

It may be helpful to open a parenthesis to show that, in practice, requirements elicitation is a continuous process that can occur at any stage of system design. In fact, as a consequence of this design choice, a new requirement can be formulated: "The pressure at which hydrogen is stored must always be higher than the pressure required by the fuel cell." This requirement could be further refined by specifying that the necessary pressure margin depends on pressure losses along the supply line. In reality, during the doctoral activity, this issue was addressed through direct interaction with the engineer responsible for the fuel cell system. From the perspective of the FCS requirements, it was determined that the output pressure from the storage system must be at least 1 bar higher than the nominal input pressure of the fuel cell to ensure that the FCS can autonomously regulate the inlet pressure within the desired tolerance range.

Looking at Fig. 5.31, the underlying logic applied to supply hydrogen at desired pressure can be depicted. The FCS send a request for hydrogen, the H_2SDSys check the actual storage pressure level and, if it is acceptable supply hydrogen, if the storage pressure level is too low it ask for electric power to make the liquid hydrogen boil so to increase the storage pressure while, if pressure increases too much, the gaseous hydrogen is vented to the environment.

Analogously, the sequence of functions to supply hydrogen at the desired temperature has been reported in Fig. 5.32. Initially, it was assumed that the hydrogen temperature could be regulated through a heat exchanger linked with the TMS, which

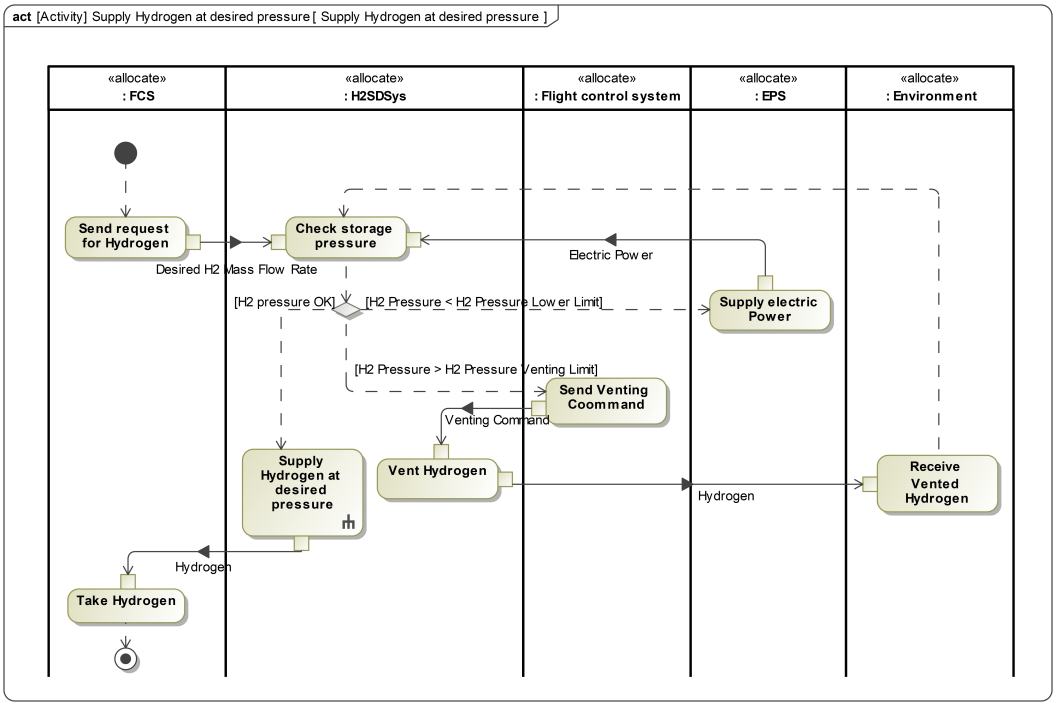

Fig. 5.31 Activity diagram of the "Supply Hydrogen at desired pressure".

was responsible for supplying coolant. Actually, the coolant is used here to heat up the hydrogen out-flowing from the H_2SDSys, not to cool it down. However, again, to avoid increasing the overall system complexity, it has been assumed that the same fluid is used to cool down all the other components and to heat up hydrogen, and to avoid misunderstandings between designers, the term coolant was used. In any case, the system was initially modelled with the heat exchanger as the only "hydrogen-heating" component, and, indeed, the Simulink model proposed (Sec. 5.6.4) has only a heat exchange. However, after a meeting between all the systems engineers, it emerged that the TMS cannot supply the coolant at a suitable temperature until steady-state conditions are reached. Specifically, at the beginning of the mission, when the UAV is started, the hydrogen must be supplied to the FCS at the desired temperature. However, since the coolant is not yet at a proper temperature, it has been proposed to heat the hydrogen using electric power that is always available. Thus, the function "Supply Desired Electric Power" has been added to the diagram together with its swimlane and the relative connections. Nonetheless, the time available to simulate the system with this additional component was not available, and it has been added to the further steps.

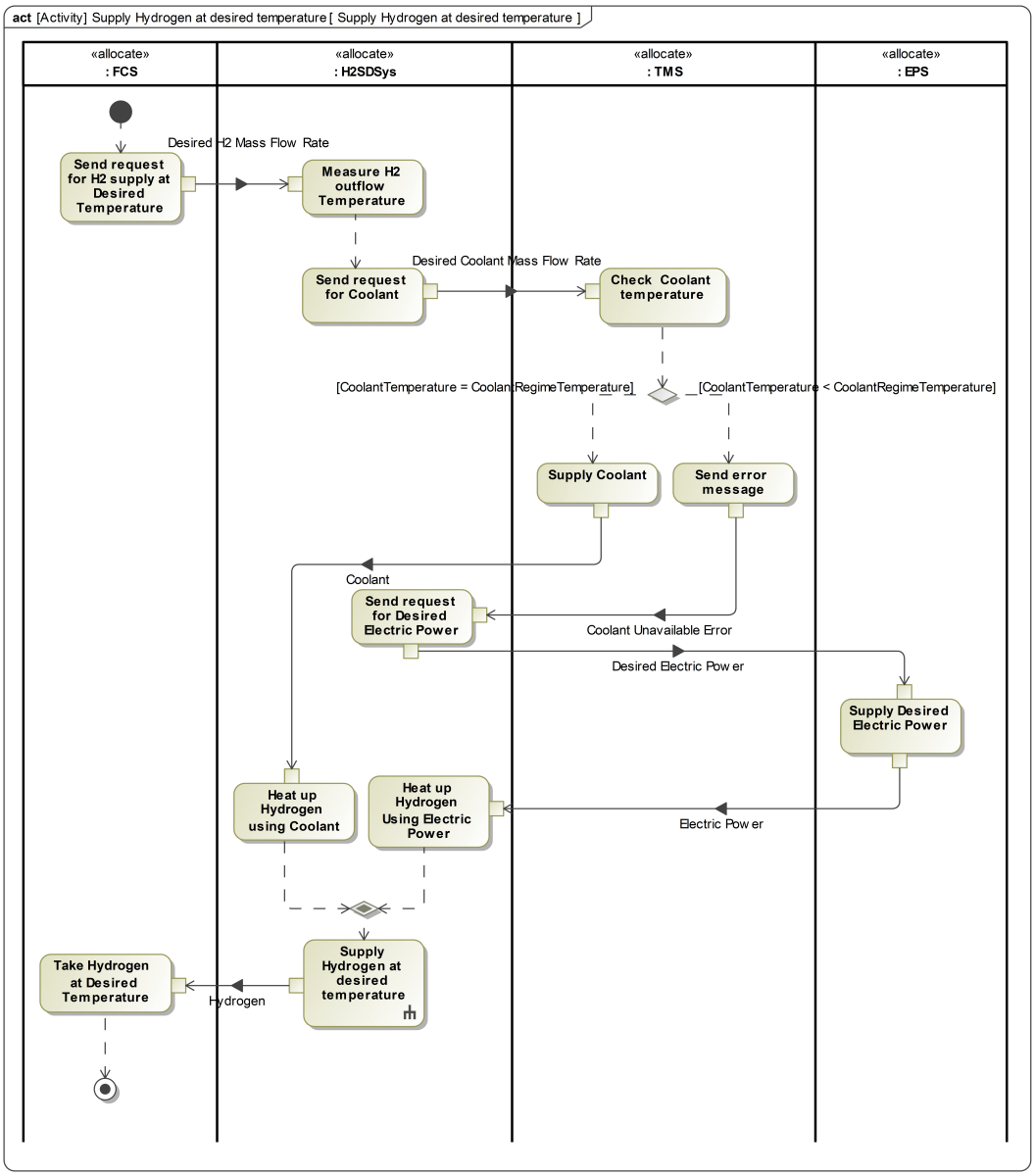

Fig. 5.32 Activity diagram of the "Supply Hydrogen at desired temperature".

After creating and refining the activity diagrams, the activity decomposition map (ADM) can be automatically created. The ADM hierarchically classify all the functions previously defined. Collecting all the functions in a unique map proved useful to both define a set of measures of effectiveness (MOE) and identify the functional subsystems and components.

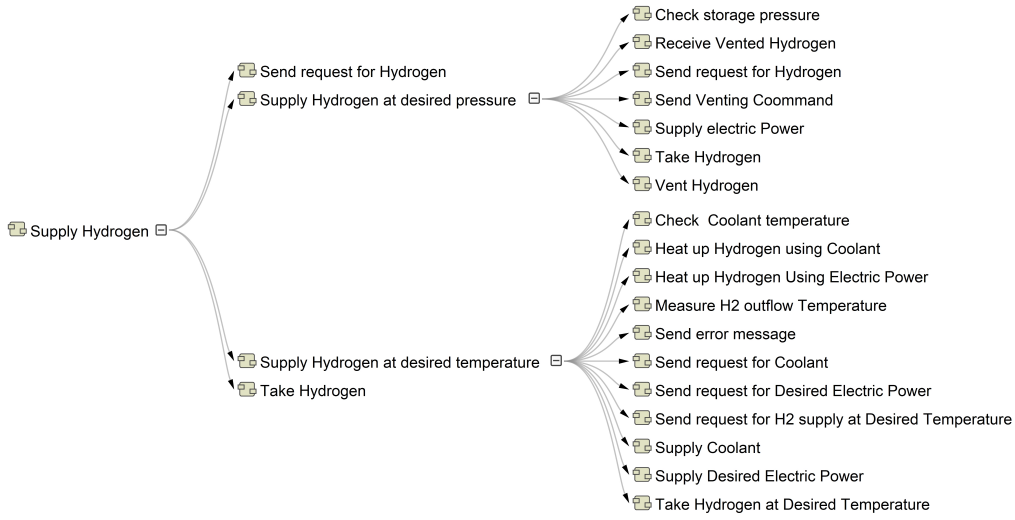

Fig. 5.33 Activities decomposition map.

The MOEs have been collected in a BDD (Fig. 5.34). Formally, the MOE are defined as "measures of success that are closely related to the achievement of the mission or operational objective being evaluated in the intended operational environment under a specified set of conditions." [211]. More precisely, MOEs are measures of the extent to which objectives are met. In the current analysis, the MOEs are practically applied to describe the attributes of the systems. Actually, this use of the MOEs does not significantly diverge from the conceptual use proposed by INCOSE. Indeed, the effectiveness of a system depends on reaching specific objectives, which often turn into measurable objectives that must be included within specific ranges. For instance, considering the use case "Supply Hydrogen at desired temperature" just mentioned, the temperature of hydrogen at the supply will be used as a measure for the effectiveness of the solution proposed. Analogously, the volume of the system will be used both to verify the relative requirement (R_H2SDsys_Max_Volume) and to compare different solutions in further design steps.
The MOEs are collected inside the block "MOEs Holder" and are inherited by the

H_2SDSys block, where the functional blocks identified through the ADM are also reported (Fig. 5.34).

At this point, the transition from black-box to white-box approach takes place. Indeed, a series of functional blocks, representing functional sub-systems or components, has been identified. Then all the functional blocks are placed inside the IBD, which will describe the system's functional architecture. However, at this stage, the functional block still has to be connected to the architecture, and to be linked, each block should show one or more interfaces, formally known as ports. For brevity, the creation of interfaces has only been shown for two blocks: "Storing Hydrogen" (Fig. 5.35) and "Regulating H2 Temperature" (Fig. 5.37). Looking at Fig. 5.35, an interface block has been created and consequently represented in the "Storing Hydrogen" functional block. Then, the exchange items are assigned to each interface block. After assigning all the interfaces to the functional block, the part representing the functional sub-system inside the IBD, which was in practice only a yellow rectangle, becomes populated with ports (Fig. 5.36).

Repeating these steps and linking the parts inside the IBD, the functional architecture has been created (Fig. 5.38). The items exchanged and their flow directions are also specified in the architecture as the result of assigning each item to an interface block, which practically means creating the ports and determining what flows through each of them.

5.6.4 Logical architecture and system dynamic simulation

The purpose of the logical analysis is to propose a preliminary architecture supporting the functional behaviour of the system [6]. Then, the physical analysis is performed, allocating each logical component to a physical one. Typically, physical analysis is performed through digital simulations to optimise time and resources. Then the off-the-shelf or customised components are bought or manufactured, acquired or fabricated for subsequent validation and testing.
Hence, the transition between logical and physical architectures implies the identification of a series of physical components associated with the logical ones. However, in the current analysis, the system's architecture is modelled through blocks that, while providing a quantitative analysis of system dynamics, represent logical components rather than physical ones. For instance, the functional block "Electric H2 Boil

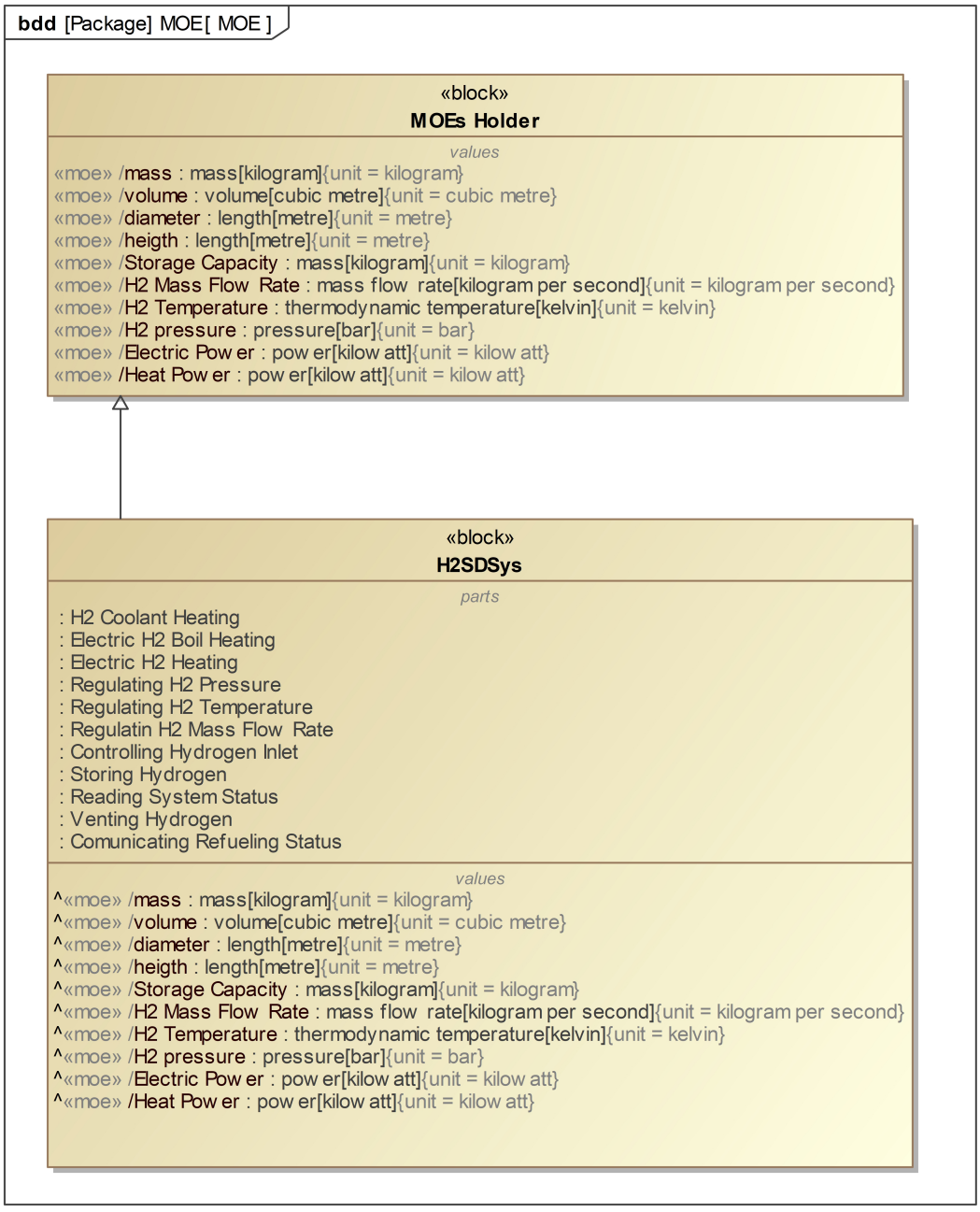

Fig. 5.34 Measure Of Effectiveness (MOE) BDD of the H_2SDSys.

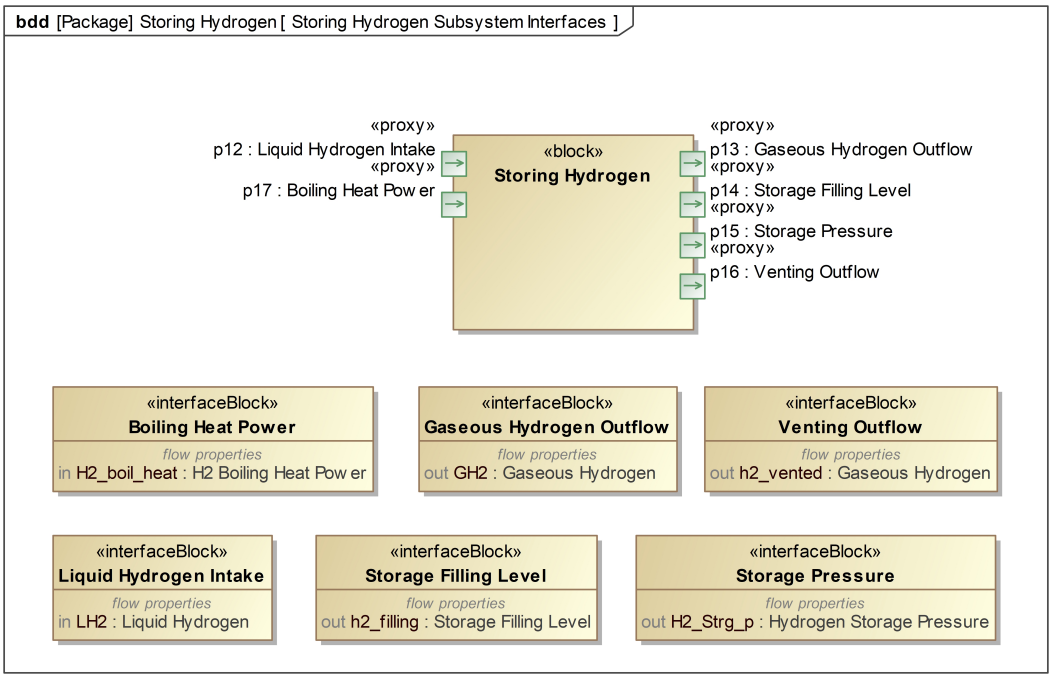

Fig. 5.35 BDD of the subsystem interfaces of the "Storing Hydrogen" functional block.

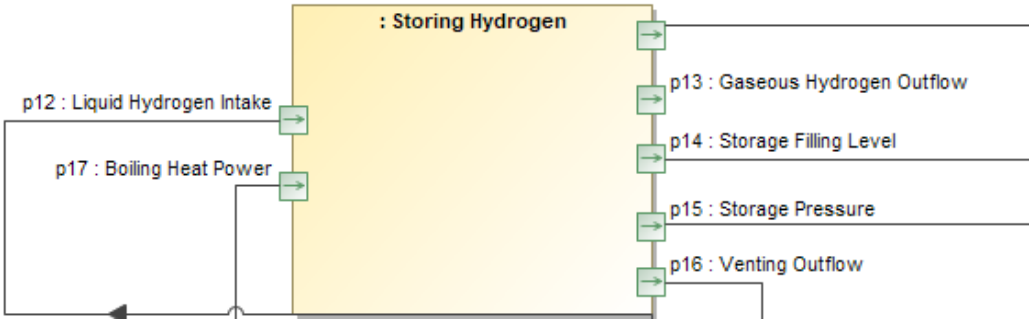

Fig. 5.36 Zoom-in of the functional block "Storing hydrogen".

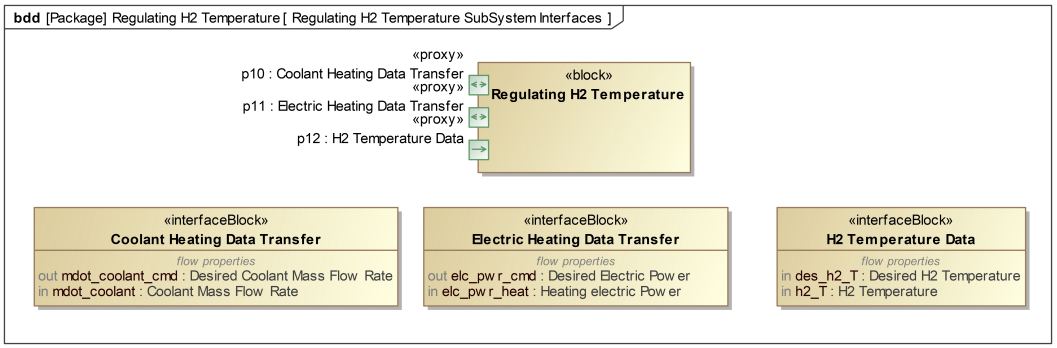

Fig. 5.37 BDD of the subsystem interfaces of the "Regulating H2 Temperature" functional block..

Heating" (Fig. 5.38), which, according to the typical "RFLP" design path, would then be modelled as the logical component "Electric-to-Heat Power Converter", and as a physical one to an electric resistance, has been actually modelled and simulated as a component that simply takes as input electric power and convert it to heat power, thus corresponding to a logical entity rather than to a physical device. From a design perspective, the ability to simulate system dynamics quantitatively while maintaining a logical abstraction of its components proves beneficial at this level, as the majority of components and subsystems are yet to be sized. Once the simulation is performed, a preliminary set of qualitative and, especially, quantitative specifications will be available, thus making interactions with potential suppliers worthwhile.

The architecture of the system is shown in Fig. 5.39, Fig. 5.40, and Fig. 5.41, while detailed images of the tank wall and the hydrogen-water glycol heat exchanger are shown in Fig. 5.42 and Fig. 5.43, respectively. The H_2SDSys modelled is basically composed of the following elements:

- Hydrogen Storage System
  - Hydrogen Tank
  - Electric-to-Heat Power Converter
  - Gaseous Hydrogen Extraction Line
  - Liquid Hydrogen Extraction Line
- Hydrogen Distribution System
  - H2-WaterGlicol HEX

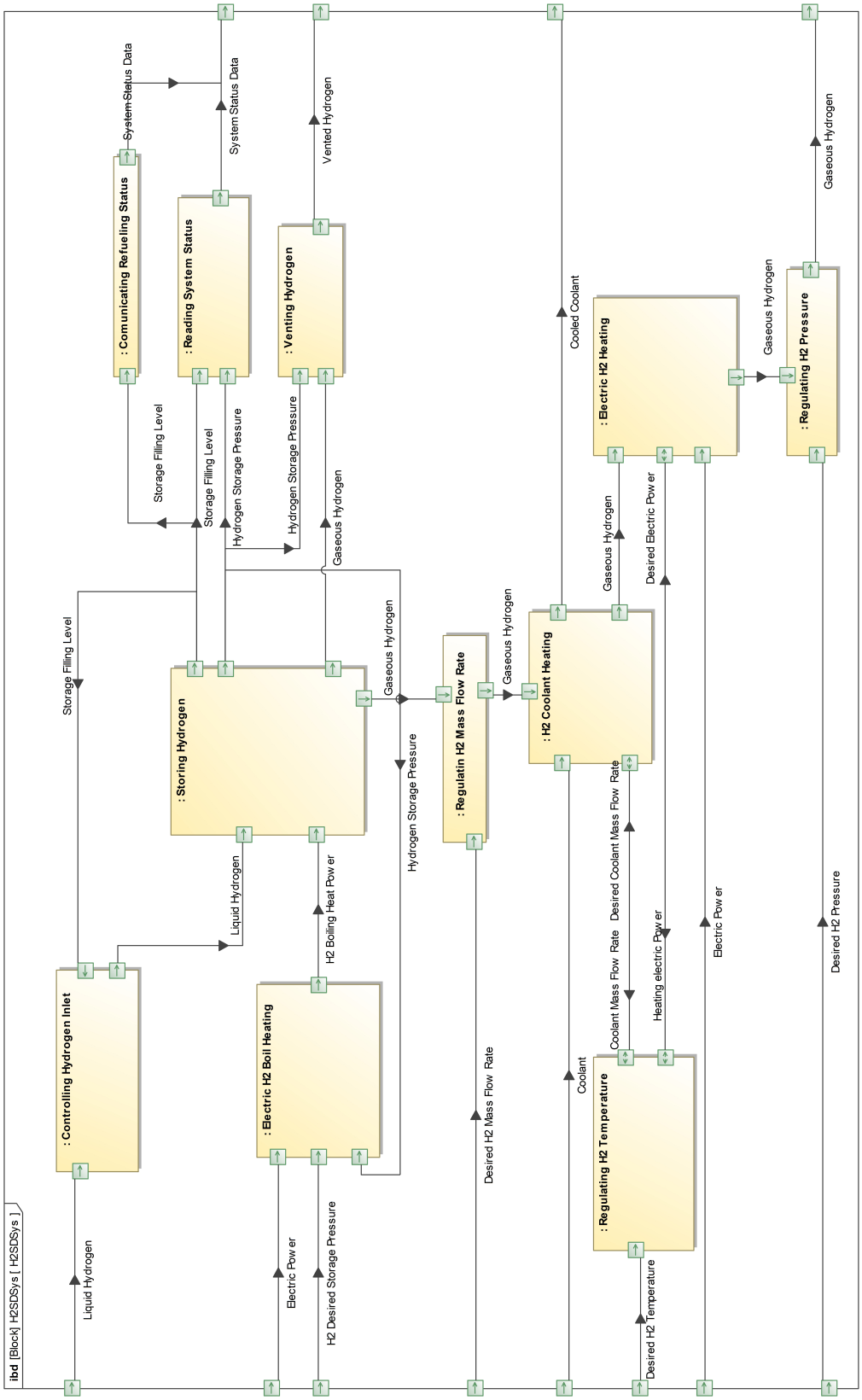

Fig. 5.38 H_2SDSys functional architecture.

  - TMS Supply Line
  - FCS Supply Line

- Hydrogen Venting System

The hydrogen liquid extraction line has been included in the model, even though it was not considered initially, as it would require an additional component to vaporise liquid hydrogen, thereby increasing system complexity. The TMS and FCS are included in the model (Fig. 5.40) due to the need to simulate the coolant and hydrogen supply, even if, as shown in the previous analysis, they are external systems. A detail of the hydrogen tank wall is proposed in Fig. 5.42. Starting

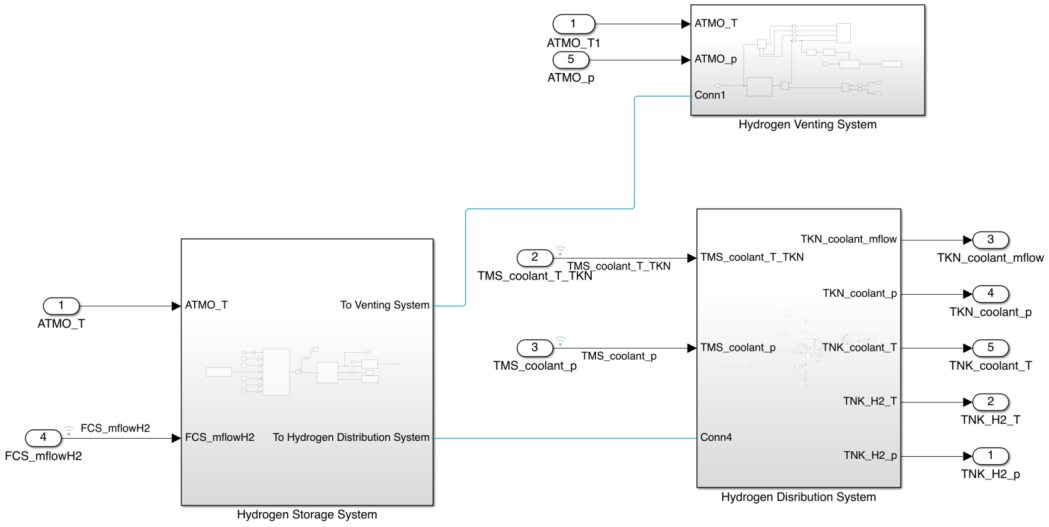

Fig. 5.39 H_2SDSys architecture.

from the left-hand side of the image, it can be seen how the external convection and radiation have been modelled. Then, dedicated blocks are used to simulate the three layers of materials composing the wall: HDPE UHMW, MLI MD low p, and Al 5083-O, as well as the heat leaks entering the tank through pipes and supports. Finally, the heat is exchanged through convection with the gaseous and liquid hydrogen.

Analogously, a magnified view of the heat exchanger is presented in Fig. 5.43, where the blue lines describe the hydrogen line while the yellow ones describe the coolant lines. The heat exchanger design was performed in collaboration with the aerospace engineer within the industrial team of mentors, who used a dedicated

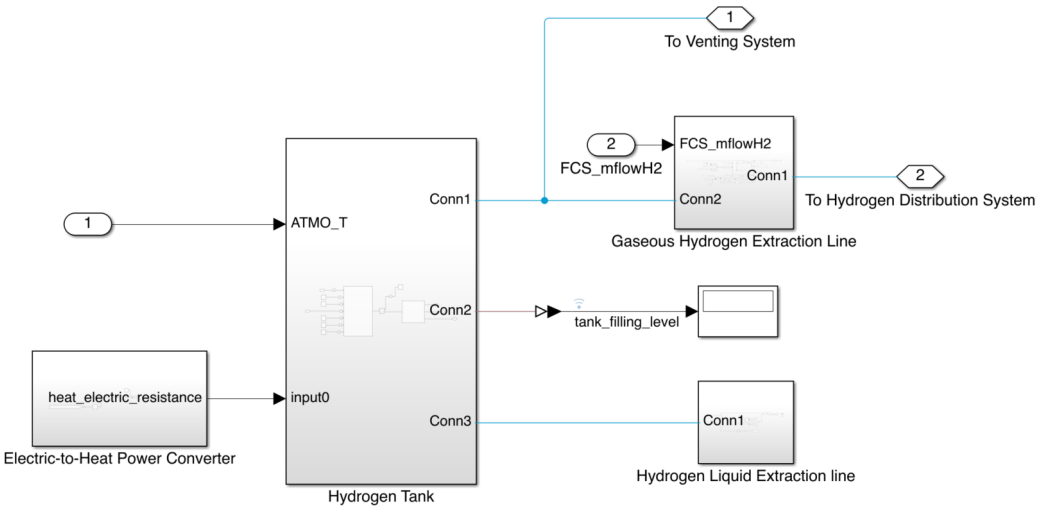

Fig. 5.40 H_2 storage subsystem architecture.

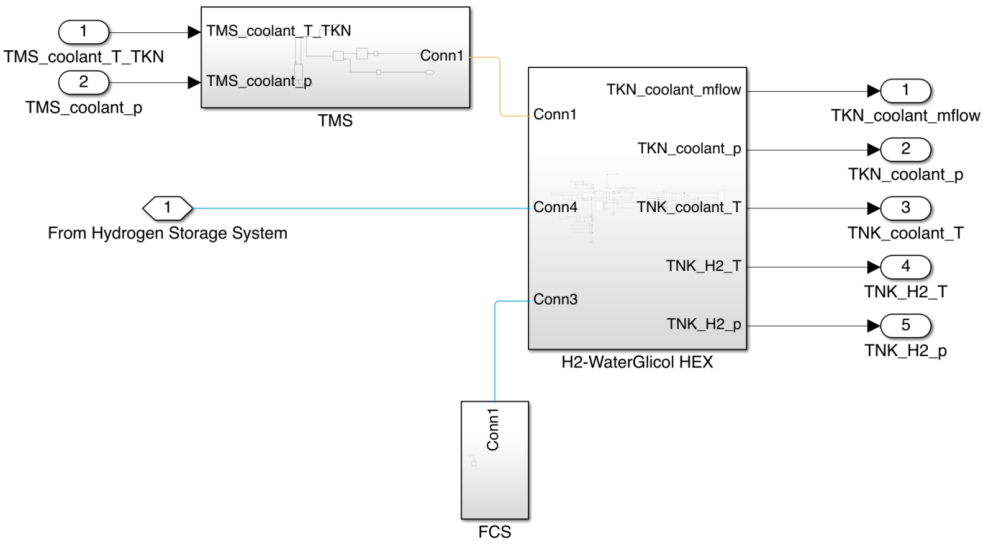

Fig. 5.41 H_2 distribution subsystem architecture.

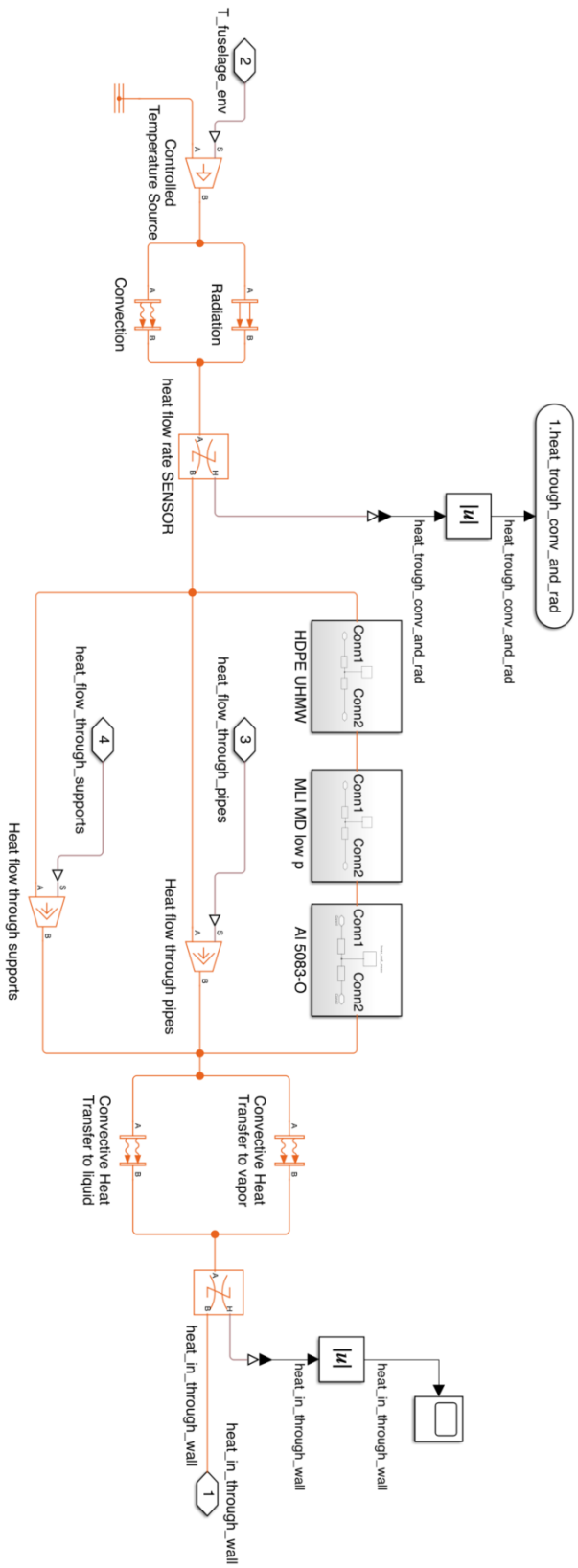

Fig. 5.42 H_2 tank wall.

design model to size the component's internal geometries. Starting from the desired specification provided by the author of the current analysis, the internal dimensions and the required mass flow rate of coolant have been computed, resulting in a heat exchanger exhibiting an efficiency around 90%. The reader can refer to the relevant publications for a more detailed discussion of this topic [212, 213].

The dynamic analysis has been performed in three different runs. The output of the Python sizing model is used as input for the first run. Then, after analysing the results, specific outputs have been changed until the third iteration, when acceptable results have been reached.
The main inputs to start the simulation have been in Table 5.12, while the hydrogen consumption profile, i.e. the mass flow rate of hydrogen requested by the FCS throughout the whole flight mission, has been derived in Ch. 3, and it is referred to as "Nominal mass flow rate" in Fig. 5.44.

The results of the first simulation run are reported in Fig. 5.44, Fig. 5.45, Fig. 5.46, and Fig. 5.47. All the variables shown are plotted along the same time interval, and, indeed, it can be useful to analyse them concurrently. Starting from time zero, it can be seen that the FCS immediately requires a small amount of hydrogen (blue curve in Fig. 5.44). Thus, the electric resistance, aimed at boiling hydrogen inside the tank, increasing its inner pressure, immediately supplies the maximum power of 1 kW (Fig. 5.46). However, this boiling process requires a certain amount of time, and the inner tank pressure takes a while to increase (Fig. 5.45). The density of liquid hydrogen increases with increasing pressure, and this is the reason why the tank filling level increases in this first time span (Fig. 5.47). When the internal tank pressure reaches the value of 4.5 bar, the hydrogen starts out-flowing, the "Mass flow rate supplied (yellow curve in Fig. 5.44 steeply increases, and the tank starts to drain (decreasing curve after the maximum in Fig. 5.47). However, the heat previously introduced through the electric resistance is still making the liquid hydrogen boil. In fact, the internal tank pressure keeps increasing until it settles at a steady value of 5 bar. Actually, after approximately 2.5 h, the hydrogen out-flowing from the tank to supply the fuel cell is not sufficient to counterbalance the increase in pressure generated by the heat entering the tank, so the system starts venting hydrogen into the external environment (green curve in Fig. 5.44). Thus, a relevant amount of hydrogen is wasted and after approximately 17 h the tank is emptied.
The results obtained with these first model settings are not acceptable. Ideally, the nominal mass flow rate curve should be superposed to the supplied mas flow rate

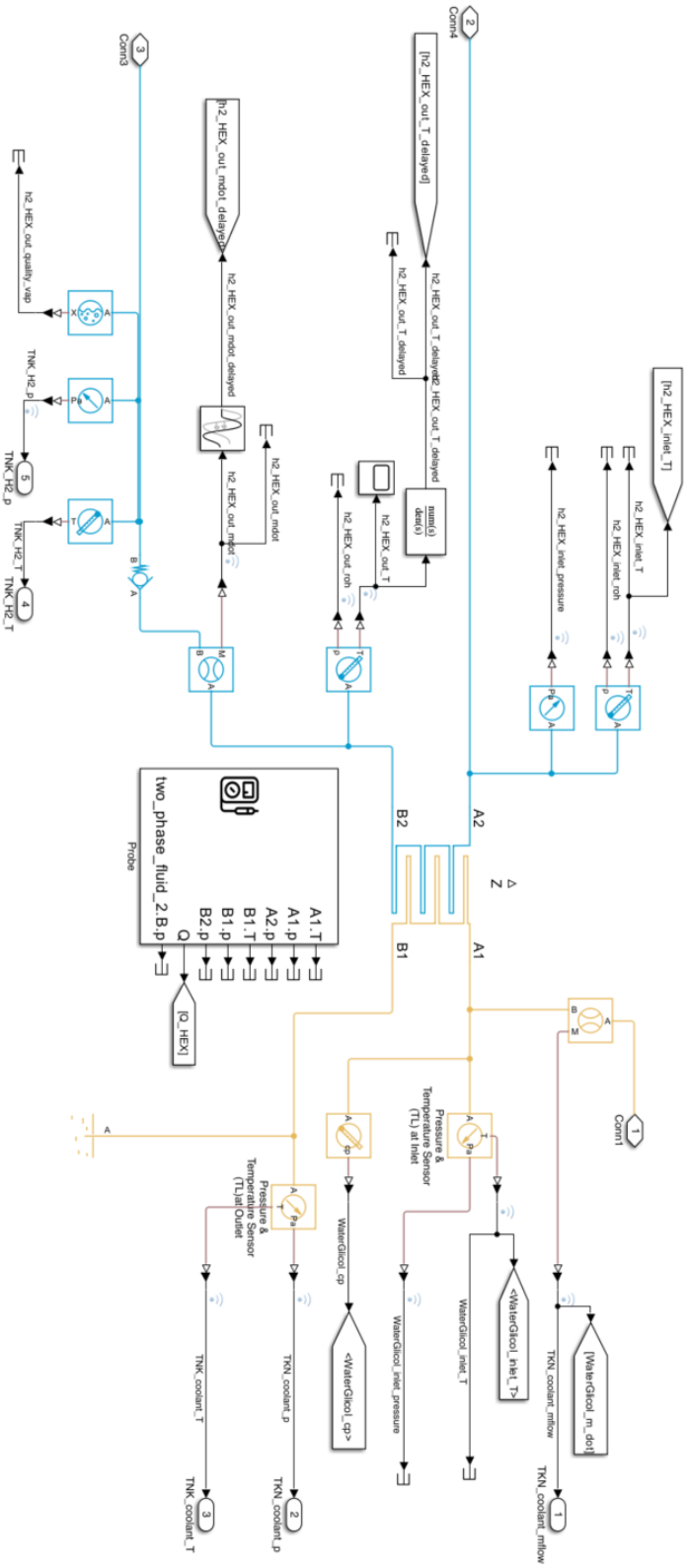

Fig. 5.43 H_2 - water glycol heat exchanger.

Table 5.12 Parameters for the dynamic analysis of the Predator UAV.

Parameters	Values
Tank inner volume (m^3)	1.840
Tank liquid vapor fraction (-)	0.800
Tank outer surface (m^2)	7.730
Tank inner surface (m^2)	7.511
Boil-off rate per hour (%/h)	1.600
Boil-off heat in (W)	212.974
Heat pipes and supports factor (-)	0.300
Heat in through pipes and supports (W)	63.892
Liner material	Al 5083-O
Liner weight (kg)	80.998
Liner specific heat (J/kgK)	900.000
Liner inner diameter (m)	1.256
Liner outer diameter (m)	1.264
Liner length (m)	1.911
Liner thermal conductivity (W/mK)	117.000
Insulation material	MLI_MD_low_p
Insulation weight (kg)	0.021
Insulation specific heat (J/kgK)	1400.000
Insulation inner diameter (m)	1.264
Insulation outer diameter (m)	1.264
Insulation length (m)	1.911
Insulation thermal conductivity (W/mK)	0.00007
Outermost tank cover material	HDPE UHMW
Outermost tank cover weight (kg)	60.847
Outermost tank cover specific heat (J/kgK)	1820.000
Outermost tank cover inner diameter (m)	1.264
Outermost tank cover outer diameter (m)	1.274
Outermost tank cover length (m)	1.921
Outermost tank cover thermal conductivity (W/mK)	0.428

Table 5.13 aviation fuel and hydrogen fuel consumption profile data.

Flight Phase	Duration	Aviation fuel		Hydrogen	
		Fuel Rate	Block fuel	Fuel Rate	Block fuel
	(hour)	(g/s)	(kg)	(g/s)	(kg)
Ground idle & Taxiing	0.42	0.54	0.82	0.19	0.29
Take-off & Climb	1.2	6.76	29.20	2.42	10.46
Cruise Ingress	3.6	3.72	48.21	1.33	17.28
Loiter	14.4	2.7	139.97	0.97	50.16
Cruise Egress	3.6	3.72	48.21	1.33	17.28
Descent & Landing	1.2	1.01	4.36	0.36	1.56

curve (blue and orange curves in Fig. 5.44). However, this only occurs for relatively short time spans, corresponding to the cruise ingress phase and to part of the loiter phase (Table 5.13). The main problems identified are a delay in starting the hydrogen supply and the relevant amount of hydrogen wasted through venting. Initially, the cause of the venting line opening was attributed to the heat introduced into the tank through the electric heater. However, the electricity is supplied at the very beginning of the flight mission and for a relatively short amount of time. In contrast, the system continues to vent hydrogen for an extended period of more than 15 h, despite the boiling effects generated by the introduced electric power being expected to be extinguished. Therefore, it was hypothesised that the cause could be the heat naturally penetrating through the tank wall.

In the second run, one hour has been added at the beginning of the simulation to pre-heat the tank and avoid a delay in the supply of hydrogen. In addition, to keep the internal tank pressure slightly lower, aiming to prevent or retard the venting, the electric power input has been set to stop when the inner tank pressure reaches 4 bar, instead of 5 bar as in the previous case. However, before analysing the main variable trends, the total heat entering the tank has been plotted to quantify the amount of parasitic heat and understand why so much hydrogen is expelled through venting (Fig 5.48). Apart from the initial values starting from 5000 W which are caused by numerical issues not linked to the physical behaviour of the system, the two curves referring to the actual and previous simulations are in practice the same. For the sake of completeness, two numerical values have been highlighted to show that actually there are two curves that, due to specific input changes, may assume different values, even though from an engineering perspective, no differences can

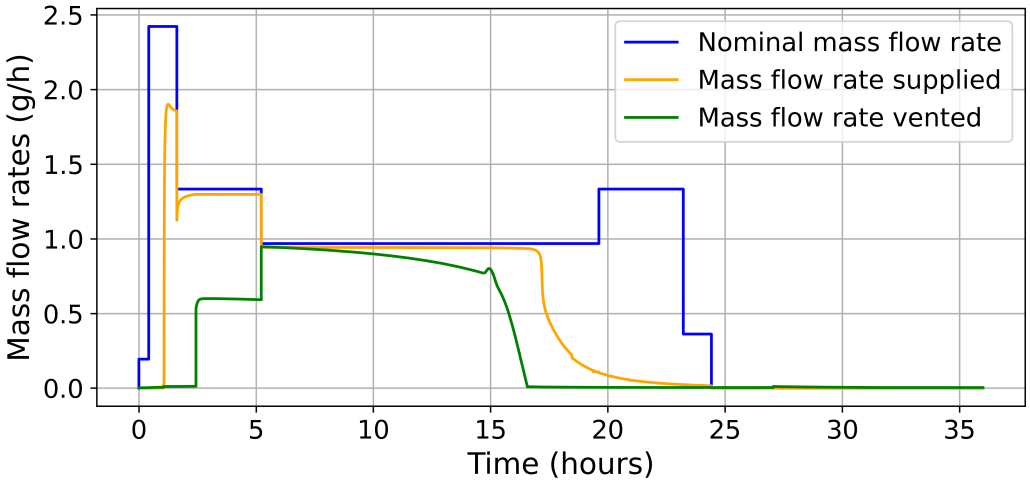

Fig. 5.44 Nominal, supplied, and venting hydrogen mass flow rates throughout flight mission (first configuration).

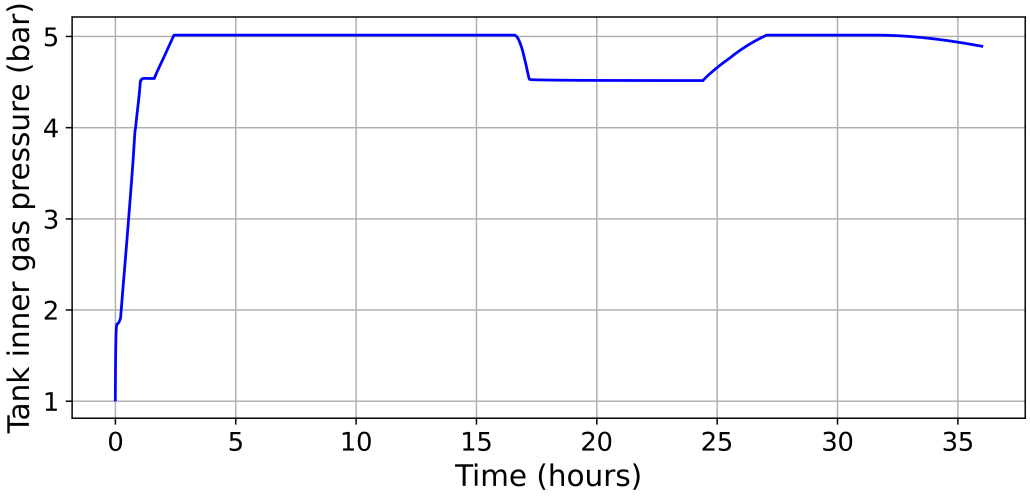

Fig. 5.45 Tank inner gas pressure throughout flight mission (first configuration).

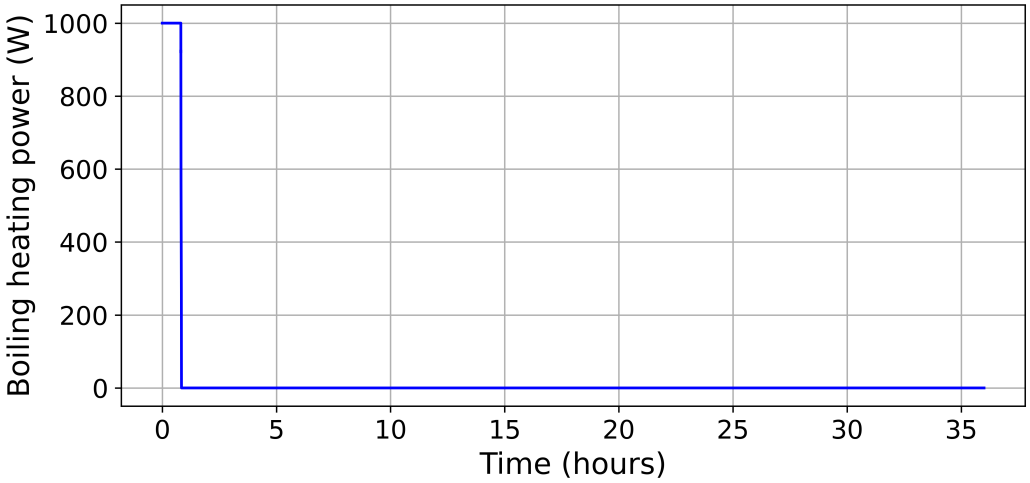

Fig. 5.46 Electric energy supplied to boil LH_2 throughout flight mission (first configuration).

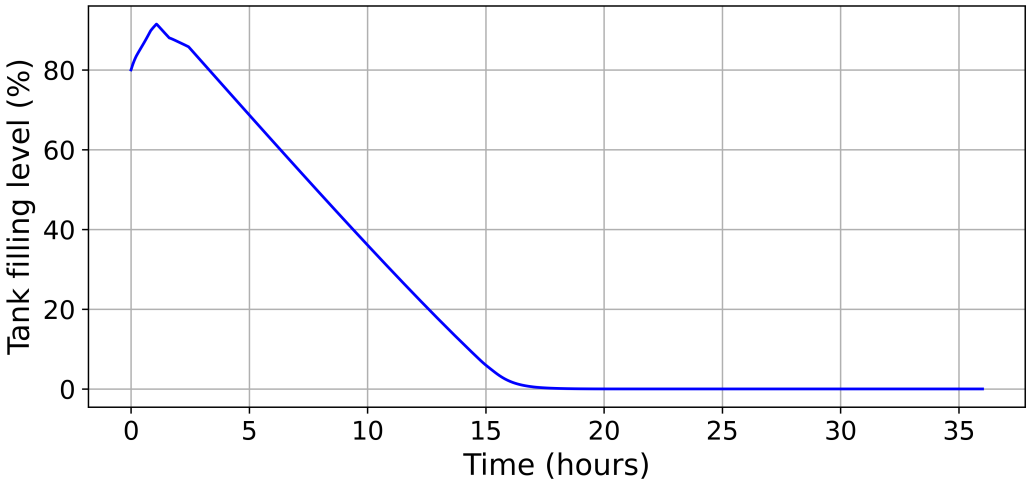

Fig. 5.47 Tank filling level throughout flight mission (first configuration).

be depicted. The heat leakages reach up to approximately 530 W for most of the mission. The insulation thickness computed through the Python model was the one generating a boil-off rate of 1.6 %h^{-1}, which turned into a mass flow rate due to boil-off around 1.7 gs^{-1}. Such a mass flow rate is clearly too high, even overcoming the values requested during most of the flight phases (Table 5.13).

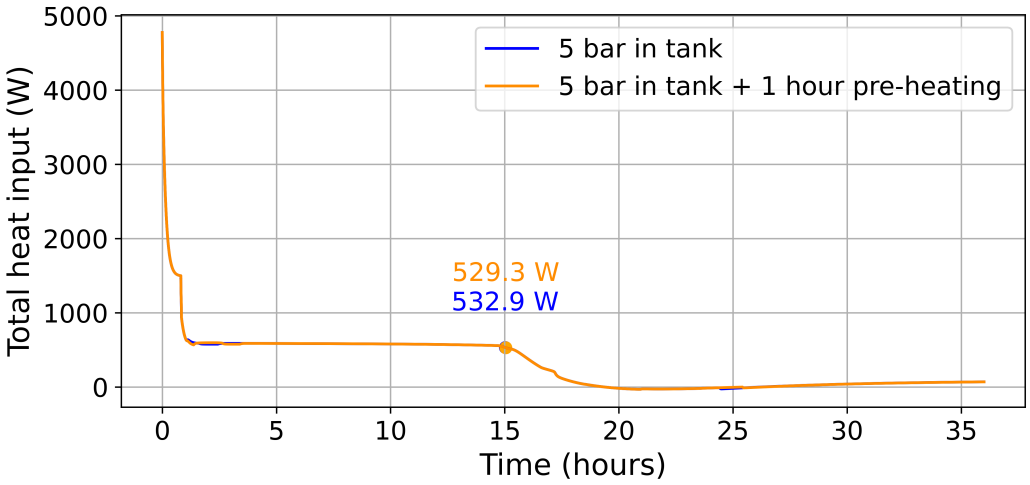

Fig. 5.48 Total heat entering the tank throughout flight mission (First and second configurations).

Then, in the third and final simulation, the BOR was then decreased by one order of magnitude (0.16 %h^{-1}), corresponding to a mass flow rate of 0.17 gs^{-1}, approximately equal to the minimum mass flow rate requested by the fuel cell ("Ground idle & Taxiing" phase in Table 5.13). The resulting insulation thickness was 4.95 mm, while it was less than 1 mm in the previous cases. Obviously, in this case, the heat leakages through the tank wall are much lower and, as a consequence, the electric power introduced to keep the internal tank pressure at the desired level is much more (Fig. 5.51). However, nominal and supplied mass flow rate curves are perfectly superposed, while hydrogen is vented only after the conclusion of the flight mission (Fig. 5.49). The tank's inner pressure level, which needs to be kept, has been lowered to 4 bar and was maintained steadily throughout the mission without the need for venting hydrogen. Finally, the tank filling level gradually decreases, and the tank was completely emptied at approximately 24 h.

The main design parameters corresponding to these final system settings have been reported in Table 5.14. Relatively high values of gravimetric and volumetric

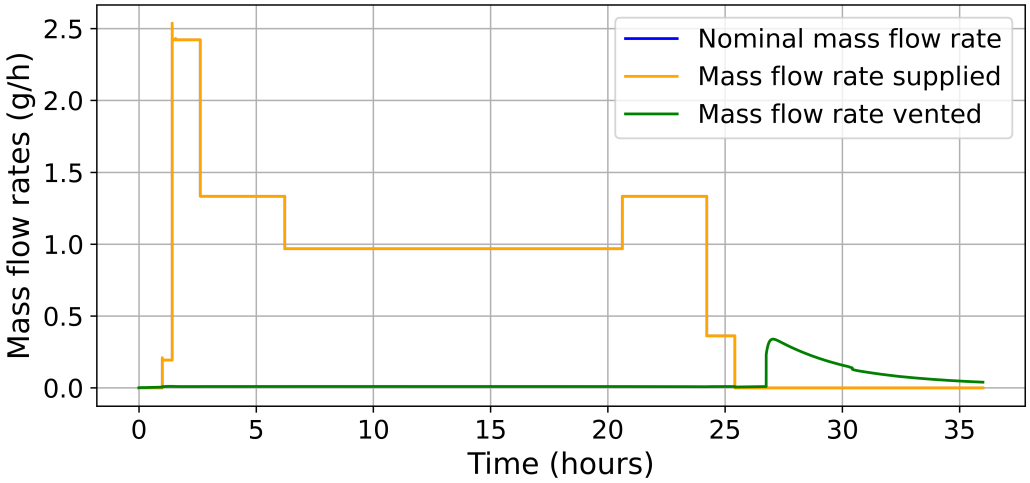

Fig. 5.49 Nominal, supplied, and venting hydrogen mass flow rates throughout flight mission (final configuration).

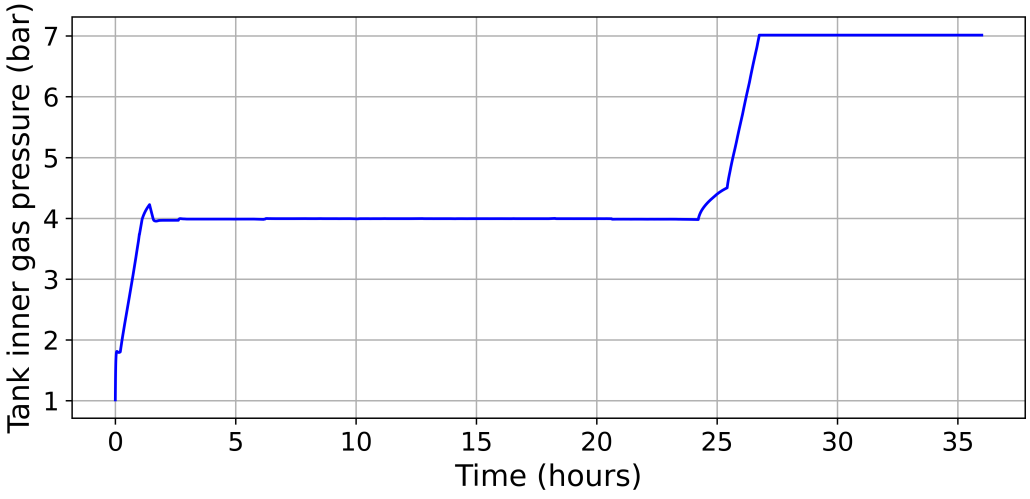

Fig. 5.50 Tank inner gas pressure throughout flight mission (final configuration).

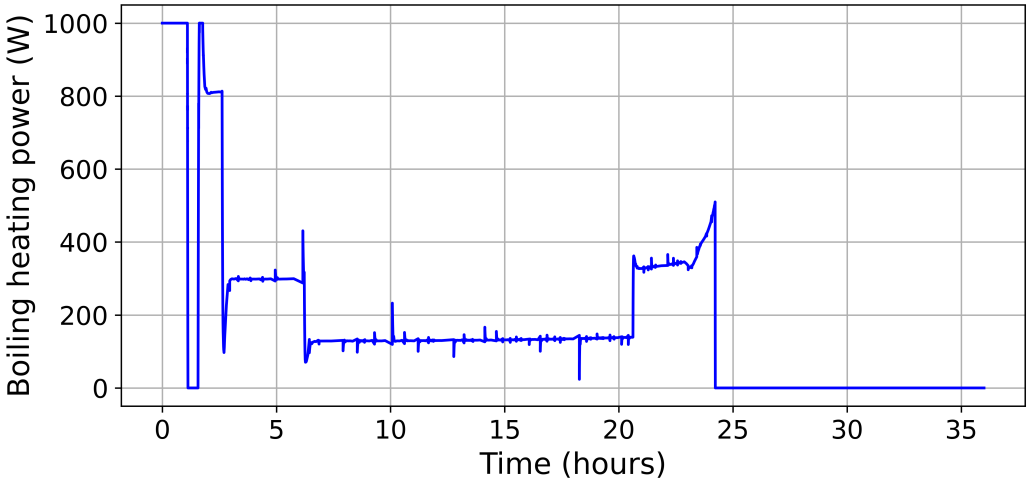

Fig. 5.51 Electric energy supplied to boil LH_2 throughout flight mission (final configuration).

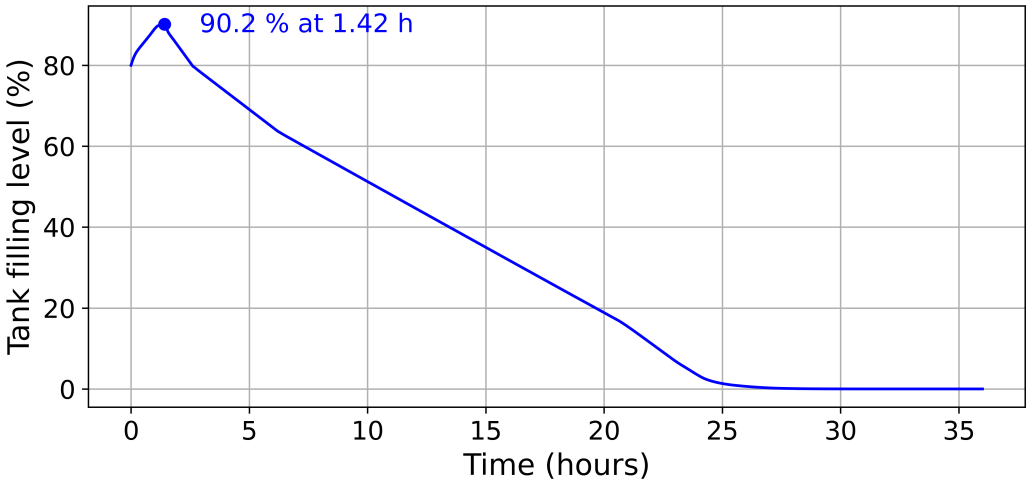

Fig. 5.52 Tank filling level throughout flight mission (final configuration).

Table 5.14 Final configuration of the liquid hydrogen tank for the MQ1 Predator UAV.

Data	Value
Liner material	Al 5083-O
Liner weight (kg)	81.00
Insulation layers materials	MLI_MD_low_p & HDPE UHMW
Insulation weight (kg)	64.32
Tank empty weight (kg)	145.32
Tank diameter (m)	1.28
Tank length (m)	1.94
Gravimetric index (%)	42.52
Volumetric index (kg/m3)	65.77

indices have been found, even though it must be remembered that the outputs of the Python model only consider the weight of the tank walls.

The very last simulation has been performed to compute the dormancy time, i.e. the period during which the hydrogen fuel remains stored in the tank without the need for venting. In practice, this parameter of the system is relevant because it increases the operational capabilities of the whole aircraft. In practice, if any unexpected event occurs after the refuelling phase, or if there is a need for refuelling the aircraft for later use, the document expresses the time interval available between the refuelling phase end and the moment when the loss of hydrogen starts due to venting. To compute the system's dormancy, it is sufficient to close the hydrogen extraction line and cut off the electrical power supply.
The mass flow rate supplied is obviously null (Fig 5.53), while the systems started to vent hydrogen after 7.41 h (Fig. 5.54), corresponding to 7 h and 25 min. Overall, the hydrogen storage and distribution system designed exhibits relevant performance. Despite being approximated, the gravimetric and volumetric indices were high. Also, the dynamic design and analysis of the system provided relevant results, taking into account both the dormancy time just calculated and the system's ability to meet the FCS demands while limiting the maximum electric power input to 1 kW and avoiding boil-off losses throughout the entire flight envelope.

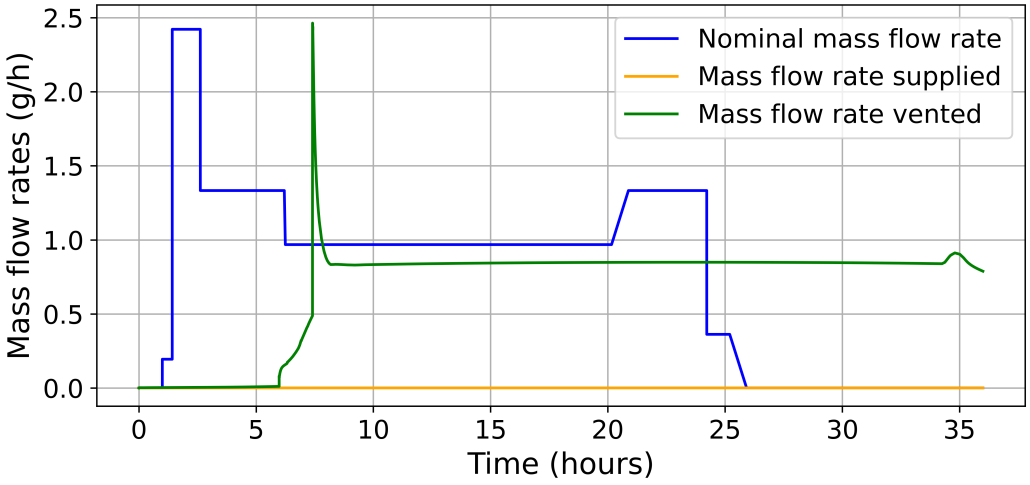

Fig. 5.53 Nominal, supplied, and venting hydrogen mass flow rates throughout flight mission (dormancy configuration).

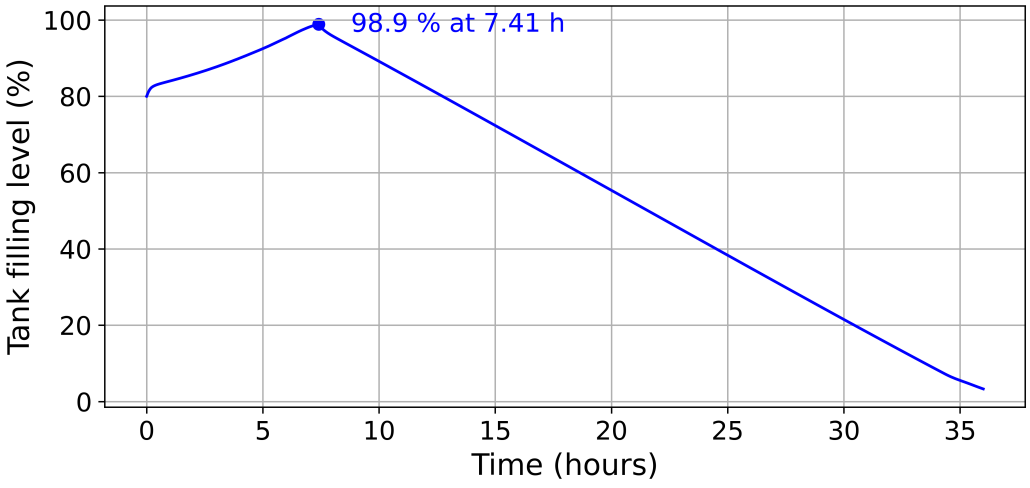

Fig. 5.54 Tank filling level throughout flight mission (dormancy configuration).

Chapter 6

Conclusion

6.1 Summary

The purpose of this thesis was to satisfy the needs of the customer by applying Systems Engineering to the design of a hydrogen storage and distribution system for aviation through the Model-Based Systems Engineering methodology. All the efforts and attempts to improve the methodology and to develop models to describe the system's behaviour have been supported by validation against data retrieved from real systems or from the literature and by the experience of industrial experts, while the methodology has been compared with the industrial platform to evaluate its feasibility.

To comply with the requests coming from the customer introduced in Chapter 1, an extended review of the literature has been conducted. In Chapter 2, Systems Engineering is introduced, together with the terminology useful in the subsequent analysis, and a description of Model-Based Systems Engineering, including the methodology, the language, namely the Systems Modelling Language (SysML), and the tools. Moreover, two sections have been added to introduce the new version of the SysML, referred to as SysML v2, and to describe the practical advantages of applying MBSE at the industrial level.
Since large UAVs have been identified by the author as promising platforms to investigate the use of hydrogen as fuel, in Chapter 3, an introduction to UAVs, to their applications and their classification is proposed. The focus then shifted to high altitude long-endurance and medium altitude long-endurance UAV classes. The data

available from the literature have been collected and compared, and two case studies have been identified: the MQ-1 Predator by General Atomics and the RQ-4 Global Hawk by Northrop Grumman. The choice fell on these two aircraft, both due to the considerable amount of data available in the literature, and because they were considered representative of their respective classes.
The use of hydrogen in aviation is anything but new. So, to understand why aviation nowadays aims at shifting towards new technologies, among which hydrogen seems to be one of the most promising, and also aimed at understanding why hydrogen has never achieved widespread adoption despite the relevant studies and demonstrators previously developed, a comprehensive review about the history of hydrogen in aviation is presented at the beginning of Chapter 4. Then, an investigation to understand why hydrogen is actually one of the most promising solutions among those available to store energy is proposed. A description of the different methods to store hydrogen is then presented, with a focus on the three physical methods for storing hydrogen.
The core of the analysis is developed in Chapter 5. The application of Systems Engineering is briefly introduced. A conceptual design path for the application of MBSE is described and applied in a simplified way to the design of the UAV, mainly to make the reader grasp the design thread linking the very initial phase, i.e., the analysis of the customer's needs, with the design of the hydrogen storage and distribution system. Then, before continuing to apply MBSE, a parametric model to perform the static preliminary design of the hydrogen tank is presented and applied to the two case studies just mentioned. Then, the requirements and functional analyses have been carried out, and a preliminary functional architecture has been developed. Finally, the dynamic design has been conducted on the whole system architecture, and the main results have been traced.

The heterogeneity of the work proposed is now evident. Both technical and methodological aspects have been investigated throughout the doctoral activity. Thus, the key findings and the implications, delineated in the following section, have been classified accordingly.

6.2 Findings and implications

Starting with the methodological findings, the application of Model-Based Systems Engineering in an industrial R&D context, as well as the limited adoption of well-established design methodologies, led to subsequent conclusions.

- The adoption of a preliminary MBSE approach facilitated early interaction among stakeholders throughout the system life-cycle.
- The parallel development of requirements, functional, logical, and physical analyses proved more effective than a strictly sequential process.
- The availability of preliminary quantitative data was essential to support early design decisions and feasibility assessments.
- The presence of a unique source of truth proved useful when integration activities have been conducted and data related to all the sub-systems was needed.

As MBSE had not been previously adopted, at the beginning of the PhD activity, attempts have been made to directly apply MBSE approaches retrieved from the literature. This strategy proved ineffective, as it was not consistent with the company's internal activity planning and was perceived as offering limited practical value.
Thus, it was referred to prioritise the development of a comprehensive, though somewhat preliminary and imprecise, framework covering all the aspects to be investigated from a high level of detail, instead of pretending to have a detailed output as a result of each design step and, only after, proceed with the subsequent steps. In this way, the outputs of the activities conducted by the R&D team were used to refine the methodology and were collected in the form of constraint requirements or functions within the model. To do so, it proved convenient to preliminarily develop requirements, functional, logical, and physical analyses with the information available, instead of elaborating in detail a certain aspect before moving to the following. By doing so, the cooperation among the team members was improved with the aim of having a useful and practical tool, which was the framework itself, that would then naturally satisfy the needs of the team and ease its adoption.
Following this approach, several issues emerged very early in the design, enhancing the dialogue between stakeholders. Moreover, in an innovative context like that of

an R&D unit, very often the technologies and solutions were not available, and if experimental activities had to be conducted, interactions with potential suppliers became mandatory and contributed to delineating the design space.

Further evidence of the relevance of promoting communication from the very early design phases was provided by modelling activity conducted during the first months of the PhD that had to be reviewed after the beginning of the cooperation with the system supplier, where mutual needs and constraints rapidly emerged. However, quantitative data provided through modelling activities was needed to engage with potential suppliers at the very beginning, even if the system was not clearly defined nor its objectives. Thus, to avoid developing unnecessary models, the author found it useful to build a parametric and flexible model exploring the main aspects all at a high level, which was somehow intended to quantify the design space rather than size a system.

An additional relevant finding emerged through the design activity was the need for a unique source of information became evident during integration activities when the need for aligning all the variables and parameters required a relevant effort, both in terms of time and work, to collect the data of the subsystems from all the stakeholders. Several design iterations were needed only to align the several inputs and outputs to enable the integration among models, because interactions in the previous phases revealed insufficient or not effective enough. A practical consequence of this issue has been shown throughout the study. Indeed, during the analysis on the interaction between the thermal management system and the hydrogen storage and distribution system, it emerged that the fluid used to heat hydrogen to bring it to the desired temperature was not available in the initial phases of the flight mission because it had to reach the steady-state conditions before being usable. However, the architecture of the model was already designed and analysed under the assumption that the heating fluid was at a constant temperature. Thus, further design iterations will be required to include these aspects.

Moving to quantitative findings related to the sizing of the hydrogen storage and distribution system, conclusions have been delineated from the outputs of static and dynamic analyses.

- The choice of insulation material should not be based only on gravimetric and volumetric efficiencies, nor should it be conducted by considering only thermal aspects.
- The increase in insulation thickness applied during the dynamic analysis of the Predator use-case to avoid boil-off losses during the mission decreased the gravimetric index from approximately 55% to 42.5%, while had minimum impact on the volumetric index which decreased from 67% to 65.75%.
- The structural aluminium layer was identified as the main contributor to overall tank mass.
- Despite the relevant gravimetric and volumetric performance derived from the hydrogen tank static sizing of the Predator and the Global Hawk UAVs, retrofitting activities proved to be not competitive with respect to fossil fuel solutions, driving further steps towards entirely new aircraft configurations.

The first general findings worth mentioning are related to the exploration of the hydrogen tank insulation materials. Being stored at cryogenic conditions, several aspects related to thermal design are explored in the literature. Concerning passive insulation, it has been highlighted in this work that relying on gravimetric or volumetric efficiencies to select a proper insulant can be misleading, due to their low influence on the final performance. Other properties or characteristics should then be identified as discriminant.
Further proof can be provided by moving to the use cases of the Predator and Global Hawk UAVs. Indeed, the choice of the insulation material had a relatively low impact on the performance of the vessel. For the Predator UAV, storing 107.5 kg of hydrogen, the gravimetric and volumetric indexes range approximately between 50% and 55% and between 67% and 68.5%, respectively. At the same time, for the Global Hawk, having a storage capacity 2811.84 kg, the gravimetric and volumetric indexes span from about 42% to 46.33%, and from 60% to 67.23%.
Two additional findings should be analysed: the decrease in gravimetric index for increasing storage capacity and the low influence of the choice of different insulating materials on the tank gravimetric and volumetric efficiency, which is even in contrast with results previously published by the same author of the present thesis.

Typically, increasing the tank capacity also increases its performance. However, the model includes a correction factor in the structural analysis, leading to an increase

in the mechanical layer to avoid buckling, which affects larger tanks to a greater extent.
Concerning the low impact of the insulation material, in the current analysis, the mechanical aluminium layer accounts for a greater portion of the total system weight due to its increased thickness to comply with the relatively high operating pressure imposed by the fuel cell, thus leading to a minimum change in the overall tank mass.

The outputs of the model were used to assess the possibility of retrofitting the two UAVs. However, comparing the tank dimensions with the estimated volume available inside the fuselage, it has been concluded that a hydrogen tank storing the same energy content as jet fuel cannot be installed onboard in either case. An existing platform has been considered useful to perform experimental operations during the development phases to be used as a flying test-bed, but retrofitting of an existing Predator or a Global Hawk UAV would likely lead to a non-competitive solution. Thus, entirely new aircraft configurations should be explored.

Due to limited time available, the outputs of the Predator UAV were only used to develop the hydrogen storage system architecture following the MBSE, and to perform dynamic analyses. The whole system's architecture was first simulated, starting from the outputs of the sizing model. The flight mission could not be completed due to the high amount of hydrogen lost through boil-off. Consequently, during the second iteration, the heat entering the tank was better analysed, and the insulation thickness was increased through a further design iteration starting from the static sizing model. The objectives were achieved, and the flight mission was completed without any boil-off loss. The resulting performance of the tank configuration was a gravimetric index of 42.5% and a volumetric index of 65.75%. Finally, a further simulation was conducted to estimate the dormancy of the vessel, which resulted in approximately seven and a half hours. The compliance with requirements deriving from operational scenarios should then be conducted.

The many conclusions delineated above have been separated according to technical and methodological aspects. However, it must be highlighted that the intercorrelations between the methodological issues, experimented through the practical application of MBSE in an industrial R&D unit, and the purely sizing ones, are one of the main results of this study. Indeed, the doctoral activity described throughout this dissertation is itself a proof of the relevance of applying a holistic approach. Systems Engineering, and specifically, Model-Based Systems Engineering, proved

to be a suitable methodology to implement this holistic approach. Through its tools, methods and language, several critical issues can be addressed, resulting in considerable efforts and resources saved.

6.3 Further developments

The work described throughout this thesis has been conducted keeping a holistic approach, which transversally covers several aspects without pretending to be exhaustive. It follows that further developments include a deeper investigation of the topics already described, as well as the analysis of those that, due to a limited amount of time, have not been mentioned.

The advantage of implementing Systems Engineering, as well as the key findings derived from the practical application of MBSE in an industrial context, have already been mentioned. However, throughout its continuous application, the methodology can be improved to align with industrial standards, methodologies, and analyses, including certification aspects related to UAVs and fuel systems, crashworthiness, hazard assessment methods, operational fault management, or system behaviour under non-nominal conditions, as well as scenario-based analyses addressing emergency situations, abnormal operating modes, and fault propagation mechanisms. This would improve model reliability, facilitate qualification, certification, and other regulatory processes, and improve design assurance.

Other key findings related to the system sizing highlighted the inefficiency of performing retrofitting activities, thus driving further design phases towards the investigation of entirely new hydrogen-based aircraft configurations.
Moving into the mechanical design, the hydrogen tank structure should be further investigated to include structural elements such as stiffeners, support columns, and annular rings, with the aim of improving the structural capabilities while reducing its weight and, mainly, to avoid the application of correction factors which may wrongly influence design choices. The analysis should also include the tank's supports that, in the current analysis, have only been modelled as sources of heat leakages in the thermal analysis. There are even studies in the literature assuming that, by selecting an insulation material with sufficient mechanical properties, the tank supports could be attached to the external insulating layer instead of the internal one, thus avoiding heat leakages through them. However, this was questioned throughout the work due

to the strict requirements typically imposed in the aviation sector. Specific standards have not been published yet, but considering that safety-critical systems should be capable of maintaining their integrity even in the case, for instance, of a hard-landing scenario, further analysis should be conducted to verify this hypothesis.

The dynamic analysis raises the need for an element that makes hydrogen evaporate during the stages of the aircraft mission when the system is operating under transient conditions, and the coolant cannot provide sufficient heat to vaporise hydrogen. It has been preliminarily assumed that during these transitions, an electrical resistance could be used. However, this possibility needs to be explored to assess its best allocation in the system architecture, to estimate the required energy, and to evaluate its integration inside an existing component or the creation of a dedicated subsystem. Moreover, dormancy has just been computed after several iterations aimed at increasing the insulation thickness to avoid boil-off losses throughout the mission. Further steps should optimise these aspects and identify the best configuration complying with requirements and constraints derived, for instance, from airport regulations or from operational scenarios.

The further developments described here, as well as the key findings mentioned above, highlight the relevance of performing system design concurrently applying MBSE and sizing the system. However, the connection between the two is mainly kept by the engineer who invests relevant effort to keep coherence among the several elements of this big picture. Actually, this tremendously increases the risk for failures as the system grows in complexity. This issue can be addressed by applying the new version of the System Modelling Language, namely SysML v2. Indeed, a relevant step to advance the design could be represented by the increased interoperability derived from the application of SysML v2. The author of this thesis investigated this new language and developed a preliminary tool to automatically verify requirements during several design iterations to limit repetitive manual operations (Appendix **??**). Due to the limited amount of time, SysML v2 has not been applied in the current work, but its potential to bridge MBSE and other design activities may lead to extraordinary advantages in the future.

References

[1] Pimchanok Su-ungkavatin, Ligia Tiruta-Barna, and Lorie Hamelin. "Biofuels, Electrofuels, Electric or Hydrogen?: A Review of Current and Emerging Sustainable Aviation Systems". In: *Progress in Energy and Combustion Science* 96 (May 1, 2023), p. 101073. ISSN: 0360-1285. DOI: 10.1016/j.pecs.2023.101073. URL: https://www.sciencedirect.com/science/article/pii/S0360128523000035 (visited on 06/14/2023).

[2] A. Boretti. "Perspectives of Hydrogen Aviation". In: *Advances in Aircraft and Spacecraft Science* (2021), pp. 199–211. URL: https://doi.org/10.12989/aas.2021.8.3.199 (visited on 06/14/2023).

[3] Candelaria Bergero et al. "Pathways to Net-Zero Emissions from Aviation". In: *Nature Sustainability* 6.4 (Apr. 2023), pp. 404–414. ISSN: 2398-9629. DOI: 10.1038/s41893-022-01046-9. URL: https://www.nature.com/articles/s41893-022-01046-9 (visited on 04/28/2024).

[4] David Timmons and Rob Terwel. "Economics of Aviation Fuel Decarbonization: A Preliminary Assessment". In: *Journal of Cleaner Production* 369 (Oct. 1, 2022), p. 133097. ISSN: 0959-6526. DOI: 10.1016/j.jclepro.2022.133097. URL: https://www.sciencedirect.com/science/article/pii/S0959652622026865 (visited on 06/14/2023).

[5] G. D. Brewer et al. *Study of the Application of Hydrogen Fuel to Long-Range Subsonic Transport Aircraft, Volume 2*. LR-26752-2. NASA, Jan. 1, 1975. URL: https://ntrs.nasa.gov/citations/19750022090 (visited on 12/09/2024).

[6] Eugenio Brusa, Ambra Calà, and Davide Ferretto. *Systems Engineering and Its Application to Industrial Product Development*. Studies in Systems, Decision and Control. Cham (CH): Springer International Publishing, 2018. ISBN: 978-3-319-71836-1. DOI: 10.1007/978-3-319-71837-8.

[7] INCOSE. *Systems Engineering Handbook: A Guide for System Life Cycle Processes and Activities*. Fifth. Hoboken, New Jersey: John Wiley & Sons, 2023. 309 pp. ISBN: 978-1-118-99940-0.

[8] SEBoK Editorial Board. *Guide to the Systems Engineering Body of Knowledge (SEBoK)*. version 2.12. BKCASE Project, May 27, 2025. URL: https://sebokwiki.org/w/images/sebokwiki-farm!w/e/e1/Guide_to_the_Systems_Engineering_Body_of_Knowledge_v2.12.pdf.

[9] Jon Holt and Tim Weilkiens. *Systems Engineering Demystified: Apply Modern, Model-Based Systems Engineering Techniques to Build Complex Systems*. Packt Publishing Ltd, July 27, 2023. 533 pp. ISBN: 978-1-80461-183-8. Google Books: rJnMEAAAQBAJ.

[10] Jeff A Estefan. "Survey of Model-Based Systems Engineering (MBSE) Methodologies". In: *INCOSE MBSE Initiative* Rev. B (May 23, 2008), pp. 1–70.

[11] Stephen J. Kapurch. *NASA Systems Engineering Handbook*. DIANE Publishing, Nov. 2010. 360 pp. ISBN: 978-1-4379-3730-5. Google Books: 2CDrawe5AvEC.

[12] Sanford Friedenthal, Alan Moore, and Rick Steiner. *A Practical Guide to SysML: The Systems Modeling Language*. Morgan Kaufmann, Oct. 2014. 631 pp. ISBN: 978-0-12-800800-3.

[13] *Getting to Know the SysML Diagrams | Enterprise Architect User Guide*. URL: https://sparxsystems.com/enterprise_architect_user_guide/17.1/guide_books/tech_sysml_gettingtoknow_diagrams.html (visited on 07/29/2025).

[14] Fabian Gilson. "Transformation-Wise Software Architecture Framework". Mar. 2, 2015. DOI: 10.13140/RG.2.1.3757.0320.

[15] *Use Case*. July 30, 2025. URL: https://dictionary.cambridge.org/dictionary/english/use-case (visited on 07/30/2025).

[16] Beatriz Bernàrdez, Amador Duràn, and Marcela Genero. "Metrics for Use Cases: A Survey of Current Proposals". In: *Metrics for Software Conceptual Models*. PUBLISHED BY IMPERIAL COLLEGE PRESS and DISTRIBUTED BY WORLD SCIENTIFIC PUBLISHING CO., Jan. 2005, pp. 59–98. ISBN: 978-1-86094-497-0. DOI: 10.1142/9781860946066_0003. URL: https://www.worldscientific.com/doi/abs/10.1142/9781860946066_0003 (visited on 10/17/2025).

[17] *Defining Blocks in Block Definition Diagram - SysML Plugin 2024x - No Magic Documentation*. URL: https://docs.nomagic.com/spaces/SYSMLP2024x/pages/136724796/Defining+Blocks+in+Block+Definition+Diagram (visited on 09/18/2025).

[18] Nicolas Jäckel et al. "Feature-Driven Specification of VTOL Air-Taxis with the Use of the Model- Based System Engineering (MBSE) Methodology CUBE". In: *77th Annual Vertical Flight Society Forum and Technology Display (FORUM 77): The Future of Vertical Flight*. Vertical Flight Society's 77th Annual Forum & Technology Display. Vol. 1 of 4. Palm Beach, Florida, USA: Curran Associates, Inc, May 11–13, 2021, pp. 2776–2784. DOI: 10.4050/F-0077-2021-16881.

[19] Matthew Hause. "The OMG Modelling Language (SYSML)". In: Fifth European Systems Engineering Conference. Cheltenham, Glos. UK: INCOSE, Sept. 18–20, 2006. URL: https://www.omg.org/sysml/The_SysML_Modelling_Language.pdf.

[20] Niamat Ullah Ibne Hossain et al. "Application of Systems Modeling Language (SysML) and Discrete Event Simulation to Address Patient Waiting Time Issues in Healthcare". In: *Smart Health* 29 (Sept. 1, 2023), p. 100403. ISSN: 2352-6483. DOI: 10.1016/j.smhl.2023.100403. URL: https://www.sciencedirect.com/science/article/pii/S2352648323000314 (visited on 10/17/2025).

[21] *SysML v2: The Next Generation Systems Modeling Language!* | *Object Management Group*. URL: https://www.omg.org/sysml/sysmlv2/ (visited on 07/31/2025).

[22] *Systems-Modeling/SysML-v2-Release*. OMG® Systems Modeling Community, July 29, 2025. URL: https://github.com/Systems-Modeling/SysML-v2-Release (visited on 07/31/2025).

[23] *No Magic*. URL: https://www.3ds.com/products/catia/no-magic (visited on 07/31/2025).

[24] *Economic Value of Systems Engineering - SEBoK*. URL: https://sebokwiki.org/wiki/Economic_Value_of_Systems_Engineering (visited on 07/31/2025).

[25] *Is There a Return on Investment from Model-Based Systems Engineering?* SlideShare. URL: https://www.slideshare.net/slideshow/is-there-an-roi-on-mbse/183242643 (visited on 07/31/2025).

[26] Stephen Cook and Shaun Wilson. "Determining Return on Investment for MBSE, SE & SoSE". In: *ASEW 2015 Workshop Proceedings*. Australian Systems Engineering Workshop. Sydney, NSW, Australia, 28 30 October 2015. URL: https://www.shoalgroup.com/wp-content/uploads/2017/06/Cook-Wilson-2015-Determining-RoI-for-MBSE-SE-SoSE-ASEW-2015.pdf.

[27] Steven W. Mitchell. "Transitioning the SWFTS Program Combat System Product Family from Traditional Document-Centric to Model-Based Systems Engineering". In: *Systems Engineering* 17.3 (2014), pp. 313–329. ISSN: 1520-6858. DOI: 10.1002/sys.21271. URL: https://onlinelibrary.wiley.com/doi/abs/10.1002/sys.21271 (visited on 08/01/2025).

[28] Edward Carroll and Robert Malins. *Systematic Literature Review: How Is Model-Based Systems Engineering Justified?* SAND–2016-2607, 1561164, 627724. Mar. 1, 2016, SAND–2016-2607, 1561164, 627724. DOI: 10.2172/1561164. URL: https://www.osti.gov/servlets/purl/1561164/ (visited on 08/01/2025).

[29] Jaume Sanso Ferrer and David Martín Rodríguez. "Benefits of Systems Engineering in Large Infrastructure Projects: The Much-Anticipated Empirical Proof." In: *INCOSE International Symposium* 32.1 (2022), pp. 514–528. ISSN: 2334-5837. DOI: 10.1002/iis2.12946. URL: https://onlinelibrary.wiley.com/doi/abs/10.1002/iis2.12946 (visited on 08/01/2025).

[30] Eric C. Honour. "2.3.1 A Practical Program of Research to Measure Systems Engineering Return on Investment (SE-ROI)". In: *INCOSE International Symposium* 16.1 (2006), pp. 299–308. ISSN: 2334-5837. DOI: 10.1002/j.2334-5837.2006.tb02744.x. URL: https://onlinelibrary.wiley.com/doi/abs/10.1002/j.2334-5837.2006.tb02744.x (visited on 08/01/2025).

[31] Azad M. Madni and Shatad Purohit. “Economic Analysis of Model-Based Systems Engineering”. In: *Systems* 7.1 (1 Mar. 2019), p. 12. ISSN: 2079-8954. DOI: 10.3390/systems7010012. URL: https://www.mdpi.com/2079-8954/7/1/12 (visited on 08/01/2025).

[32] Edward B. Rogers III and Steven W. Mitchell. “MBSE Delivers Significant Return on Investment in Evolutionary Development of Complex SoS”. In: *Systems Engineering* 24.6 (2021), pp. 385–408. ISSN: 1520-6858. DOI: 10.1002/sys.21592. URL: https://onlinelibrary.wiley.com/doi/abs/10.1002/sys.21592 (visited on 08/01/2025).

[33] Barry Boehm and Ricardo Valerdi. “The ROI of Systems Engineering: Some Quantitative Results”. In: *2007 IEEE International Conference on Exploring Quantifiable IT Yields*. 2007 IEEE International Conference on Exploring Quantifiable IT Yields. Mar. 2007, pp. 79–86. DOI: 10.1109/EQUITY.2007.14. URL: https://ieeexplore.ieee.org/abstract/document/5206402 (visited on 08/01/2025).

[34] Reg Austin. *Unmanned Aircraft Systems: UAVS Design, Development and Deployment*. 1st ed. Wiley, Apr. 16, 2010. ISBN: 978-0-470-05819-0 978-0-470-66479-7. DOI: 10.1002/9780470664797. URL: https://onlinelibrary.wiley.com/doi/book/10.1002/9780470664797 (visited on 06/14/2024).

[35] *Unmanned Aerial Vehicle*. In: *Wikipedia*. June 5, 2024. URL: https://en.wikipedia.org/w/index.php?title=Unmanned_aerial_vehicle&oldid=1227313300 (visited on 06/06/2024).

[36] Kimon P. Valavanis and George J. Vachtsevanos, eds. *Handbook of Unmanned Aerial Vehicles*. Dordrecht: Springer Netherlands, 2015. ISBN: 978-90-481-9706-4 978-90-481-9707-1. DOI: 10.1007/978-90-481-9707-1. URL: https://link.springer.com/10.1007/978-90-481-9707-1 (visited on 06/14/2024).

[37] John R. Hoehn, Kelley M. Sayler, and Michael E. (Analyst in Intelligence and National Security) Devine. *Unmanned Aircraft Systems: Roles, Missions, and Future Concepts*. United States, 2022. URL: http://catalog.gpo.gov/F/?func=direct&doc_number=001213124&format=999 (visited on 06/14/2024).

[38] Mohammad H. Sadraey. *Design of Unmanned Aerial Systems*. John Wiley & Sons, Apr. 13, 2020. 677 pp. ISBN: 978-1-119-50870-0. Google Books: Xx7RswEACAAJ.

[39] Dimitrios Mitridis et al. “An Evaluation of Fixed-Wing Unmanned Aerial Vehicle Trends and Correlations with Respect to NATO Classification, Region, EIS Date and Operational Specifications”. In: *Aerospace* 10.4 (4 Apr. 2023), p. 382. ISSN: 2226-4310. DOI: 10.3390/aerospace10040382. URL: https://www.mdpi.com/2226-4310/10/4/382 (visited on 07/03/2025).

[40] Mochammad Agoes Moelyadi, Muhammad Fikri Zulkarnain, and Nu’man Amri Maliky. “ITB High Altitude Long Endurance UAV Development: Past and Future”. In: *AIP Conference Proceedings* 2366.1 (Sept. 13, 2021), p. 030004. ISSN: 0094-243X. DOI: 10.1063/5.0060623. URL: https://doi.org/10.1063/5.0060623 (visited on 07/04/2025).

[41] Shepard. *Military Uncrewed Systems Handbook*. Issue 30. London, United Kingdom: The Shephard Press Ltd, Mar. 2022, p. 428. URL: https://mags.shephardmedia.com/legacy-handbooks/MUSH2022.pdf.

[42] *CH-6 Chang Hong-6*. URL: https://www.globalsecurity.org/military/world/china/ch-6.htm (visited on 07/04/2025).

[43] N.J.S. Stacy et al. "The Global Hawk UAV Australian Deployment: Imaging Radar Sensor Modifications and Employment for Maritime Surveillance". In: *IEEE International Geoscience and Remote Sensing Symposium*. IEEE International Geoscience and Remote Sensing Symposium. Vol. 2. June 2002, 699–701 vol.2. DOI: 10.1109/IGARSS.2002.1025623. URL: https://ieeexplore.ieee.org/document/1025623 (visited on 07/04/2025).

[44] J. Chris Naftel. "NASA Global Hawk: Project Overview and Future Plans". In: *Proceedings of the International Symposium on Remote Sensing of Environment*. International Symposium on Remote Sensing of Environment. Sydney: NASA, Apr. 10, 2011. URL: https://ntrs.nasa.gov/citations/20110011985 (visited on 07/04/2025).

[45] *Northrop Grumman RQ-4 Global Hawk*. In: *Wikipedia*. June 11, 2025. URL: https://en.wikipedia.org/w/index.php?title=Northrop_Grumman_RQ-4_Global_Hawk&oldid=1295033047 (visited on 07/10/2025).

[46] Craig L Nickol et al. *High Altitude Long Endurance UAV Analysis of Alternatives and Technology Requirements Development*. NASA/TP-2007-214861. National Aeronautics and Space Administration, Langley Research Center, 2007. URL: https://ntrs.nasa.gov/api/citations/20070017849/downloads/20070017849.pdf.

[47] *RQ-4 Global Hawk*. Air Force. URL: https://www.af.mil/About-Us/Fact-Sheets/Display/Article/104516/rq-4-global-hawk/https%3A%2F%2Fwww.af.mil%2FAbout-Us%2FFact-Sheets%2FDisplay%2FArticle%2F104516%2Frq-4-global-hawk%2F (visited on 07/04/2025).

[48] *Military Turbojet/Turbofan Specifications*. URL: https://www.jet-engine.net/miltfspec.htm (visited on 07/04/2025).

[49] *Rolls-Royce AE 3007*. In: *Wikipedia*. Mar. 27, 2024. URL: https://en.wikipedia.org/w/index.php?title=Rolls-Royce_AE_3007&oldid=1215841562 (visited on 07/09/2025).

[50] NASA Photograph by Carla Thomas. *NASA Image Acquired October 23, 2009*. 23 October 2009, 09:52. URL: https://commons.wikimedia.org/wiki/File:Global_Hawk,_NASA%27s_New_Remote-Controlled_Plane_-_October_2009.jpg (visited on 07/04/2025).

[51] *Understanding Tactical Drones vs. Strategic Drones: Key Differences - AMO*. Mar. 4, 2025. URL: https://allmilitaryoperations.com/tactical-drones-vs-strategic-drones/ (visited on 07/07/2025).

[52] Editorial Team. *An In-Depth Look at the Types of Military Drones Today - Total Military Insight*. June 28, 2024. URL: https://totalmilitaryinsight.com/types-of-military-drones/ (visited on 07/07/2025).

[53] Frank Grimsley. “The Predator Unmanned System: From Advanced Concept Demonstrator to Transformational Weapon System”. Sept. 2008. URL: https://apps.dtic.mil/sti/tr/pdf/ADA507640.pdf.

[54] Michael R. Thirtle, Robert V. Johnson, and John Birkler. *The Predator ACTD: A Case Study for Transition Planning to the Formal Acquisition Process*. Santa Monica, CA, US: National Defense Research Institute RAND, Jan. 1, 1997. URL: https://www.rand.org/pubs/monograph_reports/MR899.html (visited on 07/08/2025).

[55] *MQ-1B Predator*. Air Force. URL: https://www.af.mil/About-Us/Fact-Sheets/Display/Article/104469/mq-1b-predator/https%3A%2F%2Fwww.af.mil%2FAbout-Us%2FFact-Sheets%2FDisplay%2FArticle%2F104469%2Fmq-1b-predator%2F (visited on 07/08/2025).

[56] Triffaux. *MQ-1 Predator*. URL: https://armyrecognition.com/military-products/air/unmanned-aircraft-system/mq-1-predator (visited on 08/27/2025).

[57] *914 UL | F*. Rotax Aircraft Engines. URL: https://www.flyrotax.com/products/914-ul-f (visited on 07/08/2025).

[58] *Rotax 914*. In: *Wikipedia*. Jan. 5, 2025. URL: https://en.wikipedia.org/w/index.php?title=Rotax_914&oldid=1267610399 (visited on 07/08/2025).

[59] *ROTAX 914 UL 3 Engine Operators Manual*. ROTAX AIRCRAFT ENGINES. URL: https://manualzz.com/doc/23497760/rotax-914-ul-3-engine-operators-manual?utm_source=chatgpt.com&p=23.

[60] *General Atomics MQ-1 ‘Predator’ (Awaiting Delivery)*. FLIGHT TEST HISTORICAL FOUNDATION. URL: https://flighttestmuseum.org/portfolio/general-atomics-mq-1-predator-awaiting-delivery/ (visited on 07/08/2025).

[61] Tanvi Prakash. “High Altitude Long Endurance Unmanned Aerial Vehicles HALE-UAVs - A Brief Introduction” (Powai, India). Aut. 2012. URL: https://www.cdeep.iitb.ac.in/slides/A15/AE332/AE332-L11.pdf.

[62] Dries Verstraete. “Multi-Disciplinary Optimisation of Medium Altitude Long Endurance UAVs”. In: *31st Congress of the International Council of the Aeronautical Sciences, ICAS 2018*. 31st Congress of the International Council of the Aeronautical Sciences, ICAS 2018. Belo Horizonte, Brazil: International Council of the Aeronautical Sciences, Sept. 9–14, 2018. ISBN: 978-3-932182-88-4. URL: https://www.icas.org/icas_archive/ICAS2018/data/papers/ICAS2018_0416_paper.pdf.

[63] *General Atomics MQ-1 Predator*. In: *Wikipedia*. June 18, 2025. URL: https://en.wikipedia.org/w/index.php?title=General_Atomics_MQ-1_Predator&oldid=1296189891 (visited on 07/04/2025).

[64] James F. Marchman III. *Aerodynamics and Aircraft Performance*. 3rd edition. Blacksburg, VA: James F. Marchman III in association with the University Libraries at Virginia Tech. ISBN: 978-1-949373-63-9. DOI: https://doi.org/http://hdl.handle.net/10919/96525.

[65] Enric Pastor et al. “A Macroscopic Performance Analysis of NASA’s Northrop Grumman RQ-4A”. In: *Aerospace* 5.1 (1 Mar. 2018), p. 6. ISSN: 2226-4310. DOI: 10.3390/aerospace5010006. URL: https://www.mdpi.com/2226-4310/5/1/6 (visited on 07/10/2025).

[66] Jonathan M. Taylor, Majid T. Fard, and JiangBiao He. “A Multifunctional T-Type 4-Leg Inverter for Various Operation Modes of Electric Aircraft Propulsion”. In: *2022 IEEE Transportation Electrification Conference & Expo (ITEC)*. 2022 IEEE Transportation Electrification Conference & Expo (ITEC). June 2022, pp. 1205–1210. DOI: 10.1109/ITEC53557.2022.9813943. URL: https://ieeexplore.ieee.org/document/9813943 (visited on 07/09/2025).

[67] Hindenburg-*Class Airship*. In: *Wikipedia*. Apr. 13, 2025. URL: https://en.wikipedia.org/w/index.php?title=Hindenburg-class_airship&oldid=1285450365 (visited on 07/14/2025).

[68] Huanrong Lei and Bhupendra Khandelwal. “Chapter 10 - Hydrogen Fuel for Aviation”. In: *Aviation Fuels*. Ed. by Bhupendra Khandelwal. Academic Press, Jan. 1, 2021, pp. 237–270. ISBN: 978-0-12-818314-4. DOI: 10.1016/B978-0-12-818314-4.00007-8. URL: https://www.sciencedirect.com/science/article/pii/B9780128183144000078 (visited on 07/14/2025).

[69] NASA Technical Reports Server (NTRS). *NASA Technical Reports Server (NTRS) 19790008823: Liquid Hydrogen as a Propulsion Fuel, 1945-1959*. Jan. 1, 1978. URL: http://archive.org/details/NASA_NTRS_Archive_19790008823 (visited on 02/23/2024).

[70] *The Epic Attempts to Power Planes with Hydrogen*. Mar. 21, 2022. URL: https://www.bbc.com/future/article/20220316-the-epic-attempts-to-power-planes-with-hydrogen (visited on 07/14/2025).

[71] Gdaniel Brewer. *Hydrogen Aircraft Technology*. 1st ed. United Kingdom: Routledge, 2017. ISBN: 978-1-351-43979-4. DOI: 10.1201/9780203751480.

[72] Longbiao Li et al. “UAVs and Hydrogen Technologies Are the Future of Civil Aviation”. In: *Aeronautics - Characteristics and Emerging Technologies*. IntechOpen, Dec. 19, 2024. ISBN: 978-0-85014-858-9. DOI: 10.5772/intechopen.1008352. URL: https://www.intechopen.com/chapters/1196295 (visited on 07/14/2025).

[73] *Tu-155: A Plane Ahead of Its Time – RuAviation*. Apr. 15, 2023. URL: https://ruavia.su/tu-155-a-plane-ahead-of-its-time/?utm_source=chatgpt.com (visited on 07/14/2025).

[74] Younseok Choi and Jinkwang Lee. “Estimation of Liquid Hydrogen Fuels in Aviation”. In: *Aerospace* 9.10 (Oct. 2022), p. 564. ISSN: 2226-4310. DOI: 10.3390/aerospace9100564. URL: https://www.mdpi.com/2226-4310/9/10/564 (visited on 05/25/2023).

[75] Vittorio Cipolla et al. “A Parametric Approach for Conceptual Integration and Performance Studies of Liquid Hydrogen Short–Medium Range Aircraft”. In: *Applied Sciences* 12.14 (Jan. 2022), p. 6857. ISSN: 2076-3417. DOI: 10.3390/app12146857. URL: https://www.mdpi.com/2076-3417/12/14/6857 (visited on 06/22/2023).

[76] *X-43A Hyper-X - NASA*. URL: https://www.nasa.gov/reference/x-43a/ (visited on 07/15/2025).

[77] Saurav Tiwari, Michael J. Pekris, and John J. Doherty. "A Review of Liquid Hydrogen Aircraft and Propulsion Technologies". In: *International Journal of Hydrogen Energy* 57 (Feb. 29, 2024), pp. 1174–1196. ISSN: 0360-3199. DOI: 10.1016/j.ijhydene.2023.12.263. URL: https://www.sciencedirect.com/science/article/pii/S0360319923065631 (visited on 02/16/2024).

[78] *Antares DLR-H2: Fuel Cell-Powered Aircraft*. URL: https://www.dlr.de/en/images/2013/2/antares-dlr-h2-fuel-cell-powered-aircraft_9601 (visited on 07/15/2025).

[79] W. Xu, Q. Li, and W. Li. "Simulation of Mechanical Strength of Novel Cryogenic Liquid Hydrogen Tank for Unmanned Aerial Vehicle". In: *Zhenkong Kexue yu Jishu Xuebao/Journal of Vacuum Science and Technology* 35.8 (2015), pp. 1017–1022. DOI: 10.13922/j.cnki.cjovst.2015.08.18. PMID: null. URL: https://www.scopus.com/inward/record.uri?eid=2-s2.0-84941945771&doi=10.13922%2fj.cnki.cjovst.2015.08.18&partnerID=40&md5=3f2a9a07efe243d8a0b51660a7b5be44.

[80] *Universal Hydrogen Has Introduced a Solution That Reduces Hydrogen Loss during Fuel Tank Filling*. HydrogenWire. Apr. 26, 2024. URL: https://shorturl.at/y5IG1 (visited on 07/15/2025).

[81] *Home | HERA*. URL: https://project-hera.eu/home (visited on 07/15/2025).

[82] W. Xu, G. Yang, and P. Lou. "Design and Simulation of Airborne Liquid-Hydrogen Tank for Unmanned Aerial Vehicle". In: *Zhenkong Kexue yu Jishu Xuebao/Journal of Vacuum Science and Technology* 35.3 (2015), pp. 266–270. DOI: 10.13922/j.cnki.cjovst.2015.03.03. PMID: null. URL: https://www.scopus.com/inward/record.uri?eid=2-s2.0-84928736399&doi=10.13922%2fj.cnki.cjovst.2015.03.03&partnerID=40&md5=6052529c13aa8a3243e7de5c36b6ff62.

[83] Morten B. Ley et al. "Complex Hydrides for Hydrogen Storage – New Perspectives". In: *Materials Today* 17.3 (Apr. 2014), pp. 122–128. ISSN: 13697021. DOI: 10.1016/j.mattod.2014.02.013. URL: https://linkinghub.elsevier.com/retrieve/pii/S136970211400073X (visited on 10/21/2022).

[84] Pavlos Rompokos et al. "Synergistic Technology Combinations for Future Commercial Aircraft Using Liquid Hydrogen". In: *Journal of Engineering for Gas Turbines and Power* 143.7 (Mar. 31, 2021). DOI: 10.1115/1.4049694. URL: http://dx.doi.org/10.1115/1.4049694.

[85] K.E. Lamb and C.J. Webb. "A Quantitative Review of Slurries for Hydrogen Storage – Slush Hydrogen, and Metal and Chemical Hydrides in Carrier Liquids". In: *Journal of Alloys and Compounds* 906 (June 2022), p. 164235. ISSN: 09258388. DOI: 10.1016/j.jallcom.2022.164235. URL: https://linkinghub.elsevier.com/retrieve/pii/S0925838822006260 (visited on 10/21/2022).

[86] Eytan J. Adler and Joaquim R. R. A. Martins. “Hydrogen-Powered Aircraft: Fundamental Concepts, Key Technologies, and Environmental Impacts”. In: *Progress in Aerospace Sciences*. Special Issue on Green Aviation 141 (Aug. 2023), p. 100922. ISSN: 0376-0421. DOI: 10.1016/j.paerosci.2023.100922.

[87] Helen Webber and Stella Job. *Realising Zero-Carbon Emission Flight - Primary Energy Source Comparison and Selection*. FZ_0_6.1. Cranfield, England: Aerospace Technology Institute, Sept. 23, 2021. URL: https://www.ati.org.uk/wp-content/uploads/2021/09/FZ_0_6.1-Primary-Energy-Source-Comparison-and-Selection-FINAL-230921.pdf.

[88] U.Y. Qazi. “Future of Hydrogen as an Alternative Fuel for Next-Generation Industrial Applications; Challenges and Expected Opportunities”. In: *Energies* 15.13 (2022). DOI: 10.3390/en15134741.

[89] Vinay Prakash Chaudhary et al. “Comparative Analysis of Performance Parameters of Hydrogen Fuel, Conventional Fuels and Hydrogen Enriched Fuels in an IC Engine”. In: *Advances in Clean Energy and Sustainability*. International Conference on Advances in Energy Research. Springer, Singapore, 2023, pp. 519–528. ISBN: 978-981-99-2279-6. DOI: 10.1007/978-981-99-2279-6_45. URL: https://link.springer.com/chapter/10.1007/978-981-99-2279-6_45 (visited on 07/15/2025).

[90] Charles Bronzo Barbosa Farias et al. “Use of Hydrogen as Fuel: A Trend of the 21st Century”. In: *Energies* 15.1 (1 Jan. 2022), p. 311. ISSN: 1996-1073. DOI: 10.3390/en15010311. URL: https://www.mdpi.com/1996-1073/15/1/311 (visited on 07/15/2025).

[91] Marcel Otto et al. “Optimal Hydrogen Carrier: Holistic Evaluation of Hydrogen Storage and Transportation Concepts for Power Generation, Aviation, and Transportation”. In: *Journal of Energy Storage* 55 (Nov. 30, 2022), p. 105714. ISSN: 2352-152X. DOI: 10.1016/j.est.2022.105714. URL: https://www.sciencedirect.com/science/article/pii/S2352152X22017029 (visited on 04/05/2024).

[92] Ramin Moradi and Katrina M. Groth. “Hydrogen Storage and Delivery: Review of the State of the Art Technologies and Risk and Reliability Analysis”. In: *International Journal of Hydrogen Energy* 44.23 (May 3, 2019), pp. 12254–12269. ISSN: 0360-3199. DOI: 10.1016/j.ijhydene.2019.03.041. URL: https://www.sciencedirect.com/science/article/pii/S0360319919309656 (visited on 07/16/2025).

[93] Adriana Rincon Montenegro, Marco Sanjuan, and Mauricio Carmona. “Energy Storage Development Using Hydrogen and Its Potential Application in Colombia”. In: *International Journal of Energy Economics and Policy* 9.6 (6 Oct. 4, 2019), pp. 254–268. ISSN: 2146-4553. URL: https://www.econjournals.com/index.php/ijeep/article/view/8294 (visited on 07/16/2025).

[94] Hyun Tae Hwang and Arvind Varma. "Hydrogen Storage for Fuel Cell Vehicles". In: *Current Opinion in Chemical Engineering*. Energy and Environmental Engineering / Reaction Engineering 5 (Aug. 1, 2014), pp. 42–48. ISSN: 2211-3398. DOI: 10.1016/j.coche.2014.04.004. URL: https://www.sciencedirect.com/science/article/pii/S2211339814000446 (visited on 07/16/2025).

[95] Ibrahim Dincer and Haris Ishaq. "Chapter 1 - Introduction". In: *Renewable Hydrogen Production*. Ed. by Ibrahim Dincer and Haris Ishaq. Elsevier, Jan. 1, 2022, pp. 1–33. ISBN: 978-0-323-85176-3. DOI: 10.1016/B978-0-323-85176-3.00001-9. URL: https://www.sciencedirect.com/science/article/pii/B9780323851763000019 (visited on 07/16/2025).

[96] C. Sindt. "A Summary of the Characterization Study of Slush Hydrogen". In: *Cryogenics* 10.5 (Oct. 1, 1970), pp. 372–380. ISSN: 0011-2275. DOI: 10.1016/0011-2275(70)90003-2. URL: https://www.sciencedirect.com/science/article/pii/0011227570900032 (visited on 02/09/2024).

[97] Maria Chiara Massaro et al. "Potential of Ammonia as Hydrogen Storage for Future Electrified Aircraft". In: *Energy Conversion and Management: X* 26 (Apr. 1, 2025), p. 101034. ISSN: 2590-1745. DOI: 10.1016/j.ecmx.2025.101034. URL: https://www.sciencedirect.com/science/article/pii/S2590174525001667 (visited on 07/16/2025).

[98] Florian Franke and Stefan Kazula. "Conceptual Design of a Metal Hydride System for the Recovery of Gaseous Hydrogen Boil-Off Losses from Liquid Hydrogen Tanks". In: *Engineering Proceedings* 90.1 (1 2025), p. 17. ISSN: 2673-4591. DOI: 10.3390/engproc2025090017. URL: https://www.mdpi.com/2673-4591/90/1/17 (visited on 06/27/2025).

[99] Victor J. Bahrs et al. "Analysis of the Potential of Metal Hydride-Based Range Extenders for Electric Commuter Aircraft". In: *CEAS Aeronautical Journal* 16.1 (1 Jan. 1, 2025), pp. 255–273. ISSN: 1869-5590. DOI: 10.1007/s13272-024-00784-0. URL: https://link.springer.com/article/10.1007/s13272-024-00784-0 (visited on 07/16/2025).

[100] Maria Zafar et al. "Carbon Nanotubes for Production and Storage of Hydrogen: Challenges and Development". In: *Chemical Papers* 76.2 (2 Feb. 1, 2022), pp. 609–625. ISSN: 2585-7290. DOI: 10.1007/s11696-021-01922-2. URL: https://link.springer.com/article/10.1007/s11696-021-01922-2 (visited on 07/16/2025).

[101] Timothy Manda et al. "A Data-Guided Approach for the Evaluation of Zeolites for Hydrogen Storage with the Aid of Molecular Simulations". In: *Journal of Molecular Modeling* 30.2 (2 Feb. 1, 2024), pp. 1–14. ISSN: 0948-5023. DOI: 10.1007/s00894-024-05837-z. URL: https://link.springer.com/article/10.1007/s00894-024-05837-z (visited on 07/16/2025).

[102] Selcuk Demir et al. “Metal-Organic Frameworks for Hydrogen Storage”. In: *Handbook of Energy Materials*. Springer, Singapore, 2022, pp. 1–35. ISBN: 978-981-16-4480-1. DOI: 10.1007/978-981-16-4480-1_90-1. URL: https://link.springer.com/rwe/10.1007/978-981-16-4480-1_90-1 (visited on 07/16/2025).

[103] Marc Prewitz, Andreas Bardenhagen, and Ramon Beck. “Hydrogen as the Fuel of the Future in Aircrafts – Challenges and Opportunities”. In: *International Journal of Hydrogen Energy* 45.46 (Sept. 2020), pp. 25378–25385. ISSN: 0360-3199. DOI: 10.1016/j.ijhydene.2020.06.238. URL: http://dx.doi.org/10.1016/j.ijhydene.2020.06.238 (visited on 02/26/2024).

[104] Ahmad Baroutaji et al. “Comprehensive Investigation on Hydrogen and Fuel Cell Technology in the Aviation and Aerospace Sectors”. In: *Renewable and Sustainable Energy Reviews* 106 (May 2019), pp. 31–40. ISSN: 1364-0321. DOI: 10.1016/j.rser.2019.02.022.

[105] Fazil Qureshi et al. “Advancements in Sorption-Based Materials for Hydrogen Storage and Utilization: A Comprehensive Review”. In: *Energy* 309 (Nov. 15, 2024), p. 132855. ISSN: 0360-5442. DOI: 10.1016/j.energy.2024.132855. URL: https://www.sciencedirect.com/science/article/pii/S036054422402629X (visited on 10/16/2024).

[106] Georg Klepp. “Modelling Activated Carbon Hydrogen Storage Tanks Using Machine Learning Models”. In: *Energy* 306 (Oct. 15, 2024), p. 132318. ISSN: 0360-5442. DOI: 10.1016/j.energy.2024.132318. URL: https://www.sciencedirect.com/science/article/pii/S0360544224020929 (visited on 10/16/2024).

[107] ILK Dresden Kuhn Moritz. *English: Storage Density of Hydrogen under Certain Pressure and Tempeature Conditions. (1) Liquid Storage - LH2, (2) Pressurised Storage CGH2, (3) Transcritical Storage (Cryo Compressed)Deutsch: Speicherdichte von Wasserstoff Unter Bestimmten Druck- Und Temperaturbedingungen. (1) Flüssiggasspeicherung, (2) Druckgasspeicherung, (3) Transkritische Speicherung*. 9 July 2015, 11:08:32. URL: https://commons.wikimedia.org/wiki/File:Storage_Density_of_Hydrogen.jpg (visited on 07/15/2025).

[108] Mengxiao Li et al. “Review on the Research of Hydrogen Storage System Fast Refueling in Fuel Cell Vehicle”. In: *International Journal of Hydrogen Energy* 44.21 (Apr. 23, 2019), pp. 10677–10693. ISSN: 0360-3199. DOI: 10.1016/j.ijhydene.2019.02.208. PMID: null. URL: https://www.sciencedirect.com/science/article/pii/S0360319919308663 (visited on 07/16/2025).

[109] Tobias Brunner and Oliver Kircher. “Cryo-Compressed Hydrogen Storage”. In: *Hydrogen Science and Engineering : Materials, Processes, Systems and Technology*. John Wiley & Sons, Ltd, 2016, pp. 711–732. ISBN: 978-3-527-67426-8. DOI: 10.1002/9783527674268.ch29. URL: https://onlinelibrary.wiley.com/doi/abs/10.1002/9783527674268.ch29 (visited on 07/17/2025).

[110] *Target True Zero: Delivering the Infrastructure for Battery and Hydrogen-Powered Flight*. World Economic Forum. URL: https://www.weforum.org/publications/target-true-zero-delivering-the-infrastructure-for-battery-and-hydrogen-powered-flight/ (visited on 04/28/2024).

[111] G Correa et al. "Flight Test Validation of the Dynamic Model of a Fuel Cell System for Ultra-Light Aircraft". In: *Proceedings of the Institution of Mechanical Engineers, Part G: Journal of Aerospace Engineering* 229.5 (Apr. 1, 2015), pp. 917–932. ISSN: 0954-4100. DOI: 10.1177/0954410014541081. URL: https://doi.org/10.1177/0954410014541081 (visited on 07/21/2025).

[112] Alexander Air, Md Shamsuddoha, and B. Gangadhara Prusty. "A Review of Type V Composite Pressure Vessels and Automated Fibre Placement Based Manufacturing". In: *Composites Part B: Engineering* 253 (Mar. 15, 2023), p. 110573. ISSN: 1359-8368. DOI: 10.1016/j.compositesb.2023.110573. URL: https://www.sciencedirect.com/science/article/pii/S1359836823000768 (visited on 04/12/2024).

[113] Mariana Pimenta Alves et al. "A Review on Industrial Perspectives and Challenges on Material, Manufacturing, Design and Development of Compressed Hydrogen Storage Tanks for the Transportation Sector". In: *Energies* 15.14 (Jan. 2022), p. 5152. ISSN: 1996-1073. DOI: 10.3390/en15145152. URL: https://www.mdpi.com/1996-1073/15/14/5152 (visited on 07/22/2025).

[114] Mourad Nachtane et al. "An Overview of the Recent Advances in Composite Materials and Artificial Intelligence for Hydrogen Storage Vessels Design". In: *Journal of Composites Science* 7.3 (3 Mar. 2023), p. 119. ISSN: 2504-477X. DOI: 10.3390/jcs7030119. URL: https://www.mdpi.com/2504-477X/7/3/119 (visited on 12/13/2023).

[115] Dávid István Kis and Eszter Kókai. "A Review on the Factors of Liner Collapse in Type IV Hydrogen Storage Vessels". In: *International Journal of Hydrogen Energy* 50 (PA Jan. 1, 2024). ISSN: 0360-3199. DOI: 10.1016/j.ijhydene.2023.09.316. URL: https://www.osti.gov/biblio/2202695 (visited on 02/07/2024).

[116] Zeping Jin et al. "Review of Decompression Damage of the Polymer Liner of the Type IV Hydrogen Storage Tank". In: *Polymers* 15.10 (10 Jan. 2023), p. 2258. ISSN: 2073-4360. DOI: 10.3390/polym15102258. URL: https://www.mdpi.com/2073-4360/15/10/2258 (visited on 12/22/2023).

[117] Wei Zhou et al. "Review on Optimization Design, Failure Analysis and Non-Destructive Testing of Composite Hydrogen Storage Vessel". In: *International Journal of Hydrogen Energy* 47.91 (Nov. 15, 2022), pp. 38862–38883. ISSN: 0360-3199. DOI: 10.1016/j.ijhydene.2022.09.028. URL: https://www.sciencedirect.com/science/article/pii/S0360319922041052 (visited on 12/13/2023).

[118] Michael Ebermann et al. “Analytical and Numerical Approach to Determine Effective Diffusion Coefficients for Composite Pressure Vessels”. In: *Composite Structures* 291 (July 1, 2022), p. 115616. ISSN: 0263-8223. DOI: 10.1016/j.compstruct.2022.115616. URL: https://www.sciencedirect.com/science/article/pii/S0263822322004019 (visited on 07/20/2025).

[119] Jian Li et al. “Small-Scale High-Pressure Hydrogen Storage Vessels: A Review”. In: *Materials* 17.3 (3 Jan. 2024), p. 721. ISSN: 1996-1944. DOI: 10.3390/ma17030721. URL: https://www.mdpi.com/1996-1944/17/3/721 (visited on 04/12/2024).

[120] Abdisa Sisay Mekonnin et al. “Hydrogen Storage Technology, and Its Challenges: A Review”. In: *Catalysts* 15.3 (3 Mar. 2025), p. 260. ISSN: 2073-4344. DOI: 10.3390/catal15030260. URL: https://www.mdpi.com/2073-4344/15/3/260 (visited on 07/21/2025).

[121] Maria Mikroni et al. “Design, Analysis, and Testing of a Type V Composite Pressure Vessel for Hydrogen Storage”. In: *Polymers* 16.24 (24 Jan. 2024), p. 3576. ISSN: 2073-4360. DOI: 10.3390/polym16243576. URL: https://www.mdpi.com/2073-4360/16/24/3576 (visited on 07/21/2025).

[122] R Parello et al. “Structural Sizing of a Hydrogen Tank for a Commercial Aircraft”. In: *Journal of Physics: Conference Series* 2716.1 (Mar. 2024), p. 012040. ISSN: 1742-6596. DOI: 10.1088/1742-6596/2716/1/012040. URL: https://dx.doi.org/10.1088/1742-6596/2716/1/012040 (visited on 07/21/2025).

[123] Ashok Saxena. “High-Pressure Hydrogen Storage Vessel Designs for Hydrogen Embrittlement”. In: *International Journal of Materials Technology and Innovation* 4.2 (Dec. 1, 2024), pp. 14–29. ISSN: 2682-4299. DOI: 10.21608/ijmti.2024.331423.1113. URL: https://ijmti.journals.ekb.eg/article_399842.html (visited on 07/21/2025).

[124] George Tzoumakis, Konstantinos Fotopoulos, and George Lampeas. “Multi-Physics Digital Model of an Aluminum 2219 Liquid Hydrogen Aircraft Tank”. In: *Aerospace* 11.2 (2 Feb. 2024), p. 161. ISSN: 2226-4310. DOI: 10.3390/aerospace11020161. URL: https://www.mdpi.com/2226-4310/11/2/161 (visited on 07/21/2025).

[125] Sergio Bagarello, Dario Campagna, and Ivano Benedetti. “A Survey on Hydrogen Tanks for Sustainable Aviation”. In: *Green Energy and Intelligent Transportation* (Sept. 1, 2024), p. 100224. ISSN: 2773-1537. DOI: 10.1016/j.geits.2024.100224. URL: https://www.sciencedirect.com/science/article/pii/S2773153724000768 (visited on 07/21/2025).

[126] Erik Bigelow and Michael Lewis. *Conformable Hydrogen Storage Pressure Vessel*. DOE-CTE-06967. Center for Transportation and the Environment, Atlanta, GA (United States), July 6, 2018. DOI: 10.2172/1459184. URL: https://www.osti.gov/biblio/1459184 (visited on 02/07/2024).

[127] *Hydrogen Embrittlement*. In: *Wikipedia*. June 19, 2025. URL: https://en.wikipedia.org/w/index.php?title=Hydrogen_embrittlement&oldid=1296407384 (visited on 07/24/2025).

[128] Anka Trajkovska Petkoska et al. “Towpreg—An Advanced Composite Material with a Potential for Pressurized Hydrogen Storage Vessels”. In: *Journal of Composites Science* 8.9 (9 Sept. 2024), p. 374. ISSN: 2504-477X. DOI: 10.3390/jcs8090374. URL: https://www.mdpi.com/2504-477X/8/9/374 (visited on 07/21/2025).

[129] Ahmed I. Osman et al. “Advances in Hydrogen Storage Materials: Harnessing Innovative Technology, from Machine Learning to Computational Chemistry, for Energy Storage Solutions”. In: *International Journal of Hydrogen Energy* 67 (May 20, 2024), pp. 1270–1294. ISSN: 0360-3199. DOI: 10.1016/j.ijhydene.2024.03.223. URL: https://www.sciencedirect.com/science/article/pii/S036031992401053X (visited on 07/21/2025).

[130] Alberto Boretti and Aijun Huang. “Physical Storage in Conformal Composite Tanks Presents Clear Advantages over Material-Based Solutions for Hydrogen-Powered Aerospace Applications”. In: *International Journal of Hydrogen Energy* 68 (May 28, 2024), pp. 1297–1301. ISSN: 0360-3199. DOI: 10.1016/j.ijhydene.2024.04.258. URL: https://www.sciencedirect.com/science/article/pii/S0360319924015611 (visited on 07/21/2025).

[131] Andrei Ratoi, Corneliu Munteanu, and Dan Eliezer. “Maximizing Onboard Hydrogen Storage Capacity by Exploring High-Strength Novel Materials Using a Mathematical Approach”. In: *Materials* 17.17 (17 Jan. 2024), p. 4288. ISSN: 1996-1944. DOI: 10.3390/ma17174288. URL: https://www.mdpi.com/1996-1944/17/17/4288 (visited on 07/21/2025).

[132] CA Saias et al. “Assessment of Hydrogen Fuel for Rotorcraft Applications”. In: *INTERNATIONAL JOURNAL OF HYDROGEN ENERGY* 47.76 (Sept. 5, 2022), pp. 32655–32668. ISSN: 0360-3199. DOI: 10.1016/j.ijhydene.2022.06.316. URL: https://www.sciencedirect.com/science/article/pii/S0360319922030099 (visited on 02/23/2024).

[133] Hyun Kyu Shin and Sung Kyu Ha. “A Review on the Cost Analysis of Hydrogen Gas Storage Tanks for Fuel Cell Vehicles”. In: *Energies* 16.13 (13 Jan. 2023), p. 5233. ISSN: 1996-1073. DOI: 10.3390/en16135233. URL: https://www.mdpi.com/1996-1073/16/13/5233 (visited on 07/24/2025).

[134] Maria Chiara Massaro et al. “Optimal Design of a Hydrogen-Powered Fuel Cell System for Aircraft Applications”. In: *Energy Conversion and Management* 306 (Apr. 15, 2024), p. 118266. ISSN: 0196-8904. DOI: 10.1016/j.enconman.2024.118266. URL: https://www.sciencedirect.com/science/article/pii/S0196890424002073 (visited on 10/03/2024).

[135] Damian Maciorowski, Aleksandra Ludwiczak, and Adam Kozakiewicz. “Hydrogen, the Future of Aviation”. In: *Combustion Engines* 197.2 (May 18, 2024), pp. 126–131. ISSN: 2300-9896, 2658-1442. DOI: 10.19206/CE-178375. URL: https://www.combustion-engines.eu/Hydrogen-the-future-of-aviation,178375,0,2.html (visited on 07/24/2025).

[136] Zhenglin Cai. "Feasibility of Hydrogen Energy for High-Power Aerospace Applications: A Comprehensive Assessment". In: *E3S Web of Conferences* 606 (2025), p. 01005. ISSN: 2267-1242. DOI: 10.1051/e3sconf/202560601005. URL: https://www.e3s-conferences.org/articles/e3sconf/abs/2025/06/e3sconf_icnaoe2024_01005/e3sconf_icnaoe2024_01005.html (visited on 07/22/2025).

[137] C. M. Benson et al. "Combined Hazard Analyses to Explore the Impact of Liquid Hydrogen Fuel on the Civil Aviation Industry". In: ASME Turbo Expo 2020: Turbomachinery Technical Conference and Exposition. American Society of Mechanical Engineers Digital Collection, Jan. 11, 2021. DOI: 10.1115/GT2020-14977. URL: https://dx.doi.org/10.1115/GT2020-14977 (visited on 07/22/2025).

[138] Dimitrios Dimos and Stefanie de Graaf. "Overview of Safety Challenges Associated with Integration of Hydrogen-Based Propulsion Systems for Climate Neutral Aviation". In: *Journal of Physics: Conference Series* 2716.1 (Mar. 2024), p. 012001. ISSN: 1742-6596. DOI: 10.1088/1742-6596/2716/1/012001. URL: https://dx.doi.org/10.1088/1742-6596/2716/1/012001 (visited on 07/22/2025).

[139] Lyazid Bouhala et al. "Advancement in the Modeling and Design of Composite Pressure Vessels for Hydrogen Storage: A Comprehensive Review". In: *Journal of Composites Science* 8.9 (9 Sept. 2024), p. 339. ISSN: 2504-477X. DOI: 10.3390/jcs8090339. URL: https://www.mdpi.com/2504-477X/8/9/339 (visited on 07/22/2025).

[140] T. Michler et al. "3 - Assessing Hydrogen Embrittlement in Automotive Hydrogen Tanks". In: *Gaseous Hydrogen Embrittlement of Materials in Energy Technologies*. Ed. by Richard P. Gangloff and Brian P. Somerday. Vol. 2. Woodhead Publishing Series in Metals and Surface Engineering. Woodhead Publishing, Jan. 1, 2012, pp. 94–125. ISBN: 978-1-84569-677-1. DOI: 10.1533/9780857093899.1.94. URL: https://www.sciencedirect.com/science/article/pii/B978184569677150003X (visited on 10/26/2024).

[141] Fábio Coelho Barbosa. "Zero Carbon Emission Aviation Fuel Technology Review - The Hydrogen Pathway". In: SAE Brasil 2023 Congress. SAE International, Jan. 8, 2024. DOI: 10.4271/2023-36-0029. URL: https://saemobilus.sae.org/papers/zero-carbon-emission-aviation-fuel-technology-review-hydrogen-pathway-2023-36-0029 (visited on 07/24/2025).

[142] Jonas Martin, Anne Neumann, and Anders Oedegaard. *Sustainable Hydrogen Fuels versus Fossil Fuels for Trucking, Shipping and Aviation: A Dynamic Cost Model*. MIT Center for Energy and Environmental Policy Research, July 1, 2022, pp. 1–46. URL: https://ceepr.mit.edu/wp-content/uploads/2022/07/2022-010.pdf.

[143] Phillip J. Ansell. "Hydrogen-Electric Aircraft Technologies and Integration: Enabling an Environmentally Sustainable Aviation Future". In: *IEEE Electrification Magazine* 10.2 (June 2022), pp. 6–16. ISSN: 2325-5889. DOI: 10.1109/MELE.2022.3165721.

[144] Tawfiq Ahmed and Dilek Funda Kurtulus. "Technology Review of Sustainable Aircraft Design". In: *Sustainable Aviation*. Ed. by T. Hikmet Karakoc et al. Cham: Springer International Publishing, 2019, pp. 137–152. ISBN: 978-3-030-14195-0. DOI: 10.1007/978-3-030-14195-0_7. URL: https://doi.org/10.1007/978-3-030-14195-0_7 (visited on 06/14/2023).

[145] J. Hoelzen et al. "Hydrogen-Powered Aviation and Its Reliance on Green Hydrogen Infrastructure – Review and Research Gaps". In: *International Journal of Hydrogen Energy*. Hydrogen Energy and Fuel Cells 47.5 (Jan. 15, 2022), pp. 3108–3130. ISSN: 0360-3199. DOI: 10.1016/j.ijhydene.2021.10.239. URL: https://www.sciencedirect.com/science/article/pii/S0360319921043184 (visited on 10/14/2022).

[146] Talal Yusaf et al. "Sustainable Aviation—Hydrogen Is the Future". In: *Sustainability* 14.1 (1 Jan. 2022), p. 548. ISSN: 2071-1050. DOI: 10.3390/su14010548. URL: https://www.mdpi.com/2071-1050/14/1/548 (visited on 10/14/2022).

[147] Talal Yusaf et al. "Sustainable Hydrogen Energy in Aviation – A Narrative Review". In: *International Journal of Hydrogen Energy* 52 (Mar. 2023), S0360319923009187. ISSN: 03603199. DOI: 10.1016/j.ijhydene.2023.02.086. URL: https://linkinghub.elsevier.com/retrieve/pii/S0360319923009187 (visited on 06/14/2023).

[148] Stanislav Karpuk and Ali Elham. "Comparative Study of Hydrogen and Kerosene Commercial Aircraft with Advanced Airframe and Propulsion Technologies for More Sustainable Aviation". In: *Proceedings of the Institution of Mechanical Engineers, Part G: Journal of Aerospace Engineering* 237.9 (Dec. 12, 2022), p. 09544100221144342. ISSN: 0954-4100. DOI: 10.1177/09544100221144342. URL: https://doi.org/10.1177/09544100221144342 (visited on 06/14/2023).

[149] Sridhar Dalai et al. "Conversion of Laboratory Waste Glass into Useful Micro and Nano Materials for Energy Storage Application". In: *From Waste to Wealth*. Springer, Singapore, 2024, pp. 509–524. ISBN: 978-981-99-7552-5. DOI: 10.1007/978-981-99-7552-5_23. URL: https://link.springer.com/chapter/10.1007/978-981-99-7552-5_23 (visited on 07/24/2025).

[150] S. M Aceves, J Martinez-Frias, and O Garcia-Villazana. "Analytical and Experimental Evaluation of Insulated Pressure Vessels for Cryogenic Hydrogen Storage". In: *International Journal of Hydrogen Energy* 25.11 (Nov. 1, 2000), pp. 1075–1085. ISSN: 0360-3199. DOI: 10.1016/S0360-3199(00)00016-1. URL: https://www.sciencedirect.com/science/article/pii/S0360319900000161 (visited on 02/09/2024).

[151] Stratview Research. *Carbon Composite Pressure Vessels Market Size, Share, & Growth Analysis | Covid-19 Impact Analysis*. stratviewresearch.com. July 23, 2025. URL: https://stratviewresearch.com/3956/carbon-composite-pressure-vessels-market.html (visited on 07/23/2025).

[152] Francesco Salucci et al. “Retrofit of Hydrogen-Powered Helicopters: A Sizing Approach”. In: *AIAA AVIATION 2022 Forum*. AIAA AVIATION 2022 Forum. Chicago, IL & Virtual: American Institute of Aeronautics and Astronautics, June 27–July 1, 2022. DOI: 10.2514/6.2022-3206. URL: https://doi.org/10.2514/6.2022-3206 (visited on 12/10/2024).

[153] Ulrich Carsten Johannes Rischmüller et al. “Conceptual Design of a Hydrogen-Hybrid Dual-Fuel Regional Aircraft Retrofit”. In: *Aerospace* 11.2 (2 Feb. 2024), p. 123. ISSN: 2226-4310. DOI: 10.3390/aerospace11020123. URL: https://www.mdpi.com/2226-4310/11/2/123 (visited on 12/10/2024).

[154] B. Rietdijk and M. Selier. “Architecture Design for a Commercially Viable Hydrogen-Electric Powered Retrofitted Regional Aircraft”. In: ICAS Proceedings. Florence, Italy: International Congress of Aeronautical Science, 2024.

[155] Bassam Rakhshani, Alexandru Stan, and Tony Leslie. “A Steady-State Model-Based Evaluation of Performance Characteristics and Feasibility Analysis of Retrofit Hydrogen-Powered Aircraft Configurations”. In: *International Journal of Sustainable Aviation* 10.2 (Jan. 2024), pp. 99–123. ISSN: 2050-0467. DOI: 10.1504/IJSA.2024.138699. URL: https://www.inderscienceonline.com/doi/abs/10.1504/IJSA.2024.138699 (visited on 12/10/2024).

[156] Jayant Mukhopadhaya. *Performance Analysis of Fuel Cell Retrofit Aircraft*. Washington, DC: the International Council on Clean Transportation (ICCT), July 8, 2023, p. 40.

[157] Teresa Donateo, Antonio Ficarella, and Leonardo Lecce. “Retrofitting of Ultralight Aircraft with a Fuel Cell Power System”. In: *European Transport Studies* 1 (Dec. 1, 2024), p. 100002. ISSN: 2950-2985. DOI: 10.1016/j.ets.2024.100002. URL: https://www.sciencedirect.com/science/article/pii/S2950298524000023 (visited on 12/10/2024).

[158] FOKKER SERVICES BV. *Final Report Summary - RETROFIT (Reduced Emissions of TRansport Aircraft Operations by Fleetwise Implementation of New Technology) | FP7*. European Commission, 2012. URL: https://cordis.europa.eu/project/id/265867/reporting (visited on 12/10/2024).

[159] T. W. Reynolds. *Aircraft-Fuel-Tank Design for Liquid Hydrogen*. NACA-RM-E55F22. NASA, Aug. 9, 1955. URL: https://ntrs.nasa.gov/citations/19930088877 (visited on 06/22/2023).

[160] Anthony J Colozza, Analex Corporation, and Brook Park. *Hydrogen Storage for Aircraft Applications Overview*. NASA, 2002.

[161] D. Verstraete et al. “Hydrogen Fuel Tanks for Subsonic Transport Aircraft”. In: *International Journal of Hydrogen Energy*. Hyceltec 2009 Conference 35.20 (Oct. 2010), pp. 11085–11098. ISSN: 0360-3199. DOI: 10.1016/j.ijhydene.2010.06.060.

[162] A Onorati et al. “The Role of Hydrogen for Future Internal Combustion Engines”. In: *International Journal of Engine Research* 23.4 (Apr. 2022), pp. 529–540. ISSN: 1468-0874, 2041-3149. DOI: 10.1177/14680874221081947. URL: http://journals.sagepub.com/doi/10.1177/14680874221081947 (visited on 06/19/2024).

[163] Sebastian Nicolay et al. “Conceptual Design and Optimization of a General Aviation Aircraft with Fuel Cells and Hydrogen”. In: *International Journal of Hydrogen Energy* 46.64 (Sept. 16, 2021), pp. 32676–32694. ISSN: 0360-3199. DOI: 10.1016/j.ijhydene.2021.07.127. URL: https://www.sciencedirect.com/science/article/pii/S0360319921027920 (visited on 02/23/2024).

[164] Pavlos Rompokos et al. “Cryogenic Fuel Storage Modelling and Optimisation for Aircraft Applications”. In: *Proceedings of the ASME Turbo Expo 2021: Turbomachinery Technical Conference and Exposition*. ASME Turbo Expo 2021: Turbomachinery Technical Conference and Exposition. Vol. 6: Ceramics and Ceramic Composites; Coal, Biomass, Hydrogen, and Alternative Fuels; Microturbines, Turbochargers, and Small Turbomachines. Virtual, Online: American Society of Mechanical Engineers Digital Collection, Sept. 16, 2021, V006T03A001. ISBN: 978-0-7918-8499-7. DOI: 10.1115/GT2021-58595. URL: https://dx.doi.org/10.1115/GT2021-58595 (visited on 02/23/2024).

[165] Christopher Winnefeld et al. “Modelling and Designing Cryogenic Hydrogen Tanks for Future Aircraft Applications”. In: *Energies 11 (2018), Nr. 1* 11.1 (2018), p. 105. DOI: 10.15488/3366. URL: https://www.repo.uni-hannover.de/handle/123456789/3396 (visited on 12/13/2023).

[166] Gulru Babac, Altug Sisman, and Tolga Cimen. “Two-Dimensional Thermal Analysis of Liquid Hydrogen Tank Insulation”. In: *International Journal of Hydrogen Energy* 34.15 (15 Aug. 1, 2009), pp. 6357–6363. ISSN: 0360-3199. DOI: 10.1016/j.ijhydene.2009.05.052. URL: https://www.sciencedirect.com/science/article/pii/S0360319909007587 (visited on 03/23/2023).

[167] Linus Kameni Monkam et al. “Feasibility Analysis of a New Thermal Insulation Concept of Cryogenic Fuel Tanks for Hydrogen Fuel Cell Powered Commercial Aircraft”. In: *International Journal of Hydrogen Energy* 47.73 (Aug. 26, 2022), pp. 31395–31408. ISSN: 0360-3199. DOI: 10.1016/j.ijhydene.2022.07.069. URL: https://www.sciencedirect.com/science/article/pii/S036031992203083X (visited on 02/23/2024).

[168] Wenbing Jiang et al. “Transient Thermal Behavior of Multi-Layer Insulation Coupled with Vapor Cooled Shield Used for Liquid Hydrogen Storage Tank”. In: *Energy* 231 (Sept. 15, 2021), p. 120859. ISSN: 0360-5442. DOI: 10.1016/j.energy.2021.120859. URL: https://www.sciencedirect.com/science/article/pii/S0360544221011075 (visited on 02/23/2024).

[169] Yang Yu, Fushou Xie, and Yanzhong Li. “Study on Recovery and Utilization of Cold Energy for Insulation Design of Liquid Hydrogen Tanks”. In: *Energy* 310 (Nov. 30, 2024), p. 133167. ISSN: 0360-5442. DOI: 10.1016/j.energy.2024.133167. URL: https://www.sciencedirect.com/science/article/pii/S0360544224029426 (visited on 10/16/2024).

[170] Ping Wang et al. “Modeling and Optimization of Composite Thermal Insulation System with HGMs and VDMLI for Liquid Hydrogen on Orbit Storage”. In: *International Journal of Hydrogen Energy* 45.11 (11 Feb. 28, 2020), pp. 7088–7097. ISSN: 0360-3199. DOI: 10.1016/j.ijhydene.2019.12.110. URL: https://www.sciencedirect.com/science/article/pii/S0360319919346464 (visited on 03/23/2023).

[171] “Front Matter”. In: *Compendium of Hydrogen Energy*. Ed. by Ram B. Gupta, Angelo Basile, and T. Nejat Veziroğlu. Woodhead Publishing Series in Energy. Woodhead Publishing, Jan. 1, 2016, pp. i–iii. ISBN: 978-1-78242-362-1. DOI: 10.1016/B978-1-78242-362-1.09987-9. URL: https://www.sciencedirect.com/science/article/pii/B9781782423621099879 (visited on 10/14/2022).

[172] Saif Ghafri et al. “Hydrogen Liquefaction: A Review of the Fundamental Physics, Engineering Practice and Future Opportunities”. In: *Energy & Environmental Science* 15.7 (Apr. 21, 2022), pp. 2690–2731. ISSN: 1754-5692, 1754-5706. DOI: 10.1039/D2EE00099G. URL: http://xlink.rsc.org/?DOI=D2EE00099G.

[173] AEROSPACE TECHNOLOGY INSTITUTE. “Cryogenic Hydrogen Fuel System and Storage - Roadmap Report”. Mar. 2022. URL: https://www.ati.org.uk/wp-content/uploads/2022/03/FZO-PPN-COM-0027-Cryogenic-Hydrogen-Fuel-System-and-Storage-Roadmap-Report.pdf.

[174] Neha Singh Chauhan and Vineet Kumar Singh. “Fundamentals of Hydrogen as a Fuel”. In: *ISST Journal of Mechanical Engineering* 6 (2015), pp. 63–68. ISSN: 0976-7371.

[175] H Hemmes, Alfred Driessen, and Ronald Griessen. “Thermodynamic Properties of Hydrogen at Pressures up to 1 Mbar and Temperatures between 100 and 1000K”. In: *Journal of Physics C: Solid State Physics* 19 (Nov. 23, 2000), p. 3571. DOI: 10.1088/0022-3719/19/19/013.

[176] Jacob W. Leachman et al. *Thermodynamic Properties of Cryogenic Fluids*. International Cryogenics Monograph Series. Cham: Springer International Publishing, 2017. ISBN: 978-3-319-57833-0 978-3-319-57835-4. DOI: 10.1007/978-3-319-57835-4. URL: http://link.springer.com/10.1007/978-3-319-57835-4 (visited on 11/24/2022).

[177] Harold W. Woolley, Russell B. Scott, and F.G. Brickwedde. “Compilation of Thermal Properties of Hydrogen in Its Various Isotopic and Ortho-Para Modifications”. In: *Journal of Research of the National Bureau of Standards* 41.5 (Nov. 1948), p. 379. ISSN: 0091-0635. DOI: 10.6028/jres.041.037. URL: https://nvlpubs.nist.gov/nistpubs/jres/041/jresv41n5p379_A1b.pdf (visited on 11/21/2022).

[178] Andreas Zuttel. “Hydrogen Storage Methods”. In: *Naturwissenschaften* 91.4 (2004), p. 157. ISSN: 0028-1042. URL: https://www.academia.edu/4826927/Hydrogen_storage_methods (visited on 12/15/2022).

[179] R. D. McCarty. *Selected Properties of Hydrogen (Engineering Design Data)*. Boulder, CO, 1981, p. 536. URL: https://nvlpubs.nist.gov/nistpubs/Legacy/MONO/nbsmonograph168.pdf.

[180] Jacob Leachman. "Fundamental equations of state for parahydrogen, normal hydrogen, and orthohydrogen". M.S.M.E. Ann Arbor, United States, 2007. 124 pp. ISBN: 9780549058250. URL: https://www.proquest.com/docview/304854189/abstract/60E758799C1D4353PQ/1 (visited on 11/21/2022).

[181] Jonathan A. Lee and Stephen Woods. *Hydrogen Embrittlement*. JSC-CN-36009. Apr. 1, 2016. URL: https://ntrs.nasa.gov/citations/20160005654 (visited on 12/18/2023).

[182] John T. Hailer. "LNG Station Analysis for the Prediction of Pressure Rise and Vented Emissions". MS. West Virginia University Libraries, Jan. 1, 2015. DOI: 10.33915/etd.5735. URL: https://researchrepository.wvu.edu/etd/5735 (visited on 03/14/2023).

[183] Dries Verstraete. "The Potential of Liquid Hydrogen for Long Range Aircraft Propulsion". PhD thesis. Cranfield University / School of Engineering, Apr. 2009.

[184] Zhenzhou Wang et al. "A Review of Metallic Tanks for H2 Storage with a View to Application in Future Green Shipping". In: *International Journal of Hydrogen Energy* 46.9 (Feb. 3, 2021), pp. 6151–6179. ISSN: 0360-3199. DOI: 10.1016/j.ijhydene.2020.11.168. URL: https://www.sciencedirect.com/science/article/pii/S0360319920344141 (visited on 02/07/2024).

[185] R. P. Reed. "Aluminium 2. A Review of Deformation Properties of High Purity Aluminium and Dilute Aluminium Alloys". In: *Cryogenics* 12.4 (Aug. 1, 1972), pp. 259–291. ISSN: 0011-2275. DOI: 10.1016/0011-2275(72)90041-0. URL: https://www.sciencedirect.com/science/article/pii/0011227572900410 (visited on 02/09/2024).

[186] Subodh K. Mital et al. *Review of Current State of the Art and Key Design Issues With Potential Solutions for Liquid Hydrogen Cryogenic Storage Tank Structures for Aircraft Applications*. E-15621. Oct. 1, 2006. URL: https://ntrs.nasa.gov/citations/20060056194 (visited on 01/13/2023).

[187] Randall F. Barron. *Cryogenic Systems*. McGraw-Hill, 1966. 720 pp. ISBN: 978-0-07-003820-2. Google Books: G8FTAAAAMAAJ.

[188] Weiqiang Xu, Qianqian Li, and Minjie Huang. "Design and Analysis of Liquid Hydrogen Storage Tank for High-Altitude Long-Endurance Remotely-Operated Aircraft". In: *International Journal of Hydrogen Energy* 40.46 (Dec. 14, 2015), pp. 16578–16586. ISSN: 0360-3199. DOI: 10.1016/j.ijhydene.2015.09.028. PMID: null. URL: https://www.sciencedirect.com/science/article/pii/S0360319915300367 (visited on 03/23/2023).

[189] N. M. Garceau et al. "Performance Test of a 6 L Liquid Hydrogen Fuel Tank for Unmanned Aerial Vehicles". In: *IOP conference series. Materials Science and Engineering* 101.1 (2015), pp. 12130–12136. ISSN: 1757-8981. DOI: 10.1088/1757-899X/101/1/012130. URL: https://iopscience.iop.org/article/10.1088/1757-899X/101/1/012130 (visited on 09/20/2024).

[190] Salvador M. Aceves et al. "High-Density Automotive Hydrogen Storage with Cryogenic Capable Pressure Vessels". In: *International Journal of Hydrogen Energy* 35.3 (Feb. 1, 2010), pp. 1219–1226. ISSN: 0360-3199. DOI: 10.1016/j.ijhydene.2009.11.069. URL: https://www.sciencedirect.com/science/article/pii/S0360319909018394 (visited on 02/09/2024).

[191] Yan Yan et al. "Review on Linerless Type V Cryo-Compressed Hydrogen Storage Vessels: Resin Toughening and Hydrogen-Barrier Properties Control". In: *Renewable and Sustainable Energy Reviews* 189 (Jan. 1, 2024), p. 114009. ISSN: 1364-0321. DOI: 10.1016/j.rser.2023.114009. URL: https://www.sciencedirect.com/science/article/pii/S1364032123008675 (visited on 03/05/2024).

[192] Victor K. Poorte et al. "Structural Integration of a Full-Composite, Double-Walled, Vacuum-Insulated, Cryo-Compressed Tank for the Flying V: A Numerical Study". In: *AIAA SCITECH 2024 Forum*. AIAA SciTech Forum. American Institute of Aeronautics and Astronautics, Jan. 4, 2024. DOI: 10.2514/6.2024-0834. URL: https://arc.aiaa.org/doi/10.2514/6.2024-0834 (visited on 08/05/2025).

[193] Ming He et al. "Design and Development of Vehicle Cryo-Compressed Hydrogen Storage Vessel". In: *IOP Conference Series: Materials Science and Engineering* 1301.1 (May 2024), p. 012056. ISSN: 1757-899X. DOI: 10.1088/1757-899X/1301/1/012056. URL: https://dx.doi.org/10.1088/1757-899X/1301/1/012056 (visited on 08/05/2025).

[194] O. Kircher, Ichs, and Bmw EfficientDynamics. "Validation of Cryo-compressed Hydrogen Storage (CcH 2) – a Probabilistic Approach". In: *Proceeding of the Int. Conference on Hydrogen Safety*. Int. Conference on Hydrogen Safety. URL: https://api.semanticscholar.org/CorpusID:174787397 (visited on 01/23/2024).

[195] Romain Parello et al. "Design and Integration of a Liquid Hydrogen Tank on an Aircraft". In: *AIAA SCITECH 2024 Forum*. AIAA SciTech Forum. American Institute of Aeronautics and Astronautics, Jan. 4, 2024. DOI: 10.2514/6.2024-2638. URL: https://arc.aiaa.org/doi/10.2514/6.2024-2638 (visited on 02/26/2024).

[196] T. Hikmet Karakoc and Emre Özbek, eds. *Unmanned Aerial Vehicle Design and Technology*. Sustainable Aviation. Cham: Springer International Publishing, 2024. ISBN: 978-3-031-45320-5 978-3-031-45321-2. DOI: 10.1007/978-3-031-45321-2. URL: https://link.springer.com/10.1007/978-3-031-45321-2 (visited on 06/14/2024).

[197] A Aleksandraviciene and A Morkevicius. *Magicgrid® Book of Knowledge-a Practical Guide to Systems Modeling Using Magicgrid from No Magic*. 2nd edition. Kaunas, Lithuania: Vitae Litera, 2021. URL: https://discover.3ds.com/magicgrid-book-of-knowledge.

[198] Ferdinando Vitolo et al. "Mobile Robots and Cobots Integration: A Preliminary Design of a Mechatronic Interface by Using MBSE Approach". In: *Applied Sciences* 12.1 (Jan. 2022), p. 419. ISSN: 2076-3417. DOI: 10.3390/app12010419. URL: https://www.mdpi.com/2076-3417/12/1/419 (visited on 08/10/2025).

[199] Filippo Mazzoni et al. "Design Space Exploration through Liquid H2 Tank Preliminary Sizing and Design of Experiments Analysis". In: *International Journal of Hydrogen Energy* 95 (Dec. 2024), pp. 1252–1260. ISSN: 0360-3199. DOI: 10.1016/j.ijhydene.2024.08.017. URL: https://www.sciencedirect.com/science/article/pii/S0360319924031665 (visited on 03/22/2025).

[200] Mark Lutz. *Learning Python*. 5th ed. Beijing: O'Reilly, 2013. 1590 pp. ISBN: 978-1-4493-5573-9.

[201] F. Mazzoni et al. "Hydrogen Storage System Design: Case Studies for Airborne Application". In: *ICAS Proceedings*. 34th Congress of the International Council of the Aeronautical Sciences. Florence, Italy: International Congress of Aeronautical Science, 2024.

[202] P.C. de Boer, A.J. de Wit, and R.C. van Benthem. "Development of a Liquid Hydrogen-Based Fuel Cell System for the HYDRA-2 Drone". In: *AIAA Science and Technology Forum and Exposition, AIAA SciTech Forum 2022*. AIAA Science and Technology Forum and Exposition, AIAA SciTech Forum 2022. 2022. DOI: 10.2514/6.2022-0443. URL: https://www.scopus.com/inward/record.uri?eid=2-s2.0-85122949044&doi=10.2514%2f6.2022-0443&partnerID=40&md5=8a4140f94fbe307f22bf045ad7d275e9.

[203] *Online Materials Information Resource - MatWeb*. URL: https://matweb.com/index.aspx (visited on 05/01/2024).

[204] *Toray T300 Carbon Fiber*. URL: https://matweb.com/search/datasheet.aspx?MatGUID=86d0be5b80514c66b2c91e3357c57a1f (visited on 05/01/2024).

[205] Afshin Ghajar and Yunus Cengel. *Heat and Mass Transfer - Fundamentals and Applications*. 6th Edition. New York, NY: McGraw-Hill Education, 2020.

[206] Claire McFarland and Ramesh K Agarwal. "A Simple Model of Thermal Insulation Design for Cryogenic Liquid Hydrogen Tank". In: *Mechanical Engineering and Materials Science Independent Study* (Apr. 1, 2022). URL: https://openscholarship.wustl.edu/mems500/176.

[207] *Cryogenics Material Properties*. URL: https://trc.nist.gov/cryogenics/materials/materialproperties.htm (visited on 08/10/2025).

[208] *The Physics Factbook - An encyclopedia of scientific essays*. URL: https://hypertextbook.com/facts/2003/EvelynGofman.shtml (visited on 09/26/2025).

[209] Updated: Sep 20 and 2023. *The Predator Drone: A Pioneering Force in Modern Warfare*. HowStuffWorks. Jan. 1, 1970. URL: https://science.howstuffworks.com/predator.htm (visited on 09/03/2025).

[210] Department of the Air Force. *English: 3-View Line Drawing and Dimensions of RQ-1B Predator UAV*. URL: https://commons.wikimedia.org/wiki/File:USAF_RQ-1B_Predator_UAV_3view.jpg (visited on 09/03/2025).

[211] Garry J. Roedler and Cheryl Jones. *Technical Measurement - A Collaborative Project of PSM, INCOSE, and Industry*. INCOSE-TP-2003-020-01. PSM & INCOSE, Dec. 27, 2005, p. 65. URL: https://www.incose.org/publications/products/technical-publications (visited on 09/06/2025).

[212] Stefano Favre et al. "Fuel-Based Thermal Management System Architectures and Tank Temperature Evolution Models for Aviation". In: Florence, Italy: International Congress of Aeronautical Science, 2024. URL: https://iris.polito.it/handle/11583/2994352 (visited on 09/07/2025).

[213] Stefano Favre et al. "Innovative Thermal Management Systems for Fuel Cell Electric Aircraft". In: *International Journal of Mechanics and Control* (2025). DOI: 10.69076/jomac.2025.0014. URL: https://iris.polito.it/handle/11583/3001430 (visited on 09/07/2025).

Appendix A

Systems Engineering terminology: stakeholder, customer, and user

Considering the widespread adoption of the terms stakeholder, customer, client, and user across various disciplines, it has been deemed helpful to provide definitions to clarify their meanings.

The ISO/IEC/IEEE 15288 standard provides a proper definition of stakeholder.

A stakeholder is any entity (individual or organisation) with a legitimate interest in the system.

The *customer* is the entity that commissions the system. The system can be a product or a service. Typically, if it is a product, the term customer is used to refer to the buyer, while the term client is sometimes used as a substitute for customer if the system is a service. However, in SE, the term client is avoided in favour of customer, which is generally more appropriate.

Finally, the *user* is any entity that directly interacts with the system to perform an operational activity. Users are defined here as entities that directly interact with the system during its lifecycle.

A simple example can be made. Assuming the SoI is an aircraft, a potential stakeholder would be the Air traffic management institution. The customer could be a company, such as an airline like Air France, KLM, or ITA Airways. At the same time, the users would include the passengers, the pilot, the maintenance personnel,

as well as those interacting with the SoI before its deployment, such as engineers performing testing activities.

In general, the stakeholder definition also encompasses customers and users, although this is not always the case. A user can also be the customer and vice versa. In practice, the distinction between the different roles is not always clear, but, given that consistency is maintained throughout the design, the most suitable solution must be found on a case-by-case basis [8, 7, 6].

Appendix B

Industrial CH_2 tank data

Table B.1 Type III and IV high-pressure vessel commercial data.

Service pressure (bar)	Capacity (kg)	Empty weight (kg)	Length (mm)	Diam. (mm)	Vol. (L)	Grav. index (%)	Company	Source
Type III tanks								
350	0.1	3	450	125	4	3.23	Steelhead	Catalogue
350	0.5	14	2500	125	22	3.45	Steelhead	Catalogue
350	0.6	17	760	280	28	3.41	Steelhead	Catalogue
350	0.9	23	850	330	40	3.77	Steelhead	Catalogue
350	1	26	740	340	42	3.70	Luxfer	Catalogue
350	1.3	29	875	340	52	4.29	Luxfer	Catalogue
350	1.8	39	900	400	74	4.41	Luxfer	Catalogue
350	1.8	49	880	425	80	3.54	Steelhead	Catalogue
350	2.07	70	1016	435	90	2.87	Steelhead	Catalogue
350	2.3	48	1458	340	94	4.57	Luxfer	Catalogue
350	2.9	58	3	280	125	4.76	Steelhead	Catalogue
350	3	100	1422	435	133	2.91	Steelhead	Catalogue
350	3.6	73	1614	415	150	4.70	Luxfer	Catalogue
350	3.8	75	2600	330	165	4.82	Steelhead	Catalogue
350	4.85	135	2110	435	205	3.47	Steelhead	Catalogue
350	5	95	2110	415	205	5.00	Luxfer	Catalogue
350	6.2	165	2616	435	270	3.62	Steelhead	Catalogue
350	6.2	132	2600	425	270	4.49	Steelhead	Catalogue
350	6.5	118	2743	419	280	5.23	Luxfer	Catalogue
350	7	168	1372	660.4	290	4.00	AST	Brochure
350	7.3	129	3048	419	310	5.35	Luxfer	Catalogue
350	7.8	138	3165	415	322	5.35	Luxfer	Catalogue
350	10.8	222	1963	660.4	445	4.64	AST	Brochure
Type IV tanks								
700	0.4	10	735	170	9	3.85	Steelhead	Catalogue
700	1	24	1750	170	26	4.00	Steelhead	Catalogue
700	1.4	33	921	332	36	4.07	Hexagon Purus	Brochure
700	2.1	36	900	350	53	5.51	ILJIN Hysolus	Website
700	2.1	37	878	368	53.4	5.37	Hexagon Purus	Brochure
700	2.4	50	860	410	63	4.58	Steelhead	Catalogue
700	3.1	59	1050	440	76	4.99	Hexagon Purus	Brochure
700	4.1	66	1653	350	103	5.85	ILJIN Hysolus	Website
700	4.6	79	123	445	115	5.50	ILJIN Hysolus	Website
700	7	118	2100	410	180	5.60	Steelhead	Catalogue
700	7.4	117	1850	445	185	5.95	ILJIN Hysolus	Website
700	9.8	188	2154	530	244	4.95	Hexagon Purus	Brochure
700	14.6	191	2060	600	364	7.10	Hexagon Purus	Brochure
700	18.4	272	2078	705	457	6.34	Hexagon Purus	Brochure

Appendix C

Publications produced throughout the PhD

Filippo Mazzoni, Eugenio Brusa, Cristiana Delprete, Camilo Andrés Manrique-Escobar, Alberto Dagna, Grazia Accardo. *Bridging Requirements and Design in MBSE: Leveraging SysML v2 for Automatic Verification*. Accepted to 2025 IEEE International Symposium on Systems Engineering (ISSE), Paris, France, 2025.

Filippo Mazzoni, Roberta Biga, Camilo Andrés Manrique-Escobar, Eugenio Brusa, Cristiana Delprete. *Design space exploration through liquid H_2 tank preliminary sizing and design of experiments analysis*. International Journal of Hydrogen Energy, Volume 95, 2024, pp. 1252–1260. DOI: 10.1016/j.ijhydene.2024.08.017.

Filippo Mazzoni, Grazia Accardo, Roberta Biga, Eugenio Brusa, Cristiana Delprete, Camilo Andrés Manrique-Escobar, Valeria Vercella. *Hydrogen storage system design: case studies for airborne application*. 34th Congress of the International Council of the Aeronautical Sciences, 2024.

Filippo Mazzoni, Roberta Biga, Camilo Andrés Manrique-Escobar, Eugenio Brusa, Cristiana Delprete. *Design space exploration through liquid H_2 tank preliminary sizing and design of experiments analysis*. European Fuel Cells and Hydrogen Conference, 2023.

Filippo Mazzoni, Eugenio Brusa, Cristiana Delprete, Camilo Andrés Manrique-Escobar, Grazia Accardo. *Quantitative assessment of hydrogen fuel tank design optimisation on hydrogen-powered regional aircraft weight and UAV endurance*. Under peer review.

Eugenio Brusa, Cristiana Delprete, Lorenzo Giorio, Filippo Mazzoni. *Design pathways for Additively Manufactured metal components supported by the Systems Engineering Methodology*. Under peer review.